



# DISSERTATION

Titel der Dissertation

„The Role of Fibroblast Growth Factor Receptor 4 in  
Colorectal Cancer“

Verfasserin

Mag.rer.nat. Christine Heinzle

angestrebter akademischer Grad

Doktorin der Naturwissenschaften (Dr.rer.nat.)

Wien, 2011

Studienkennzahl lt. Studienblatt: A 091 490

Dissertationsgebiet lt. Studienblatt: Molekulare Biologie

Betreuerin / Betreuer: A.o.Univ.Prof. Dr. Brigitte Marian



## **Acknowledgements**

As I am coming to the end of my PhD years there are several acknowledgements I want to express. This thesis would not have been possible unless the help of some people to whom I am sincerely grateful.

First of all I owe my deepest gratitude to my supervisor Brigitte Marian, who inspired me not only with her scientific knowledge but also with her patient and understanding handling of all kind of problems. I would like to thank her for supporting me in any way during my thesis, for always having an open ear for any concerns and for the great atmosphere in the lab. Thank you for giving me the opportunity to work within our team!

I am also deeply indebted to our FGF-group namely Walter Berger, Bettina Grasl-Kraupp, Michael Grusch, Klaus Holzmann and their teams for the inspiring and supporting discussions and advices as well as their help in daily laboratory practice.

Many special thanks also to Andrea Gsur and her lab, for genotyping such a large cohort and providing us with very valuable patient information, to Wolfgang Mikulits and his lab, who supported us with all kinds of EMT-issues, and finally to Martin Filipits, who, together with Sabine El Gazzar and Elisabeth Rabensteiner, has greatly helped me with immunohistological procedures and interpretations.

I am also thankful to Christine Gauglhofer, who, especially during my first two years, was a great support in all kinds of FGF-related and technical issues. Furthermore I would also like to thank Petra Heffeter for helping me with the in vivo experiments.

Special thanks also to Irene Herbacek, who helped me with all those numerous FACS analyses, and Paul Breit, for taking all those excellent pictures.

I am also very grateful to Xenia Hudec and Zeynep Erdem for their extensive support in the lab. I am really looking forward to work with you for the next years!

I would also like to thank my colleagues Kerstin, Edith, Inga, Andrea M. und Andrea P. for any help and all the laughs we had in (and outside) the lab.

Certainly I do not want to forget to thank my family and friends for supporting me during my studies in any sense.

Last but not least I am deeply thankful to Thomas Klaghofer who helped me out with all kinds of computer-issues, helped me correcting my thesis, and (although not working in a scientific field) shows great interest in my work.

# TABLE OF CONTENTS

<b>1</b>	<b>INTRODUCTION.....</b>	<b>1</b>
1.1	DEFINITION OF CANCER.....	1
1.2	EPIDEMIOLOGY .....	1
1.2.1	<i>Epidemiology of cancer worldwide.....</i>	<i>1</i>
1.2.2	<i>Epidemiology of colorectal cancer worldwide.....</i>	<i>4</i>
1.2.3	<i>Epidemiology of cancer in Austria.....</i>	<i>5</i>
1.2.4	<i>Epidemiology of colorectal cancer in Austria.....</i>	<i>8</i>
1.3	CANCEROGENESIS .....	9
1.3.1	<i>The three-stage model: Initiation – Promotion – Progression .....</i>	<i>10</i>
1.3.1.1	Tumor initiation .....	10
1.3.1.2	Tumor promotion .....	11
1.3.1.3	Tumor progression .....	12
1.4	THE HALLMARKS OF CANCER .....	13
1.4.1	<i>Self-sufficiency in growth signals.....</i>	<i>13</i>
1.4.2	<i>Insensitivity to anti-growth signals .....</i>	<i>14</i>
1.4.3	<i>Evading apoptosis.....</i>	<i>14</i>
1.4.4	<i>Limitless replicative potential.....</i>	<i>15</i>
1.4.5	<i>Sustained angiogenesis .....</i>	<i>15</i>
1.4.6	<i>Tissue invasion and metastasis .....</i>	<i>15</i>
1.4.7	<i>Additional hallmarks.....</i>	<i>16</i>
1.4.7.1	Evasion of Immunosurveillance .....	16
1.4.7.2	DNA damage and DNA replication stress.....	17
1.4.7.3	Proteotoxic stress .....	17
1.4.7.4	Mitotic stress.....	17
1.4.7.5	Metabolic stress.....	17
1.4.7.6	Oxidative Stress .....	18
1.4.7.7	Inflammatory microenvironment.....	18
1.5	COLORECTAL CANCER (CRC).....	19
1.5.1	<i>Anatomy of the colon .....</i>	<i>19</i>
1.5.2	<i>Histology of the colon tissue .....</i>	<i>20</i>
1.5.3	<i>Development of colorectal cancer .....</i>	<i>22</i>
1.5.4	<i>Molecular biology of colorectal cancer.....</i>	<i>24</i>
1.5.4.1	Vogelstein-model .....	24
1.5.4.2	APC and the Wnt-pathway.....	25
1.5.4.2.1	The canonical Wnt/ $\beta$ -catenin cascade.....	25
1.5.4.2.2	The role of APC and $\beta$ -catenin in colorectal cancer .....	26
1.5.4.3	K-ras, a member of the Ras-family .....	29
1.5.4.3.1	Ras signaling: the MAP-kinase and PI3-kinase pathway.....	30
1.5.4.3.2	The role of K-Ras in colorectal cancer .....	31

1.5.4.4	P53.....	32
1.5.4.5	LOH at chromosome 18: Smad2 and Smad4.....	33
1.5.5	<i>Tumor staging in colorectal cancer</i> .....	34
1.6	RECEPTOR TYROSINE KINASES.....	37
1.6.1	<i>The function of receptor tyrosine kinases</i> .....	37
1.6.2	<i>Receptor tyrosine kinases in cancer</i> .....	39
1.7	FIBROBLAST GROWTH FACTOR RECEPTORS (FGFRs).....	40
1.7.1	<i>FGFRs in general</i> .....	40
1.7.1.1	Structure of FGF and FGFR.....	40
1.7.1.2	Interaction between FGFR and FGF/extracellular matrix.....	41
1.7.1.3	FGFR dimerization.....	43
1.7.1.4	Receptor activation.....	44
1.7.1.5	FGFR downstream signaling.....	45
1.7.1.6	Crosstalk between FGF- and Wnt-signaling.....	47
1.7.1.7	Regulation and termination of FGF-mediated signaling.....	49
1.7.2	<i>FGFR Family</i> .....	51
1.7.2.1	FGFR1.....	51
1.7.2.2	FGFR2.....	52
1.7.2.3	FGFR3.....	52
1.7.2.4	FGFR4.....	53
1.7.2.4.1	FGFR4 and its role in cancer.....	53
1.7.2.4.2	FGFR4 G388R polymorphism.....	54
1.7.2.4.3	The role of FGFR4 G388R polymorphism in various cancer types.....	55
1.7.2.4.4	The role of FGFR4 G388R polymorphism in colorectal cancer.....	56
1.7.2.4.5	Interaction of FGFR4 G388 polymorphism with metalloproteinase.....	57
1.7.3	<i>FGF-Family</i> .....	57
1.7.3.1	Intracellular subfamily: FGF11-14 (iFGF).....	59
1.7.3.2	Hormone-like subfamily: FGF19, FGF21, FGF23.....	60
1.7.3.3	Canonical subfamily.....	61
1.7.3.3.1	FGF1 subfamily: FGF1 and FGF2.....	61
1.7.3.3.2	FGF4 subfamily: FGF4, FGF5, FGF6.....	63
1.7.3.3.3	FGF7 subfamily: FGF3, FGF7, FGF10, FGF22.....	63
1.7.3.3.4	FGF8 subfamily: FGF8, FGF17, FGF18.....	64
1.7.3.3.5	FGF9 subfamily: FGF9, FGF16, FGF20.....	65
1.7.4	<i>Deregulation of FGF-signaling in cancer</i> .....	67
1.7.4.1	Activating mutation.....	67
1.7.4.2	FGFR gene amplification.....	68
1.7.4.3	Chromosomal translocation.....	69
1.7.4.4	Autocrine and paracrine signaling.....	69
1.7.4.5	Germline single nucleotide polymorphism.....	70
1.7.4.6	Alteration of FGFR-splicing.....	71
1.7.5	<i>Role of FGF-signaling in colorectal cancer</i> .....	71
1.7.6	<i>Therapeutic strategies affecting FGF-signaling in cancer</i> .....	73

1.7.6.1	Small molecule FGFR kinase inhibitors.....	73
1.7.6.2	Antagonistic antibodies to FGFRs.....	74
<b>2</b>	<b>AIMS OF THIS PROJECT .....</b>	<b>77</b>
<b>3</b>	<b>MATERIALS AND METHODS .....</b>	<b>79</b>
3.1	CELL BIOLOGY.....	79
3.1.1	<i>Materials used for cell culture</i> .....	79
3.1.2	<i>Cell lines</i> .....	79
3.1.3	<i>Passaging of cells</i> .....	80
3.1.4	<i>Viability assays</i> .....	80
3.1.4.1	Neutral red uptake .....	80
3.1.4.2	MTT assay: EZ4U.....	81
3.1.5	<i>Colony formation assay</i> .....	81
3.1.6	<i>Filter migration assay</i> .....	81
3.1.7	<i>Anchorage independent growth: soft agar assay</i> .....	82
3.1.8	<i>H<sup>3</sup>-thymidine incorporation</i> .....	82
3.1.9	<i>Fluorescence Activated Cell Sorting (FACS)</i> .....	83
3.1.9.1	Cells expressing GFP .....	83
3.1.9.2	Immuno-flow-cytometry with PE directly labeled antibody: FGFR4 .....	83
3.1.9.3	Immuno-flow-cytometry with PE indirectly labeled antibody: E-Cadherin .....	84
3.1.9.4	Cell cycle distribution .....	84
3.1.9.5	Induction of Apoptosis: JC-1-FACS .....	85
3.1.10	<i>Cell Sorting</i> .....	85
3.1.11	<i>Immunofluorescence staining</i> .....	85
3.1.12	<i>Plasmids</i> .....	86
3.1.13	<i>Transfection</i> .....	87
3.1.14	<i>Selection</i> .....	87
3.1.15	<i>Small interfering RNA (siRNA) mediated gene knock down</i> .....	88
3.1.16	<i>Luciferase</i> .....	89
3.2	MOLECULAR BIOLOGY: RNA.....	90
3.2.1	<i>RNA isolation</i> .....	90
3.2.2	<i>Complementary DNA (cDNA) synthesis</i> .....	91
3.2.3	<i>Standard Polymerase Chain Reaction (PCR)</i> .....	91
3.2.4	<i>Polyacrylamid Gel Electrophoresis</i> .....	93
3.2.5	<i>Real-time PCR</i> .....	94
3.2.5.1	TaqMan <sup>®</sup> Assays .....	95
3.2.5.2	TaqMan <sup>®</sup> Genotyping assay for FGFR4 .....	96
3.2.5.3	SybrGreen .....	97
3.2.6	<i>Restriction Fragment Length Polymorphism (RFLP) for FGFR4</i> .....	98
3.2.6.1	PCR.....	98
3.2.6.2	Restriction enzyme digest .....	99

3.2.6.3	Gel .....	99
3.3	TET-OFF ADVANCED INDUCIBLE GENE EXPRESSION SYSTEM .....	100
3.3.1	<i>Principles of the tet-off-system</i> .....	100
3.3.1.1	K5-vector .....	101
3.3.1.2	pTet-Off-Advanced-Vector .....	101
3.3.1.3	pTRE-Tight-vector .....	102
3.3.2	<i>Restriction digest</i> .....	103
3.3.3	<i>DNA-isolation with gel-extraction-kit</i> .....	104
3.3.4	<i>Ligation</i> .....	105
3.3.5	<i>Transformation of bacteria</i> .....	105
3.3.6	<i>Plasmid preparation: Mini-, midi-, and maxi-preps</i> .....	105
3.4	PROTEIN CHEMISTRY.....	106
3.4.1	<i>Western blotting</i> .....	106
3.4.1.1	Total protein isolation.....	107
3.4.1.2	Membrane Protein Isolation.....	107
3.4.1.3	Evaluation of protein concentration: Coomassie blue assay .....	108
3.4.1.4	SDS-Polyacrylamid Gel Electrophoresis (PAGE).....	108
3.4.1.5	Western blot.....	110
3.4.1.6	Ponceau S staining.....	110
3.4.1.7	Immunological detection of protein.....	111
3.5	IN VIVO EXPERIMENTS .....	113
3.5.1	<i>Tissue specimens</i> .....	113
3.5.2	<i>Blood samples</i> .....	113
3.5.3	<i>Local tumor growth in SCID mice</i> .....	114
3.5.4	<i>Metastatic in vivo model: tail vein injection</i> .....	114
3.5.5	<i>Tissue fixation and paraffinization</i> .....	114
3.5.6	<i>Hämatoxylin-Eosin staining</i> .....	115
3.5.7	<i>Immunohistochemical staining</i> .....	116
3.6	STATISTICAL EVALUATION OF DATA.....	116
<b>4</b>	<b>RESULTS.....</b>	<b>117</b>
4.1	FGFR4 IN HUMAN COLORECTAL CANCER.....	117
4.1.1	<i>Genotyping FGFR4 G388R polymorphism in blood samples</i> .....	117
4.1.2	<i>FGFR4 expression and G388R polymorphism in human CRC tissue specimen</i> .....	118
4.1.2.1	FGFR4 expression in human CRC tissue specimen.....	118
4.1.2.2	Correlation of FGFR4 expression and TMN-staging.....	119
4.1.2.3	Allelic expression of FGFR4 in human CRC tissue specimen.....	120
4.1.2.4	Correlation of allelic FGFR4 expression and TMN-staging .....	122
4.2	EXPRESSION DATA OF CRC CELL LINES.....	125
4.2.1	<i>FGFR4 expression in CRC cell lines</i> .....	125
4.2.2	<i>Expression of FGFR4 ligands in CRC cell lines</i> .....	126
4.3	FGFR4 G388R POLYMORPHISM IN CRC CELL LINES .....	129



4.3.1	<i>Establishment of FGFR4<sup>Gly</sup> and FGFR4<sup>Arg</sup> over-expressing cells</i>	129
4.3.2	<i>Viability of FGFR4 over-expressing cells</i>	131
4.3.3	<i>Proliferation of FGFR4 over-expressing cells</i>	132
4.3.4	<i>Migration of FGFR4 over-expressing cells</i>	133
4.3.5	<i>Colony formation of FGFR4 over-expressing cells</i>	134
4.3.6	<i>Anchorage independent growth of FGFR4 over-expressing cells</i>	135
4.3.7	<i>Signaling of FGFR4 over-expressing cells</i>	136
4.3.8	<i>FGFR4 over-expressing SW480 xenografts in SCID mice</i>	138
4.3.8.1	Immunohistological evaluation of tumor xenografts	139
4.3.8.2	Immunohistological evaluation of lung sections and metastasis	142
4.3.9	<i>In vivo metastasis model of FGFR4 over-expressing SW480 transfectants</i>	144
4.4	<b>FGFR4 G388R POLYMORPHISM AND ITS ROLE IN EMT</b>	146
4.4.1	<i>E-Cadherin</i>	146
4.4.1.1	mRNA expression: real-time PCR	146
4.4.1.2	Protein expression: FACS	147
4.4.1.3	Protein expression: immunofluorescence staining	147
4.4.2	<i>β-catenin</i>	148
4.4.2.1	Protein expression: immunofluorescence staining	148
4.4.2.2	β-catenin localization: luciferase assay	149
4.5	<b>DOWN-REGULATION OF FGFR4</b>	151
4.5.1	<i>Down-regulation of FGFR4 via siRNA</i>	151
4.5.1.1	Knock down efficiency of FGFR4 on mRNA- and protein-level	151
4.5.1.2	Viability	153
4.5.1.3	Proliferation	154
4.5.1.4	Colony formation	155
4.5.1.5	Migration	156
4.5.1.6	Anchorage independent growth	157
4.5.1.7	Signaling	158
4.5.2	<i>Down-regulation of FGFR4 via dominant negative adenovirus</i>	160
4.5.2.1	mRNA expression	160
4.5.2.2	Protein expression	162
4.5.2.3	Viability	162
4.5.2.4	Colony Formation	163
4.5.2.5	Migration	164
4.5.2.6	Anchorage independent growth	165
4.5.3	<i>Tet-inducible down-regulation of FGFR4</i>	167
4.5.3.1	Cloning of a tet-inducible dominant negative FGFR4 construct	167
4.5.3.1.1	Excision of K5 and GFP	167
4.5.3.1.2	Transformation of pTet-off and pTRE-tight into Jm109 bacteria strain	169
4.5.3.1.3	Preparative digest of pTRE-tight for cloning	169
4.5.3.1.4	Ligation, transformation into XL1Blue bacteria strain and verification	170
4.5.3.2	Transfection of tet-inducible system into CRC cell lines	171
4.5.3.2.1	Expression and function of the tet-off-system in cell model	171

4.5.3.2.2	Establishment of pTet-off expressing stable cells .....	173
4.5.3.2.3	Establishment of pTet-off/pTRE-tight-K5 and -GFP stable cells.....	175
4.5.3.2.4	Expression of GFP and K5 in pTet-off/pTRE-tight stable cells .....	176
4.5.3.3	Influence of Doxycycline dependent K5 expression on cell biology .....	177
4.5.3.3.1	Viability .....	177
4.5.3.3.2	Cell cycle: FACS analysis.....	178
4.5.3.3.3	Apoptosis: JC1-FACS.....	179
4.5.3.3.4	Cell migration .....	180
4.5.3.3.5	Colony formation .....	181
4.5.3.3.6	Anchorage independent growth.....	181
<b>5</b>	<b>DISCUSSION .....</b>	<b>183</b>
5.1	SUMMARY OF OUR RESULTS .....	183
5.2	ROLE OF THE FGFR4 G388R POLYMORPHISM IN HUMAN CRC .....	184
5.2.1	<i>Expression of FGFR4 in CRC tissue .....</i>	<i>184</i>
5.2.2	<i>Correlation between FGFR4 allele and expression.....</i>	<i>184</i>
5.2.3	<i>FGFR4 G388R polymorphism and CRC initiation and development .....</i>	<i>185</i>
5.2.4	<i>FGFR4 G388R polymorphism and histopathological parameters.....</i>	<i>186</i>
5.2.5	<i>FGFR4 G388R polymorphism and survival.....</i>	<i>187</i>
5.3	FGFR4 G388R POLYMORPHISM IN VIVO AND IN VITRO: CELL CULTURE MODEL .....	188
5.3.1	<i>FGFR4 G388R polymorphism and cell growth.....</i>	<i>188</i>
5.3.2	<i>FGFR4 G388R polymorphism and cell migration and cell adhesion .....</i>	<i>189</i>
5.3.3	<i>FGFR4 G388R polymorphism in SCID mouse xenografts.....</i>	<i>190</i>
5.3.4	<i>FGFR4 G388R polymorphism and epithelial mesenchymal transition.....</i>	<i>190</i>
5.3.5	<i>FGFR4 dependent cell signaling.....</i>	<i>191</i>
5.4	FGFR4 KNOCK DOWN VIA siRNA .....	193
5.5	TOOL DEVELOPMENT FOR STABLE AND INDUCIBLE FGFR4 INHIBITION.....	194
5.5.1	<i>Introduction of a dominant negative FGFR4 construct .....</i>	<i>194</i>
5.5.1.1	<i>Influence of dominant negative FGFR4 adenovirus on cell growth, migration and adhesion ....</i>	<i>195</i>
5.5.1.2	<i>Establishment of an inducible tet-off system for dominant negative FGFR4 construct.....</i>	<i>196</i>
5.6	CONCLUSION .....	196
<b>6</b>	<b>ABSTRACT .....</b>	<b>199</b>
<b>7</b>	<b>ZUSAMMENFASSUNG .....</b>	<b>201</b>
<b>8</b>	<b>BIBLIOGRAPHY .....</b>	<b>203</b>
<b>9</b>	<b>CURICULUM VITAE .....</b>	<b>217</b>

## TABLE OF FIGURES

Figure 1: Cancer incidence and mortality worldwide in 2008 .....	2
Figure 2: Worldwide incidence and mortality of most common cancer types.....	3
Figure 3: Worldwide incidence rate of colorectal cancer among men and women .....	4
Figure 4: Causes of death in Austria 1970 and 2010 .....	6
Figure 5: Incidence and mortality of various cancer types in Austrian men and women 2007 .....	7
Figure 6: Colorectal cancer incidence and mortality rate from 1990 to 2007 in Austria .....	8
Figure 7: Cancerogenesis and Darwinian selection .....	9
Figure 8: Multi-step tumorigenesis in determined cancer types .....	10
Figure 9: The hallmarks of cancer .....	13
Figure 10: Two key signaling pathways to achieve self-sufficiency in growth signaling.....	14
Figure 11: The new hallmarks of cancer.....	16
Figure 12: Anatomy of the colon .....	20
Figure 13: The five layers of the intestine .....	21
Figure 14: Histology of colon tissue .....	22
Figure 15: Development of colorectal cancer .....	23
Figure 16: Carcinogenesis of colorectal cancer: Vogelstein-model.....	24
Figure 17: Wnt-signaling pathway.....	26
Figure 18: APC/ $\beta$ -catenin and the biology of colonic crypts.....	28
Figure 19: Familial adenomatous polyposis .....	29
Figure 20: The regulation of Ras activity .....	30
Figure 21: Ras signaling: MAP-kinase and PI3-kinase pathway .....	31
Figure 22: Pathways of p53 .....	33
Figure 23: TGF- $\beta$ /Smad4 signaling .....	34
Figure 24: Tyrosine kinase receptors .....	38
Figure 25: Signaling pathways activated by the RTK FGFR.....	39
Figure 26: Structure of FGFR.....	41
Figure 27: Ligand binding of FGF and receptor dimerization .....	42
Figure 28: Molecular surface representation of the 2:2:2 FGF2-FGFR1-heparin-complex.....	43
Figure 29: FGFR activation .....	45
Figure 30: Intracellular FGF-dependent signaling .....	47
Figure 31: Induction of EMT by FGF-signaling.....	48
Figure 32: GSK3 $\beta$ crosslinks Wnt-signaling and FGF-signaling pathways .....	49
Figure 33: Inhibition of FGF-mediated signaling by sprouty .....	50
Figure 34: Structure of FGFR4-G388R polymorphism .....	55
Figure 35: Evolutionary relationship of mouse FGFs.....	59
Figure 36: 3-dimensional structure of FGF2, a prototypical FGF .....	63
Figure 37: Role of different FGF-splice variants in the tissue crosstalk .....	66
Figure 38: Binding affinity of FGF towards their receptors .....	67

Figure 39: Chemical structure of JC-1 .....	85
Figure 40: Bioluminescent reaction catalyzed by firefly and renilla luciferase .....	89
Figure 41: The principle of Standard PCR.....	92
Figure 42: The principles of real-time PCR .....	95
Figure 43: Gel of RFLP of FGFR4 G388R polymorphism.....	99
Figure 44: Principles of the Tet off system.....	100
Figure 45: K5-vector: a dominant negative construct for FGFR4.....	101
Figure 46: pTet-off-Advanced vector .....	102
Figure 47: pTRE-Tight-vector: the response plasmid .....	103
Figure 48: FGFR4 expression of 71 colorectal tumor tissues normalized to normal mucosa.....	119
Figure 49: Correlation of FGFR4 expression in CRC with histopathological parameters.....	120
Figure 50: Straight calibration line to analyze allelic expression of FGFR4 in tissue specimen .....	121
Figure 51: Allelic expression of FGFR4 in colon tumor and normal mucosa tissue.....	121
Figure 52: FGFR4 expression versus allelotype in human CRC tissue .....	122
Figure 53: Correlation of FGFR4 genotype with tumor histopathological parameters in human CRC ...	123
Figure 54: FGFR4 expression of CRC cell lines.....	125
Figure 55: Expression of FGFR4-ligands in CRC cell lines .....	126
Figure 56: G388R polymorphism in CRC cell lines .....	127
Figure 57: Pictures of SW480, HCT116 and HT29 FGFR4 transfectants .....	129
Figure 58: FGFR4 RNA expression of transfected SW480, HCT116 and HT29 stable clone pools.....	130
Figure 59: Total FGFR4 protein expression of SW480 transfectants .....	131
Figure 60: Cell surface expression of FGFR4 in SW480, HCT116, and HT29 FGFR4-transfectants.....	131
Figure 61: Viability of FGFR4 <sup>Arg</sup> and FGFR4 <sup>Gly</sup> tranfectants.....	132
Figure 62: Proliferation of FGFR4 over-expressing cells .....	133
Figure 63: Migration of FGFR4 over-expressing cells .....	134
Figure 64: Colony formation of FGFR4 over-expressing cells.....	135
Figure 65: Anchorage independent growth of FGFR4 over-expressing cells .....	136
Figure 66: Impact of FGFR4 over-expressing SW480 on FRS and PCL $\gamma$ .....	137
Figure 67: Impact of FGFR4 over-expressing SW480 on ERK, S6, GSK and Src.....	138
Figure 68: Local tumor growth of SW480 FGFR4 <sup>Arg</sup> , FGFR4 <sup>Gly</sup> and GFP xenografts in SCID mice.....	139
Figure 69: Immunohistochemical stainings of FGFR4 over-expressing tumor xenografts.....	140
Figure 70: Apoptotic-, mitotic-, and proliferation-rate of FGFR4 tumor sections .....	141
Figure 71: Cell density of FGFR4 <sup>Arg</sup> , FGFR4 <sup>Gly</sup> and control tumor sections .....	142
Figure 72: Ki67 staining and classification of FGFR4 over-expressing xenograft lungs .....	143
Figure 73: Metastatic score of FGFR4 over-expressing xenografts and control.....	144
Figure 74: Body weight of FGFR4 transfectants in metastasis model in vivo .....	145
Figure 75: Ki67 positive nodules of SW480 FGFR4 <sup>Arg</sup> metastasis in rodent lung .....	145
Figure 76: E-cadherin mRNA expression of FGFR4 over-expressing cells .....	146
Figure 77: FACS analysis of E-cadherin in FGFR4 over-expressing cells.....	147
Figure 78: Immunofluorescence staining of E-cadherin in FGFR4 over-expressing .....	148

Figure 79: Immunofluorescence staining of $\beta$ -catenin in FGFR4 over-expressing .....	149
Figure 80: FGFR4 over-expression and $\beta$ -catenin dependent promoter activity .....	150
Figure 81: mRNA expression of FGFR4 after knock down in CRC cell lines .....	152
Figure 82: FGFR4 protein knock down efficiency of SW480 – western blot.....	152
Figure 83: FGFR4 protein knock down efficiency of HCT116 and HT29 - FACS.....	153
Figure 84: Cell viability after FGFR4 knock down in CRC cell lines .....	154
Figure 85: Proliferation of FGFR4 knock down in CRC cell lines.....	155
Figure 86: Colony formation of FGFR4 knock down in CRC cell lines .....	156
Figure 87: Migration of FGFR4 knock down in CRC cell lines .....	157
Figure 88: Anchorage independent growth of FGFR4 knock down in CRC cell lines.....	158
Figure 89: Signaling of FGFR4 knock down via siRNA in HT29 and SW480.....	159
Figure 90: K5 mRNA expression of K5-adenovirally infected CRC cell lines: real-time PCR .....	161
Figure 91: K5 mRNA expression of K5-adenovirally infected CRC cell lines: standard PCR .....	161
Figure 92: Expression of the K5-protein.....	162
Figure 93: Cell viability of CRC cell lines infected with K5 adenovirus .....	163
Figure 94: Colony formation of CRC cell lines infected with K5 adenovirus.....	164
Figure 95: Migration of CRC cell lines infected with K5 adenovirus .....	165
Figure 96: Anchorage independent growth of CRC cell lines infected with K5 adenovirus .....	166
Figure 97: Excision of K5 and GFP.....	168
Figure 98: Control restriction digest of pTet-off and pTRE-tight.....	169
Figure 99: Preparative digest of pTRE-tight for cloning .....	170
Figure 100: Control restriction digests of pTRE-tight-GFP and pTRE-tight-K5.....	171
Figure 101: Protein expression of TetR in a transient cell model.....	172
Figure 102: Function of tet-off-system in a transient cell model.....	173
Figure 103: Stable expression of pTet-off in SW480 and HCT116.....	175
Figure 104: mRNA expression of GFP/K5 in pTet-off/pTRE-tight-K5 and –GFP stable cells.....	177
Figure 105: Viability of pTRE-tight-K5 and –GFP expressing cells +/- Doxycycline .....	178
Figure 106: Cell cycle of pTRE-tight-K5 and –GFP expressing cells +/- Doxycycline .....	179
Figure 107: Apoptosis of pTRE-tight-K5 and –GFP expressing cells +/- Doxycycline .....	179
Figure 108: Migration of pTRE-tight-K5 and –GFP expressing cells +/- Doxycycline .....	180
Figure 109: Colony formation of pTRE-tight-K5 and –GFP expressing cells +/- Doxycycline.....	181
Figure 110: Malignant growth of pTRE-tight-K5 and –GFP expressing cells +/- Doxycycline .....	182

## LIST OF TABLES

Table 1: Colorectal cancer staging according to the American Joint Committee of Cancer .....	36
Table 2: FGF-knockout mice: phenotype and physiological role of FGF1-23 .....	58
Table 3: FGFR kinase inhibitors .....	75
Table 4: Description of CRC cell lines .....	80
Table 5: Vectors used in this work.....	87
Table 6: Selection conditions for cell lines .....	88
Table 7: Primer for standard PCR.....	93
Table 8: TaqMan <sup>®</sup> assay kits.....	96
Table 9: Antibodies used for western blot .....	112
Table 10: Categories of study population and their genotype in relation to allelic FGFR4 expression ...	117
Table 11: Genotype of FGFR4 polymorphism and carcinoma incidence .....	118
Table 12: Correlation of FGFR4 genotype with tumor stage in human CRC .....	124
Table 13: CRC cell lines chosen for FGFR4 over-expression and down-regulation models .....	128
Table 14: Classification of metastatic score for Ki67 positive stained lungs.....	142

## LIST OF ABBREVIATIONS

A. bidest	water two times distilled
AJCC	American Joint Committee of Cancer
ATCC	American Type Culture Collection
ALK	Anaplastic Lymphoma Kinase
APC	Adenomatous Polyposis Coli
APS	Ammoniumperoxodisulfat
ATP	Adenosine Tri-Phosphate
BAKS	Burgenländer Arbeitskreis für Sozial- und Vorsorgemedizin
BSA	Bovine Serum Albumin
cDNA	complementary DNA
CFP	Cyan Fluorescent Protein
CIAP	Calf Intestinal Alkaline Phosphatase
CK1	Caseine Kinase 1
cm	centimeter
COX-1/2	Cyclooxygenase 1/2
Cox as virus	unrelated noncoding virus
CRC	Colorectal Cancer
DAG	Diacylglycerol
DEPC	Diethylpyrocarbonate
DNA	Desoxyribonucleic Acid
Dox	Doxycycline
EDTA	Ethylenediaminetetraacetic Acid
EGF	Epidermal Growth Factor
EGFR	Epidermal Growth Factor Receptor
EMS	8p11 Myeloproliferative Syndrome
EMT	Epithelial Mesenchymal Transition
EtOH	Ethanol
FACS	Fluorescence Activated Cell Sorting
FAM	Carboxyfluorescein
FAP	Familiar Adenomatous Polyposis
FCS	Fetal Calf Serum

FELASA	Federation of European Laboratory Animal Science Associations
FGF	Fibroblast Growth Factor
FGFR	Fibroblast Growth Factor Receptor
FGFR4 <sup>Arg</sup>	Fibroblast Growth Factor Receptor 4 R388
FGFR4 <sup>Gly</sup>	Fibroblast Growth Factor Receptor 4 G388, “wild-type”
FRS2	FGFR Substrate 2
g	gram
GAP	GTPase-Activating Protein
GAPDH	Glyceraldehyde 3-Phosphate Dehydrogenase
GDP	Guanosine Di-Phosphate
GEF	Guanine nucleotide Exchange Factor
GFP	Green Fluorescent Protein
GIT	Gastro Intestinal Tract
GSK3	Glycogen Synthase Kinase 3
GTP	Guanosine Tri-Phosphate
h	hour
H&E staining	Hematoxylin & Eosin staining
HIF-1	Hypoxia-Inducible Factor 1
HGF	Hepatocyte Growth Factor
HPSG	Heparan Sulphate Proteoglycan
HRP	Horse Radish Peroxidase
iFGF	intracellular Fibroblast Growth Factor
Ig loops	Immunoglobulin-like loops
IGF1R/INSR	Insulin-like Growth Factor 1 Receptor
IL	Interleukin
Ins(1,4,5)P3	Inositol 1,4,5-trisphosphate
IRES	Internal Ribosome Entry Site
kDa	kilo Dalton
LAR II	Luciferase Assay Reagent II
LEF	Lymphoid Enhancer Factor
LOH	Loss of Heterozygosity
LRP	LDL-Receptor Related Protein



m	meter
M	molar
MAP-kinase	Mitogen-Activated Protein kinase
MBq	Megabecquerel
mCi	millicurie
MCS	Multiple Cloning Site
MEM	Minimum Essential Medium
mg	milligram
MGB	Minor Groove Binder
min	minute
ml	milliliter
mm	millimeter
mM	millimolar
MOI	Multiplicity Of Infection
MT1-MMP	Membrane Type 1 Matrix Metalloproteinase
μg	microgram
μl	microliter
μm	micrometer
NCI	National Cancer Institute
NGF	Nerve Growth Factor
nm	nanometer
NTRK1	Neurotrophic Tyrosine Kinase Receptor type 1
OD	Optical Density
PAGE	Polyacrylamid Gel Electrophoresis
PAH	Polycyclic Aromatic Hydrocarbons
PBS	Phosphate Buffered Saline
PCR	Polymerase Chain Reaction
PDGF	Platelet-derived Growth Factor
PDGFR	Platelet-derived Growth Factor Receptor
PDK	Phosphoinositide-Dependent Kinase
PE	Phycoerythrin
PH	Pleckstrin Homology

PI	Inositol Phospholipid
PI3-kinase	Phosphatidylinositol 3-Kinase
PKB	Protein Kinase B
PKC	Protein Kinase C
PLC $\gamma$	Phospholipase-C $\gamma$
PMSF	Phenylmethylsulfonylfluoride
PP2A	Protein Phosphatase 2A
pRb	Retinoblastoma protein
PSA	Prostate-Specific Antigen
PTB	Phosphor Tyrosine Binding
PtdIns(4,5)P <sub>2</sub>	Phosphatidylinositol 4,5-bisphosphate
PVDF	Polyvinylidene Fluoride
RET	Rearranged during Transfection
RFLP	Restriction Fragment Length Polymorphism
RISC	RNA-Induced Silencing Complex
RNA	Ribonucleic Acid
ROS	Reactive Oxygen Species
rpm	revolutions per minute
RTK	Receptor Tyrosine Kinase
SCID	Severe Combined Immunodeficiency
SDS	Sodiumdodecylsulfate
Sef	Similar Expression to FGF-genes
SFM	Serum Free Medium
SH2/3	Src Homology 2/3
siRNA	small interfering RNA
SNP	Single Nucleotide Polymorphism
Spry	Sprouty
STAT	Signal Transducer and Activator of Transcription
TAE buffer	Tris base, Acetic acid and EDTA buffer
TBS	Tris-Buffered Saline
TCF	T-Cell Factor
TEMED	Tetramethylethylenediamine

Tet	Tetracycline
TetO	Tet-Operator
TetR	Tet-Repressor
TGF- $\alpha$	Transforming Growth Factor $\alpha$
TGF- $\beta$	Transforming Growth Factor $\beta$
T/N ratio	Tumor/Normal mucosa ratio
TNF	Tumor Necrosis Factor
tTA-protein	Tetracycline-controlled Transactivator protein
TRE	Tet-Responsive Element
VEGF	Vascular Endothelial Growth Factor
VEGFR	Vascular Endothelial Growth Factor Receptor
WHO	World Health Organization



# **1 Introduction**

## **1.1 Definition of cancer**

The National Cancer Institute (NCI) defines cancer as “a term used for diseases in which abnormal cells divide without control and are able to invade other tissues. Cancer cells can spread to other parts of the body through the blood and lymph systems” (NCI 17.6.2011). The medical term for cancer is malignant neoplasm. According to the NCI cancer can be grouped into five broad categories:

- carcinomas, which originate from epithelial cells
- sarcomas, which originate from mesoderm or supporting tissue (like bones, cartilage, fat, muscle, blood vessels, etc.)
- leukemia, which originates from blood forming tissue (bone marrow) and affects the blood cells
- lymphoma and myeloma, which originate from cells of the immune system
- central and nervous system cancers, which arise from cells of the central and peripheral nervous system

Tumors are divided into benign and malignant tumors. Benign tumors are not cancerous and do not invade or metastasize to other parts of the body. Therefore, they can be removed surgically and mostly do not return. Malignant tumors are defined as cancer and can invade nearby tissues and metastasize.

## **1.2 Epidemiology**

### **1.2.1 Epidemiology of cancer worldwide**

Cancer is the second of the leading causes of death (following heart diseases) in economically developed countries and the third leading cause of death in developing countries (following heart diseases and diarrheal diseases) (Garcia et al. 2007). 2008 the World Health Organization (WHO) reported 12,7 million new cancer cases. In 2008 7,6 million people died of cancer which are around 13% of all deaths. 70% of all cancer

## Introduction

deaths occur in low- and middle-income countries (WHO 11.6.2011). The highest incidences of cancer are mainly seen in developed regions like Australia, New Zealand, Northern America and Europe. The lowest incidence rates are observed in Africa (except South Africa) and South-Central Asia. Although cancer incidence rates in developed countries are higher than in developing countries, mortality rates are almost the same (Globoscan 11.6.2011). The incidence rate of cancer in developing countries is increasing due to reduced childhood mortality and reduced deaths of infectious diseases leading to higher age. But also adopting western lifestyle behavior like smoking, high saturated fat and calorie dense diet connected with reduced physical activity raises the rates of cancer in these regions (Garcia et al. 2007).

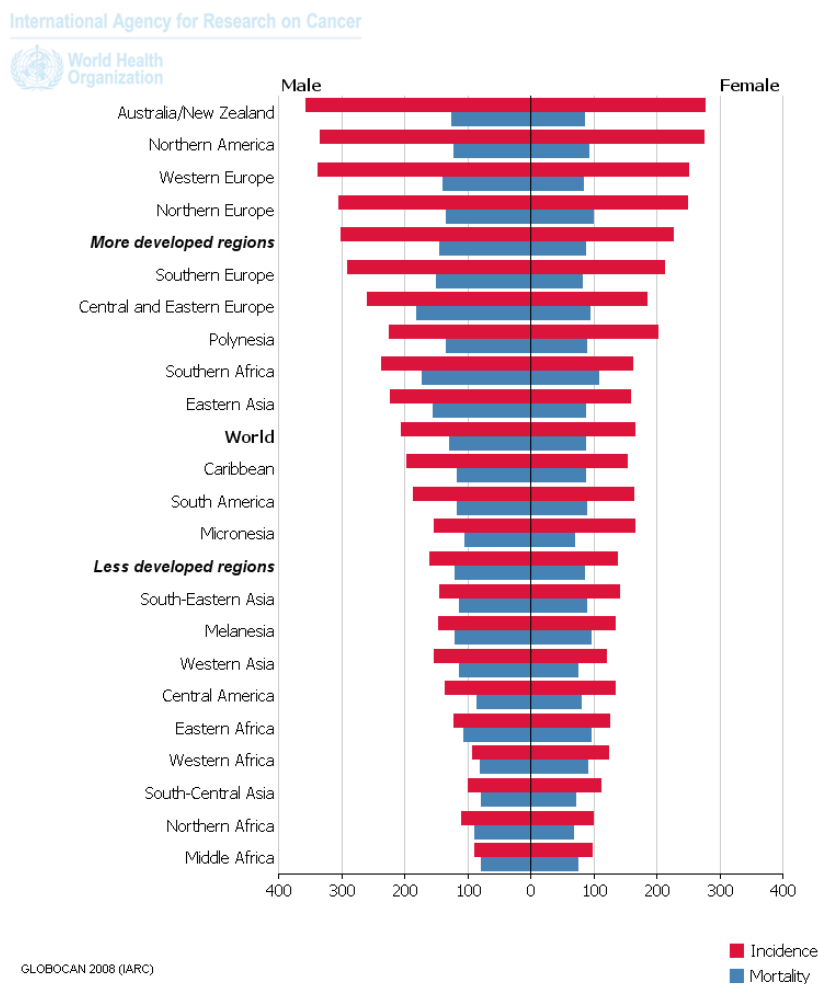


**Figure 1:** Cancer incidence and mortality worldwide in 2008

(Globoscan 11.6.2011)

## Introduction

Apart from genetic factors cancer can be induced by physical carcinogens, chemical carcinogens and biological carcinogens (see chapter 1.3.1.1). Avoiding these external carcinogens and risk factors like alcohol abuse, smoking, overweight, poor diet and physical inactivity can prevent a considerable percentage of cancer deaths (WHO 11.6.2011). About 15% of all cancers worldwide are caused by infection. In developing countries this percentage is three times higher (26%) than in developed countries (8%), caused by reduced availability and use of medical practices like cancer screening and treatment. Stomach cancer is the most infection-related cancer followed by liver and cervix cancer (Garcia et al. 2007).

Worldwide the most frequent cancer types in men are lung cancer, prostate cancer, colorectal cancer, stomach cancer and liver cancer whereas lung cancer presents the most lethal cancer for men. The most common cancer for women is breast cancer which has also the highest mortality among all cancer types for women (Globoscan 11.6.2011).

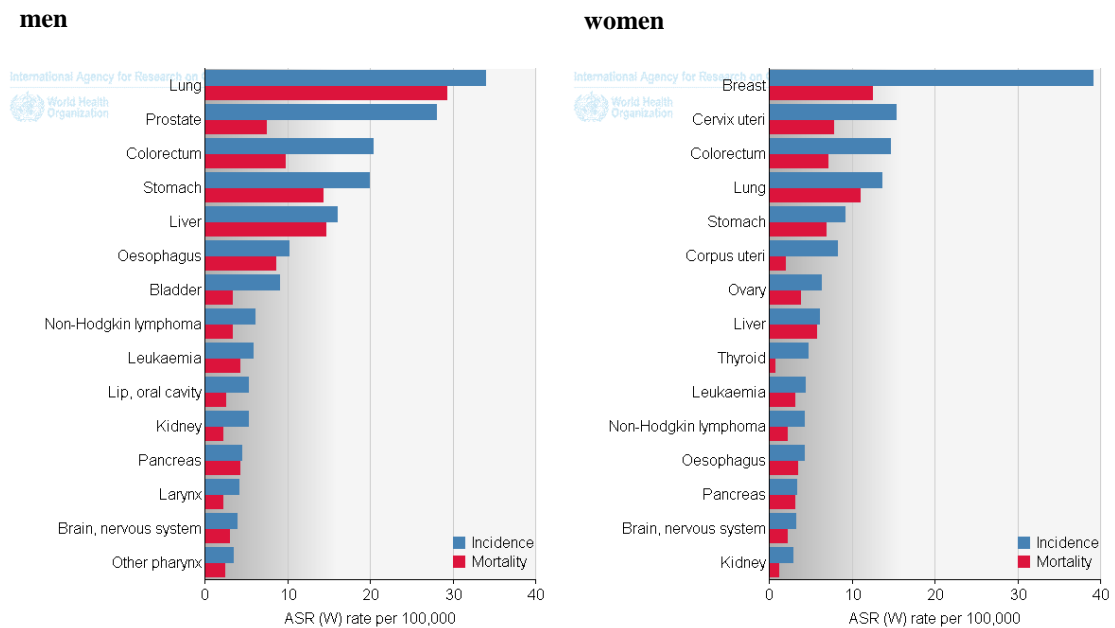


**Figure 2:** Worldwide incidence and mortality of most common cancer types

(Globoscan 11.6.2011)

## Introduction

### 1.2.2 Epidemiology of colorectal cancer worldwide

Colorectal cancer (CRC) is the third common (9-10%) cancer in both sexes and the fourth most common cause of death from cancer (8%) worldwide. 60% of CRC cases occur in developed countries like Australia, New Zealand, Europe and Northern America. The lowest incidence rates for CRC are estimated in Africa (excluding South Africa), Central America and South Central Asia. Also in countries in which the risk for CRC was historically low like Japan or Puerto Rico, the incidence rate is increasing. The greatest increase of CRC incidence is reported for Asia (Japan, Hong Kong, Singapore) and Eastern Europe (Hungary and Poland) as well as Israel and Puerto Rico. Changes in dietary patterns and increased obesity in these regions are quoted as reasons. The decrease of CRC rate which was observed in Northern America results from an increase of cancer detection and removal of precancerous lesions (Garcia et al. 2007).

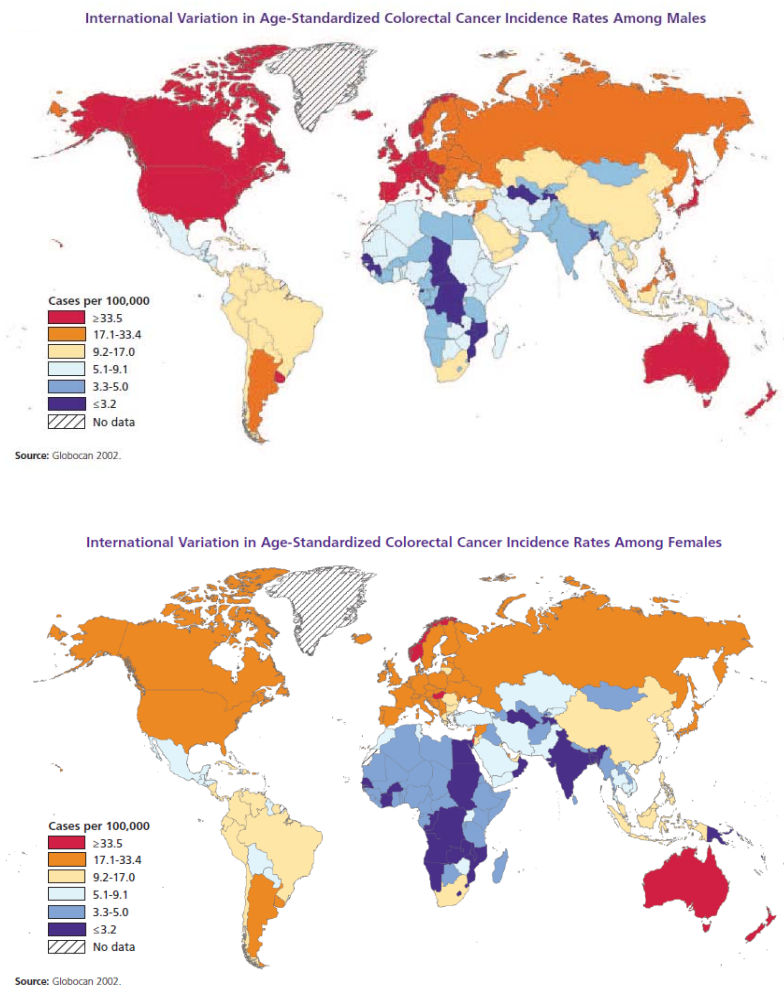


**Figure 3:** Worldwide incidence rate of colorectal cancer among men and women (Garcia et al. 2007)



## Introduction

Although screening for CRC increases survival rates and reduces mortality, only few countries have implemented organized national or regional screening programs. The five-year survival rate can reach 90% when CRC is detected at an early and localized stage. During 1982-1992 the survival rate for men in five developing countries (China, Cuba, India, the Philippines, and Thailand) was only 28%-42%. Today, for instance in the United States, the five-year survival rate for CRC is 64%. (Garcia et al. 2007).

### **1.2.3 Epidemiology of cancer in Austria**

In 2010 77.199 people died in Austria. Among these, 43% died of cardiovascular diseases which were the major cause of death in Austria followed by cancer. Although cardiovascular diseases demonstrate the largest part of deaths, the percentage is declining compared to 1970. According to *Statistik Austria* approximately 25% of all events of death in 2010 were attributed to cancer. In contrast to cardiovascular diseases the percentage of cancer related deaths is increasing compared to 1970, caused by an increase of the life expectancy. People aged between 65 and 74 display the statistically highest risk for developing cancer. Other causes of death are respiratory diseases, injuries and intoxications as well as diseases of the gastro intestinal tract (GIT) (StatistikAustria 15.6.2011).

## Introduction

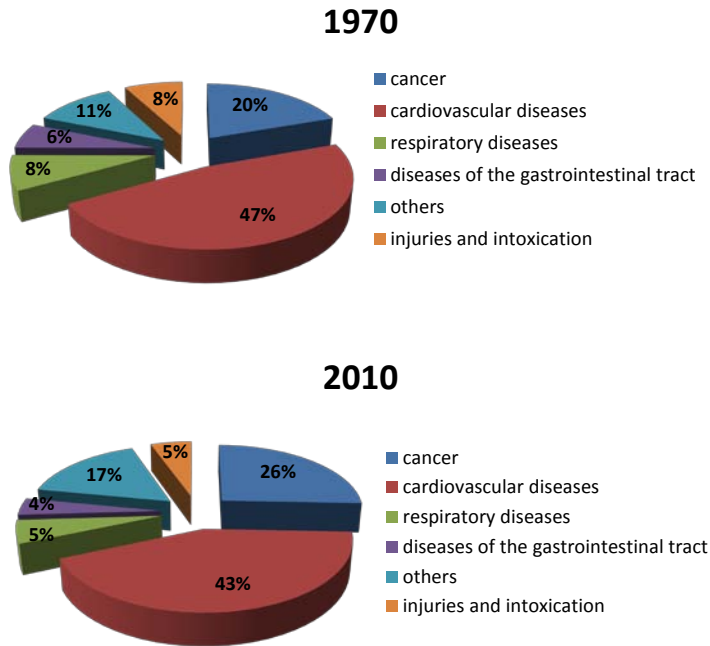


**Figure 4:** Causes of death in Austria 1970 and 2010

(StatistikAustria 15.6.2011)

Since 1994 prostate cancer is the most frequent cancer type in Austrian men. Before 1994 lung cancer was the predominant cancer type in men. In women breast cancer is the most frequent cancer type. In the last decade the incidence for prostate and breast cancer in Austria increased about 14% partly because of extended screening programs. In contrast, the incidence for gastric cancer in Austria has sharply dropped since 1987 and also the incidence and mortality of cervical carcinoma in women decreased. The risk and mortality rate for lung cancer was increasing for women and decreasing for men during the last decade (Zielonke 2010).

Breast cancer still presents the highest mortality rate of all cancer types in women. For men lung cancer displays the highest mortality followed by CRC. The mortality rate for CRC in women is at the third place behind lung cancer (Zielonke 2010).

# Introduction

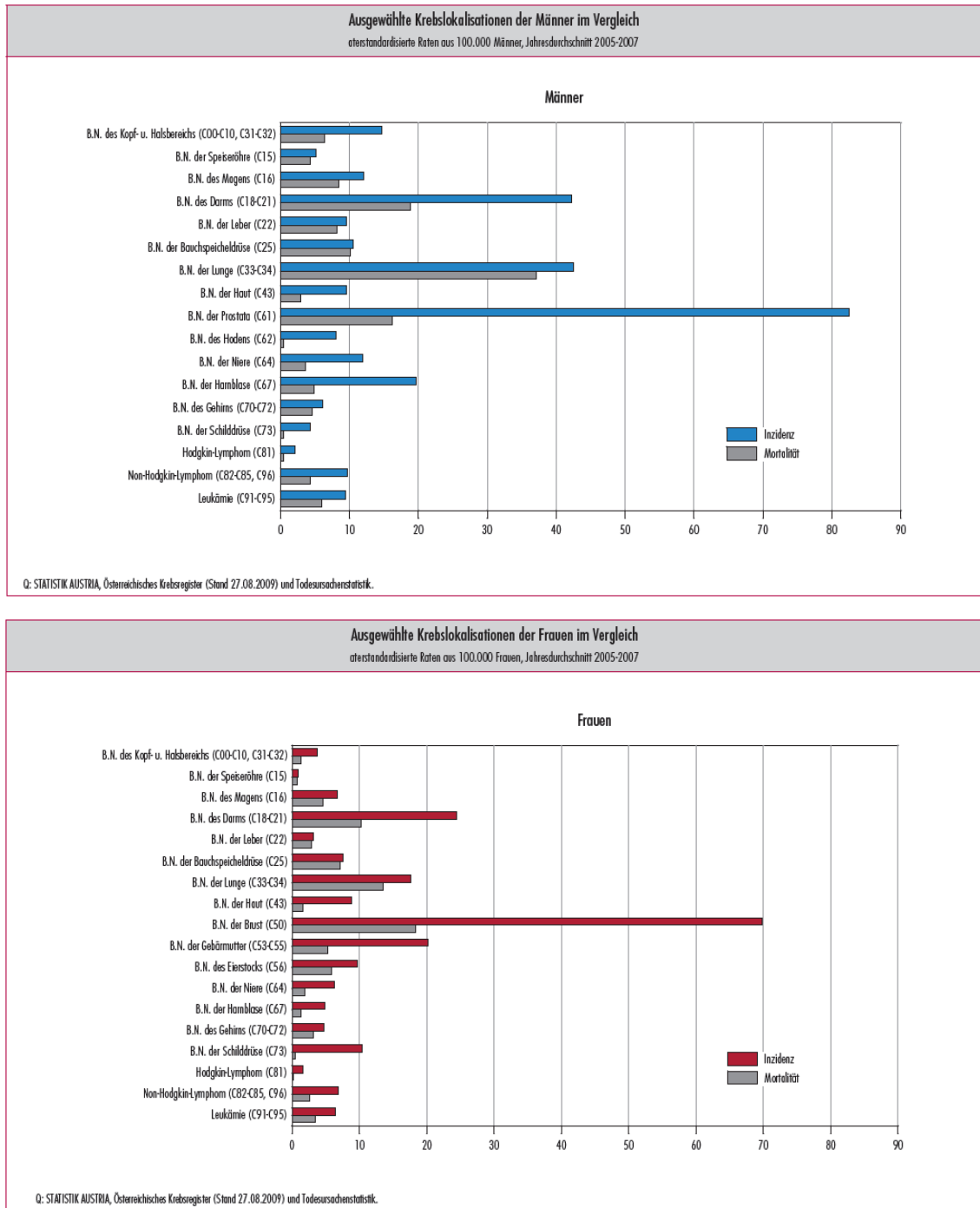


**Figure 5:** Incidence and mortality of various cancer types in Austrian men and women 2007

In the upper panel cancer incidence is presented by the blue bars for men, in the lower panel by the red bars for women. The grey bars present cancer mortality (Zielonke 2010).

From 2005-2007 84% of all malignant tumors were carcinomas. Among these 45% were adenocarcinomas (cancer of the epithelia originated from glandular tissue) and

## Introduction

10% squamous cell carcinoma. 1% of all malignant neoplastic diseases were sarcomas and 8% were leukemia (Zielonke 2010).

### 1.2.4 Epidemiology of colorectal cancer in Austria

Each year between 4.400 and 5.000 malignant colorectal tumors are diagnosed in Austria. This presents about 13% of all newly diagnosed malignant diseases. About 2.200 people each year die from CRC in Austria. The risk to suffer from CRC is higher for men than for women. Nevertheless the age standardized incidence rate for CRC dropped about 24% and also the mortality rate decreased about 28% over the last decade. 60% of women and 53% of men with diagnosed CRC display a survival rate of more than 5 years in Austria (Zielonke 2010).

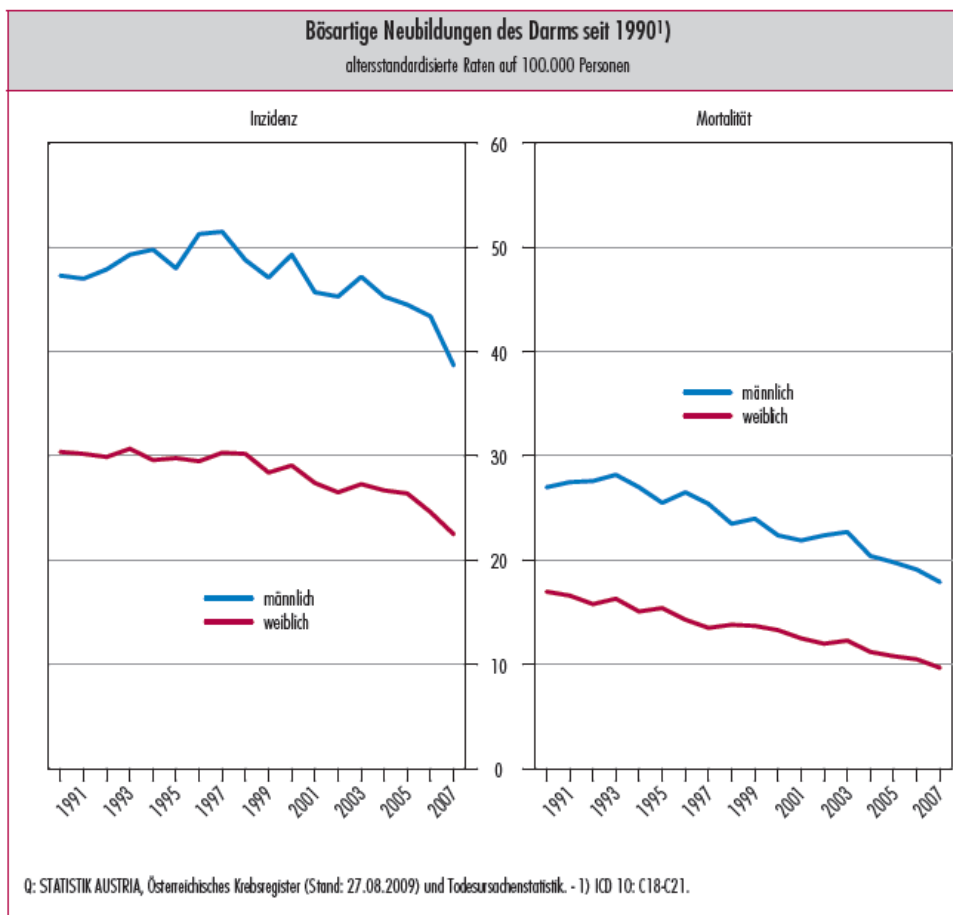


**Figure 6:** Colorectal cancer incidence and mortality rate from 1990 to 2007 in Austria

The left panel shows incidence rate, the right panel shows mortality. Blue lines represent men, red lines women (Zielonke 2010).

### 1.3 Cancerogenesis

Cancerogenesis is the process of a normal cell developing into a malignant tumor. This transformation is a complex process which involves changes on cellular and genetic levels to reprogram cells and acquire malignant characteristics. During a process resembling Darwinian evolution, these characteristics are acquired by genetic modifications followed by the natural selection of cells capable to proliferate and survive more effectively than their neighbors (Stratton et al. 2009).

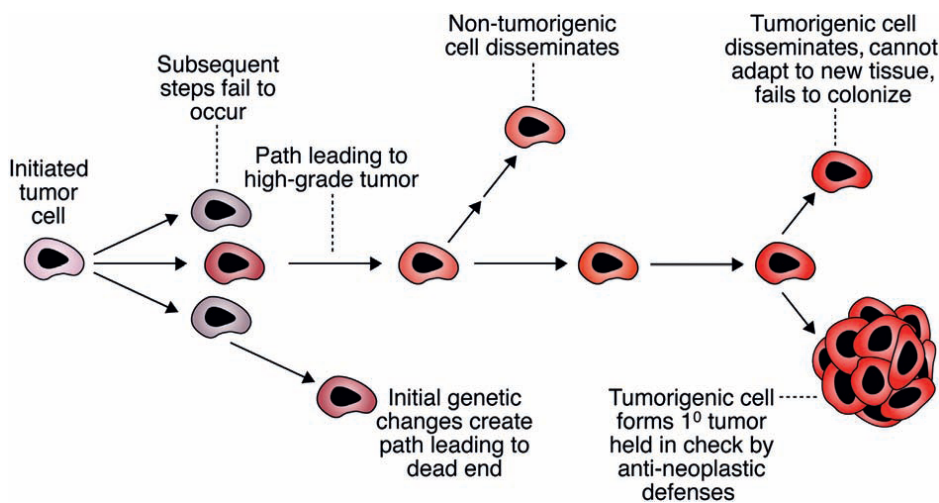


**Figure 7:** Cancerogenesis and Darwinian selection

(Weinberg 2008)

Using a mouse model for skin cancer, the mechanism of carcinogenesis was described for the first time in 1941 by Berenblum. Treatment of the mouse skin with either polycyclic aromatic hydrocarbons (PAH) or inflammation inducing croton-oil alone could not cause cancer. But together a unique treatment by PAH followed by continuous treatment with croton-oil was sufficient to support cancer development. The sequence of treatment in this experiment was crucial leading to the assumption that carcinogenesis follows a defined order which was described in a **three-stage model: initiation, promotion and progression**. The theory of carcinogenesis as a **multi-step process** also in humans is nowadays confirmed. The intermediate stages do not always automatically lead into advanced tumor growth but could also represent a dead end (see Figure 7). Alternatively, it has been proposed for a variety of epithelial cancer to skip the intermediate states and to enter highly malignant growth right after early

## Introduction

hyperplastic growth. In many tissues these intermediate stages reach from hyperplastic, dysplastic to adenomatous growth. All of them are benign precursors of carcinomas. In CRC the multi-stage tumorigenesis is best described (see chapter 1.5.4) (Weinberg 2007).

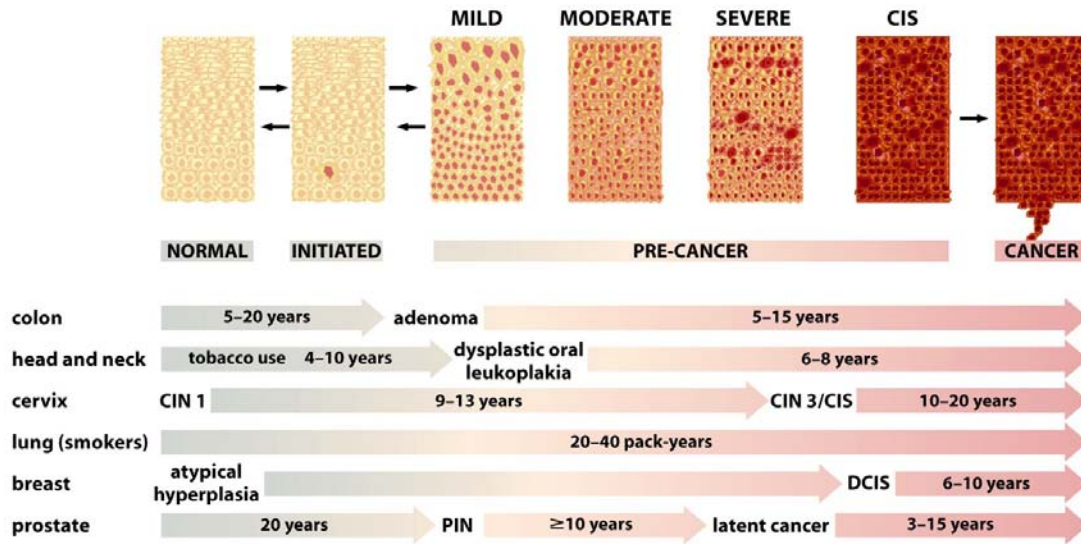


Figure 11-7 The Biology of Cancer (© Garland Science 2007)

**Figure 8:** Multi-step tumorigenesis in determined cancer types

(Weinberg 2007)

### 1.3.1 The three-stage model: Initiation – Promotion – Progression

#### 1.3.1.1 Tumor initiation

Initiation is the first step of cancerogenesis and occurs relatively infrequent and only in proliferating cells. It is a spontaneous process and induces an advantage for growth and survival in the affected cells. Actively proliferating cells are genetically altered which can be triggered by exogenous carcinogens or endogenous replication errors. Exogenous carcinogens initiating tumor development are:

- chemicals: e.g. aflatoxin, 3-methylcholanthrene in tobacco smoke, polycyclic aromatic hydrocarbons, asbestos, arsenic etc.
- physical impacts: e.g. UV-lights and X-rays

## Introduction

- biological components: e.g. hepatitis B and C viruses, *Helicobacter pylori*, human papilloma virus, etc.

DNA damage caused by carcinogens occurs quite often but is removed by DNA damage repair systems very efficiently (only 1 error per  $10^9$  nucleotides manifests in normal dividing cells). Genetic errors which are not eliminated by DNA-repair processes or apoptosis do manifest and mutations are transmitted to descendent cells. Initiation is an irreversible process. Genes which are affected by initiating mutation processes are often involved in cell cycle control, apoptosis or cell differentiation. In context with tumorigenesis these genes are also called oncogenes or tumor suppressor genes. So far more than 100 oncogenes and 30 tumor suppressor genes have been identified. In manifest tumors many of them are found to be mutated. Famous oncogenes are genes belonging to the Ras-family (see chapter 1.5.4.3) or myc. p53 is one of the best described tumor suppressor genes and mutated in 50% of human tumors. p53 plays a major role in proliferation control, cell cycle arrest and DNA-repair and induces apoptosis if the DNA cannot be repaired (see chapter 1.5.4.4) (Schulte-Hermann R. 2004). Another example for a tumor suppressor gene is APC, which, because of its important role in CRC, will be gone deeper into in chapter 1.5.4.2.

### 1.3.1.2 Tumor promotion

Promotion occurs over a long period (months or years) and in contrast to initiation and progression it is a reversible process. During promotion initiated cells are proliferating preferentially as compared to not initiated cells. The homeostasis between cell replication and apoptosis rate is shifted towards a higher proliferation rate. This can be caused by stimulation of cell growth or decrease in apoptosis compared to normal cells. Initiated cells are more sensitive to growth stimulatory effects. Therefore, in initiated cells the replication rate is induced more by tumor promoters than in normal cells. (Schulte-Hermann et al. 1992). Pre-neoplastic or malignant cells can be also quite sensitive to growth inhibiting conditions. In this case promoted cell growth is regressing, which is called “anti-promotion”. Reducing tumor promoting factors like hormones, tobacco or diet result in a higher apoptosis rate and shrinkage of pre-stage tumors (Bursch et al. 1991; Grasl-Kraupp et al. 1994; Mao et al. 1997).

## Introduction

Tumor promoting factors are from different exogenous or endogenous origins. Endogenous tumor promoting factors are for instance signal proteins reacting with growth receptors, kinases and transcription factors. Examples for such signal proteins are hormones like estrogens and androgens and growth factors like Transforming Growth Factor  $\alpha$  (TGF- $\alpha$ ) which promotes its own expression by an autocrine loop. Other promoting factors are prostaglandins. They are produced by cyclooxygenase (COX-1, COX-2) which are over-expressed in many human tumors. Apart from endogenous factors also nutrition and inflammation which results in a release of mitogenic signals are attributed to tumor promotion (Schulte-Hermann R. 2004).

### 1.3.1.3 Tumor progression

During tumor progression cellular signaling pathways are impaired by multiple mutations in various oncogenes and tumor suppressor genes. But how many different sequential changes are required to transform cells and tissues in human cancer? Mutations of oncogenes and tumor suppressor genes were found to be synergistic in many cases. For example cotransfection of mutated Ras and myc leads to the malignant phenotype in murine cells (Land et al. 1983). In human cells more than two oncogenic mutations are essential to transform cells into a malignant phenotype. To accumulate mutations genetic instability is required. In normal cells DNA-repair processes avoid accumulation of mutations. Therefore, in many tumors these repair genes are affected and inactivated. Consequently, mutations occur in a higher frequency than usual, not least because of the increased proliferation capacity discussed earlier. Due to the various mutations, cell signaling is dramatically changed which finally affects hundreds or thousands of different genes (Schulte-Hermann R. 2004). But also epigenetic changes like hyper- or hypomethylation of promotor regions lead to alterations in gene expression in tumor cells (Esteller et al. 2000). All these changes result in the manifestation of a malignant phenotype of cancer which has been defined in “*The hallmarks of cancer*” by Hanahan and Weinberg as described below.



## 1.4 The hallmarks of cancer

In 2000 Hanahan and Weinberg characterized six classical hallmarks of cancer: *self-sufficiency in growth signals*, *insensitivity to anti-growth signals*, *limitless replication*, *evasion of apoptosis*, *sustained angiogenesis* and *tissue invasion and metastasis*. These six capabilities are shared in common in most human tumors (Hanahan and Weinberg 2000).

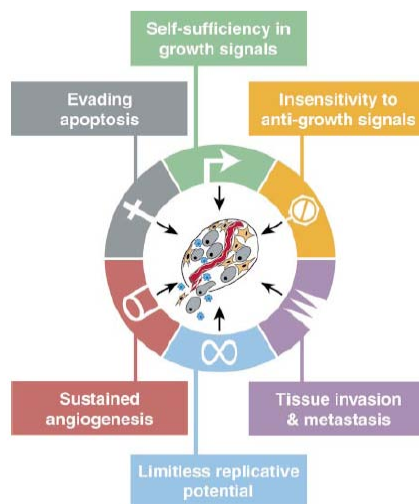


**Figure 9:** The hallmarks of cancer

(Hanahan and Weinberg 2000)

### 1.4.1 Self-sufficiency in growth signals

There are two key signal-transducing kinase pathways which can be activated by binding of growth signals to receptor tyrosine kinases (RTKs): the ERK-pathway (via Ras-Raf-MAPK) and the PI3K-pathway. Both of them activate mTOR which leads to a stimulation of cell proliferation. mTOR activity is also controlled by the availability of nutrients (glucose, amino acid and oxygen). In most cancers master regulators of these two pathways like K-Ras, H-Ras, N-Ras, B-Raf, the p110 (a PI3K subunit), and RTKs as well as their downstream effectors like Akt or PDK1 are mutated. Furthermore negative regulators can be affected by inactivating mutations (Shaw and Cantley 2006). But also the autonomous generation of growth signals by the tumor itself reduces its

## Introduction

dependence from the normal tissue microenvironment and alters homeostatic mechanisms (Hanahan and Weinberg 2000).

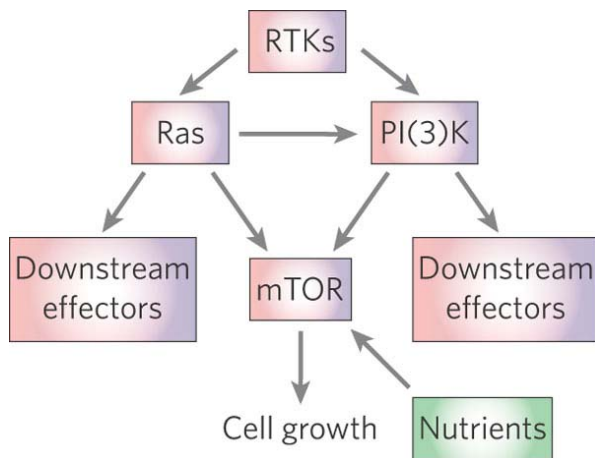


**Figure 10:** Two key signaling pathways to achieve self-sufficiency in growth signaling (Shaw and Cantley 2006)

### 1.4.2 Insensitivity to anti-growth signals

Anti-proliferative signals play an important role in cellular quiescence and tissue homeostasis. Like growth signals they act via a transmembrane cell surface receptor and start a signaling cascade. They block proliferation by forcing the cell into a quiescent state (G0) or entering a postmitotic state usually associated with differentiation. Retinoblastoma protein (pRb) for instance blocks proliferation and its signaling pathway, also governed by Transforming Growth Factor  $\beta$  (TGF- $\beta$ ). pRb is disrupted in a variety of ways in many cancer types (Hanahan and Weinberg 2000).

### 1.4.3 Evading apoptosis

Apoptosis is a process which is also called the programmed cell death. Intracellular apoptotic signals result in loss of cell membrane symmetry, cell attachment, cell shrinkage, nuclear fragmentation, chromatin condensation and chromosomal DNA fragmentation which finally lead to the death of the cell. Evading apoptosis is therefore a crucial step for cancer development but also for chemotherapy resistance. Consequently, cancer cells often manifest resistance against mitochondrial membrane

permeabilization which is an important step of apoptosis (Kroemer and Pouyssegur 2008).

### **1.4.4 Limitless replicative potential**

As observed in cell culture, normal human cells have the capacity for 60-70 doublings. Limitless replication requires growth signal autonomy, insensitivity to antigrowth signals and resistance to apoptosis. One of the most important regulators of apoptosis is p53. p53 reacts on DNA-damage, oxidative stress, and osmotic shock and initiates cell cycle arrest, DNA repair, and apoptosis. To achieve limitless replicative potential, p53 is mutated or lost in more than 50% of the human tumors. But also the induction of telomerase which prevents the chromosomal ends from shortening during replication results in an unlimited replicative potential of the cell (Hanahan and Weinberg 2000).

### **1.4.5 Sustained angiogenesis**

Angiogenesis is important to supply required nutrients to the tumor. It also serves to transform the tumor into a malignant state and metastasize, where single cells break away from the tumor, enter the blood vessels and are carried to another part of the body via blood stream where they can implant and grow to a secondary tumor. Stimulators of angiogenesis like VEGF and FGF are often up-regulated in tumors (Hanahan and Weinberg 2000).

### **1.4.6 Tissue invasion and metastasis**

E-cadherin plays an essential role in the maintenance of intercellular contacts within epithelia. Loss or inactivated E-cadherin goes in common with epithelial mesenchymal transition (EMT), a process which leads to metastasis. Development of metastasis causes 90% of human cancer deaths (Weinberg 2007).

### 1.4.7 Additional hallmarks

There are other common features of malignant cells like an induced anabolic metabolism, avoidance of immune response and several stress phenotypes (Kroemer and Pouyssegur 2008). Kroemer and Pouyssegur added 2008 the “*Evasion of immune surveillance*” as a seventh hallmark of cancer. 2009 the hallmarks of Hanahan and Weinberg were expanded by Lou et. al. by five additional hallmarks, the stress phenotypes of cancer: *DNA damage/replication stress*, *proteotoxic stress*, *mitotic stress*, *metabolic stress* and *oxidative stress*.

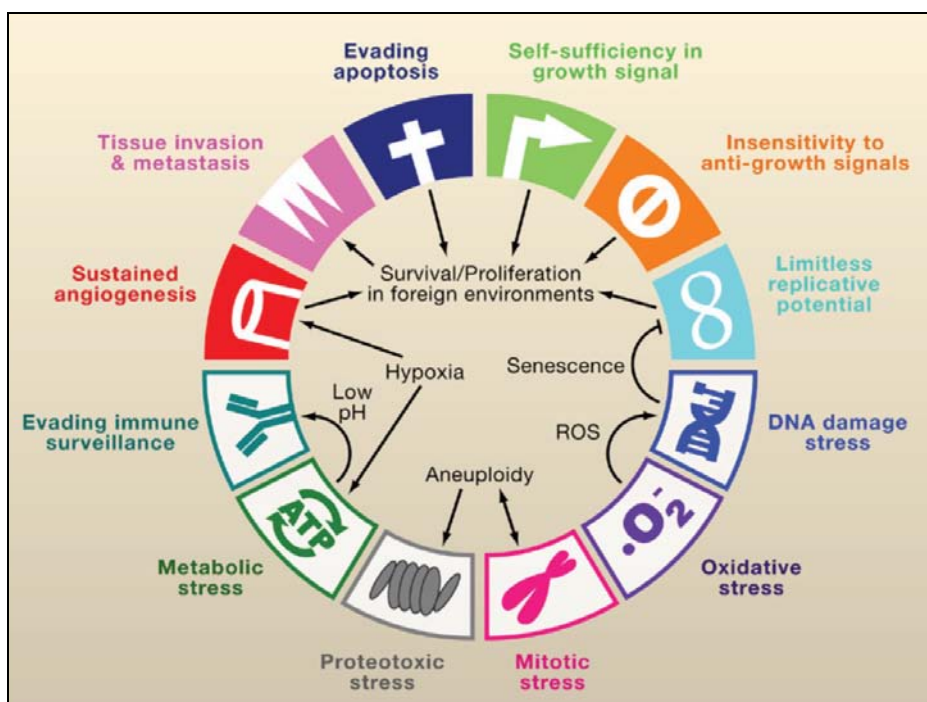


**Figure 11:** The new hallmarks of cancer

(Luo et al. 2009)

#### 1.4.7.1 Evasion of Immunosurveillance

Cytotoxic T-lymphocytes and natural killer cells act in an anti-tumor response and are frequently inhibited by the microenvironment of tumor cells. Furthermore, tumor cells attract inflammatory cells which participate in tumor progression (Kroemer and Pouyssegur 2008).

### **1.4.7.2 DNA damage and DNA replication stress**

Usually, the genome of cancer cells is altered by the accumulation of point mutations, deletions, complex chromosomal rearrangements, and aneuploidy. In normal cells DNA damage leads to a proliferation stop and induces DNA damage stress response pathways and DNA repair programs or apoptosis. Cancer cells have overcome these anti-proliferative effects of DNA damage and continue to replicate in the presence of DNA damage (Luo et al. 2009).

### **1.4.7.3 Proteotoxic stress**

Aneuploidy and gene copy-number changes result in an increase and decrease of transcript levels of certain genes. This leads in consequence to a stoichiometric imbalance of protein complex subunits which increases an amount of toxic unfold protein aggregates in the cell. Thus, protein folding and degradation machineries are stressed to overcome this imbalance which results in a proteotoxic stress for the cell. Heat shock response pathway which promotes the proper folding or/and degradation of proteins are therefore frequently activated in tumor cells (Luo et al. 2009).

### **1.4.7.4 Mitotic stress**

During mitosis in many tumors the chromosomes are not segregated properly which leads to a certain kind of chromosome instability phenotype. This phenotype results from defective pathways, from defective mitotic proteins which are responsible for chromosome segregation and from defects in the spindle assembly checkpoint which coordinates the alignment of the chromosomes to the spindle. But also double strand breaks and chromosomal instability lead to mitotic stress (Luo et al. 2009).

### **1.4.7.5 Metabolic stress**

Normal cells receive their energy from mitochondrial oxidative phosphorylation. Tumor cells instead predominantly produce energy glycolysis which is less efficient and leads to the excretion of large amount of lactic acid (Warburg 1956). This has been referred to

## Introduction

as the Warburg effect which helps the tumor to adapt to low oxygen environment. The excretion of lactic acid leads to an acidification of the surrounding environment which helps the tumor to invade and to suppress the immune surveillance. (Kroemer and Pouyssegur 2008; Luo et al. 2009).

### **1.4.7.6 Oxidative Stress**

Oxidative stress is induced by reactive oxygen species (ROS) which due to their high reactivity contribute to DNA damage. In cancer cells ROS are typically generated more than in normal cells. ROS can also promote the activity of the transcription factor HIF-1 (Hypoxia-Inducible Factor) by hypoxia which leads to glycolytic switch and angiogenesis in the tumor (Luo et al. 2009).

### **1.4.7.7 Inflammatory microenvironment**

2009 Colotta and his group defined another hallmark: the *inflammatory microenvironment*. There is a relation between inflammation and cancer. As studies have revealed, chronic inflammation advantages the development of different cancer types. But there can also be found an inflammatory environment to most neoplastic tissues with no relation to obvious inflammatory processes. The cancer-related inflammation is linked to infiltration of white blood cells like tumor-associated macrophages, but also with polypeptide messengers of inflammation like cytokines such as tumor necrosis factor (TNF), interleukin (IL-)1 and IL-6, chemokines such as CCL2 and CXCL8 as well as tissue remodeling and angiogenesis.

There are two pathways linking cancer and inflammation: intrinsic and extrinsic. The intrinsic pathway shows expression of inflammation-related program due to genetic events in the course of cancer development which leads to an inflammatory microenvironment. In contrast the extrinsic pathway describes that cancer development is facilitated by inflammation via infection (e.g. *Helicobacter pylori* for gastric cancer, papilloma virus and hepatitis virus for cervical and liver carcinoma), autoimmune disease (e.g. inflammatory bowel disease for colon cancer), and inflammatory conditions of uncertain origin (e.g. prostatitis for prostate cancer) (Colotta et al. 2009).

## **1.5 Colorectal Cancer (CRC)**

### **1.5.1 Anatomy of the colon**

The lower gastrointestinal tract is divided into two parts: the small intestine and the large intestine. The large intestine consists of the cecum, colon, rectum, and anal canal. The human large intestine measures about 1,5m. In contrast to the small intestine the large intestine does not play a major role in absorbing food but is important for absorption of water, potassium and some fat soluble vitamins from the solid wastes before elimination from the body. The colon also harbors a bacterial flora which ferments unabsorbed material.

The human colon consists of four different sections called the ascending colon, the transverse colon, the descending colon and the sigmoid colon. The 25cm long ascending colon is located at the right side of the abdomen behind the peritoneum (retroperitoneal) and connects the cecum with the transverse colon at the hepatic flexure. The transverse colon is encased in the peritoneum and consequently mobile and leads to the splenic flexure into the descending colon. In the descending colon food is stored until it is emptied into the rectum. The sigmoid colon is located between the descending colon and the rectum and is named after its S-shaped morphology. The colon is further characterized by multiple haustra which are small pouches caused by sacculations and gives the colon a segmented appearance.

## Introduction

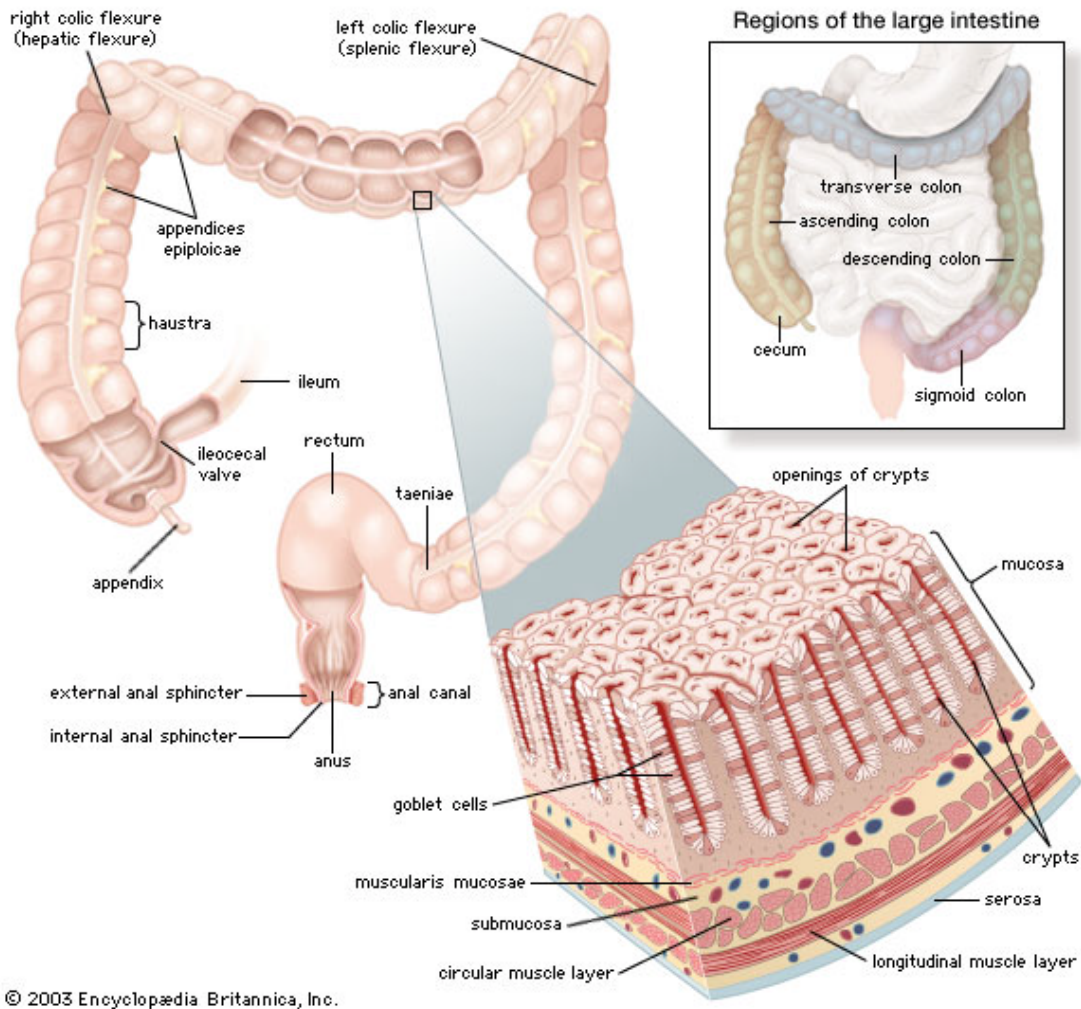


**Figure 12:** Anatomy of the colon

(Picture from website: <http://media.web.britannica.com/eb-media/19/74319-004-68DBB5D6.jpg>; 30.6.11)

### 1.5.2 Histology of the colon tissue

The intestine is structured in five layers. The first layer which faces the interior cavity (lumen) of the gastrointestinal tract is the mucosa, a one-cell epithelial layer which absorbs nutrients, fat and proteins. The second layer underlying these epithelia is a basement membrane which is called muscularis mucosa. It forms part of the extracellular matrix and anchors the epithelial cells. Furthermore, it presents a barrier between the mucosa and the submucosa, the third layer. The submucosa consists of mesenchymal cells which are large fibroblasts and is also rich in vessels and immune cells. The fourth layer is a thick layer of smooth muscle and called the muscularis propria



## Introduction

which is responsible for moving the content of the colonic lumen. The fifth and outermost layer is the serosa.

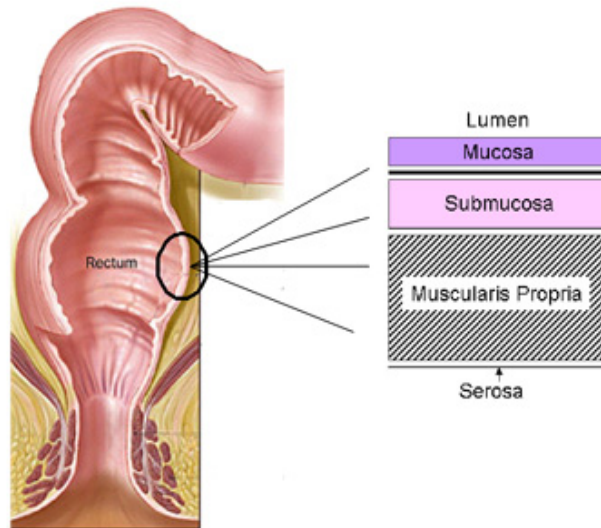


**Figure 13:** The five layers of the intestine

(Picture from website: [http://www.hopkinscoloncancercenter.org/CMS/CMS\\_Page.aspx?SS=&CurrentUDV=59&CMS\\_Page\\_ID=0B34E9BE-5DE6-4CB4-B387-4158CC924084](http://www.hopkinscoloncancercenter.org/CMS/CMS_Page.aspx?SS=&CurrentUDV=59&CMS_Page_ID=0B34E9BE-5DE6-4CB4-B387-4158CC924084); 18.6.11)

The epithelium of the gut is a rapidly self-renewing tissue which is ordered into numerous villis and crypts. Stem cells are sitting near the bottom of the crypts. In the crypts the cells are proliferating resulting in precursor cells whereas at the villis cells are differentiated. Transient amplifying cells arrest their cell cycle and differentiate once they reach the crypt-villus-junction. As soon as they reach the tip of the villis the differentiated cells undergo apoptosis. This results in a contiguous sheet of cells which is perpetually moving upwards. In the large intestine there are abundant goblet cells which secret mucins that together with water form mucus. A loss of the proliferation control in the crypt is the cause for colorectal cancer.

## Introduction

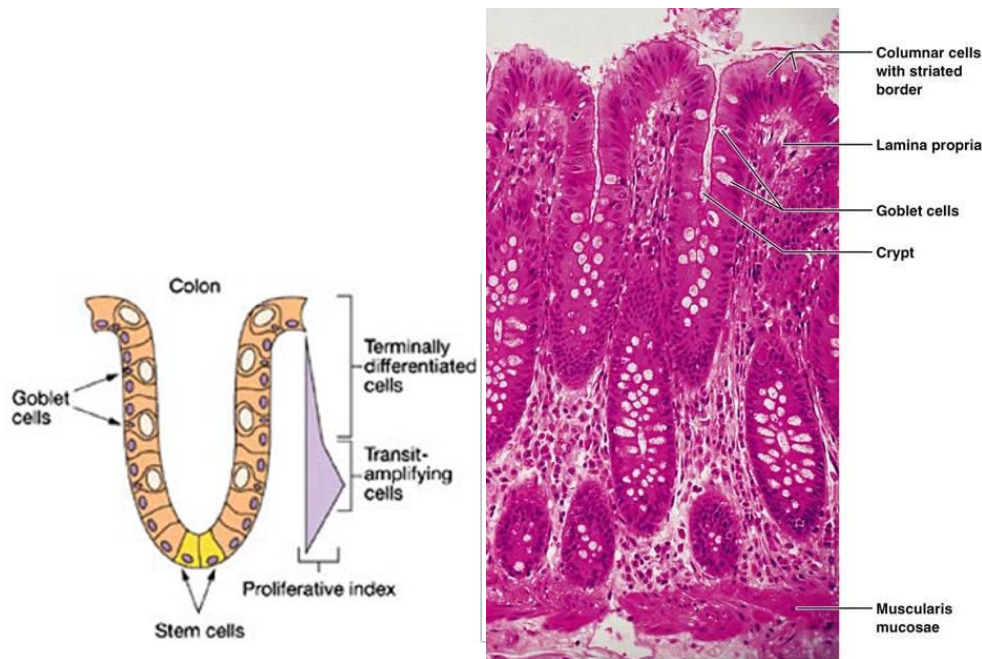


**Figure 14:** Histology of colon tissue

The left panel shows a schematic picture of a colonic crypt (Picture from website: <http://img.medscape.com/fullsize/migrated/532/504/gastro532504.fig1.gif>; 30.6.11).

The right panel shows a histological staining of a colonic crypt (picture from website: <http://classes.midlandstech.com/carterp/Courses/bio211/chap23/Slide44.JPG>; 30.6.11)

### 1.5.3 Development of colorectal cancer

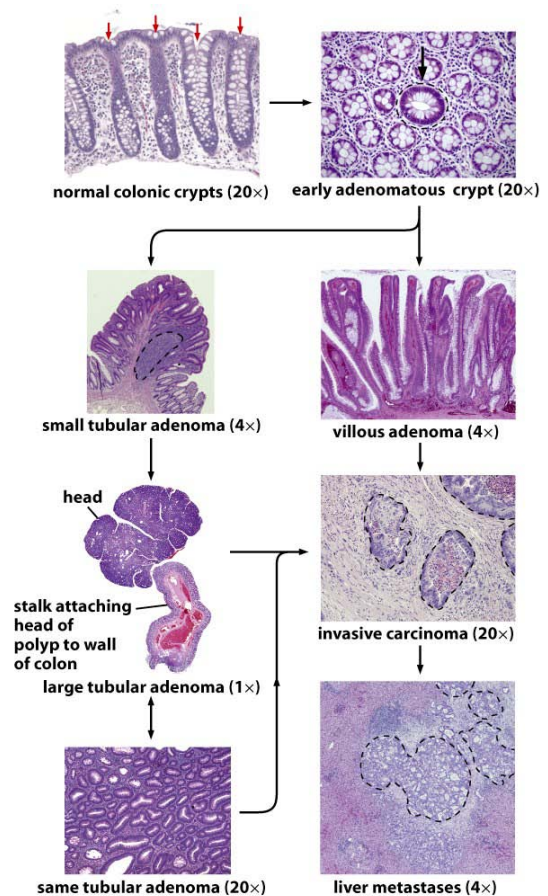
Most pathological changes which lead to colon carcinomas occur in the epithelium. Colon carcinoma develops during a multi-step tumorigenesis beginning with hyperplastic, dysplastic crypts and adenomatous growth leading to cancerous growth. Cells growing hyperplastically exhibit almost normal histology and appearance. Hyperplastic areas however display an unusual high cell division rate which leads to a thicker-than-normal epithelium. The well-ordered epithelial cell layer is now altered and also the morphology of the individual cells changes subtly and later progressively, which is called dysplasia. Larger areas of dysplastic cells growing more deviant are called polyp or adenoma. Polyps can be directly attached to the colonic wall or can be tethered by a stalk and share the morphology of a mushroom. As long as they do not break through the basement membrane, polyps are referred to as benign and can be easily removed by colonoscopy. Usually, CRC begins with the formation of a benign polyp. With increasing size of the adenomatous polyp the risk for development into

## Introduction

cancer is elevated. Malignant adenomas are called adenocarcinomas and begin to break through the basement membrane and invade all colonic tissue layers. In advanced stages cancerous cells detach and metastasize into the circulatory system, invading other organs of the body like liver and lungs. 95% of colorectal cancer grows directly out from adenomatous polyps (Weinberg 2007).

**Figure 15:** Development of colorectal cancer

Different stages of colorectal cancer development are presented in histological sections (Weinberg 2007).



Abnormal cell growth and inflammation can cause dysplasia which presents another pre-cancerous condition for CRC. Chronic inflammation of the colon, as it occurs in patients suffering from Morbus Crohn, exposes them to a higher risk for developing CRC.

## 1.5.4 Molecular biology of colorectal cancer

### 1.5.4.1 Vogelstein-model

1988 Vogelstein et. al. presented a new model which explained the molecular mechanism behind the CRC development. Searching for genetic alterations they found a loss of heterozygosity (LOH) in the long arm of chromosome 5 in many early adenomas. LOH is the loss of the normal function of one allele (in context of cancerogenesis of a tumor suppressor gene) by e.g. deletion or point mutation in which the other allele has already been inactivated. The region on chromosome 5 affected by LOH is carrying the gene Adenomatous Polyposis Coli (APC) which is an important tumor suppressor. In slightly larger adenomas about 50% additionally display a mutated K-ras oncogene. A high rate of LOH on the long arm of chromosome 18 was found in even larger adenomas. Half of the carcinomas showed in addition a LOH on the short arm of chromosome 17 which harbors p53. These observations led to the assumption that genetic changes, which were acquired by an epithelial cell during the process of cancerogenesis, involved the activation of one proto-oncogen and the inactivation of at least three tumor suppressor genes. However, alterations of the APC- $\beta$ -catenin pathway usually come first whereas the other genetic changes do not have to happen in a determined order (Vogelstein et al. 1988; Weinberg 2007).

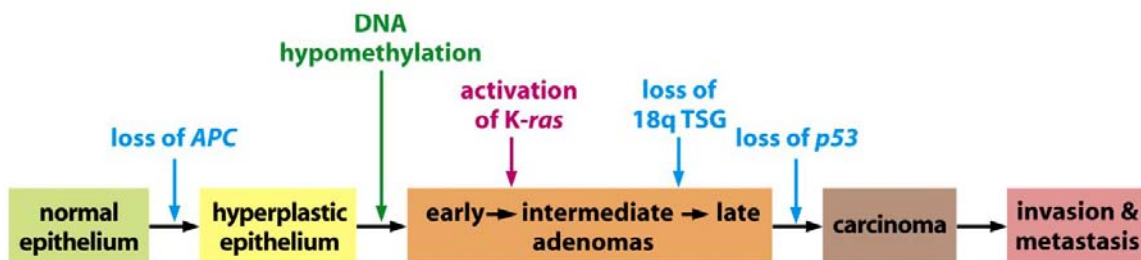


Figure 11-10 The Biology of Cancer (© Garland Science 2007)

**Figure 16:** Carcinogenesis of colorectal cancer: Vogelstein-model

(Weinberg 2007)

### 1.5.4.2 APC and the Wnt-pathway

#### 1.5.4.2.1 *The canonical Wnt/ $\beta$ -catenin cascade*

The discovery of Wnt is traced back to a wingless *Drosophila* mutant and a related gene termed *int-1* which was found up-regulated by mouse mammary tumor virus in mouse (Nusse et al. 1991). The human Wnt-family consists of 19 secreted glycoproteins that are involved in regulation of cell proliferation, cell morphology, cell motility and cell fate (Dale 1998; Katoh 2006a). Wnt proteins are tethered tightly to the extracellular matrix and bind the extracellular domain of transmembrane frizzled receptor. In addition to frizzled, Wnt also binds to a co-receptor protein, the LDL-receptor-related protein (LRP) (Alberts 2002).

$\beta$ -catenin is associated with the transmembrane adhesion protein cadherin but also located in the cytoplasm. The  $\beta$ -catenin-cadherin-complex is located at cell-cell adherent junctions where  $\beta$ -catenin helps to link cadherin to the actin cytoskeleton. In the absence of Wnt-signaling free and unbound  $\beta$ -catenin is degraded rapidly by a complex which consists of axin, Glycogen Synthase Kinase 3 (GSK3), Casein Kinase 1 (CK1) and APC. Axin acts as the scaffold of this complex because it directly interacts with all components of this complex. Unbound  $\beta$ -catenin is first phosphorylated by CK1 and GSK3 at highly conserved Serine/Threonin residues, ubiquitinated and finally degraded by proteasomes (Alberts 2002).

As soon as the canonical Wnt-pathway is activated by Wnt binding to frizzled and LRP, Dishellved is recruited to the plasma membrane where it is activated and inhibits the axin-GSK3-APC-complex.  $\beta$ -catenin is therefore not proteolytically degraded and can now enter the nucleus and interact with Lymphoid Enhancer Factor/T-Cell Factor (LEF/TCF) transcription factor family. In the absence of  $\beta$ -catenin TCF acts as a transcriptional repressor by forming a complex with the protein Groucho.  $\beta$ -catenin displaces Groucho by interacting with TCF and converts it into an activator. Many TCF target genes have been identified in diverse biological systems including genes which are also involved in tumor progression. Examples for Wnt-controlled target genes are *c-myc*, *cyclin D*, *survivin*, *c-met*, *VEGF*, proteinases like *MMPs*, *CD44* but also *FGF18* and *FGF20* (Behrens and Lustig 2004; Clevers 2006).

## Introduction

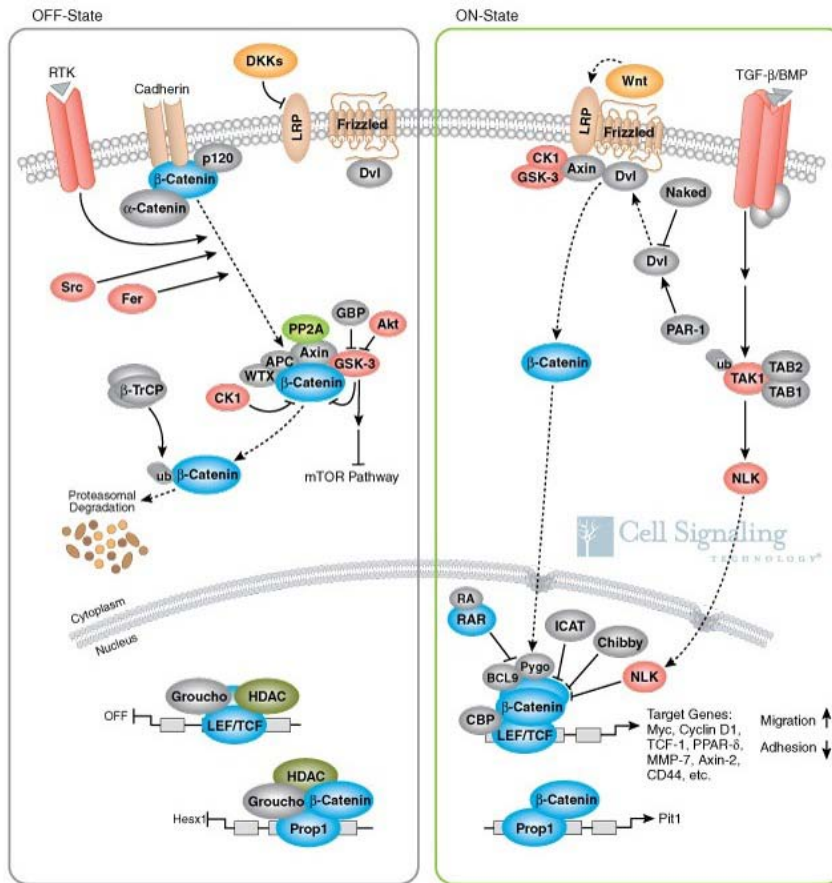


**Figure 17:** Wnt-signaling pathway

(Picture from website: [http://www.cstj.co.jp/reference/pathway/images/Wnt\\_beta\\_Catenin.jpg](http://www.cstj.co.jp/reference/pathway/images/Wnt_beta_Catenin.jpg); 30.6.11)

### 1.5.4.2.2 The role of APC and $\beta$ -catenin in colorectal cancer

The Wnt cascade is implicated in controlling cell fate along the crypt-villus axis. At the bottom of the crypts stem cells are located. Their progenies are moving upwards and out of the crypt where they form the epithelial lining of the gut. Stromal cells near the bottom of the crypt release Wnt proteins which affect the enterocytes at the bottom of the crypt. In these enterocytes intracellular  $\beta$ -catenin level is high, giving them a stem cell-like character. This leads to increased proliferation and increased differentiation of these cells based on the interaction with TCF/LEF transcription factors. By moving upwards the crypt towards the lumen, cells lose the stimulation via Wnt-signaling and proliferation is turned off due to  $\beta$ -catenin degradation. Cells are now differentiating and after 4 days they enter apoptosis (Weinberg 2007). Inhibition of Wnt-signaling results in the complete loss of crypts in adult mice which identifies Wnt as an essential

## Introduction

mitogen for crypt progenitor cells. On the other hand, over-activation of Wnt-signaling leads to a massive hyperproliferation of intestinal crypts (Clevers 2006).

APC plays a crucial role in the early development of CRC. The APC gene is located on the long arm of chromosome 5 (5q21) and is mutated in 35-80% of all sporadic carcinomas and 29-63% of all sporadic adenomas (Powell et al. 1992). APC negatively controls  $\beta$ -catenin level in the cytosol and is essential for its degradation. APC is not expressed in the colonic crypts but its level increases with the upwards migrating cells out of the crypts. Mutated APC leads to an accumulation of  $\beta$ -catenin in the cells even without Wnt-signaling. Cells are proliferating but do not differentiate while migrating upwards the crypt. Finally, they are unable to migrate further and due to the increased proliferation they develop an adenomatous polyp in the crypt (Weinberg 2007).

Even in colon carcinomas carrying the wild-type APC allele, intracellular level of  $\beta$ -catenin was affected by epigenetic silencing of the APC promoter region or by point mutations of the  $\beta$ -catenin gene. Patients with point mutations in  $\beta$ -catenin, which affect its degradation or mutated axin2, display also a predisposition to CRC (Weinberg 2007).



## Introduction

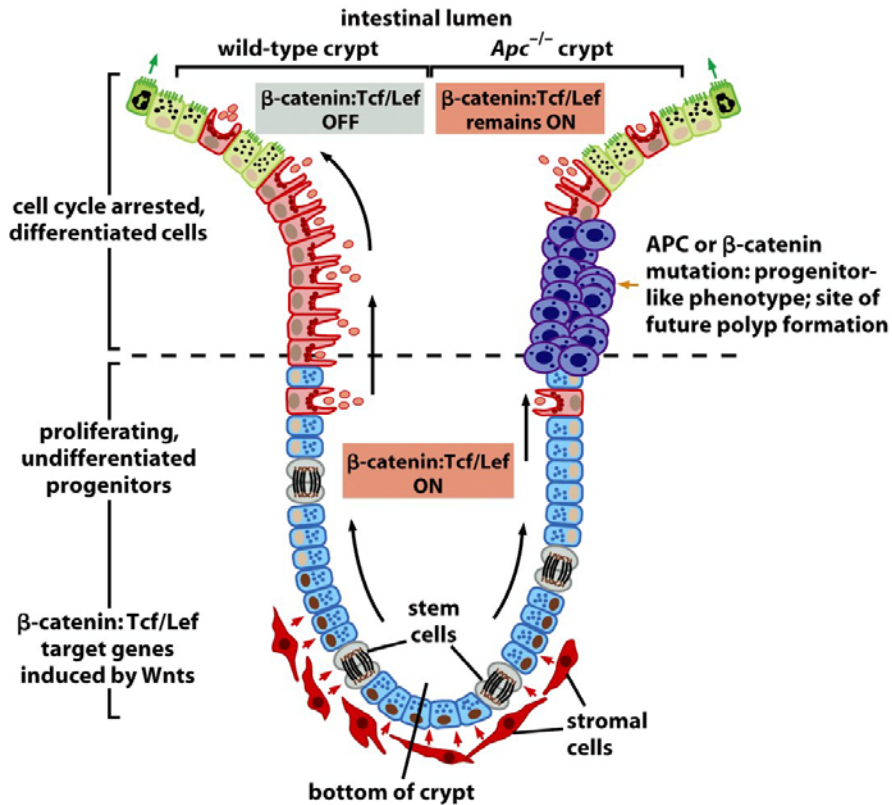


Figure 7-24a The Biology of Cancer (© Garland Science 2007)

**Figure 18:** APC/ $\beta$ -catenin and the biology of colonic crypts

(Weinberg 2007)

A germline APC mutation is the genetic cause for a hereditary cancer syndrome named Familial Adenomatous Polyposis (FAP). One defective APC allele results in subtle shifts in growth and differentiation control. It also destabilizes the genome so that the normal APC allele is lost causing development of benign polyps. People suffering from FAP develop hundreds of adenomatous polyps in the colon which are themselves not malignant but are susceptible to develop into carcinoma. FAP is relatively rare and is identified in less than 1% of all colon cancers in the western population.



## Introduction



Figure 7-22 The Biology of Cancer (© Garland Science 2007)

### **Figure 19:** Familial adenomatous polyposis

On the left picture a section of the colon of a FAP patient is presented whereas on the right picture the colon of a healthy person is shown. The wall of the colon of a FAP patient is carpeted with adenomatous polyps (Weinberg 2007) .

Aberrant Wnt-signaling might also play a role in other cancer variants. APC mutations are also present in 76% of sporadic gastric adenomas. Mutations in  $\beta$ -catenin were found in 40% of endometrial carcinomas, in ovarian carcinomas, in up to 70% of hepatoblastomas, 25% of hepatocellular carcinomas, 61% of sporadic anaplastic thyroid carcinomas, and in Wilms tumor (common childhood renal malignancy). In 30% of prostate cancer cases as well as in medulloblastomas Wnt-signaling is involved. High levels of  $\beta$ -catenin but not mutated  $\beta$ -catenin was also found in melanomas and osteosarcomas (Behrens and Lustig 2004).

Mutation of APC has also been found to increase chromosomal instability. This derives from the fact that APC is also localized to components of the microtubule array and consequently also involved in the formation of the mitotic spindle. Loss of APC results in an inappropriate segregation of chromosomes during mitosis, which alters the number of critical growth-promoting and growth-inhibiting genes in the progeny cells (Weinberg 2007).

### **1.5.4.3 K-ras, a member of the Ras-family**

The members of the Ras-family are small GTPase involved in cellular signaling transduction affecting cell growth, differentiation and survival. The name Ras is traced back to **rat sarcoma** because the Ras-gene was first identified in cancer causing viruses in rat sarcoma. There are three Ras genes designed: N-Ras, K-Ras and H-Ras. About

## Introduction

30% of human tumors have a hyperactive Ras mutation. Ras is anchored to the cell membrane at the cytoplasmic face and acts in two conformations: active when Guanosine Tri-Phosphate (GTP) is bound and inactive when Guanosine Di-Phosphate (GDP) is bound. Ras activation is controlled by two kinds of proteins called Guanine nucleotide Exchange Factors (GEFs) and GTPase-Activating Proteins (GAPs). GEFs stimulate the dissociation of GDP and the uptake of GTP from the cytosol. GAPs increase the hydrolysis of GTP and therefore inactivate Ras. Hyper-activating mutations of Ras inhibit the interaction with GAP and leave Ras permanently active (Alberts 2002).

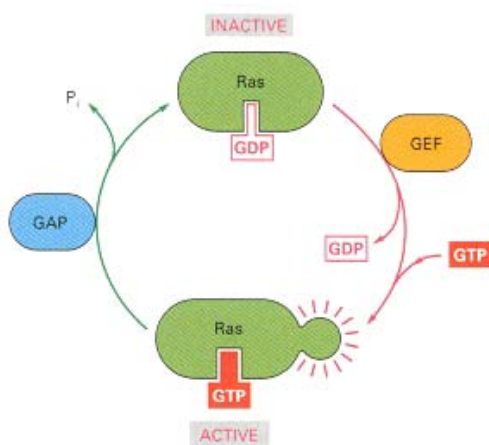


**Figure 20:** The regulation of Ras activity

(Alberts 2002)

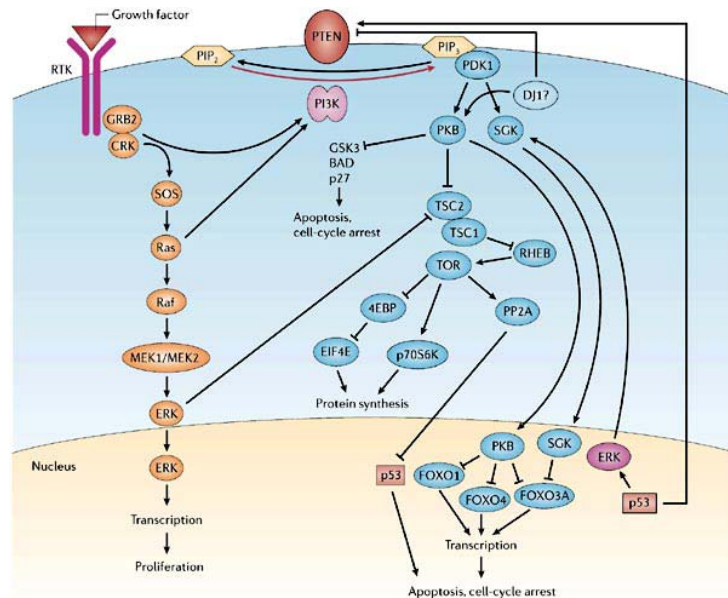
### 1.5.4.3.1 Ras signaling: the MAP-kinase and PI3-kinase pathway

Receptor tyrosine kinases activate Ras by activating GEFs or inhibiting GAPs via Grb2 protein. Grb2 protein binds through a SH2 domain specific phosphotyrosines on activated receptor tyrosine kinases and through a SH3 domain the proline-rich motif on a special GEF called Sos. Activated Ras itself activates various other signaling proteins.

One of the downstream signaling pathways activated by Ras is the Mitogen-Activated Protein kinase (MAP-kinase) pathway. Ras activates Raf which again phosphorylates MEK. MEK finally activates the MAP-kinase ERK which phosphorylates gene regulatory proteins in the nucleus and other protein kinases and stimulates cell division.

## Introduction

Another pathway activated by Ras is the Phosphatidylinositol 3-kinase (PI3-kinase) pathway which is involved in the control of cell growth and cell survival. The PI3-kinase can be activated by receptor tyrosine kinases as well as other types of cell-surface receptors directly or G-protein-linked e.g. by Ras. PI3-kinase phosphorylates Inositol Phospholipids (PI) generating PI(3,4)P<sub>2</sub> or PI(3,4,5)P<sub>3</sub>. The phosphorylated PI serve as docking sites for many intracellular signaling proteins, amongst them PDK1 which in turn activates the Protein Kinase B (PKB), also called Akt. Once activated, Akt interacts with a variety of proteins for example BAD, a protein which encourages cells to undergo apoptosis. Akt further activates p70S6 kinase via mTor which phosphorylates and activates the S6 subunit of ribosomes and consequently increases translation (Alberts 2002).



Copyright © 2006 Nature Publishing Group  
Nature Reviews | Cancer

**Figure 21:** Ras signaling: MAP-kinase and PI3-kinase pathway

(Cully et al. 2006)

### 1.5.4.3.2 The role of K-Ras in colorectal cancer

K-Ras is a proto-oncogene and is found mutated in 10% of adenomas smaller than 1cm, 40-58% of larger adenomas and 47-60% of colorectal carcinomas (Vogelstein et al. 1988). A single point mutation (mostly in codon 12) resulting in the substitution of one

## Introduction

amino acid leads to a growth factor independent persisting stimulation of K-Ras. Malignant CRC cell lines carrying a K-Ras mutation show typical features of transformed cells like the ability to grow anchorage independent. K-Ras mutation itself leads to self-limiting hyperplastic lesions in colorectal cells. K-Ras mutation occurring after a previous APC mutation promotes cancerogenesis (Weitz J. 2004).

### **1.5.4.4 P53**

p53 is one of the most important tumor suppressor genes mutated or deleted in more than 50% of various human tumor types. As the “guardian of the genome” p53 plays a crucial role in the regulation of the cell cycle. The key role for p53 is to detect genomic stress and to decide whether DNA is repaired or the cell undergoes apoptosis. MDM2 regulates p53 by recruiting it to the cytoplasm and inducing its degradation by ubiquitination. p53 itself stimulates its own degradation by stimulating the expression of MDM2 (Alberts 2002).

Physical or chemical agents causing DNA damage induce p53-dependent physiological response. Gamma irradiation activates ATM which further activates p53 by phosphorylation. Phosphorylated p53 modifies the protein and inhibits the binding to MDM2. ATM also activates ABL which phosphorylates MDM2 and neutralizes its function as p53 inhibitor. Consequently, p53 is accumulated in the nucleus which arrests the cell cycle in G1. DNA repairing enzymes are activated and repair the DNA damage. Alternatively, instead of arresting the cell cycle p53 can induce apoptosis of the genomic stressed cell. But also other cellular disturbances like oncogene activation, hypoxia, or abnormal cellular ribonucleotide concentrations lead to the accumulation of p53 (Soussi 2000).

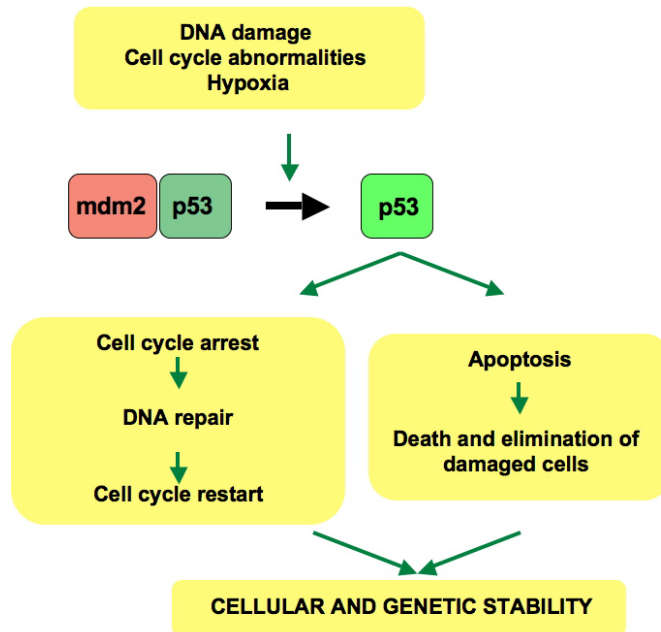


**Figure 22:** Pathways of p53

(Picture from website [http://en.wikipedia.org/wiki/File:P53\\_pathways.jpg](http://en.wikipedia.org/wiki/File:P53_pathways.jpg), 02.07.11)

Mutations of p53 are often accompanied by LOH and in most cases are caused by point mutations in four of the five evolutionary conserved domains of the protein. More than 90% of mutations in p53 affect the DNA-binding affinity of the protein. Cells harboring mutated p53 are less stable by accumulating mutations and give rise to malignant potential. Mutations of p53 are rare in polyps but common in carcinomas, suggesting that they occur later during colon cancerogenesis. They are found in 50-60% of sporadic CRCs and occur preferentially during the transition of adenomas to invasive adenocarcinomas. Germline mutations of p53 lead to the Li-Fraumeni syndrome which predisposes affected members to cancer (Bartram 2004).

#### 1.5.4.5 LOH at chromosome 18: Smad2 and Smad4

In 60% of human CRCs the long arm of chromosome 18 is affected by LOH. The identity of genes in this region contributing tumorigenesis is not completely clear so far. One candidate gene is DPC4/MADH4 which expresses Smad4, a protein involved in the transition of growth-inhibitory signals from TGF- $\beta$  receptor to the cell nucleus. However, this gene is only mutated in fewer than 15% of colon cancers. Another

## Introduction

protein affected by LOH of chromosome 18 is Smad2 which is inactivated even less frequently than Smad4 (Weinberg 2007). Smad4 and Smad2 are considered as tumor suppressors regulating the TGF- $\beta$  transduction pathway. TGF- $\beta$  binds to a single-pass transmembrane serine/threonine kinase receptor which is then activated and binds intracellular Smad2 and Smad3 or Smad1, Smad5 and Smad8. Phosphorylation of these Smads leads to dissociation and binding to Smad4 with either one of the Smads. This complex moves into the nucleus where it associates with other transcription factors and activates specific target genes (Alberts 2002).

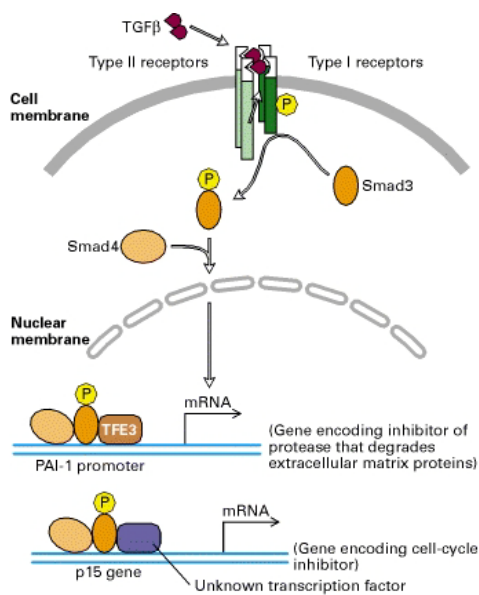


**Figure 23:** TGF- $\beta$ /Smad4 signaling

(H. Lodish 2000)

Target genes affect a diverse range of biological activities like cell cycle, differentiation, apoptosis, gastrulation and embryonic development. Furthermore, TGF- $\beta$ -Smad signaling is implicated in epithelial growth and extracellular matrix proteins which are important for tumor development and metastasis.

### 1.5.5 Tumor staging in colorectal cancer

Survival rates of colon cancer are higher if the disease is diagnosed at an early localized stage than in patients with advanced tumors. Therefore, tumor staging is important for

## Introduction

therapy administration, as a prognostic factor, for statistical evaluation of therapy, for clinical and international information exchange and for cancer research. There have been established some systems for cancer classification and the first one was founded in 1932 by Dr. Cuthbert Dukes, called the *Dukes classification*. This classification has been modified and complemented and today is known as the *Astler-Coller-version* of the Dukes classification (MAC) (Schölmerich J. 2005).

Today the TNM-classification of malignant tumors for international clinical and pathological staging is used. The TNM-classification was developed 1943-1952 when Pierre Denoix tried to characterize solid tumor stages using the size and extension of the tumor, lymphatic involvement and presence of metastasis as parameters. Since that time the TNM-classification has been adapted and modified various times.

**T:** describes size of primary tumor and invasion into nearby tissue (AJCC 26.6.2011)

- TX: primary tumor cannot be assessed
- T0: no evidence of primary tumor
- Tis: carcinoma in situ: intraepithelial or invasion of lamina propria
- T1: tumor invades submucosa
- T2: tumor invades muscularis propria
- T3: tumor invades through muscularis propria into pericolorectal tissue
- T4a: tumor penetrates to the surface of the visceral peritoneum
- T4b: tumor directly invades or is adherent to other organs or structures

**N:** describes regional lymph node involvement (AJCC 26.6.2011)

- NX: regional lymph node cannot be assessed
- N0: no regional lymph node metastasis
- N1: metastasis in 1-3 regional lymph nodes
- N1a: metastasis in 1 regional lymph node
- N1b: metastasis in 1-3 regional lymph nodes
- N1c: Tumor deposit(s) in the subserosa, mesentery, or non-peritonealized pericolic or perirectal tissues without regional nodal metastasis
- N2: Metastasis in 4 or more regional lymph nodes
- N2a: Metastasis in 4–6 regional lymph nodes
- N2b: Metastasis in 7 or more regional lymph nodes

## Introduction

**M:** describes the presence of distant metastasis (AJCC 26.6.2011)

- M0: no distant metastasis
- M1: distant metastasis
- M1a: metastasis confined to one organ or site (for example, liver, lung, ovary, non-regional node)
- M1b: metastases in more than one organ/site or the peritoneum

Tumor stage is stated as I-IV and is determined by the TNM-classification. Most stage I tumors are curable and most stage IV tumors are inoperable.

ANATOMIC STAGE/PROGNOSTIC GROUPS					
Stage	T	N	M	Dukes*	MAC*
0	Tis	N0	M0	—	—
I	T1	N0	M0	A	A
	T2	N0	M0	A	B1
IIA	T3	N0	M0	B	B2
IIB	T4a	N0	M0	B	B2
IIC	T4b	N0	M0	B	B3
IIIA	T1–T2	N1/N1c	M0	C	C1
	T1	N2a	M0	C	C1
IIIB	T3–T4a	N1/N1c	M0	C	C2
	T2–T3	N2a	M0	C	C1/C2
	T1–T2	N2b	M0	C	C1
IIIC	T4a	N2a	M0	C	C2
	T3–T4a	N2b	M0	C	C2
	T4b	N1–N2	M0	C	C3
IVA	Any T	Any N	M1a	—	—
IVB	Any T	Any N	M1b	—	—

NOTE: cTNM is the clinical classification, pTNM is the pathologic classification. The y prefix is used for those cancers that are classified after neoadjuvant pretreatment (for example, ypTNM). Patients who have a complete pathologic response are ypT0N0cM0 that may be similar to Stage Group 0 or I. The r prefix is to be used for those cancers that have recurred after a disease-free interval (rTNM).  
 \* Dukes B is a composite of better (T3 N0 M0) and worse (T4 N0 M0) prognostic groups, as is Dukes C (any TN1 M0 and Any T N2 M0). MAC is the modified Astler-Coller classification.

**Table 1:** Colorectal cancer staging according to the American Joint Committee of Cancer (AJCC 26.6.2011)

Additional, the differentiation state of tumor tissue compared to normal tissue is determined by pathologists analyzing the tissue under the microscope. Tumor tissue is



divided into “low-grade” (G1, G2) and “high-grade” (G3, G4) groups (Schölmerich J. 2005).

- Gx: differentiation cannot be determined
- G1: well differentiated, carcinoma shows normal histological and cellular characteristics
- G2: moderately differentiated
- G3: poorly differentiated, carcinoma shows different histological and cellular characteristics compared to normal tissue
- G4: undifferentiated, no typical glandular or epithelial characteristics of the tumor tissue

## **1.6 Receptor Tyrosine Kinases**

### **1.6.1 The function of receptor tyrosine kinases**

58 receptor tyrosine kinases (RTK) belonging to 20 families have been detected in the human genome. In general protein kinases transfer phosphate groups from Adenosine Tri-Phosphate (ATP) to a protein side chain. As this is a very rapid reaction that has high impact on protein domain structures, it is frequently used for intracellular signal transduction. RTKs use a tyrosine to bind phosphate groups in contrast to serine-threonine kinase receptors. They consist of three main domains: an extracellular domain for ligand binding, signaling peptide and dimerization, a transmembrane domain and an intracellular domain containing the kinase domain and an auto- and transphosphorylation side. Whereas the extracellular ligand binding domain differs strongly between the different RTK-families the kinase domain is quite conserved (Alberts 2002).

## Introduction

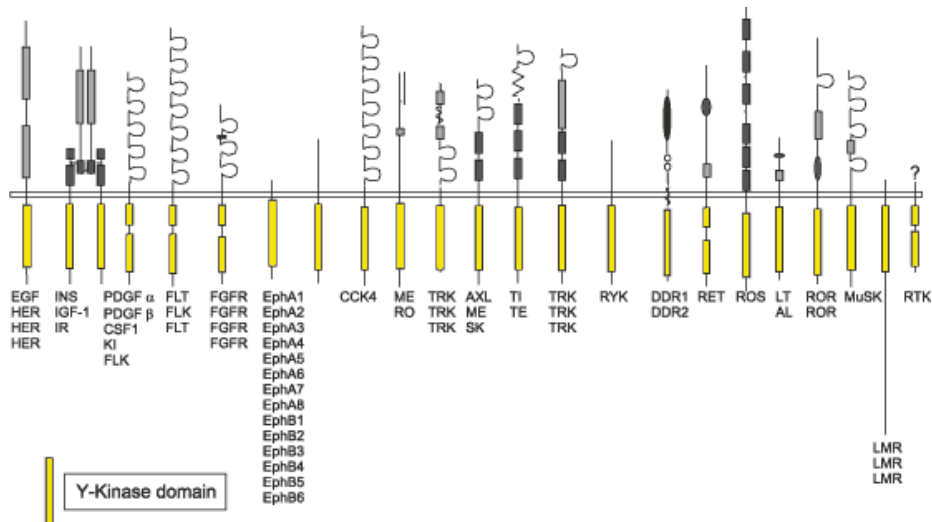


**Figure 24:** Tyrosine kinase receptors

(Picture from website [http://journals.prous.com/journals/servlet/xmlxsl/pk\\_journals.xml\\_summary\\_pr?p\\_JournalId=2&p\\_RefId=857184&p\\_IsPs=N; 30.6.11](http://journals.prous.com/journals/servlet/xmlxsl/pk_journals.xml_summary_pr?p_JournalId=2&p_RefId=857184&p_IsPs=N; 30.6.11))

The kinase domain contains an ATP-binding side and a substrate binding side. Ligand binding to the extracellular domain leads to receptor homo- or hetero-dimerization and the kinase domain is auto- or transphosphorylated. The resulting phosphotyrosines create the docking site for proteins containing a SH2 (Src Homology 2) or a PTB (Phosphor Tyrosine Binding) domain. Additionally, docking domains like the SH3 (Src Homology 3) and the PH (Pleckstrin Homology) domain recruit targets that transduce the signal further down-stream towards the nucleus. RTKs activate several signaling cascades controlling cell survival, proliferation and migration. Activated RTKs are then down-regulated by endocytosis and degradation (Alberts 2002).

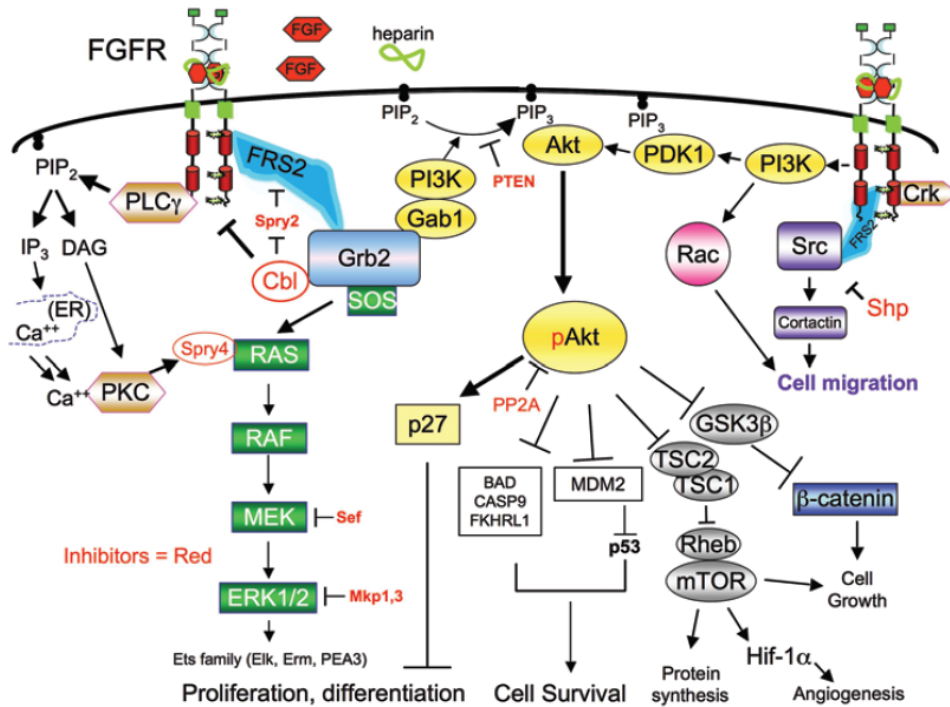


**Figure 25:** Signaling pathways activated by the RTK FGFR

(Acevedo et al. 2009)

### 1.6.2 Receptor tyrosine kinases in cancer

Due to the involvement of RTKs in cell proliferation, cell survival and cell migration they are often affected in various cancer types. Aberrations of RTK signaling are caused for instance by gene amplification, mutations, and increased transcription of the receptor but also by increased production of ligands and decrease of antagonists. Epidermal Growth Factor Receptor (EGFR)-family, Vascular Endothelial Growth Factor Receptor (VEGFR)-family, Insulin-like Growth Factor 1 Receptor (IGF1R/INSR)-family, and FGFR-family are mutated and act as oncogenes in cancer. One of the most prominent examples is HER-2 gene amplification in breast cancer (Slamon et al. 1987). Consequently, a lot of effort has been undertaken to target RTKs and since 1998 clinical application of RTK targeted therapies have been developed. RTKs can be targeted by antibodies or small molecule kinase inhibitors.

## **1.7 Fibroblast Growth Factor Receptors (FGFRs)**

### **1.7.1 FGFRs in general**

The importance of Fibroblast Growth Factor (FGF) signaling through their receptors (FGFRs) is extensive. Not only embryonic development (mesodermal patterning in the early embryo as well as organogenesis) but also different physiological functions in the adult organism like control of the nervous system, tissue repair, wound healing and angiogenesis are partly controlled by FGFs and FGFRs. They regulate cell proliferation, differentiation and survival and consequently play an important role in the development of cancer (Eswarakumar et al. 2005; Turner and Grose 2010).

Germline mutations of FGFR which lead to a gain-of-function result in various diseases like craniosynostosis (malformed cranium due to premature closure of sutures of a developing skull), dwarfing syndromes or cancer. Especially germline mutations of FGFR2 and 3 cause distinctly different patterns of limb development – e.g. normal hands and feet in the Crouzon syndrome, broader thumbs and toes in the Pfeiffer syndrome and severe fusion of the bones in the hands and feet in the Apert syndrome. Most of the germline mutations which cause skeletal syndromes lead to the development of cancer when they are somatic. Heterozygous mutations of FGFR1-3 contribute significantly to disorders of bone patterning and growth (Beenken and Mohammadi 2009; Webster and Donoghue 1997).

#### **1.7.1.1 Structure of FGF and FGFR**

FGFRs belong to the family of RTKs. Their extracellular domains consist of three Immunoglobulin-like (Ig) loops IgI, IgII, and IgIII. Between IgI and IgII a stretch of eight consecutive acidic residues (acid box) is located. IgII, IgIII and the linker between these two domains are important for ligand binding (Plotnikov et al. 1999). IgI and the acid box do not contribute to ligand binding but possess an auto-inhibitory function. The acid box interacts with the highly basic heparin-binding side of IgII. IgI interacts directly with the IgII-IgIII fragment (Olsen et al. 2004).

Further diversity is also reached by alternative splicing of FGFR1-3. Especially the exon 8 and 9 in the IgIII leads to the expression of either the IIIb or IIIc receptor

## Introduction

isoform. These two isoforms are expressed in a tissue specific manner. Thus, the expression of the IIIb isoform is predominant in epithelia, whereas IIIc isoform is more expressed in mesenchymal tissue. Ligands can also distinguish between the two isoforms. For example the FGF7 subfamily is expressed in mesenchyme and binds preferentially to FGFR2IIIb, whereas the FGF8 subfamily activates IIIc splice forms of FGFRs and is expressed in epithelial tissue (Ornitz and Itoh 2001; Zhang et al. 2006). The intracellular domain consists of a juxta-membrane domain, a split kinase domain, and a carboxy-terminal tail.

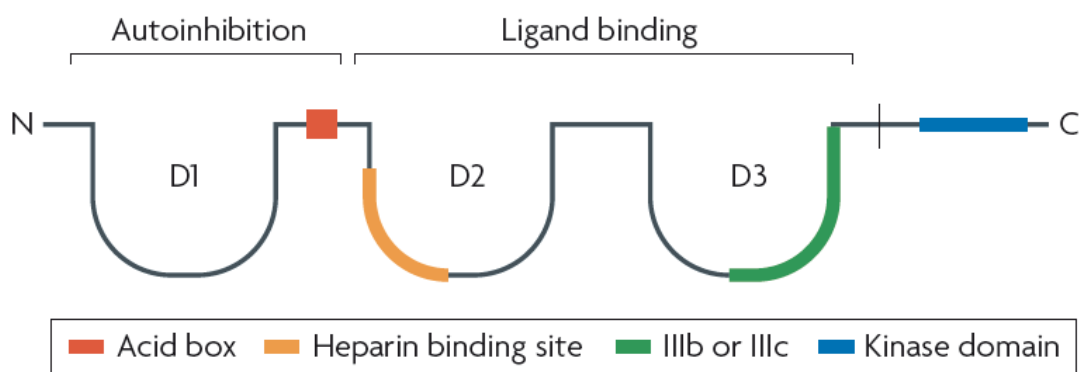


**Figure 26:** Structure of FGFR

(Beenken and Mohammadi 2009)

### 1.7.1.2 Interaction between FGFR and FGF/extracellular matrix

FGFs are glycoproteins and after secretion they are bound to the extracellular matrix and the cell surface by heparin or Heparan Sulphate Proteoglycans (HPSGs) (Hacker et al. 2005). HPSGs are polysulphated acidic glycoproteins which contain a larger carbohydrate than protein moiety. Specifically, they consist of a core protein, to which glycosaminoglycan chains are attached at specific sites. They reside in the extracellular matrix or are attached to the cell membrane.

Heparin is a highly sulfated polysaccharide which due to its structural similarity mimics the action of heparan sulphates but is not expressed on the cell surface (Berman et al. 1999; Ostrovsky et al. 2002). Heparins are shorter than heparan sulphate chains (Harmer 2006).

## Introduction

FGFs interact with the sulphated domains of heparan sulfate, heparan sulfate proteoglycans, and heparin. Heparan sulphate not only provides an extracellular reservoir of FGFs but also protects them from heat inactivation and proteolytic degradation (Vlodavsky et al. 1996)

Heparinases, proteases and specific FGF-binding proteins release FGFs from the extracellular matrix HSPGs and FGFs can bind to the cell surface HSPGs (Turner and Grose 2010). HSPGs are low affinity receptors which do not transmit a biological signal (Eswarakumar et al. 2005).

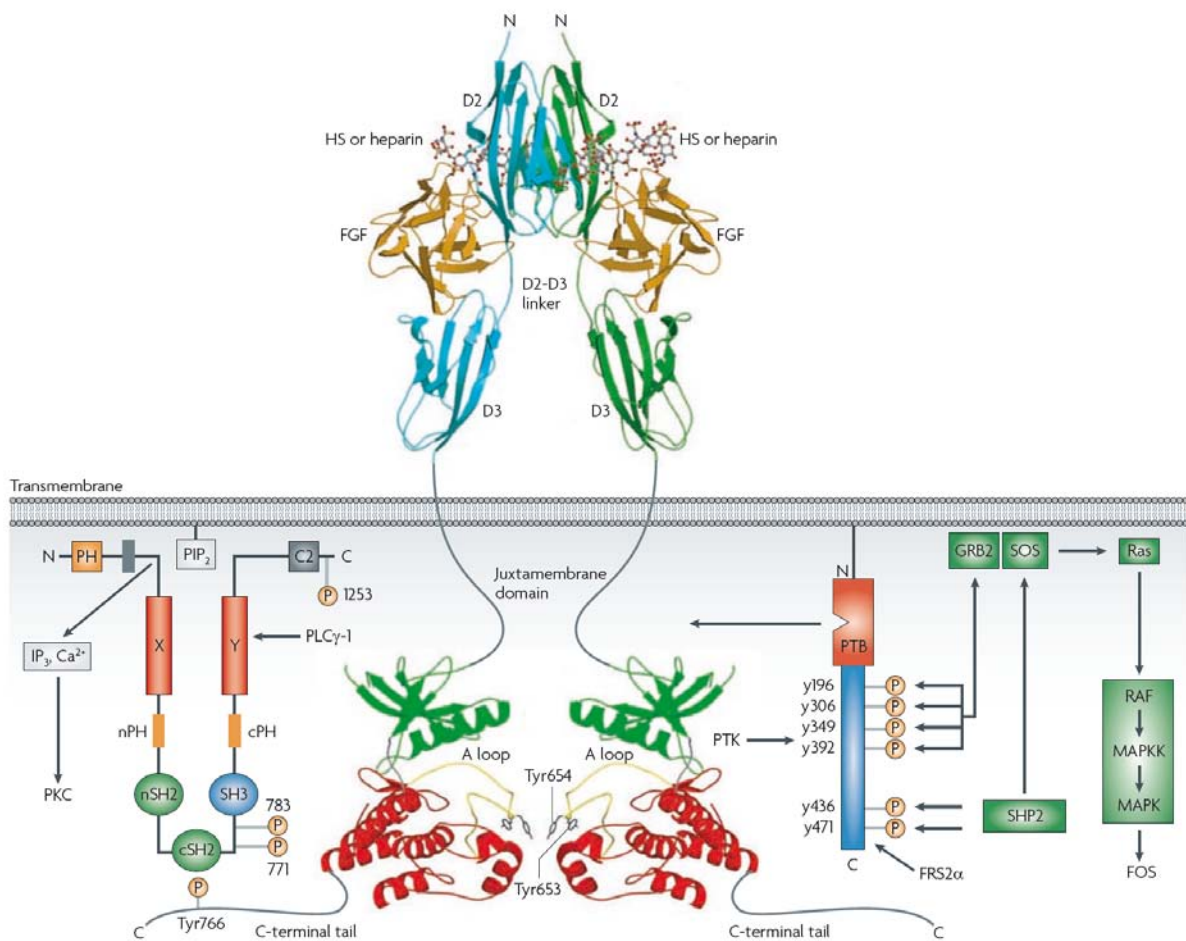


**Figure 27:** Ligand binding of FGF and receptor dimerization

(Beenken and Mohammadi 2009)

### 1.7.1.3 FGFR dimerization

Heparin facilitates the formation of FGF-dimers but also stabilizes the formation of FGF-FGFR-complexes (Ornitz et al. 1996). FGFR dimerization is induced by binding to an FGF-heparan proteoglycan/heparin sulphate complex. In the absence of heparan proteoglycan and heparin FGF is unable to bind to FGFR (Schlessinger et al. 1995). The length of glycosaminoglycan and heparin sulphation patterns can also determine binding of different FGFs to different FGFRs and their isoforms (Ostrovsky et al. 2002). One heparan sulphate saccharide can bind multiple FGF complexes depending on its length and sulphation. This leads to the suggestion that signaling plaques are formed due to the building of FGFR aggregates co-localized on the cell surface (Harmer 2006).

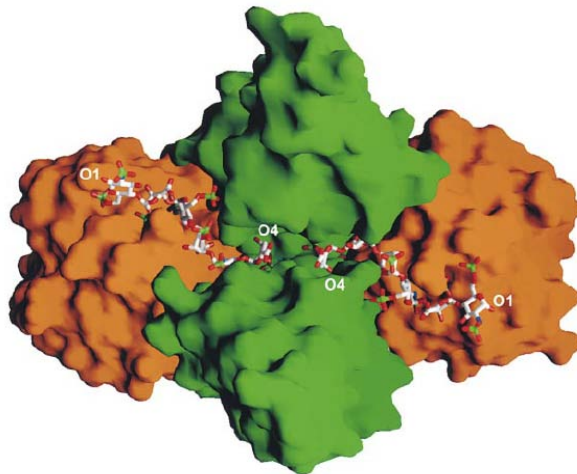


**Figure 28:** Molecular surface representation of the 2:2:2 FGF2-FGFR1-heparin-complex

FGF2 is colorized orange and the IgII of FGFR1 is green. The view is from the top looking into the heparin canyon. Heparin is presented here only with the first 6 sugar rings (Schlessinger et al. 2000).

Two 1:1 FGF-FGFR complexes form a symmetric dimer. Interaction between both receptors of each FGF-FGFR complex as well as interaction between ligand and receptor stabilizes the dimer. There is no interaction between the two ligands observed. IgII domains of both receptors form a canyon of positive potential, where heparin binds and bridges the two receptor-ligand complexes (Plotnikov et al. 2000; Schlessinger et al. 2000).

## Introduction

The expression of heparan sulphate and its biosynthetic enzymes as well as the expression of the core proteins to which heparan sulphates are attached changes during the embryonic development suggesting an important mechanism to regulate FGF-signaling (Allen and Rapraeger 2003).

### **1.7.1.4 Receptor activation**

Ligand dependent dimerization of the FGFRs leads to conformational changes in the receptor structure which activate the intracellular kinase domain.

Auto-phosphorylation of RTKs regulates catalytic activity and initiates downstream signaling. FGFR is auto-phosphorylated in trans by a strictly ordered reaction which indicates that different signaling pathways are recruited and activated within a certain time. For FGFR1 there are seven tyrosine residues which act as the major autophosphorylation sites: Y463, Y583, Y585, Y653, Y654, Y730, and Y766. Whereas pY766 acts as binding site for the SH2 domain of Phospholipase-C $\gamma$ , Y653 and Y654 are in the active loop and essential for tyrosine kinase activation. The other tyrosine auto-phosphorylation sites act as docking sites for signal proteins. Y653 is first phosphorylated which enhances the catalytic activity of FGFR 50-100fold and recruits signal proteins. Y583, Y463, Y766, and Y585 are then phosphorylated and further recruit SH2- and PTB-domain containing proteins. Y654 is auto-phosphorylated subsequently and increases the catalytic activity up to 500-1000fold (Furdui et al. 2006; Knights and Cook 2010).



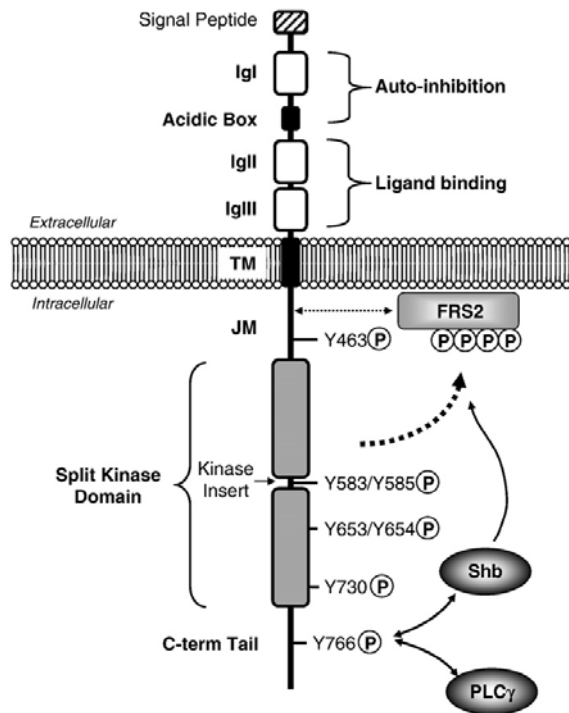


**Figure 29:** FGFR activation

TM ... transmembrane, JM ... juxta-membrane; (Knights and Cook 2010)

### 1.7.1.5 FGFR downstream signaling

There are two main substrates of FGFRs: FGFR Substrate 2 (FRS2) and Phospholipase- $C\gamma$  (PLC $\gamma$ ). Unlike other RTKs FGFRs do not directly bind Grb2, which links the activation of RTKs to the Ras/MAPK signaling pathway (Olsen et al. 2003). Phosphorylation of FGFR leads to the direct phosphorylation of the 90kDa Protein FRS2 and Shc. Shc and FRS2 both recruit Grb2/Sos-complex. FRS2 is associated with the cell membrane and contains a PTB domain, which binds the phosphotyrosine. FRS2 phosphorylation is stimulated by FGF and Nerve Growth Factor (NGF) but not by Epidermal Growth Factor (EGF), Platelet-Derived Growth Factor (PDGF) or insulin (Wang et al. 2002). FRS2 is a key adaptor protein and quite specific for FGFR but it interacts also with other RTKs like Neurotrophic Tyrosine Kinase Receptor type 1 (NTRK1), RET (Rearranged during Transfection) and Anaplastic Lymphoma Kinase (ALK) (Turner and Grose 2010).

For maximal activation of Ras/MAPK signaling pathway, an adaptor protein Shb which binds to the tyrosine 766 is required. Shb regulates Shp2 phosphorylation and its

## Introduction

interaction with FRS2 (Feik et al. 2010). Recruitment of Grb2 and Shp2 are necessary for FGF-mediated MAPK activation, leading to cell proliferation and differentiation. Grb2 binds to FRS via a SH2 domain and a 2:2 complex of Grb2 and FRS recruits another protein Gab1, a guanine nucleotide releasing factor which is phosphorylated and activates PI3-kinase. Grb2 binds to a proline-rich region of Gab1 via its c-terminal SH3 domain. The binding and phosphorylation of Gab1 generates a binding site of the SH2 domain of p85, the regulatory subunit of PI3-kinase which leads to recruitment and activation of PI3-kinase (Hacker et al. 2005). PI3-kinase phosphorylates PIP<sub>2</sub>, generating PIP<sub>3</sub> (Phosphatidylinositol-3,4,5-triphosphate) which translocates Akt, a serine/threonine kinase to the plasma membrane. There Akt is phosphorylated and activated by the Phosphoinositide-Dependent Kinase (PDK) and phosphorylates by itself a variety of substrates like GSK3 $\beta$ , mTor, FOXO1 and FOXO3 (Katoh 2006a).

Grb2 also binds to Sos, another guanine nucleotide releasing factor via its n-terminal SH3 domain. Sos activates G-proteins of the Ras-family and catalyzes the exchange of GDP by a GTP. Ras itself can activate different signaling pathways: RAF-MEK1/2-ERK1/2, PI3K-PDK1-PKB and PLC $\epsilon$ -IP<sub>3</sub>/DAG-PKC (Knights and Cook 2010).

PLC $\gamma$  by contrast binds directly to FGFR1 at the Y766. Since Y766 binds also the adaptor protein Shb, it is conceivable that PLC $\gamma$  and Shb compete with each other for binding to activated FGFR. Probably, the activation of PLC $\gamma$  or Shb differs temporarily or depends on different pools of activated receptors.

PLC $\gamma$  catalyzes the hydrolysis of the minor membrane phospholipid Phosphatidylinositol 4,5-bisphosphate (PtdIns(4,5)P<sub>2</sub>) which produces two intracellular secondary messengers: Diacylglycerol (DAG) and Inositol 1,4,5-trisphosphate (Ins(1,4,5)P<sub>3</sub>). Ins(1,4,5)P<sub>3</sub> binds to Ins(1,4,5)P<sub>3</sub> receptors which are large calcium channels and reside in the membranes of intracellular calcium stores like the endoplasmatic reticulum. Channels are opened by binding and Ca<sup>2+</sup> is released into the cytosol where it activates Ca<sup>2+</sup> dependent protein kinases like calmodulin-dependent kinases, Ca<sup>2+</sup>- and DAG-dependent proteins, and Protein Kinase C (PKC)-family of kinases (Knights and Cook 2010; Sugiyama et al. 2010b).

There are also other pathways which are activated by FGF-signaling including Signal Transducer and Activator of Transcription (STAT) signaling (Turner and Grose 2010).

## Introduction

Constitutively activated FGFR1, FGFR3 and FGFR4 mutants showed activation of STAT transcription factors like STAT1, STAT3, STAT5a and STAT5b (Zhong et al. 2006). How precisely FGFRs can activate STAT is unclear so far.

ERK1/2 and PKB pathways promote cell cycle progression and cell survival for example by inhibiting pro-apoptotic proteins like BIM and BAD or by promoting expression of pro-survival proteins like BCL-x<sub>L</sub> or MCL-1 (Knights and Cook 2010).

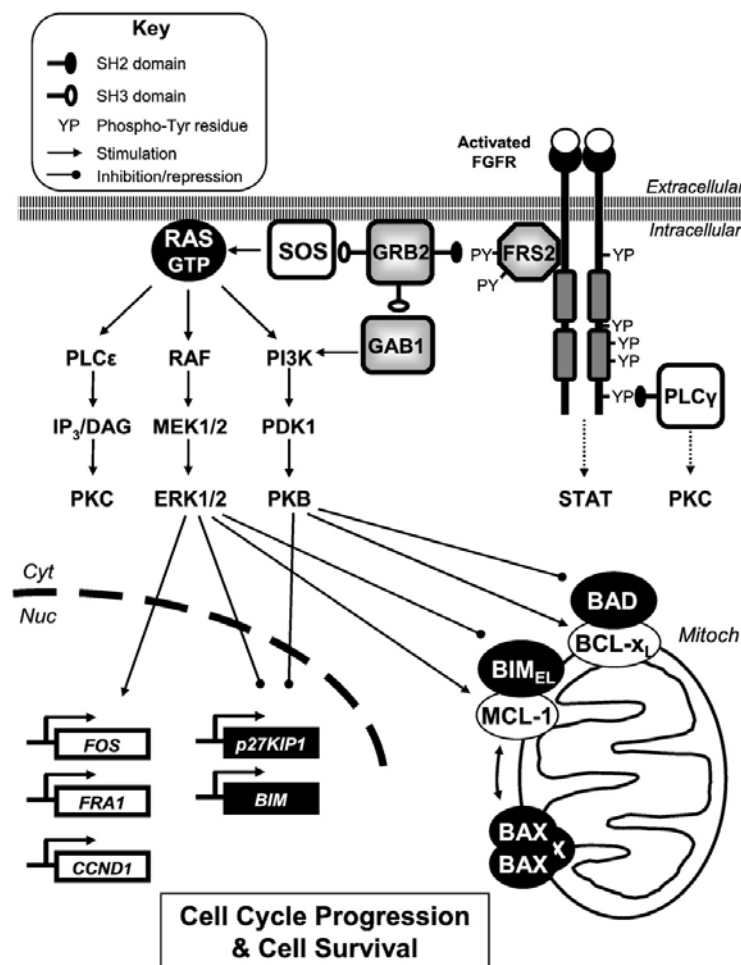


**Figure 30:** Intracellular FGF-dependent signaling

(Knights and Cook 2010)

### 1.7.1.6 Crosstalk between FGF- and Wnt-signaling

FGF-signaling pathways and WNT-signaling pathways interfere with each other in a variety of cellular processes like early embryogenesis, body-axis formation, limb-bud

## Introduction

formation, neurogenesis, hematogenesis, hepatogenesis, gastrointestinal morphogenesis, MMTV-induced mammary carcinogenesis, and human colorectal carcinogenesis. FGF16, FGF18 and FGF20 are targets of the canonical Wnt-pathway (Katoh 2006b).

Whereas GSK3 $\beta$  is responsible for the degradation of  $\beta$ -catenin in the canonical Wnt-pathway, GSK3 $\beta$  is phosphorylated due to FGF-dependent signaling via PI3K and Akt which results in the down-regulation of GSK3 $\beta$  activity. GSK3 $\beta$  binds and phosphorylates SNAIL, a transcriptional repressor of CDH1 gene encoding E-cadherin. Phosphorylated SNAIL is cytoplasmically translocated and cannot repress the transcription of E-cadherin. This leads to the assumption that inhibition of GSK3 $\beta$  activity in the FGF-signaling pathway results in a development of EMT by down-regulating E-cadherin (Katoh 2006a).

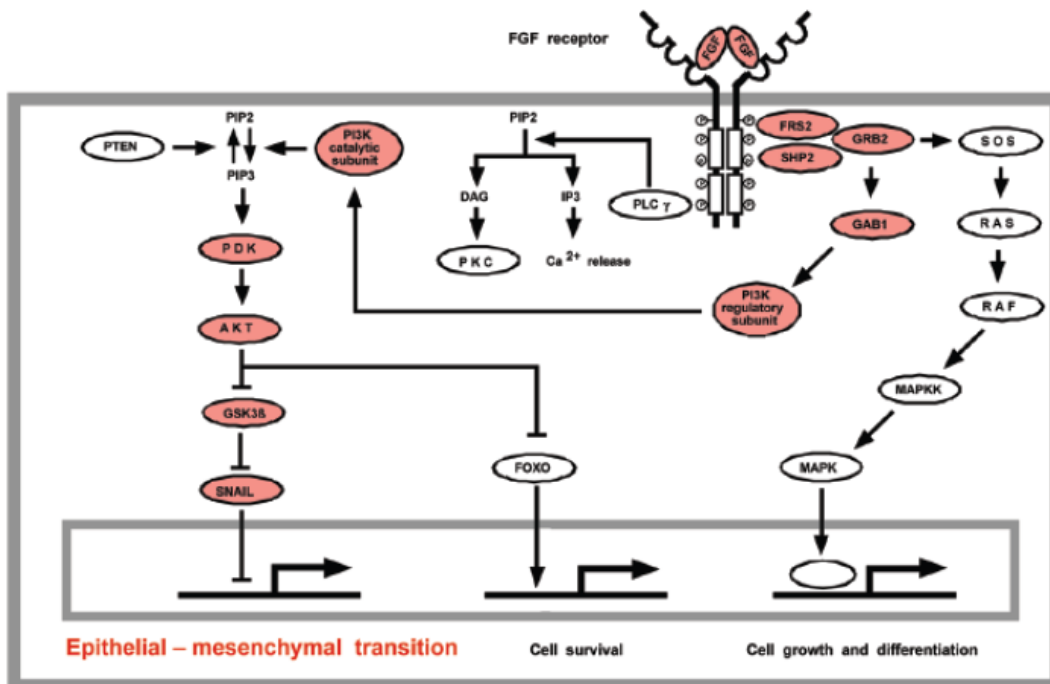


**Figure 31:** Induction of EMT by FGF-signaling

(Katoh 2006a)

There is a cross-talk between Wnt- and FGF-signaling during a variety of cellular processes. Since FGF18 and FGF20 are target genes of the Wnt-pathway, activation of the canonical Wnt-pathway, for example during carcinogenesis, also influences and activates FGF-signaling. GSK3 $\beta$  is down-regulated by both Wnt- and FGF-signaling.

There might be different pools of GSK3 $\beta$  available for the two pathways. Furthermore, a simultaneous activation of FGF- and Wnt-signaling leads to a potentiation of the Wnt-signaling because translocation of  $\beta$ -catenin is promoted by the FGF-signaling via PI3K-Akt (Katoh 2006a).

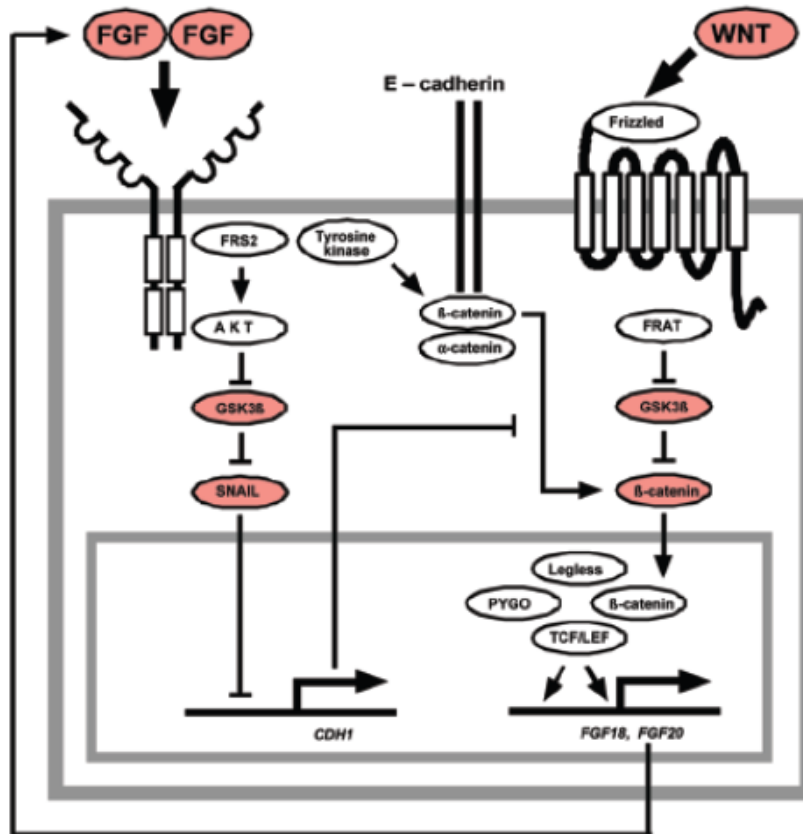


**Figure 32:** GSK3 $\beta$  crosslinks Wnt-signaling and FGF-signaling pathways

(Katoh 2006a)

### 1.7.1.7 Regulation and termination of FGF-mediated signaling

One possibility to regulate FGF-mediated signaling is auto-inhibition of the receptor. Auto-inhibition can be mediated by the IgI and the linker sequence IgI-IgII, the acid box. IgI directly interacts with the IgII-IgIII region of FGFR. The flexible nature of the IgI-IgII sequence facilitates also intramolecular interaction between the acid box and the highly basic heparin-binding site of IgII. These interactions lead to a low-affinity state of the FGFR where its affinity to FGF and heparin is reduced. The length of the IgI-IgII linker region as well as the number of consecutive acidic residues determines the

## Introduction

strength of auto-inhibition. FGFR1 has a very long linker region and therefore is stronger auto-inhibited as for example FGFR4 (Goldfarb et al. 2007).

Another mechanism regulating FGF-signaling is via c-Cbl. In response to FGF stimulation, c-Cbl is recruited by Grb2 and binds to FRS2 which results in ubiquitination of FRS and FGFR. This process is highly significant because other proteins in the multi-protein complex associated with FRS like Grb2, Gab1, or Shp2 are not ubiquitinated (Yayon et al. 1991).

Possible ways for termination of FGF-mediated signaling are achieved via a protein tyrosine phosphatase which has been identified in *Caenorhabditis elegans* so far but is currently unknown in mammalian cells (Knights and Cook 2010).

Apart from receptor auto-inhibition and receptor degradation there are several ways to modify the FGF-signaling by feedback inhibition, above all affecting Ras-Raf-MEK1/-ERK1/2 signaling pathway. MAPK phosphatases for example are expressed due to ERK1/2 activation and inactivate ERK1/2 by dephosphorylation (Knights and Cook 2010).

An efficient regulator of FGF, VEGF or EGF downstream signaling is Sprouty (Spry). Spry2 binds to Grb2 and inhibits FGF-induced MAPK pathway. Spry2 itself is activated by a protein phosphatase 2A (PP2A). Spry is synexpressed to FGFs and can also bind and inhibit Sos1 and Raf1 (Harmer 2006).

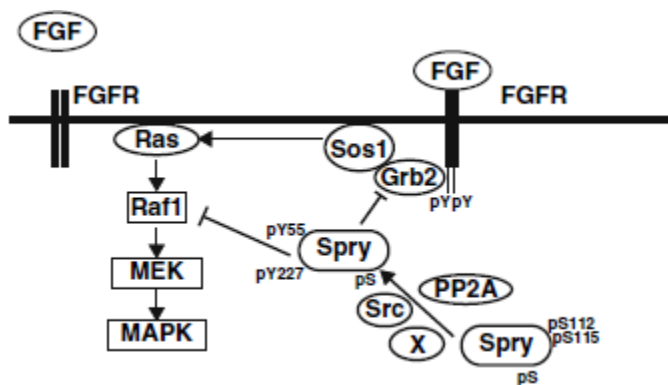


**Figure 33:** Inhibition of FGF-mediated signaling by sprouty

(Cabrita and Christofori 2008)

Thirdly, Similar Expression to FGF-genes (Sef) encodes a transmembrane protein and is also synexpressed to FGFs. Overexpression of Sef reduces FGF-mediated tyrosine phosphorylation of FGFR1 and FRS2 and therefore activation of ERK1/2 and Akt is inhibited (Ostrovsky et al. 2002).

### **1.7.2 FGFR Family**

Four FGFRs (FGFR1-4) which share a protein homology of 55%-72% are known to date (Powers et al. 2000). A fifth FGFR has been described (FGFR5 or FGFR1) that binds FGFs but lacks a tyrosine kinase domain. Its role has not been detected yet (Wiedemann and Trueb 2000). Due to the different expression patterns of all different FGFRs, including their splice variants, a remarkable FGFR diversity is achieved. Imbalances in FGFR signaling are associated with diverse pathologies like skeletal disorders and cancer.

#### **1.7.2.1 FGFR1**

There are three genetic disorders attributed to the mutation of FGFR1: Kallman's syndrome, osteoglophonic dysplasia and Pfeiffer syndrome.

A loss-of-function mutation of FGFR1 results in Kallman's syndrome which is manifested in hypogonadotropic hypogonadism and anosmia, a deficiency of the sense of smell. The development of the olfactory bulb in humans is sensitive to FGFR1 (Dode et al. 2003).

Osteoglophonic dysplasia is a bone disorder. Its symptoms are dwarfism, vertebral fragility, craniosynostosis, multiple unerupted teeth and failure to thrive. Missense mutation of FGFR1 leads to a constitutive activation of the receptor which is associated with the development of osteoglophonic dysplasia (Shankar et al. 2010).

Pfeiffer syndrome is manifested in an autosomal dominant craniosynostosis syndrome with craniofacial anomalies and characteristic broad thumbs and big toes. A missense mutation of FGFR1 C755G causes a Pro252Arg substitution and is related to the Pfeiffer syndrome (Muenke et al. 1994).

## Introduction

Dominant gain-of-function mutation of FGFR1 causes craniosynostosis and fails morphogenesis of olfactory bulbs (Dode et al. 2003). In the kinase domain it also leads to glioblastoma (Rand et al. 2005).

### 1.7.2.2 FGFR2

Germline mutations in FGFR2 kinase domain are found in patients with various craniosynostosis syndromes like Crouzon's syndrome and Pfeiffer syndrome. These mutations constitutively activate FGFR2 by disengaging an auto-inhibitory sequence in the kinase domain (Chen et al. 2007).

The majority of mutations of FGFR2 occur in IgIIIa (exon 8) or IgIIIc (exon 10) or in the intron sequence flanking IgIIIc. Alternative splicing joins IgIIIa to IgIIIb or IgIIIc and generates different isoforms of FGFR2 which show different FGF-binding properties and are tissue specific. Mutations in IgIII also lead to Crouzon, Pfeiffer or Apert syndrome (Kan et al. 2002).

Truncated forms of FGFR2, which result in a c-terminal deletion or aberrant splicing, have been described. The truncated forms interfere with receptor internalization and therefore prevent a potential mechanism for signal attenuation and increase receptor stability and activation. This was also observed in gastric cancer cell lines (Missiaglia et al. 2009; Yamaguchi et al. 1994).

### 1.7.2.3 FGFR3

Most FGFR3 mutations, which were found in cancer, are identical to the FGFR3 mutations involved in skeletal disorders. A transmembrane mutation of FGFR3 leads to Gly380Arg and results in nearly all cases in achondroplasia, which is a common genetic form of dwarfism (Webster and Donoghue 1997).

Germline mutations, which affect the kinase domain of FGFR3, cause three different dwarfing syndromes: hypochondroplasia (mild dwarfism syndrome with nearly normal cranial and facial characteristics), thanatophoric dysplasia type II (lethal neonatal skeletal dysplasia) and severe achondroplasia with developmental delay and *Acanthosis*



*nigricans* syndrome (dwarfism syndrome with neurological disorders and a hyperpigmentation of the skin).

### **1.7.2.4 FGFR4**

#### *1.7.2.4.1 FGFR4 and its role in cancer*

FGFR4 plays an important role in the liver where it controls the systemic cholesterol/bile acid metabolism and lipid metabolism (Huang et al. 2009). Disruption of FGFR4 in the mouse germline does not show an aberrant phenotype. Mice are still fertile and also liver morphology is comparable to control mice. But liver-associated organs like gallbladder are affected. Gallbladder is small and depleted and the excreted and total bile pools are elevated which leads to an elevated cholesterol metabolism (Yu et al. 2000).

The expression of FGFR4 is up-regulated in various cancer types like prostate cancer (Sahadevan et al. 2007; Wang et al. 2008), rhabdomyosarcoma (Taylor et al. 2009), breast and gynecological cancers (Jaakkola et al. 1993), or gastric cancer (Ye et al. 2011). FGFR4 is clearly involved in initiation and progression of prostate cancer. All FGFs found in prostate cancer tissue are activators of FGFR4. Strong expression of FGFR4 in prostate cancer is associated with increased clinical stage and tumor grade and decreased patient survival (Wang et al. 2008). In breast cancer there is an association between up-regulated expression of FGFR4 and chemoresistance (Roidl et al. 2009).

In contrast to FGFR1-3 there are no reports about splice variants in the Ig-loop III of FGFR4. However in human intestinal epithelial cell lines a 120bp shorter splice variant of FGFR4 was found. In this particular splice form exon 9, which encodes for the transmembrane domain, is substituted by an intron. This receptor is therefore not anchored in the cell membrane but is secreted as a soluble receptor. The soluble form of FGFR4 has not only been found in gastrointestinal epithelial cells but also in pancreas, gastric, colon and pancreatic cancer cell lines (Takaishi et al. 2000).

FGF19 has high affinity for FGFR4 and binds nearly exclusively to this receptor. It is expressed in several tissues like fetal cartilage, skin, retina, adult gall bladder but also in

## Introduction

colon cancer cell lines like Colo201 (Xie et al. 1999). FGF19 and FGFR4 are both expressed in conjunction, e.g. in colon adenocarcinoma, lung squamous cell carcinoma and hepatocellular carcinoma. An anti-FGF19 monoclonal antibody which blocks the interaction of FGF19 with FGFR4 inhibits growth of colon carcinoma xenografts (Desnoyers et al. 2008).

Drafahl et al showed a correlation between FGFR4 expression and the reduction of NFκB induced apoptosis. FGFR4 expression and/or FGF19 stimulated FGFR4 leads to a decrease of the kinase activity of IKKβ complex (which rescues NFκB from proteosomal degradation) as well as to a reduced nuclear localization of NFκB indicating a down-regulation of NFκB-signaling. Additionally in prostate cancer cells FGF19 stimulation results in a reduced TNFα-induced apoptosis (Drafahl et al. 2010).

### *1.7.2.4.2 FGFR4 G388R polymorphism*

A single nucleotide polymorphism in the transmembrane domain has been described causing the exchange of a glycine to an arginine at position 388 (rs351855). FGFR4<sup>Gly</sup> (FGFR4-G388) is represented in the majority of the population and therefore referred to as the “wild-type” FGFR4. Usually charged amino acids like arginine do not occur in transmembrane domains of receptor tyrosine kinases and have been previously associated with diseases like achondroplasia and Crouzon syndrome (Bange et al. 2002). The G388R polymorphism is prevalent in the white population with approximately 45% of the individuals studied so far are hetero- or homozygous for the FGFR4<sup>Arg</sup> (FGFR4-R388) allele (Wang et al. 2008).

## Introduction

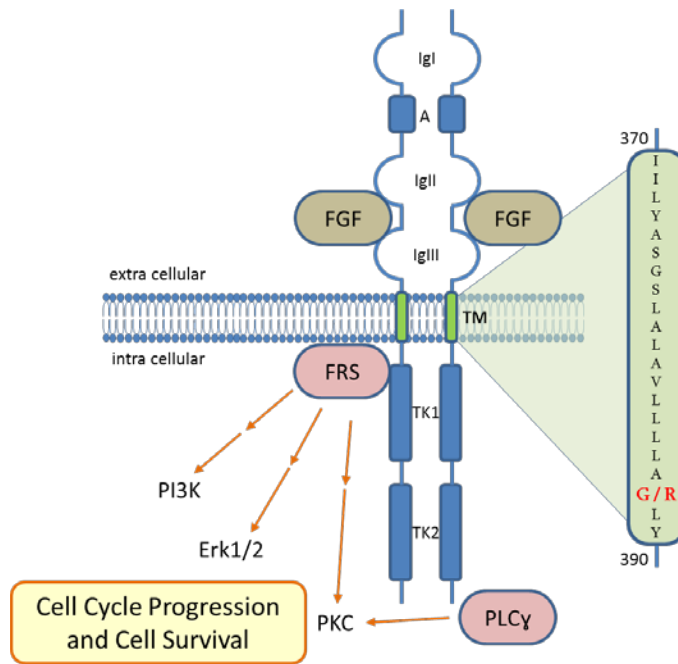


**Figure 34:** Structure of FGFR4-G388R polymorphism

### 1.7.2.4.3 The role of FGFR4 G388R polymorphism in various cancer types

FGFR4 G388R polymorphism and its impact on tumor initiation, development, clinicopathological parameters like tumor stage and lymph node involvement, as well as disease free survival and overall survival has been studied and described in various publications for many cancer types. 2011 Frullanti et al. summarized 21 studies and published a “Meta and pooled analysis of FGFR4 Gly388Arg polymorphism as a cancer prognostic factor”. They included studies on G388R polymorphism in different types of cancers affecting brain, breast, colorectal, head and neck, larynx, lung, melanoma, prostate and sarcomas. The overall conclusion was a significant association between the Arg388Arg genotype and nodal involvement in the meta-analysis whereas in the pooled analysis the Arg-allele was correlated with increased hazard of poor overall survival compared to patients with a homozygous Gly-genotype. The FGFR4<sup>Arg</sup> allele was furthermore identified to be a potential risk factor for developing and progressing prostate cancer (Frullanti et al. 2011). FGFR4<sup>Arg</sup> promotes initiation and progression in prostate cancer probably due to increased stability and prolonged activity of the receptor. But also the “wild-type” variant FGFR4<sup>Gly</sup> is stabilized after ligand stimulation by another protein called HIP1 (Wang et al. 2008).

## Introduction

The presence of the FGFR4<sup>Arg</sup> allele in breast cancer cell lines correlates with high expression of FGFR4. FGFR4<sup>Arg</sup> is not associated with initiation of breast cancer and lung adenocarcinoma but is connected to aggressive tumor progression like high tumor stage and axillary lymph node involvement in breast cancer patients (Bange et al. 2002; Spinola 2005). Furthermore, FGFR4<sup>Gly</sup> was associated with motility inhibition in breast cancer and prostate cancer cell lines (Stadler et al. 2006; Wang et al. 2004).

Similarly, in head and neck squamous cell carcinoma high expression of FGFR4<sup>Arg</sup> allele was significantly associated with reduced overall survival and advanced tumor stage (Dacostaandrade et al. 2007; Streit et al. 2004). In another approach FGFR4<sup>Gly</sup> was found to increase the risk for head and neck-squamous cell carcinoma and carriers of the FGFR4<sup>Arg</sup> allele showed an increased sensitivity for cisplatin (Ansell et al. 2009).

In soft tissue sarcoma there are no differences regarding the phenotype compared to control which indicates no association of the FGFR4 single nucleotide polymorphism (SNP) with the initiation of soft tissue sarcoma. But FGFR4<sup>Gly</sup> homozygous patients seem to have a better prognosis concerning overall and metastasis-free survival. For osteosarcoma such observations concerning overall and metastasis-free survival were not found (Morimoto et al. 2003).

### *1.7.2.4.4 The role of FGFR4 G388R polymorphism in colorectal cancer*

The situation of the G388R polymorphism in CRC is diffuse. Hitherto, very few reports have been published about this topic and these are contradictory. To date there are three reports about the FGFR4 G388R polymorphism in CRC available. Bange and his colleagues were the first who described the FGFR4 G388R polymorphism in 2002. They also found a significant correlation between the Arg-allele and metastatic lymph nodes as well as advanced tumor stage in 37 CRC patients. Furthermore they reported an association between the Arg-allele and a significantly reduced overall survival over a 16-month follow up time. A long term follow up of seven years did not show this effect (Bange et al. 2002).

2005 Spinola et al. published their study on 179 CRC patients compared to 220 controls but could not associate the Arg-allele to any kind of cancer risk, survival or other

prognostic parameters. In contrast to Bange and colleagues Spinola, despite a higher number of patients, found no association between the presence of an Arg-allele and nodal status in CRC (Spinola et al. 2005).

In 2006, another work of Gordon and colleagues studied 21 germline polymorphisms to predict tumor recurrence on chemoradiation-treated rectal cancer patients. For this purpose, 90 patients with diagnosed stage II and III adenocarcinoma of the rectum, who have been treated with chemoradiation, were genotyped. In this study a risk tree was identified including not only node status, IL-8, intracellular adhesion molecule-1, TGF- $\beta$  but also FGFR4. These findings indicate a correlation between the FGFR4 polymorphism and risk for developing tumor recurrence (Gordon et al. 2006).

#### *1.7.2.4.5 Interaction of FGFR4 G388 polymorphism with metalloproteinase*

FGFR4<sup>Arg</sup> was also found to induce and stabilize Membrane Type 1 Matrix Metalloproteinase (MT1-MMP, MMP14) and collagen invasion by decreasing lysosomal degradation of MT1-MMP. Because of its collagenase activity MT1-MMP is used by tumor cells for invasion and metastasis. Interaction of FGFR4<sup>Arg</sup> with MT1-MMP also results in epithelial-mesenchymal transition (EMT) by preventing the accumulation of basement membrane and altering cadherin. FGFR4<sup>Gly</sup> also induces MT1-MMP phosphorylation but results more in down regulation of MT1-MMP (Sugiyama et al. 2010a; Sugiyama et al. 2010b).

### **1.7.3 FGF-Family**

FGF-signaling has been implicated in different physiological and pathological processes reaching from angiogenesis to tumor development and progression. But the most important role of FGF-signaling is embryonic development. Studies with FGF-knockout mice show different phenotypes ranging from early embryonic lethality to very mild and no effects. This reflects the redundancy of the FGF-family and the uniqueness of their expression in specific tissue.

## Introduction

FGF	Phenotype of knockout mouse	Physiological role
FGF1	normal	not established
FGF2	loss of vascular tone, slight loss of cortex neurons	not established
FGF3	inner ear agenesis in humans	inner ear development
FGF4	embryonic lethal	cardiac valve leaflet formation, limb development
FGF5	abnormally long hair	hair growth cycle regulation
FGF6	defective muscle regeneration	myogenesis
FGF7	matted hair reduced nephron branching in kidney	branching morphogenesis
FGF8	embryonic lethal	Brain, eye, ear and limb development
FGF9	postnatal death, gender reversal lung hypoplasia	gonadal development, organogenesis
FGF10	failed limb and lung development	branching morphogenesis
FGF16	embryonic lethal	heart development
FGF17	abnormal brain development	cerebral and cerebellar development
FGF18	delayed long-bone ossification	bone development
FGF19	increased bile acid pool	bile acid homeostasis, lipolysis, gall bladder filling
FGF20	no knockout model	neurotrophic factor
FGF21	no knockout model	fasting response, glucose homeostasis, lipolysis and lipogenesis
FGF22	no knockout model	presynaptic neural organizer
FGF23	hyperphosphataemia, hypoglycaemia, immature sexual organs	phosphate homeostasis, vitamin D homeostasis

**Table 2:** FGF-knockout mice: phenotype and physiological role of FGF1-23

(Beenken and Mohammadi 2009)

22 structurally related FGFs are known in mammals. They all have in common a homologous core region of 120-130 amino acids which is arranged into 12 antiparallel  $\beta$ -strands and is flanked by amino and carboxyl termini (Knights and Cook 2010). FGF11-FGF14 are not generally considered as members of the FGF-family. Although they share a high sequence identity with the FGF-family, they cannot activate the FGFRs. FGF15 is a mouse orthologue of human FGF19 (Beenken and Mohammadi 2009).

## Introduction

The mammalian FGF-family can be divided into three groups:

1. Intracellular subfamily: FGF11 subfamily: FGF11-14 (iFGFs)
2. Hormone-like subfamily: FGF19 subfamily: FGF19, 21 and 23 (hFGFs)
3. Canonical subfamily: further divided into five subfamilies based on differences in sequence homology and phylogeny:
  - FGF1 subfamily: FGF1 and FGF2
  - FGF4 subfamily: FGF4, FGF5, FGF6
  - FGF7 subfamily: FGF3, FGF7, FGF10, FGF22
  - FGF8 subfamily: FGF8, FGF17, FGF18
  - FGF9 subfamily: FGF9, FGF16, FGF20

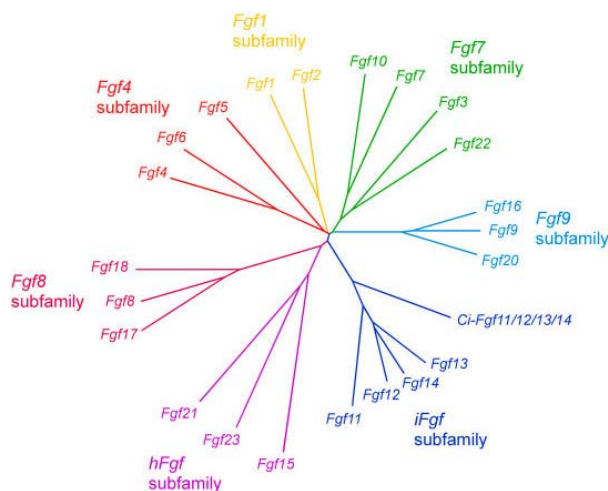


**Figure 35:** Evolutionary relationship of mouse FGFs

(Itoh and Ornitz 2008)

### 1.7.3.1 Intracellular subfamily: FGF11-14 (iFGF)

FGF11-14 share high sequence identity with the FGF9 subfamily. They all lack a secretory signal sequence but unlike the FGF9 subfamily FGF11-14 remain intracellular. Furthermore, they can bind heparin with high affinity but are not able to activate FGFRs (Olsen et al. 2003).

## Introduction

iFGF act in a FGFR-independent manner and bind to the intracellular domains of voltage-gate sodium channels which are expressed in excitable cells like neurons, skeletal muscle, and cardiac muscle and opened in response to membrane depolarization. They also bind to the neuronal MAP-kinase scaffold protein, islet-brain-2, which is expressed in developing and mature neurons, olfactory epithelium, and pancreatic islet cells (Goldfarb 2005; Goldfarb et al. 2007; Olsen et al. 2003). Expression is almost exclusively occurring in neuronal cells (Goldfarb 2005).

FGF13 is not detected in embryos or in normal trophoblastic stem cells (TS cells) but can be induced by 24h hyperosmolar stress (Zhong et al. 2006).

FGF14 is expressed in the developing and adult central nervous system and suggests a role in neuronal development and adult brain function. FGF14-deficient mice are viable, fertile and anatomically normal but show muscle weakness and movement disorder probably due to aberrant basal forebrain activity (Wang et al. 2002).

FGF12-deficient mice show little demonstrable phenotype like muscle weakness but less severe than FGF14-deficient mice (Goldfarb 2005).

### **1.7.3.2 Hormone-like subfamily: FGF19, FGF21, FGF23**

Hormone-like FGFs have an endocrine function like regulating bile acid, cholesterol, glucose, vitamin D and phosphate homeostasis. The heparin binding affinity of hormone-like FGFs is reduced compared to the other FGFs whereas FGF19 and FGF23 need a cofactor called klotho for binding to their FGF receptors (Itoh 2010). At high concentrations (compared to FGF1) they activate FGFRIIIc isoforms and FGFR4 (Zhang et al. 2006).

FGF19 is the human orthologue of FGF15 in the mouse (Ornitz and Itoh 2001). FGF15/19 plays an important role in the development of heart and brain at embryonic stages. FGF15<sup>-/-</sup> mice die because of heart defects. Furthermore bile excretion is elevated in FGF15<sup>-/-</sup> mice. FGF15/19 is highly involved in the regulation of bile acid metabolism in the liver. Intestinally produced FGF15/19 regulates hepatic bile acid synthesis by binding and activating hepatic FGFR4 (Inagaki et al. 2005; Itoh 2010)



FGF21 serves as a metabolic regulator by improving glycemic control (improved insulin sensitivity) and lipid metabolism (Berglund et al. 2009). Serum FGF21 level is elevated in obese people and associated with an increased risk for metabolic syndrome (Zhang et al. 2008)

FGF23 is synthesized by osteocytes and osteoblasts and controls the phosphate balance by modulating phosphate excretion and absorption. It is also involved in the regulation of 1,25-dihydroxyvitamin D (calcitriol) (Prie and Friedlander 2010). Biallelic mutations of FGF23 result in hyperphosphatemic familial tumoral calcinosis or hyperostosis-hyperphosphatemia syndrome (Ichikawa et al. 2010). FGF23 needs klotho, a membrane protein to bind to FGFRs (Prie and Friedlander 2010; Urakawa et al. 2006).

### **1.7.3.3 Canonical subfamily**

Most FGFs of this group are secreted from the cell, bind to FGFRs and can act in a paracrine and an autocrine way. They also have binding sites for acidic glycosaminoglycans like heparin and heparin sulfate.

#### *1.7.3.3.1 FGF1 subfamily: FGF1 and FGF2*

FGF1 and FGF2 are the prototypic FGFs and were first isolated from bovine pituitary extracts. FGF1 has a high affinity to all FGFRs and their splice variants and probably defines the core FGF-binding domain (Ornitz et al. 1996). Both FGFs do not contain a signal peptide for the classical secretory pathway so they must be secreted by another way. FGF1 and FGF2 possess a nuclear localization signal so they are found in the cytosol and associated with the nucleus (Powers et al. 2000). Removal of the nuclear localization signal in FGF1 causes abrogation of its mitogen effect (Imamura et al. 1990). FGF1 also stimulates DNA synthesis without binding to a cell-surface receptor (Wiedlocha et al. 1994).

The physiological role of FGF1 and FGF2 remains still unclear. Both factors are found highly expressed in the adult brain, but in different compartments so a potential role of FGF1 and FGF2 for the brain development is suggested. FGF2<sup>-/-</sup> mice are fertile and viable and show relatively mild defects like changes in the number of neurons in the

## Introduction

cerebral cortex, a delay in the healing of epithelial wounds and defects in the regulation of blood pressure. No phenotypic defects at all could be seen in FGF1<sup>-/-</sup> mice. Interestingly a FGF1-FGF2 double knockout mouse shows only the same mild defects like the FGF2<sup>-/-</sup> mouse which excludes the suggestion that FGF1 and FGF2 compensate each other (Miller et al. 2000).

It is also likely that FGF1 and FGF2 play a physiological role in the maintenance of vascular tone. Administration of FGF1 and FGF2 lowers blood pressure. FGF2 has also angiogenic properties like stimulating migration and proliferation of endothelial cell, anti-apoptotic activity as well as inducing development of large collateral vessels (Beenken and Mohammadi 2009). But also FGF1 shows angiogenic properties inducing microvascular branching of endothelial cells as well as antiapoptotic activity (Beenken and Mohammadi 2009; Uriel et al. 2006).

By inducing proliferation of airway smooth muscle cells FGF2 seems to play a role in the development of asthma (Bosse and Rola-Pleszczynski 2008). FGF1 was found to stimulate human preadipocytes in a paracrine manner suggesting an important role in human adipogenesis (Hutley et al. 2004). It has also been associated with the regeneration of nerve injuries (Lin et al. 2005).

Inhibiting FGF1 and FGF2 reveals a potential cancer therapy. Thalidomide, which inhibits FGF2-induced angiogenesis, as well as Suramin, which mimics heparin and therefore interferes with FGF-signaling, were tested in clinical trials and show benefits in prostate and renal cancer (Kathir et al. 2006; Kraemer et al. 2009; Vogelzang et al. 2004).

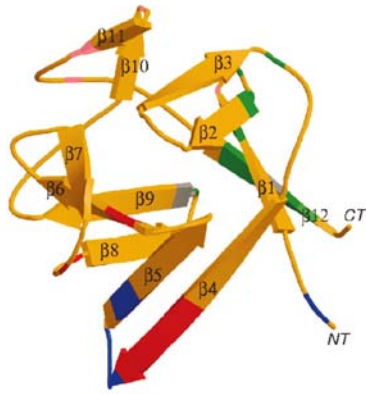


**Figure 36:** 3-dimensional structure of FGF2, a prototypical FGF

(Ornitz and Itoh 2001)

### 1.7.3.3.2 *FGF4 subfamily: FGF4, FGF5, FGF6*

Members of the FGF4 subfamily are expressed in epithelial and mesenchymal cells and specifically activate the FGFR3c splice variant (Ornitz et al. 1996).

FGF4 is very important in developing processes which include the formation of cardiac valve leaflet or limb development (Sugi et al. 2003). FGF4<sup>-/-</sup> mice are not viable. Embryos undergo uterine implantation but cannot develop properly. In vitro the absence of FGF4 results in impaired proliferation of the inner cell mass (Feldman et al. 1995).

FGF5 expression is found in hair follicles and negatively regulates hair growth. FGF5<sup>-/-</sup> mice show an abnormally long hair phenotype (Hebert et al. 1994; Housley and Venta 2006).

FGF6 expression is restricted to developing skeletal muscle and is also up-regulated after muscle injuries, suggesting that FGF6 affects myogenesis. FGF6<sup>-/-</sup> mice show defective muscle regeneration and increased fibrosis after freeze-crush injury (Armand et al. 2006).

### 1.7.3.3.3 *FGF7 subfamily: FGF3, FGF7, FGF10, FGF22*

Members of the FGF7 subfamily strongly activate FGFR2IIIb. FGF10 and FGF22 additionally show a weak activity towards FGFR1IIIb. All the other FGFRs are not activated by this subfamily (Zhang et al. 2006).

## Introduction

FGF3 plays an important role in the development of the inner ear at a very early stage. Homozygous deletion of FGF3 leads to hereditary deafness in humans and a few dental defects like widely spaced teeth. (Tekin et al. 2007).

FGF7 is also known as keratinocyte growth factor and is synthesized by skin fibroblasts. FGF7<sup>-/-</sup> mice develop matted fur but no abnormalities concerning epidermal growth or wound healing and are viable and fertile (Guo et al. 1996). FGF7 and its receptors are also expressed by or around the growing ureteric bud in the developing kidney suggesting a role in kidney morphogenesis. Kidneys of mature FGF7<sup>-/-</sup> mice show 30% fewer nephrons and exogenous FGF7 can increase the number of nephrons by approximately 50% (Qiao et al. 1999).

FGF10 is expressed in mesenchymal tissue and signals to epithelial FGFR2IIIb. It is important for limb and lung formation in the embryo because it is required for a normal branching program and for proper proximal-distal patterning in the lung (Abler et al. 2009; Zhang et al. 2006). FGF10<sup>-/-</sup> mice die at birth. They show development of trachea but fail to form a lung. Furthermore, mutated mice have truncated fore- and hind limbs (Sekine et al. 1999).

Like FGF7 and FGF10 FGF22 is a presynaptic organizing molecule in the mammalian brain and may play a role in the synaptogenesis (Umemori et al. 2004).

### *1.7.3.3.4 FGF8 subfamily: FGF8, FGF17, FGF18*

Members of the FGF8 subfamily are expressed in epithelial cells and exclusively activate FGFR3IIIc (above all FGFR3IIIc) splice forms and FGFR4. The FGF8, 17 and 18 are expressed in the midbrain-hindbrain area (Zhang et al. 2006).

FGF8 is important for organizing the midbrain-hindbrain patterns in the embryonic development. FGF17 is expressed later and broader. FGF17<sup>-/-</sup> mice are born alive but reveal significant tissue loss in midbrain and vermis cerebellum whereas FGF8<sup>-/-</sup> mice do not undergo gastrulation and are not viable suggesting an important role for FGF8 in the early embryonic development of the brain (Xu et al. 2000).

## Introduction

FGF18 also plays a role in the regulation of endochondral, periosteal and intramembranous bone growth. FGF18<sup>-/-</sup> mice survive embryonic development but die in the early neonatal period. They are 10-15% smaller and die of cyanosis within the first 30min after birth, probably due to respiratory failure. They also show decreased expression of osteogenic markers and delayed long-bone ossification (Liu et al. 2002).

### *1.7.3.3.5 FGF9 subfamily: FGF9, FGF16, FGF20*

The FGF9 subfamily binds to all FGFRIIIc isoforms, FGFR4 and FGFR3IIIb.

FGF9 is expressed in epithelial-like and neuronal tissues during the embryonic development and is important for lung, heart, inner ear, digestive system, and testes development (Zhang et al. 2006). FGF9<sup>-/-</sup> mice die at birth because of lung hypoplasia. Additional FGF9 seems to play a role in sex determination and testicular embryogenesis because until E18.5 mice undergo a male-to-female sex reversal (Colvin et al. 2001a).

The FGF9 subfamily signals from epithelium to mesenchyme whereas the FGF7 subfamily signals in a reciprocal way from mesenchyme to epithelium. Therefore, FGF9 stimulates the mesenchymal expression of the FGF7 subfamily members. By knocking out FGF9 this epithelial-mesenchymal signaling loop is disturbed and the reduced mesenchymal proliferation leads to an decrease of FGF3, 7, 10 and 22 which is the proximate cause for lung hypoplasia in FGF9<sup>-/-</sup> mice (Beenken and Mohammadi 2009; Colvin et al. 2001b).

## Introduction

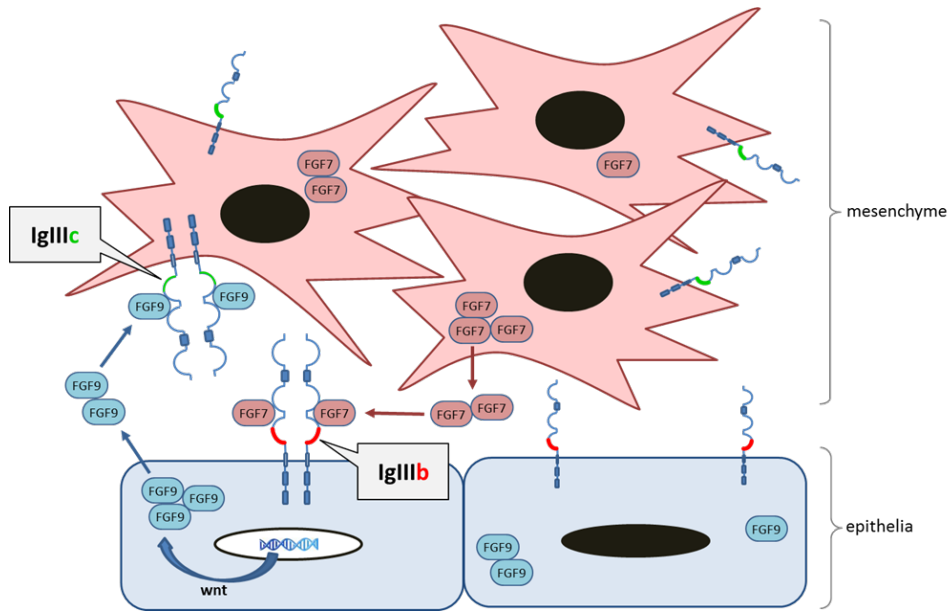


**Figure 37:** Role of different FGF-splice variants in the tissue crosstalk

(Heinzle et al. 2011)

FGF16 is required for embryonic heart development. Elimination of FGF16 expression in mice results in hemorrhage in the heart and ventral body region of the embryo as well as facial defects and embryonic death because of cardiac defects (Lu et al. 2008).

A single nucleotide polymorphism which leads to an increased translation in FGF20 has been related with Parkinson disease (van der Walt et al. 2004).

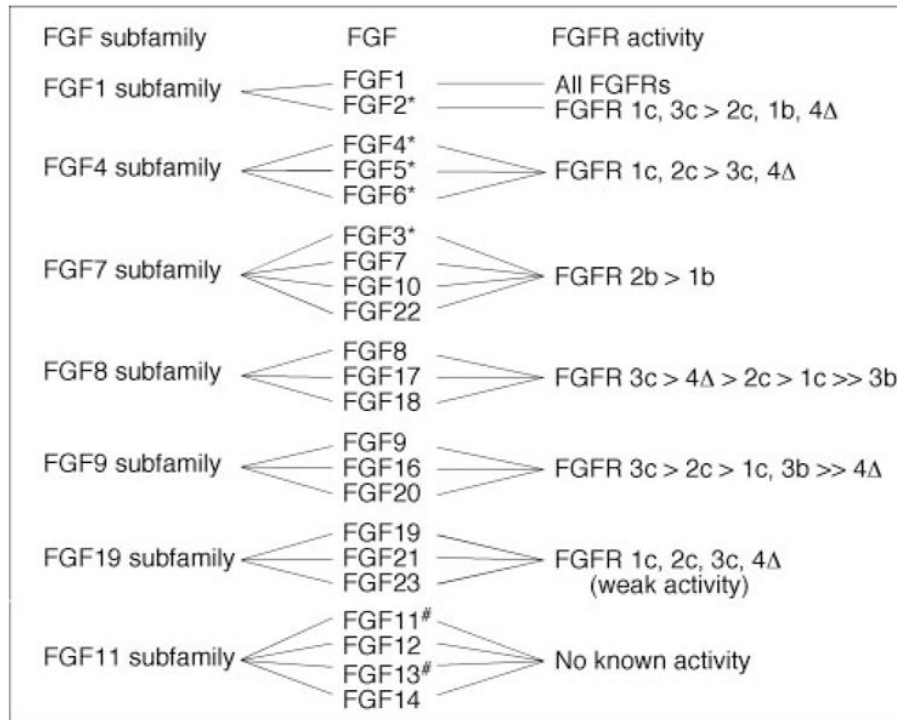


**Figure 38:** Binding affinity of FGF towards their receptors

#... not tested (Ornitz et al. 1996; Zhang et al. 2006)

#### 1.7.4 Deregulation of FGF-signaling in cancer

Deregulation of FGF-signaling promotes tumor development by driving cancer cell proliferation and survival as well as supporting tumor angiogenesis.

Genomic aberrations like activating mutations, gene amplifications, and translocations lead to ligand independent constitutive activation of FGFRs. Another way to deregulate FGF-signaling is the alterations of autocrine production of FGFR ligands in the cell or paracrine production of ligands by stromal cells.

##### 1.7.4.1 Activating mutation

Activating mutations of FGFRs occur in various cancer types. For instance in bladder cancer a lot of FGFR mutations have been described. In more than 30% of all bladder cancers there are somatic mutations of FGFR3 which correspond to the germline mutations found in skeletal dysplasia syndromes (Martinez-Torrecuadrada et al. 2005).

## Introduction

More than half of the FGFR3 mutations in bladder cancer occur in the extracellular domain at a single position which leads to a constitutive dimerization and activation of the receptor. There are also mutations found in the transmembrane domain and in the kinase domain (Trudel et al. 2006).

Apart from bladder cancer, activating mutations of FGFR3 are also found in cervical carcinoma (1,7% mutation rate in FGFR3 worldwide) (Giri et al. 1999), in multiple myeloma (an incurable B-cell malignancy), prostate cancer (above all in low-grade cancers) (Nicholes et al. 2002), as well as in colon carcinoma (Desnoyers et al. 2008) and benign skin tumors (Logie et al. 2005).

Extracellular mutations of FGFR2, which cause craniosynostosis syndromes in germlines, were also found as somatic mutations in gastric (Desnoyers et al. 2008), endometrial, cervical and squamous lung cancer (Powers et al. 2000).

Somatic mutations of FGFR4 in the kinase domain lead to overexpression of FGFR4 and are associated with increased risk of rhabdomyosarcomas (Taylor et al. 2009).

### **1.7.4.2 FGFR gene amplification**

Gene amplifications have been described especially for FGFR1 and 2. FGFR2 gene amplification is mainly observed in gastric cancer. Amplification and activating mutations have been found in FGFR2 in approximately 10% of primary gastric cancer (Knights and Cook 2010; Turner and Grose 2010). Gastric cancer cell lines with amplified FGFR2 showed good response to a VEGFR/FGFR inhibitor (Kunii et al. 2008). Their proliferation and survival is dependent on FGFR2 expression. Blocking of FGFR2 leads to growth arrest and in some cases to apoptosis. There seems to be a crosstalk between FGFR2 and EGFR family kinases, because in FGFR2-amplified cell lines EGFR and ErbB3 phosphorylation was elevated dependent on FGFR2 kinase activity (Kunii et al. 2008).

In normal breast tissue FGF and FGFRs are highly expressed during ductal morphogenesis. Therefore, FGFs are potent mitogens in the mammary gland which, when deregulated could lead to mammary tumorigenesis. In 10-15% of breast cancers



## Introduction

the amplicon 8p11-12p which includes FGFR1 was found. In 4-12% of breast cancers the 10q26 amplicon including FGFR2 is present (Berman et al. 1999).

Further FGFR1 amplification were found in oral squamous cell carcinoma (Simon et al. 2001), ovarian cancer (Gorringe et al. 2007), in 3,4% of bladder cancer (Freier et al. 2007), squamous cell lung cancer (Weiss et al. 2010), and in rhabdomyosarcoma (Cha et al. 2009).

### **1.7.4.3 Chromosomal translocation**

Chromosomal translocations occur mostly in haematological malignancies. Several intragenic translocations affecting FGFRs have been identified. They result typically in a fusion protein where the N-terminus of a transcription factor is fused to an FGFR kinase domain (Turner and Grose 2010).

*Multiple myeloma:* due to translocation on chromosome 14 FGFR3 is brought under the control of the IgH enhancer region and therefore the expression is elevated. FGFR3 inhibition in FGFR3-positive multiple myeloma cell lines showed decreased proliferation and increased apoptosis (Knights and Cook 2010).

*8p11 myeloproliferative syndrome (EMS):* chimeric proteins which contain the kinase domain of FGFR1 fused to a number of unrelated partners are very frequent in EMS. Ligand-independent dimerisation of the fusion protein results in an activation of FGFR1 kinase (Knights and Cook 2010).

### **1.7.4.4 Autocrine and paracrine signaling**

Deregulation of autocrine and paracrine production of FGFR ligands can also lead to aberrant signaling. An autocrine loop between FGF2 and FGFR1 could be shown in melanoma (Wang and Becker 1997). In ovarian cancer tissue amplification of FGF1 showed increased angiogenesis which results in paracrine and autocrine stimulation of cancer cells (Birrer et al. 2007).

In different cancer types there are elevated plasma levels of FGF2 and other FGFs which results partly from tumor invasion and degradation of extracellular matrix and

## Introduction

consequently release of FGFs. Tumor cells induce the release of FGF2 from stromal inflammatory infiltrate which also promotes angiogenesis and therefore acts in a paracrine loop (Turner and Grose 2010).

FGF2 is up-regulated in prostate cancer cells that were stimulated in a paracrine way through elevated expression of FGF2 by surrounding stromal and endothelial cells. Additional, FGFR1 and FGFR2 are both over-expressed in prostate cancer epithelial cells (Giri et al. 1999).

FGF2 is up-regulated in lung cancer where it shows intracrine action. In rapid growing lung cancer cells for example a large fraction of FGF2 is not secreted but stored in the cells where it stimulates proliferation. Due to the intracrine activity of FGF2 in lung cancer these cells are insensitive to exogenous modulation of FGF2-signaling. In later stages a paracrine activity of FGF2 may occur by cytolysis of the cells within the tumor tissue and therefore release of FGF2 (Berger et al. 1999). In breast cancer stroma there are also higher levels of FGF1, FGF2, and FGF7 than in normal breast stroma (Turner and Grose 2010).

Over-expression of FGF5 has been observed in many tumor types, e.g. renal cell carcinoma, prostate carcinoma, breast cancer cell lines (Hanada et al. 2001), in astrocytic brain tumor tissue (Allerstorfer et al. 2008) and in melanomas (Metzner et al. 2011).

Elevated levels of hormonal FGFs like FGF19 lead to hepatocellular cancer in transgenic mice, which shows an endocrine action in the tumor. FGF19 was also found over-expressed in liver, colonic and lung squamous carcinomas (Nicholes et al. 2002). Blockage of FGF19 inhibits interaction with FGFR4 and leads to inhibition of growth of colon tumor xenografts (Desnoyers et al. 2008).

### **1.7.4.5 Germline single nucleotide polymorphism**

Germline polymorphisms can be associated with different susceptibilities for various diseases like diabetes, hypertension and also cancer but also other non-pathological phenotypes. There are numerous examples of these cancer-associated genetic variations in humans (Hunter and Crawford 2006). A SNP in intron 2 of FGFR2 was associated

with an increased risk for breast cancer (Furdui et al. 2006). Little is known about how the SNP in FGFR2 increases the breast cancer risk. One possible explanation is the modification of the binding site of two transcription factors OCT1 and RUNX2 (Turner and Grose 2010).

Another SNP is described in FGFR4. The importance of the G388R polymorphism in cancer is explained in detail in chapter 1.7.2.4.3.

### **1.7.4.6 Alteration of FGFR-splicing**

There are a variety of FGFR isoforms generated by differential splicing of the FGFR RNA. Differential splicing in the IgIII-loop region results in two isoforms: IIIb and IIIc. The two isoforms IIIb and IIIc occur in FGFR1-3 but not in FGFR4 and display different ligand-binding characteristics. Furthermore, they can be expressed in different tissues, e.g. FGFR2IIIb isoform which is only expressed in epithelial cells and FGFR2IIIc which is exclusively expressed in mesenchymal cells (Eswarakumar et al. 2005).

In malignant cells altered splicing leads to the expression of mesenchyme-specific FGFR (IIIc) which expands the range of binding FGFs (Zhang et al. 2006). Therefore, a switch of IIIb to IIIc expression can result in tumor progression, EMT and invasiveness. For example FGFR2IIIb down-regulation is associated with bladder cancer (Ricol et al. 1999) and prostate cancer (Matsubara et al. 1998).

In CRC FGFR3IIIb is down-regulated. The IIIc/IIIb ratio is therefore increased but not due to a higher expression of FGFR3IIIc. Inhibition of FGFR3IIIc in CRC results in decreased growth and survival in vivo and in vitro (Sonvilla et al. 2010).

### **1.7.5 Role of FGF-signaling in colorectal cancer**

FGF7 and FGFR2IIIb were found to be co-expressed in colon cancer tissue. A high FGF7 expression was also detected in neuroendocrine cells which are lying in close proximity to the cancer cells suggesting an autocrine and paracrine stimulation of FGF7 in colon cancer cells (Watanabe et al. 2000). FGF7, which is usually expressed by

## Introduction

mesenchymal cells and acts via FGFR2IIIb on epithelial cells, raises the expression of VEGF-A whereas the expression of FGF2 and hepatocyte growth factor (HGF) remains low in colorectal cell lines. VEGF-A, FGF2 and HGF are very important angiogenic growth factors contributing to the formation of microvessels adjacent to the tumor cells. The reason why FGF7 stimulates VEGF-A but not FGF2 and HGF remains unclear (Narita et al. 2009). FGF2, which acts as a lymphangiogenic growth factor, was found to be down-regulated in human CRC tissue compared to normal mucosa (Sundlisaeter et al. 2009).

FGFR3 is expressed ubiquitously in normal human colorectal epithelial cells. In human CRCs the expression of FGFR3 is decreased by aberrant splicing which results in altered and inactive FGFR3 transcripts (Jang et al. 2000). Whereas FGFR3 (FGFR3IIIb) expression is decreased, expression of FGFR1 (FGFR1IIIc) in CRC cell lines is elevated. Disruption of FGFR1 expression leads to an increase of FGFR3 expression, which assumes a reciprocal relationship between the expression of FGFR1 and FGFR3 (Jang 2005). Another study reported a strong correlation of FGFR1 over-expression and presence of liver metastasis in CRC patients (Sato et al. 2009).

Although there are only few reports about the role of FGFR4 in CRC, one group found FGFR4 to be elevated in blood serum of CRC patients by using a protein microarray (Babel et al. 2009). The impact of the FGFR4 G388R polymorphism in CRC has already been described in chapter 1.7.2.4.4

There might be a potential involvement of FGF19 and FGFR4 interaction with the regulation of E-cadherin/ $\beta$ -catenin system. Exogenous FGF19 stimulates the tyrosine phosphorylation of  $\beta$ -catenin which leads to a loss of E-cadherin/ $\beta$ -catenin binding and results in increased cell growth and invasiveness in colon carcinoma cell lines. Blocking of FGF19 or FGFR4 leads to an inhibition of  $\beta$ -catenin activation and also shows impact on  $\beta$ -catenin target genes (Pai et al. 2008).

The Wnt-pathway is often affected in CRC. FGF18, which is another ligand to FGFR4, is a target of the canonical Wnt-pathway and consequently affected by Wnt-signaling alterations. Furthermore, FGF18 has an oncogenic role in CRC. In a small cohort of CRC specimen FGF18 was found to be almost generally over-expressed compared to normal mucosa. This could also be shown in vitro: adenoma cell lines showed lower

## Introduction

FGF18 expression than CRC cell lines. Up-regulation of FGF18 in CRC stimulates both cell proliferation and cell survival (Sonvilla et al. 2008).

Apart from FGF18 also FGF16 and FGF20 are targets of the canonical Wnt-pathway. FGF20 together with FGF2 are the major FGFs implicated in embryogenesis and tissue regeneration in colon. Like FGF18 FGF20 is up-regulated in CRC with activated Wnt-signaling (Katoh 2006b).

### **1.7.6 Therapeutic strategies affecting FGF-signaling in cancer**

Since FGFR deregulation in cancer leads to activation of Raf-MEK1/2-ERK1/2 and PI3K-PKB pathways, inhibition of FGFRs results in decreased proliferation and induced apoptosis. Therefore, different approaches for inhibition of FGFRs should be considered.

#### **1.7.6.1 Small molecule FGFR kinase inhibitors**

Several small molecule inhibitors against FGFRs have been developed in the past decade but have not been successful in clinical trials so far. Because of the broad expression pattern of FGFRs throughout the whole body, the side effects of FGFR-inhibitors can be severe. For instance PD173074 is a small molecule FGFR kinase inhibitor which inhibits FGFR1-3 and therefore FGFR-dependent growth and survival in different cancer cell lines. Due to toxicity issues PD173074 has been dropped from clinical development (Knights and Cook 2010; Kunii et al. 2008).

Most of the FGFR kinase inhibitors also act on VEGFR and PDGFR because of their structural similarities to the FGFR. This means that VEGFR kinase inhibitors also act on FGFR. Therefore, it is not surprising that most FGFR kinase inhibitors which have reached clinical phase II/III are combined with VEGFR and/or PDGFR inhibitors. Although the inhibition spectrum is broader the side effects (fatigue, hypertension and gastrointestinal complications) are quite mild compared to conventional cytotoxic chemotherapies (Knights and Cook 2010).

### **1.7.6.2 Antagonistic antibodies to FGFRs**

Due to their high specificity antibodies can not only be produced against each FGFR but also target different splice variants which are over-expressed in tumor cells. This high specificity should also result in less systemic side effects.

A ligand-competitive antibody binding to FGFR3 stopped cell proliferation in bladder carcinoma cells (Martinez-Torrecedrada et al. 2005) and in multiple myeloma cell lines (Qing et al. 2009; Trudel et al. 2006). It is active against wild-type and mutated forms of FGFR3 and did also enter into clinical trial.

Another antibody blocking FGFR1IIIc variant could indeed block potently FGF-signaling but also resulted in severe anorexia in an animal model (Sun et al. 2007). These results demonstrate that even in the case of high specific targeting of FGFR3 side effects can still represent a relevant problem.

A more successful strategy could be targeting autocrine/paracrine FGFs like FGF19 which blocks interaction with FGFR4 and inhibits growth of colon tumor xenografts in mice (Desnoyers et al. 2008). Unfortunately no comments on side effects of the antibody are given from this study.

Both small molecule kinase inhibitors and blocking antibodies have been described successfully for FGFR1-3. FGFR4 is less affected by these strategies; at least there are only few reports about effectually targeting FGFR4. As described in Table 3 the  $IC_{50}$  values for many FGFR kinase inhibitors are much higher for FGFR4 than for the other FGFRs. This leads to the assumption that the kinase domain of FGFR4 may be different compared to FGFR1-3. These findings together with the fact that FGFR4<sup>-/-</sup> as well as FGF19<sup>-/-</sup> mice develop normally without gross abnormalities (Desnoyers et al. 2008) identify the FGFR4 as an interesting therapeutic target.

## Introduction

compound	Activity towards specific receptors IC <sub>50</sub> in nM							
	FGFR1	FGFR2	FGFR3	FGFR4	VEGFR1/2	PDGFR	EGFR	
BIBF1120	70	40	110	610	13-34	60	>50000	
CHIR-258	8	n.d.	9	n.d.	10-13	200	20000	
PD173074	20-30					18	>50000	
PD166866								
brivanib	148	n.d.	n.d.	n.d.	380	>6000	>1900	
pazopanib	140	n.d.	130	800	10-50	70-80	n.d.	
ponatinib	2.2				1.5	1.1		
SU5402	20-30	20-30	20-30		0.4	60	100000	
RO4383596	29					44	33	310

**Table 3:** FGFR kinase inhibitors

(Heinzle et al. 2011)





## 2 Aims of this project

So far there are few reports concerning the impact of FGFR4 signaling on colorectal cancer. Regarding the role of FGFR4 G388R polymorphism the reports are even contradictory. Hence it was the intention of this work to clarify the role of FGFR4 and the G388R polymorphism in human colorectal cancer. For this purpose the following issues were to be addressed:

- The cellular effects of FGFR4 over-expression in colorectal cancer cell lines.
- Differences in biological impact in vitro and in vivo between FGFR4<sup>Arg</sup> and the FGFR4<sup>Gly</sup> polymorphic variants.
- The role of the FGFR4 expression and the G388R polymorphism in the pathogenesis of human colorectal cancers and in relation to histopathological parameters.
- Assessment of FGFR4 inhibiting strategies for growth inhibition in colorectal cancer.

Conclusions from evaluated data should discuss the suitability of FGFR4 and FGFR4 G388R polymorphism as a therapeutic target in colorectal cancer at best.



### 3 Materials and methods

#### 3.1 Cell Biology

##### 3.1.1 Materials used for cell culture

Petri dishes, 10cm and 6 cm:	Sarsted, Nümbrecht, G
6-well plates, 24-well plates and 96-well plates:	Sarsted
Eagles Minimal Essential Medium (MEM):	Sigma-Aldrich, St. Louis, MO, US
RPMI-1640 Medium 10x:	Sigma
Penicillin/Streptomycin (Penstrep):	PAA, Pasching, A
Fetal Calf Serum (FCS):	PAA
Phosphate Buffered Saline (PBS):	Sigma
PBS/EDTA: 10mM EDTA in PBS	Merck, Darmstadt, G
Trypsin/PBS 10x: for use diluted 1:10 in PBS,	PAA
L-Glutamine 200mM:	PAA
Bovine Serum Albumin (BSA):	Sigma
G418 (Genticin):	PAA
Doxycycline:	Sigma
Puromycine:	Sigma

##### 3.1.2 Cell lines

Cell lines used are SW480, HCT116 and HT29 and were obtained from the American Type Culture Collection (ATCC).

## Materials and methods

Cells	Source	Characteristics	Medium	Doubling time
<b>SW480</b>	human colorectal adenocarcinoma, male	Chromosome number is hypertriploid, elevated expression of p53, positive expression of c-myc, K-ras, H-ras, N-ras, myb, sis and fos oncogenes, mutation in codon 12 of ras protooncogene	MEM with 10% FCS and 4% Penstrep	24h
<b>HCT116</b>	human colorectal carcinoma, male	diploid, mutation in codon 13 of ras protooncogene	MEM with 10% FCS and 4% Penstrep	24h
<b>HT29</b>	human colorectal adenocarcinoma, female	hypertriploid, elevated expression of p53 antigen, positive expression of c-myc, K-ras, H-ras, N-ras, myb, sis and fos oncogenes,	MEM with 10% FCS and 4% Penstrep	36h

**Table 4:** Description of CRC cell lines

### 3.1.3 Passaging of cells

SW480, HCT116 and HT29 cells are split when they reach a confluence of 90%. Medium is aspirated and cells are washed with 5-10ml of PBS/EDTA. After removal of PBS/EDTA cells are trypsinized with 0,5ml Trypsin/PBS and incubated for 5-10min at 37°C. The detached cells are taken up in 10ml medium and passaged into new 10cm Petri dishes. SW480 and HCT116 are usually split 1:10, for HT29 a ratio of 1:5 was used.

### 3.1.4 Viability assays

#### 3.1.4.1 Neutral red uptake

Neutral red is taken up by intact cells and stored in their lysosomes, where due to the acidic pH-value it changes its color into pink red. Dead cells cannot store neutral red and are therefore not stained.

Cells were seeded at different densities (from  $1 \cdot 10^4$ - $5 \cdot 10^4$  in 24-well plates, from  $1 \cdot 10^3$ - $1 \cdot 10^4$  in 96-well plates). After treatment or after specific time a neutral red solution is prepared by dissolving 50µg neutral red (Merck) per 1ml serum free medium (SFM) and incubated for 1h at 37°C. After filtration 500µl are added to each 24-well (200µl for each 96-well) and the plates are incubated at 37°C for 2h. Neutral red solution is aspirated, cells are washed with PBS and incubated with 250µl (100µl in 96-

## Materials and methods

well) 70% Ethanol + 1% acetic acid for 5min at room temperature on a shaker. Color extinction is measured at 562nm wavelength using 620nm wavelength as reference by microplate reader Synergy H1 (Szabo Scandic, Vienna, A).

### **3.1.4.2 MTT assay: EZ4U**

Water soluble yellow tetrazolium salt is taken up by viable cells and reduced to an intense colored formazan by chemical reduction through mitochondrial enzyme succinate dehydrogenase and NADH/NADPH producing enzymes of the endoplasmatic reticulum.

$1 \cdot 10^3$  cells are seeded into 96-well plate and after treatment or various time points medium is replaced by 100 $\mu$ l of freshly prepared EZ4U solution (EZ4U, Biomedica, Vienna, A). Cells are incubated for 2h and color extinction is measured at 450nm wavelength with 620nm as a reference each 15min for 1h by microplate reader Synergy H1 (Szabo Scandic).

### **3.1.5 Colony formation assay**

Cells are seeded at very low density (100 and 200 cells/well) into 6-well plates. Therefore cells are forced to attach and grow independently without any cell-cell-contact. After 24h medium is replaced and the plates are incubated for various days. After reaching a desirable size of the colonies, medium is aspirated. The plates are washed with PBS and fixated with 100% methanol for at least 20min at -20°C. After removing methanol the plates are washed with PBS and stained for 5min with 0,01% crystal violet solution in PBS. The plates are washed two times with PBS and dried colonies are counted.

### **3.1.6 Filter migration assay**

PET track-etched membranes (VWR, Vienna, A) with a pore size of 8 $\mu$ m are connected to 24-well plates. 800 $\mu$ l medium is added to the lower chamber whereas cells are seeded at a concentration of  $2 \cdot 10^4$  cell/200 $\mu$ l medium on the membrane. After 48h (SW480 and HCT116) or 72h (HT29) migration time the membrane filters are removed and

## Materials and methods

migrated cells in the lower chamber are grown for another three days. Wells are washed with PBS and cells are fixed with 100% ice cold methanol for 20min at -20°C. After washing with PBS cells are stained with 0,01% crystal violet solution in PBS for 5min. Wells are washed two times with PBS, dried and stained area is calculated by Lucia Morphometry Software (Laboratory Imaging, Praha, CZ)

### **3.1.7 Anchorage independent growth: soft agar assay**

Soft agar assay is an advanced version of colony formation assay and used to determine malignant growth of cells. Cells are forced to grow in 3-dimensional colonies without attachment to a surface suspended in an agar matrix.

51 ml soft agar medium is prepared freshly following the recipe:

10ml	10x RPMI
2ml	1,31M NaHCO <sub>3</sub>
1ml	L-Glutamine
17ml	A. bidest
50µl	folic acid solution (20mg folic acid diluted in 10ml 1,31M NaHCO <sub>3</sub> )

pH-value is adjusted on 8 and the solution is sterile filtered. 20ml FCS and 1ml Penstrep are added.

6-well plates are coated with 1,5ml of a 1:1 mixture of 1% agar and soft agar medium. On the next day 5.000 cells are diluted in 750µl soft agar medium and 750µl 0,5% agar and are carefully plated on the prepared agar plates, strictly avoiding air bubbles. After 2-3 weeks colonies of five representative fields of view of each well are counted under the microscope.

### **3.1.8 H<sup>3</sup>-thymidine incorporation**

H<sup>3</sup>-thymidine is incorporated into new synthesized DNA strands during mitotic division. Therefore the H<sup>3</sup>-thymidine incorporation assay gives information about the proliferation activity of cells.

## Materials and methods

Cells are seeded into 96-well plates at three different concentrations: 2.500, 5.000 and 10.000 cells per well. After 24h the medium is replaced by 50µl H<sup>3</sup>-thymidine solution (1mCi/ml) (Perkin Elmer, Waltham, MA, US) and incubated for 90min for SW480 and HCT116 and 3h for HT29. H<sup>3</sup>-thymidine solution is discarded and cells are washed three times with 200µl PBS. Cells are lysed with 100µl lysis buffer (0,2 % TritonX100 and 2mM EDTA in PBS) and transferred into scintillation vials. 100µl PBS are added to the wells and transfused to the corresponding vial. 2ml scintillation buffer (Zinsser Analytic, Frankfurt, G) are added to each vial and H<sup>3</sup>-thymidine incorporation is measured by a Liquid Scintillation Analyzer (Canberra Packard, Meriden, CT, US) for 2min per vial.

### H<sup>3</sup>-thymidine solution:

5 µl	H <sup>3</sup> -thymidine (1ml H <sup>3</sup> -thymidine = 37MBq (1mCi))
1 ml	MEM

### **3.1.9 Fluorescence Activated Cell Sorting (FACS)**

FACS is used to divide cells according to their size, complexity and fluorescence emission. Single cells pass an excitation laser and the emitted light is evaluated by different filters and a photomultiplier.

#### **3.1.9.1 Cells expressing GFP**

Cells expressing a GFP protein are trypsinized and washed twice with PBS. Finally, the pellet is resuspended in 200-500µl PBS, transferred into FACS vials and measured by FACS Calibur (BD, Franklin Lakes, NJ, US).

#### **3.1.9.2 Immuno-flow-cytometry with PE directly labeled antibody: FGFR4**

Cells are trypsinized after reaching a confluence of 50-70%. After counting, 0,25-1\*10<sup>6</sup> cells for each sample are washed with PBS and resuspended in 100µl PBS. Cells are blocked with 30µl FCS for 10min. 13µl PE-conjugated FGFR4 antibody (PE anti-human CD334, #324305, Biolegend, San Diego, CA, US) (to reach a final dilution of

## Materials and methods

1:10) are added and incubated for 2h at room temperature avoiding light. For negative control a Rat Anti-Mouse IgG1 PE antibody (RAM  $\gamma$ 1, #340270, BD) is used in same concentration. Cells are washed twice with PBS, resuspended in 200-500 $\mu$ l PBS and transferred into FACS vials and measured by FACS Calibur.

### 3.1.9.3 Immuno-flow-cytometry with PE indirectly labeled antibody: E-Cadherin

Immuno-flow-cytometry with E-Cadherin antibody is performed as described in chapter 3.1.9.2 except for using 10 $\mu$ g E-Cadherin antibody (monoclonal antibody to E-cadherin (HECD-1), #ALX-804-201-C100, Eubio, Vienna, A) per ml instead of 13 $\mu$ l PE-conjugated antibody. After 2h incubation on ice cells are washed two times with PBS and incubated with 20 $\mu$ l Rat Anti-Mouse IgG1 PE antibody (RAM  $\gamma$ 1; #340270, BD) under light protection for 1h on ice. After washing with PBS cells are transferred into FACS vials and measured by FACS Calibur.

### 3.1.9.4 Cell cycle distribution

Trypsinized cells are washed with PBS and lysed with 1ml Nuclear Isolation buffer for 5min on ice. Nuclei are prepared and separated using a syringe. Quality of isolated nuclei is checked under the microscope. Nuclei are centrifuged at 2.000rpm for 5min at 4°C and the pellet is resuspended in 0,5ml staining solution and transferred into FACS vials. Vials need to be light protected. Cell cycle is measured using FACS Calibur.

#### Nuclear Isolation buffer

10,5g citric acid  
0,5ml Tween 20  
up to 100ml aqua bidest

#### RNAse stock solution

10mg RNAse A  
10ml PBS  
incubate 15 min 100°C  
put on ice immediately; store at -20°C

#### Propidium Iodide (PI) stock solution

5mg Propidium Iodide  
10ml PBS

#### Staining solution

0,05ml RNAse stock solution  
0,05ml PI stock solution  
5ml PBS

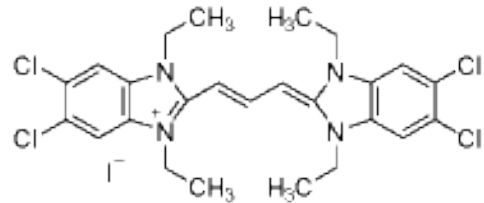


### 3.1.9.5 Induction of Apoptosis: JC-1-FACS

At higher mitochondrial membrane potential the green-fluorescent monomer JC-1 forms red-fluorescent “J-aggregates” which can be measured by FACS. JC-1 is obtained by Sigma.

**Figure 39:** Chemical structure of JC-1

(Picture from website: [http://www.sigmaaldrich.com/catalog/ProductDetail.do?lang=de&N4=T4069|SIGMA&N5=SEARCH\\_CONCAT\\_PNO|BRAND\\_KEY&F=SPEC](http://www.sigmaaldrich.com/catalog/ProductDetail.do?lang=de&N4=T4069|SIGMA&N5=SEARCH_CONCAT_PNO|BRAND_KEY&F=SPEC); 11.7.2011)



Harvested cells by trypsination are centrifuged down and resuspended in JC-1-solution (10µg JC-1 per 1ml MEM). Negative control for each sample is not mixed with JC-1-solution. After 10min light protected incubation at 37°C cells are washed two times with PBS and resuspended in 200-500µl PBS. Apoptosis is measured by FACS Calibur.

### 3.1.10 Cell Sorting

Cells are trypsinized after reaching 50-70% confluence and spun down. Cell pellet is resuspended in 1ml SFM with Penstrep and transferred into FACS vials. Cells expressing a fluorescent protein (e.g. GFP) are sorted directly whereas non-fluorescent cells are first incubated with PE-conjugated antibodies according to the protocol described in chapters 3.1.9.2 and 3.1.9.3. Sorting is carried out by FACS Calibur and cells are sorted into BSA-coated 50ml tubes which contain 5ml medium. Sorted cells are centrifuged and transferred into Petri dishes with prewarmed medium.

### 3.1.11 Immunofluorescence staining

$2 \cdot 10^4$  cells are seeded on collagen coated glass slides in 96-well flexiPERM (Greiner-Bio-One, Frickenhausen, G) and incubated over night. After removing the flexiPERM and washing the slides two times with cold PBS, cells are fixed either with methanol/aceton 3:1 for 2-5min at -20°C or 4% formaldehyd-solution (Roti<sup>®</sup>-Histofix 4%, Carl Roth GmbH + Co. KG, Karlsruhe, G) for 30min at room temperature. Formaldehyd fixed cells are additionally incubated with 47mM NH<sub>4</sub>Cl solution for

## Materials and methods

5min. After washing with cold PBS for 5min, incubating with 0,5% TritonX in PBS for 5min and again washing with cold PBS for 5min, the cells are blocked with 0,2% fish gelatine in PBS for 30min at room temperature. 1<sup>st</sup> antibody is diluted 1:100 in 0,2% fish gelatine/PBS solution and is added for 1h after discarding the blocking solution. Slides are then washed three times with cold PBS each for 5min and the 2<sup>nd</sup> antibody (1:1.000 in blocking solution) is added for 45min. TO-PRO<sup>®</sup>-3 iodide (642/661) (Invitrogen, San Diego, CA, US) was used as counterstaining and diluted at a concentration of 1:10.000 into the 2<sup>nd</sup> antibody-solution.

After incubation slides are washed three times with PBS and one time with A.bidest. Cells are mounted with a few drops Mowiol and a 24x40mm cover slide.

### 1<sup>st</sup> Antibodies

Purified Mouse Anti- $\beta$ -Catenin, (# 610154, BD)

Purified Mouse Anti-E-Cadherin, (#610182, BD)

### 2<sup>nd</sup> Antibody

Alexa Fluor<sup>®</sup> 488 goat anti-mouse IgG (H+L) (#A-11001, Invitrogen)

### **3.1.12 Plasmids**

Plasmids are circular double-stranded DNA-molecules which are naturally found in bacteria. They are a separate form of DNA and can also be replicated independently from the chromosomal DNA. Because they are transferable genetic elements, plasmids play a crucial role for gene-transfer into eukaryotic cells, multiplication and expression of particular genes. Plasmids used for genetic engineering are called 'vectors'. They usually contain a polylinker or multiple cloning sites, which consist of dozens of restriction enzyme recognition sites. Multiple cloning sites are essential for excision or insertion of any DNA fragment. Apart from the multiple cloning site plasmids also have two selection markers which are usually gene-sequences for a particular antibiotic-resistance. One antibiotic-gene serves for bacterial selection marker and the other one for eukaryotic selection marker.

## Materials and methods

Name	Promoter	Resistance in E.coli	Resistance in human cells	Description
pcDNA3 VSV/FGFR4 G388R	CMV	Ampicilin	G418	Mammalian expression vector for FGFR4 which consists of a transmembrane point mutation glycine to arginine at position 388 with VSV tag
pcDNA3 VSV/FGFR4 WT	CMV	Ampicilin	G418	Mammalian expression vector for FGFR4 with VSV tag
pK5-IRESneo	CMV	Ampicilin	G418	See 3.3.1.1
pcDNA3	CMV	Ampicilin	G418	Mammalian expression vector which is used as control vector
EGFP	CMV	Kanamycin	G418	Mammalian expression vector which encodes for green fluorescent protein (GFP)
pTet-Off-Advanced	CMV	Ampicilin	G418	See 3.3.1.2
pTRE-Tight	Tet-responsive P <sub>tight</sub> promoter	Ampicilin	---	See 3.3.1.3

**Table 5:** Vectors used in this work

Both FGFR4 over-expression vectors were kindly provided by Axel Ullrich.

### 3.1.13 Transfection

There are various ways to integrate a DNA sequence into cells: physical, chemical and viral. One of the easiest ways is lipofection. For this purpose, DNA is packed into lipid micelles which can attach to the cell surface and are taken up by the cell via endocytosis. For stable integration of DNA sequences into the cellular genome the transfected vector needs a selection marker which is usually an antibiotic resistance gene. Antibiotic treatment after transfection kills all cells which have not integrated the plasmid into their genome.

24-48h before transfection 6-well plates are inoculated with  $3 \times 10^5$  cells per well. Medium is aspirated before transfection and 1,5ml new medium is added. Transfection is carried out with TransFectin<sup>TM</sup> Lipid Reagent (Bio-Rad, Philadelphia, PA, US). 10 $\mu$ l TransFectin is mixed with 250 $\mu$ l SFM. 2 $\mu$ g plasmid is mixed with 250 $\mu$ l SFM. Plasmid and TransFectin solution are gently mixed together and after 20min added to the plate. After 6h DNA-TransFectin complexes are replaced by new medium.

### 3.1.14 Selection

24h after transfection cells are transferred from 6-well plates into 10cm Petri dishes. For most of our experiments Geneticin (G418) is used as selection agent and added 48h

## Materials and methods

after transfection. G418 is an aminoglycoside antibiotic which blocks protein synthesis. For each transfection untransfected cells were used as G418-negative control and therefore as a marker for the selection efficiency. After 3-5 weeks the first clones were picked by using cloning rings or cells were grown to mixed clone population. The concentration of G418 necessary for selection depends on the cell line (see Table 6)

Cell line	G418 concentration for selection [mg/ml]	G418 concentration for cell culture [mg/ml]
SW480	0,6	0,3
HCT116	1,0	0,5
HT29	0,9	0,45

**Table 6:** Selection conditions for cell lines

### 3.1.15 Small interfering RNA (siRNA) mediated gene knock down

Small interfering RNAs are double-strand RNAs and consist of 21-28 nucleotides. After entering the nucleus they are integrated into a protein complex called RNA-Induced Silencing Complex (RISC) and bind specifically to the mRNA. Due to the endonuclease activity of RISC the mRNA is degraded. Three different siRNAs against FGFR4 (#4390824, Ambion, Applied Biosystems, Carlsbad, CA, US) were tested and two are used for experiments. A scrambled siRNA Silencer<sup>®</sup> Select Negative Control (#4390844, Ambion) was used as negative control.

Cells are seeded at various densities into plates (6-well plate:  $3 \cdot 10^5$ /well, 24-well plate:  $1 \cdot 10^4$ /well; 96-well plate:  $2,5 \cdot 10^3$ ,  $5 \cdot 10^3$  and  $1 \cdot 10^4$ / well). After 24-48h medium is replaced. For transfection siLentFect<sup>™</sup> Lipid Reagent (Bio-Rad) is mixed with SFM according to the instruction manual (for 6-well plate:  $3 \mu\text{l}/125 \mu\text{l}$  SFM; 24-well plate:  $1 \mu\text{l}/25 \mu\text{l}$  SFM; 96-well plate:  $0,2 \mu\text{l}/10 \mu\text{l}$  SFM). In a separate vial siRNA is mixed with SFM ( $125 \mu\text{l}$ ,  $25 \mu\text{l}$  or  $10 \mu\text{l}$ ) so that a final concentration of 10nM is reached. siRNA and siLentFect are gently mixed together and after 20min added to the cells. Medium is aspirated after 6h (SW480) or after 24h (HCT116 and HT29) and new medium is added. 48h after transfection HCT116 are used for assays. 72h after transfection SW480 and HT29 are seeded for assays.

### 3.1.16 Luciferase

For the dual-luciferase reporter system two different constructs are essential: a vector carrying a firefly luciferase which is the “experimental reporter” downstream of the promoter element of interest and a vector carrying a renilla luciferase downstream of a constitutive promoter which acts as a “control reporter”. The activity of the experimental reporter is normalized to the activity of the control reporter and therefore differences in pipetting volumes, transfection efficiency etc. are minimized.

Renilla and firefly luciferase are both capable to catalyze a chemical reaction that causes light to be emitted.

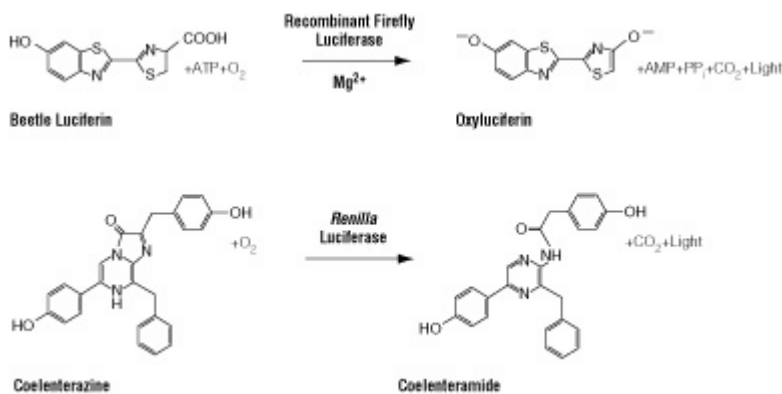


**Figure 40:** Bioluminescent reaction catalyzed by firefly and renilla luciferase

(Picture from website: <http://www.promega.com/paguide/chap8.htm>; 11.7.2011)

In our experiments  $\beta$ -catenin dependent promoter activity was determined using two different firefly luciferase constructs: Top and Fop. The Top promoter element consists of repeats of the  $\beta$ -catenin-binding consensus sequence so that luciferase vector can be expressed, when  $\beta$ -catenin is localized into the nucleus and binds to the luciferase promoter region. Fop sequence serves as a negative control because it carries a mutation preventing  $\beta$ -catenin binding to the promoter and therefore no luciferase can be expressed.

To carry out the luciferase assay the Dual-Luciferase<sup>®</sup> Reporter Assay System from Promega (Madison, WI, US) is used.  $5 \times 10^4$  cells are seeded in each well of a 24-well-plate. On the next day cells are transfected with 1ng renilla plasmid and with either 1 $\mu$ g

## Materials and methods

Top or 1µg Fop plasmid by using Transfectin (Bio-Rad) and the corresponding protocol (see chapter 3.1.13). 24h later cells are treated with 10mM lithiumchlorid. After waiting another 24h cells are washed with PBS and lysed with 100µl Passive Lysis Buffer by shaking for 15min at room temperature. Lysates are transferred into Eppendorfer tubes, exposed to ultrasound for 10min, and centrifuged for 5min at 15.000rpm. 10µl supernatant is pipetted onto a 96-well plate (Greiner-Bio-One) and 50µl Luciferase Assay Reagent II (LAR II) is added. LAR II leads to light emission triggered by firefly and chemoluminescence is measured for 10sec at the luminoscan RS-luminometer (Labsystems, Franklin, MA, US). By adding 50µl Stop&Glow-reagent firefly luciferase activity is inhibited and renilla luciferase is activated. Chemiluminescence is again measured for 10sec.

### 3.2 Molecular Biology: RNA

#### 3.2.1 RNA isolation

The culture supernatant is aspirated. 1ml Trifast (Peqlab, Erlangen, G) is added per 10cm Petri dish and incubated for 5min on ice. Cells and Trifast are scraped of the dish using RNase free scrapers (incubated for 10min in 0,1N NaOH, then 10min in 70% EtOH) and transferred into an Eppendorfer tube. 200µl (1/5 of the Trifast amount) Chloroform is added and the tube is vortexed for 30sec and incubated on ice for 10min. The tubes are centrifuged for 15min at 15.000rpm and 4°C. The transparent phase is collected and transferred into a new tube. 500µl isopropanol is added, the tube is vortexed for 30sec and incubated on ice for 10min for the RNA to precipitate. After centrifugation at 12.200rpm for 10min at 4°C the RNA pellet is washed with 1ml 75% EtOH, centrifuged at 15.000 for 15min at 4°C and dried. The pellet is then dissolved into 30-50µl RNase-free-water (DEPC water) and heated for 10min to 65-70°C to denature and dissolve the RNA. The amount of RNA is measured photometrically at 260/280nm by Nano Drop spectrophotometer (Peqlab). RNA is stored at -80°C.

$$\text{Calculation of quantity: } \mu\text{g}/\mu\text{l} = \frac{\text{OD (260nm)} \times 40 \times \text{dilution factor}}{1.000}$$

### 3.2.2 Complementary DNA (cDNA) synthesis

cDNA is complementary to the RNA and synthesized by a reverse transcriptase enzyme.

5µg RNA in 10µl nuclease free water is prepared into sterile PCR-Tubes (Biozym, Hessisch Oldendorf, G). 2,5µl Random Hexamer Primer Master Mix (100µM) is added and heated up to 70°C using a PCR cycler. After 5min 6,5µl Master Mix is added and incubated at 25°C for another 5min. Finally, 1µl Revert Aid™ M-MuLV reverse transcriptase is added and first incubated 10min at 25°C, then heated up to 42°C for 60min before incubating for 10min at 70°C. 80µl nuclease free water is added and the cDNA is stored at -20°C. (Hexa-Primer, dNTP, RNase Inhibitor and Revert Aid™ M-MuLV reverse transcriptase are obtained from Fermentas, St. Leon-Rot, G)

<u>Random Hexamer Primer Master Mix</u>		<u>Master Mix</u>	
Hexa-Primer 100µM	1µl	5x first strand buffer	4µl
DEPC water	1,5µl	dNTP-Mix	2µl
		RNase Inhibitor (20 units)	0,5µl

### 3.2.3 Standard Polymerase Chain Reaction (PCR)

Based on total RNA expression any gene of interest can be qualified and at least semi-quantified by PCR. For this purpose cDNA is used as the template. To separate the double strands cDNA is first denaturized by heating. By lowering the temperature small oligomers, called primers, can bind to specific sequences of a gene. Primers flank a defined sequence of a defined length of the gen of interest. The temperature is raised again so the Taq polymerase, a heat stable polymerase derived from the bacterium *Thermus aquaticus*, can bind to the primer and extends the strand in 5'-3' direction. This cycle (denaturation, annealing and extension) is repeated various times.

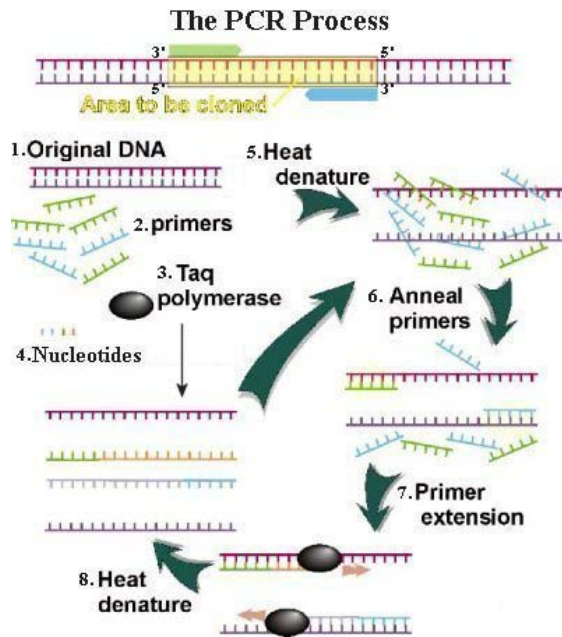


**Figure 41:** The principle of Standard PCR

(Picture from website <http://universe-review.ca/I11-50-PCR.jpg>; 18.7.2011)

PCR is performed on an “iCycler” (Bio-Rad). Components of PCR are pipetted into PCR strips. GAPDH is always taken as reference. (PCR mastermix is obtained from Fermentas)

Components

3' primer	1µl
5' primer	1µl
cDNA	1µl
Mastermix	12,5µl
DEPC water	9,5µl



## Materials and methods

### Conditions

Initial denature:	2 min	94°C
Denature:	40 sec	94°C
Annealing:	40 sec	56°C
Elongation:	40 sec	72°C
Final extension:	7 min	74°C

Name	Sequence: - upstream - downstream	Annealing temperature (°C)	Product size (bp)	Cycles
<b>FGF1</b>	GAAGCCAAACTCCTCTACTGTAGC TGTTGTAATGGTTCTCCTCCAGC	57	259	45
<b>FGF2</b>	CTGTACTGCAAAAACGGG AAAGTATAGCTTTCTGCC	45	349	45
<b>FGF6</b>	AACGTGGGCATCGGCTTTCACCTCC CCCGCTTACCCTCATTTGC	56	301	40
<b>FGF16</b>	ACGTGCCCTTAGCTGACTCC GTTTAGCTGTATCCCTCCCG	56	467	40
<b>FGF17</b>	TGCTGCCAACCTCACTC TCTTGCTCTCCCGCTG	53	361	35
<b>FGFR4</b>	AGCACTGGAGTCTCGTGATG CATAGTGGGTCGAGAGGTAG	56	525	35
<b>GFP</b>	TCGTGACCACCTGACCTGG TCTTTGCTCAGGGCGGAC	54	500	39
<b>GAPDH 53°</b>	CGGGAAGCTTGTGATCAATGG GGCAGTGATGGCATGGACTG	53	369	22
<b>GAPDH 68°</b>	GGCTCTCCAGAACATCATCCCTGC GGGTGCTCGCTTTGAAGTCAGAGG	68	269	22

**Table 7:** Primer for standard PCR

### 3.2.4 Polyacrylamid Gel Electrophoresis

DNA is negatively charged so that it migrates towards the positively charged anode in gel electrophoresis. Due to the net-like gel matrix the DNA is separated according to its size.

6% polyacrylamid gels are cast in a casting stand using 1mm spacers and the reaction mix listed below. When the polymer has formed, 10µl of the PCR-product together with 2µl of 6x loading dye (Fermentas) are loaded onto the gel. For marker, 1µl of a 100bp ladder (Fermentas) with 2µl 6x loading dye is used. The gel is run for 1h at 95V in TAE-buffer. (Gel apparatus and casting stand are obtained from Bio-Rad). Then the gel is stained with ethidiumbromide (0,5mg/ml PBS) (Sigma) that can intercalate in the

## Materials and methods

DNA. The bands are visualized with UV-light using the Gel Doc2000 (Bio-Rad) and quantified using the corresponding software ImageQuant® Version 5.0 (Molecular Dynamics).

### 6% polyacrylamide gel

TAE 50x	150µl
Acrylamide 40%	1,125ml
H <sub>2</sub> O bidest	6,175ml
TEMED	5µl
APS 10%	50µl

### 50x TAE

Tris	242g
acetic acid	57,1ml
0,5 M EDTA	100ml
A. bidest	up to 1l

### 6x loading buffer

urea	0,24g
sucrose	0,4g
bromphenolblue	1mg
xyleneolblue	1mg
1x TAE	up to 1ml

### **3.2.5 Real-time PCR**

The principles of a real-time PCR are quite similar to the Standard PCR but additionally the PCR products can be quantified in real-time (which means at each time point during the PCR) by measuring fluorescence. One possibility is the use of TaqMan® probes that are labeled with a fluorescent reporter dye and with a quencher molecule. As long as the reporter is close to the quencher, no light can be emitted by the reporter. Due to the exonuclease activity of the polymerase the reporter is released from the probe and fluorescence can be measured.

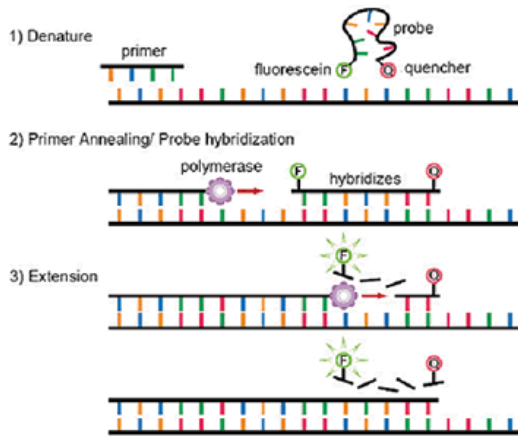


**Figure 42:** The principles of real-time PCR

(Picture from website: [http://biomed.lsu.edu/images/PCR\\_TPM.gif](http://biomed.lsu.edu/images/PCR_TPM.gif); 11.7.2011)

Another possibility to measure fluorescence during real-time PCR is to use a dye which intercalates into the DNA: SybrGreen. The more PCR product is produced the more dye can be integrated and the more light is emitted. To avoid unspecific light emission (for example primer dimers) a melting curve analysis is performed after the PCR run. Double stranded DNA is heated to 95°C for denaturation. The temperature at which the DNA strands are separated is specific for the exact sequence. Larger PCR products have higher melting temperatures than shorter primer dimers so that they can be easily distinguished.

### 3.2.5.1 TaqMan<sup>®</sup> Assays

TaqMan<sup>®</sup> gene expression arrays consist of primers and 6-carboxyfluorescein (FAM) labeled TaqMan<sup>®</sup> probes as well as a dihydrocyclopyrroloindole tripeptide minor groove binder (MGB) as a quencher. The assay is performed on a 96-well plate for real-time arrays. Gene expression quantification is performed as a two-step reverse transcription PCR on the ABI PRISM 7000 instrument using the corresponding software. Gene expression is normalized to a housekeeping gene GAPDH. All TaqMan<sup>®</sup> Assays, cyclers, probes and material are obtained from ABI (Applied Biosystems, Carlsbad, CA, US).

## Materials and methods

### Components

cDNA	1 $\mu$ l
TaqMan <sup>®</sup> probe	1 $\mu$ l
Master Mix	10 $\mu$ l
DEPC water	8 $\mu$ l

### Conditions

Initial denature	10 min	95°C
Denature:	15 sec	95°C
Annealing/Elongation	1 min	60°C

40 cycles

Name	Assay number	Exon
<b>FGFR4</b>	Hs01106913_g1	5-6
<b>FGFR4</b>	Hs00242558_m1	8-9
<b>FGF19</b>	Hs00391591_m1	3
<b>FGF18</b>	Hs00818572_m1	4-5
<b>FGF9</b>	Hs00181829_m1	2-3
<b>E-Cadherin</b>	Hs00170423_m1	3-5
<b>GAPDH</b>	Hs99999905_m1	3

**Table 8:** TaqMan<sup>®</sup> assay kits

### **3.2.5.2 TaqMan<sup>®</sup> Genotyping assay for FGFR4**

A TaqMan<sup>®</sup> Genotyping assay is performed, whereas the probe for Arg388 is labeled with FAM and the probe binding to Gly388 is labeled with VIC. Both probes contain a MGB as a quencher. Components are pipetted on a 96-well Fast plate for real-time PCR and the assay is carried out on the ABI PRISM 7500 instrument using the corresponding software.

## Materials and methods

### Components

3'Primer	0,09µl
5'Primer	0,09µl
Probe Arg388	0,01µl
Probe Gly388	0,01µl
cDNA	2µl
Genotyping Master Mix	5µl
DEPC water	2,8µl

### Conditions

Initial denaturation:	2 min	50°C
Denaturation:	10 sec	95°C
Annealing:	15 sec	95°C
Elongation:	1 min	60°C
40 cycles		

### Sequences

Probe Arg388: FAM-CTG GCC AGG CTG AT-MGB

Probe Gly388: VIC-TGG CCG GGC TGT A-MGB

Primer FGFR4:      forward:      5' CGG GAG AGC TTC TCC ACA CT 3'  
   reverse:      5' GCC AGG TAT ACG GAC ATC ATC CT 3'

### **3.2.5.3 SybrGreen**

QuantiTect® Primer assays (Quiagen) are used and the assay is performed on a 96-well plate for fast real-time arrays. Gene expression quantification is performed as a two-step reverse transcription PCR on the ABI PRISM 7500 instrument using the corresponding software. Gene expression is normalized to a housekeeping gene GAPDH. Primers are the same also used for standard PCR and described in Table 7.

## Materials and methods

### Components

4µl	Maxima™ SYBR Green qPCR Master Mix (Fermentas)
0,3µl	3' Primer
0,3µl	5' Primer
0,1µl	cDNA
3,3µl	nuclease free water

### Conditions

Initial denaturation	10 min	95°C
Denaturation:	15 sec	95°C
Annealing/Elongation	1 min	60°C
40 cycles		

### **3.2.6 Restriction Fragment Length Polymorphism (RFLP) for FGFR4**

#### **3.2.6.1 PCR**

A standard PCR is performed using the protocol described in chapter 3.2.3.

### Conditions

Initial denature:	12 min	94°C
Denature:	30 sec	94°C
Annealing:	30 sec	66(first 5 cycles)/62°C
Elongation:	40 sec	72°C
Final extension:	7 min	72°C
35 cycles		

### Primer

Reverse:	5'-TGC-TGG-AGT-CAG-GCT-GTC-AC-3'
Forward:	5'-GGC-CAG-TCT-CAC-CAC-TGA-CC-3'

### 3.2.6.2 Restriction enzyme digest

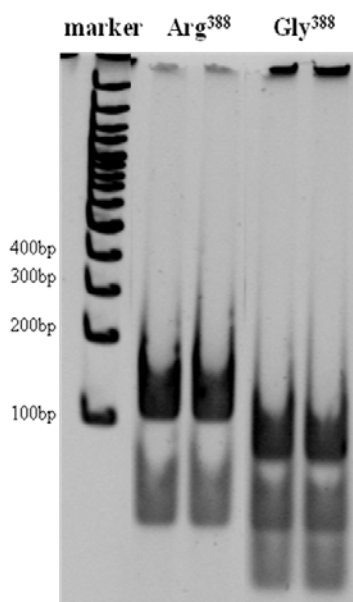
PCR product, enzyme and buffer are prepared in a tube and incubated with MspI for 1h at 37°C and afterwards brought to a polyacrylamid gel.

#### Reaction mix

PCR product	10µl
10x Tango buffer	1,5µl
MspI enzyme	1µl
Water	2,5µl

### 3.2.6.3 Gel

5µl digested PCR product is loaded together with 1µl 6x loading dye on a polyacrylamid gel. The gel is run for 1h at 125V and stained with ethidiumbromide (0,5µg/ml aqua bidest) as described in chapter 3.2.4.



#### Gel compounds

5x TBE	2,4ml
Polyacrylamid 40%	2,76ml
Water	6,48ml
APS	100µl
TEMED	10µl

Undigested PCR product: 167bp

Arg388: ~50bp and 115bp

Gly388: ~30bp, ~50bp and 85bp

**Figure 43:** Gel of RFLP of FGFR4 G388R polymorphism

### 3.3 Tet-Off advanced inducible gene expression system

Tetracycline-controlled transcriptional activation systems are used to induce the transcription of a gene of interest in a reversible mode by presence or absence of the antibiotic tetracycline or one of its derivatives. In this work the Tet-Off<sup>®</sup> Advanced system (Clontech, Mountain View, CA, USA) and Doxycycline as a tetracycline derivative was utilized.

#### 3.3.1 Principles of the tet-off-system

Using the tet-off-system two vectors are necessary: a tet-off-vector and a tetracycline sensitive vector. Both vectors need to be introduced to the cell either by cotransfection or by independent transfection. The tet-off-vector contains the sequence for a tetracycline-controlled transactivator protein (tTA-protein) whereas the tetracycline sensitive vector contains the gene of interest under the control of a Tet-responsive element (TRE). In the absence of tetracycline the tTA-protein binds to the tet-operator (tetO) which is located on the TRE-sequence. Once bound to the tetO, a coupled and modified CMV-promoter is activated which leads to the transcription of the gene of interest. By adding tetracycline, tTA is hindered to bind to the TRE and the gene of interest cannot be transcribed.

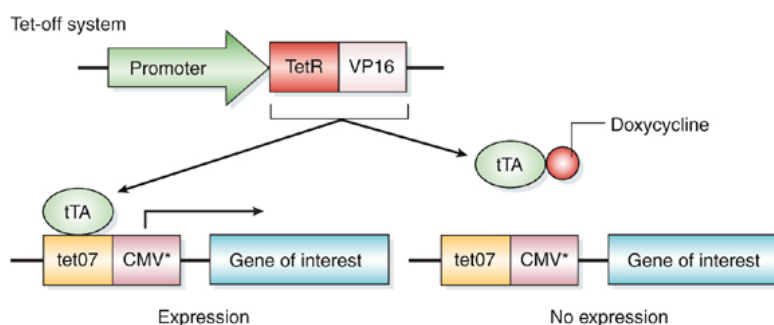


**Figure 44:** Principles of the Tet off system

(Kohan 2008)

Plasmids used for tet-off gene expression system used in this work are *K5*, *pTet-Off-Advanced*, *pTRE-Tight*, and *GFP*.



### 3.3.1.1 K5-vector

The K5-vector contains a dominant negative FGFR4-construct. The kinase-domain of the FGFR4 was substituted by a cyan fluorescent protein (CFP)-molecule which results in a 78kDa artificial protein acting as a decoy-FGFR4. Additionally, an Internal Ribosome Entry Site (IRES) segment is located between the K5 construct and the selection marker neomycin for eukaryotic cells. The IRES-segment forces the cell to translate the K5 construct together with the selection marker and therefore reduces the occurrence of 'fake clones'. An ampicillin-resistance-gene serves as a selection marker in bacteria.

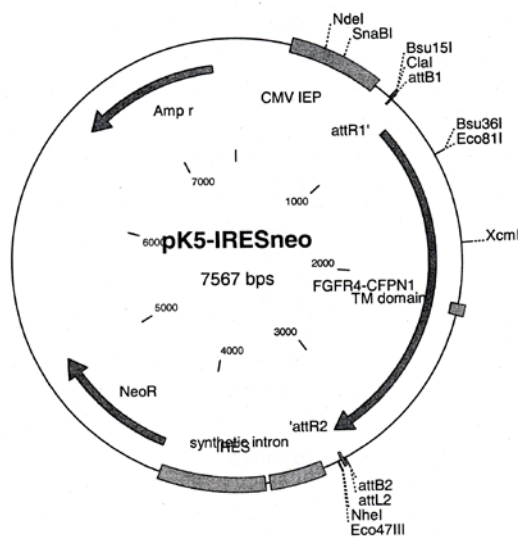


**Figure 45:** K5-vector: a dominant negative construct for FGFR4

### 3.3.1.2 pTet-Off-Advanced-Vector

The pTet-Off-Advanced-vector expresses a completely synthetic protein which is a tetracycline-controlled transactivator protein called tTA-Advanced. This protein consists of 1-207 amino acids of a Tet-Repressor (TetR) and 39 amino acids which contain three minimal transcriptional activation domains from the VP16 protein of herpes simplex virus. The vector contains also a neomycin-resistance for eukaryotic cells and an ampicillin-resistance for bacteria.

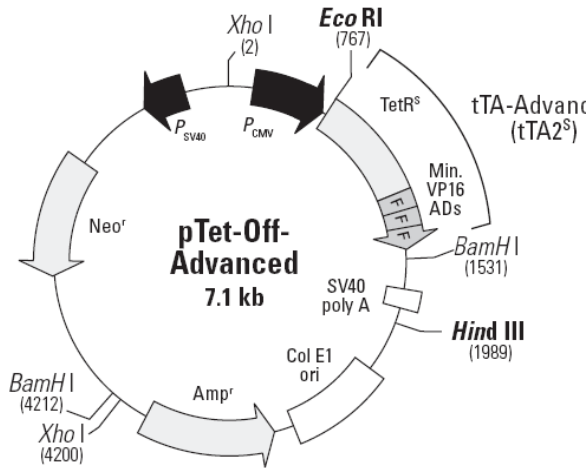


**Figure 46:** pTet-off-Advanced vector

### 3.3.1.3 pTRE-Tight-vector

The pTRE-Tight-vector is the response plasmid to pTet-off-Advanced vector and contains a multiple cloning site (MCS) for the insertion of the gene of interest downstream of the Tet-responsive  $P_{\text{tight}}$  promoter. The  $P_{\text{tight}}$  promoter contains a modified Tet response element ( $Tet_{\text{mod}}$ ) with seven direct repeats of a 36bp sequence that contains a 19bp Tet-Operator sequence ( $TetO$ ). The  $Tet_{\text{mod}}$  is located upstream of a minimal CMV promoter ( $P_{\text{minCMV}\Delta}$ ) which lacks the enhancer (part of a complete CMV-promoter).  $P_{\text{tight}}$  is silenced if no binding to the  $TetO$ -sequence occurs. The pTRE-Tight-vector contains an ampicillin-resistance gene for bacteria but no resistance gene for eukaryotic cells. Consequently a linear puromycin-marker is cotransfected to permit selection of stable transfectants.

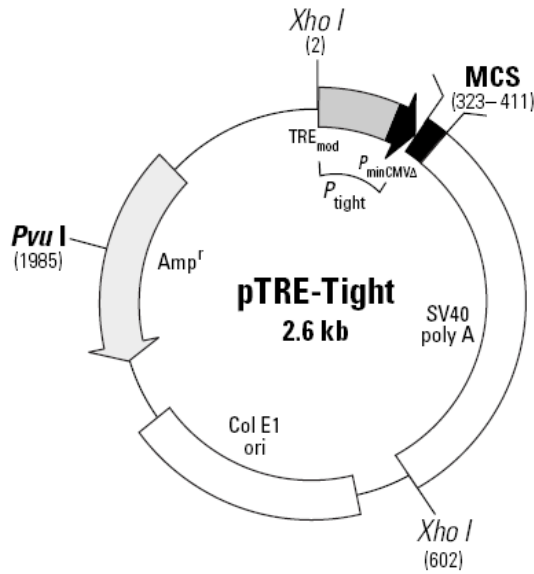


**Figure 47:** pTRE-Tight-vector: the response plasmid

### 3.3.2 Restriction digest

DNA is cut using restriction enzymes at a very specific nucleotide sequence, the restriction site. The conditions for the restriction digest vary with the restriction enzyme. Each enzyme needs a specific 10x-restriction-buffer. Enzymes and buffers are obtained from Fermentas.

For **control restriction digests** the following approach was used:

- 50-150ng Plasmid
- 0,5-1µl enzyme 1
- 0,5-1 µl enzyme 2
- 1µl 10x restriction buffer

fill up with A.bidest to 10µl

For **preparative restriction digests** the following approach was used:

- 4-5µg Plasmid
- 2-3µl enzyme 1
- 2-3µl enzyme 2
- 10µl 10x restriction buffer

fill up with A.bidest to 1000µl

Restriction digest approaches were incubated over night at 37-38°C.

Digested fragments were loaded on a 1% agarose-gel and proper bands were monitored and eventually cut out of the gel.

Big DNA-fragments (e.g. plasmid) need to be incubated with a Calf Intestinal Alkaline Phosphatase (CIAP) (Promega, Madison, WI, USA) enzyme before added to the gel. CIAP prevents the recircularization and relegation of linearized cloning vehicle DNA by removing phosphate groups of the 5'-end of the molecule by hydrolysis.

2µl CIAP were added to 100µl of the preparative restriction digest approach and incubated 30min at 37°C and then 30min at 50°C. This procedure is repeated once more with another 2µl CIAP. To inactivate the enzyme, tubes are incubated 15min at 85°C.

### **3.3.3 DNA-isolation with gel-extraction-kit**

DNA is isolated from the gel according to the protocol of the QIAquick Gel Extraction Kit (Quiagen, Hilden, G). The gel containing the DNA is dissolved by adding three volumes of the buffer QG and incubating for 10min at 50°C. One gel volume of isopropanol is added and the sample is applied to the QIAquick column which is centrifuged for 1min. The DNA binds in the column and the flow-through is discarded. Another 0,5ml of the QG buffer is added to the column and centrifuged again for 1min. The bound DNA is washed with 0,75ml of the PE buffer which needs to be removed completely by centrifugation at 17.900g for 1min. The DNA is eluted with 50µl 10mM Tris-Cl, pH8.5.

### 3.3.4 Ligation

Before ligating the gene-fragments (containing the gene of interest) with the vector, the open and linearized vector needs to be incubated with CIAP (see chapter 3.3.2). For ligation of the cut vector with an insert 40-60ng vector and 50-90ng insert were used. 1µl ligase and 1µl 10x ligase-buffer were added and filled up with A.bidest to 10µl. Approaches were incubated at 16°C over night.

### 3.3.5 Transformation of bacteria

For transformation in this work a XL1Blue *E.coli* bacteria strain was used. 3µl of a 50ng/µl plasmid-solution was added to 100µl bacteria and incubated for 30min on ice. After incubating 1min on 42°C, 1ml SOC-media with a temperature of 4°C was added. Bacteria were agitated for 1,5h on 37°C and finally centrifuged and plated on agar-plates containing ampicillin. Plates were incubated over night at 37°C and clones were picked on the next day for mini-, midi-, or maxi-preps.

### 3.3.6 Plasmid preparation: Mini-, midi-, and maxi-preps

For mini-preps the **boiling-lysis-preparation method** was used. 2ml bacteria culture with appropriate antibiotic selection was incubated over night. On the next day 1ml was transferred into a tube and centrifuged for 1min at 16.000g. The supernatant was discarded and the pellet was resuspended in 700µl STET-buffer (50mM Tris pH8,0; 50mM EDTA pH8,0; 8% sucrose; 5% tritonX) with 13µl lysozyme (10mg/ml) and incubated for 1min at 99°C. Tube was centrifuged for 10min at 14.000g and the pellet was removed with a sterile pipette-tip and discarded. 750µl isopropanol was added and incubated for 20min at -20°C. After centrifugation for 10min at 20.000 and 4°C, supernatant was poured off and pellet was washed briefly with cold 70% ethanol. Tube was centrifuged for 5min at 16.000g and supernatant was discarded while pellet was dried. Pellet was dissolved in 15µl TE-buffer with 0,2µl RNase A.

## Materials and methods

For midi- and maxi-preps the **Pure Yield™ Plasmid Midiprep System** from Promega was used.

For midi-prep 100ml and for maxi-prep 200ml bacteria culture with appropriate antibiotic selection is incubated over night. Bacteria are centrifuged at 5.000g for 10min and the pellet is resuspended in 3ml/6ml of a resuspension solution. 3ml/6ml of a lysis buffer is added and tubes are inverted 3-5 times. Bacteria are lysed for 3min and lysis is stopped by adding 5ml/10ml neutralization buffer. Lysated bacteria are centrifuged for 15min at 15.000g. Lysate is added to a clearing column which was previously added to a binding column. Using a vacuum manifold the supernatant passes through the clearing and binding column. The clearing column is removed and the DNA which binds in the binding column is washed with 5ml endotoxin removal washing buffer and finally with 20ml column washing solution. Binding column is dried for 30-60sec and the DNA is eluted with 400-600µl nuclease free water using the Eluator™ vacuum Elution Device.

### 3.4 Protein Chemistry

#### 3.4.1 Western blotting

During the western blot procedure proteins are isolated and immunologically detected using specific antibodies. Equal amounts of protein lysates are brought on a polyacrylamid gel containing Sodiumdodecylsulfate (SDS). Secondary and tertiary structures (hydrogenbonds and disulfid bridges) of protein are dissolved by adding SDS and  $\beta$ -Mercaptoethanol (in sample buffer) to the lysates and heating prior gel electrophoresis. SDS also charges the proteins negatively so the proteins can be separated via gel electrophoresis due to their size. Proteins are transmitted onto a Polyvinylidene Fluoride (PVDF) membrane and incubated with antibodies specific for a certain protein. A secondary antibody contains an enzymatic label, a horse radish peroxidase, which oxidizes a chemiluminescent substrate. A photosensitive film detects the emitted light.

### 3.4.1.1 Total protein isolation

Cells are washed with cold tris-buffered saline (TBS) containing phosphatase inhibitors (1 $\mu$ l/ml Na<sub>3</sub>VO<sub>4</sub> and 10 $\mu$ l/ml 1M NaF) and lysed with hepes lysis buffer. Cell lysates are homogenized by forcing them three times through a 0,6-mm-in-diameter needle and transferred into Eppendorfer tubes. Lysates are held on ice and during a period of 30-45min and vortexed three times. Afterwards, the tubes are exposed to ultrasound for 10min and centrifuged at 15.000rpm for 5min. Supernatant is transferred into new tubes.

#### Hepes lysis buffer

1ml	1M Hepes
10ml	1M NaCl
40 $\mu$ l	0,5M EDTA solution
200 $\mu$ l	1M NaF solution
100 $\mu$ l	1M NaVO <sub>4</sub> solution
200 $\mu$ l	Igepal (NP40)
30 $\mu$ l	1M MgCl <sub>2</sub> solution
2 tablets	complete (phosphatase inhibitor cocktail tablet)
8,03ml	aqua bidest.

### 3.4.1.2 Membrane Protein Isolation

Adherent cells are scraped down from the Petri dish, transferred into an Eppendorfer tube and washed two times with ice-cold PBS. Cells are resuspended in 3ml ice-cold Dounce buffer and incubated for 10min on ice. To break the cell structure suspended cells are forced 50 times through a 0,6-mm-in-diameter needle and checked microscopically. 1ml Tonicity buffer is added and destroyed cells are centrifuged for 5min at 500g and 4°C. Supernatant is transferred in a tube for ultracentrifugation and 80 $\mu$ l 0,25M EDTA (pH 7,6) is added (to reach a final concentration of 5mM EDTA) and centrifuged for 90min at 100.000g and 4°C. Supernatant is discarded and pellet is resuspended in hepes lysis buffer (see chapter 3.4.1.1)

## Materials and methods

### Dounce Buffer

10mM Tris HCl, pH 7,6

0,5 mM MgCl<sub>2</sub>

20µl/ml complete

10µl/ml 0,1M PMSF (in isopropanol)

### Tonicity Buffer

10mM Tris HCl, pH 7,6

0,5 mM MgCl<sub>2</sub>

0,6M NaCl

5µl/ml complete

10µl/ml 0,1M PMSF (in isopropanol)

### **3.4.1.3 Evaluation of protein concentration: Coomassie blue assay**

Standard curve as well as protein sample is determined in duplicates. For standard curve BSA solution (1µg/µl) and hepes lysis buffer are pipetted into a 96-well plate conforming to following scheme:

<b>BSA concentration [µg/µl]</b>	<b>0</b>	<b>1</b>	<b>2</b>	<b>3</b>	<b>4</b>	<b>5</b>	<b>6</b>	<b>7</b>	<b>8</b>	<b>9</b>
Aqua bidest [µl]	9	8	7	6	5	4	3	2	1	0
Hepes lysis buffer [µl]	1	1	1	1	1	1	1	1	1	1
BSA [µl]	0	1	2	3	4	5	6	7	8	9
Total volume [µl]	10	10	10	10	10	10	10	10	10	10

For protein samples 1µl protein lysate and 9µl A. bidest are mixed in a 96-well. 150µl of a 1:5 diluted Coomassie Protein Assay Dye Reagent Concentrate (Bio-Rad) solution is added to each well of the standard curve and protein samples.

Absorption is measured at 590nm by microplate reader Synergy H1 (Szabo Scandic) and protein concentration of samples is calculated according to the standard curve.

### **3.4.1.4 SDS-Polyacrylamid Gel Electrophoresis (PAGE)**

First a SDS separating gel is prepared and overlaid with ethanol. After 45min the separating gel is polymerized and ethanol is removed neatly using filter paper. The separating gel is overlaid with a SDS collecting gel.



## Materials and methods

Before loading the gel, 20-40µg protein are mixed with 4x sample buffer and heated up to 80°C for 5min. 5µl protein ladder (PageRuler™ Prestained Protein Ladder, Fermentas) is also loaded. The gel is running in electrophoresis buffer first for 15min with 60 Volt and then for 1h hour at 125 Volt. Gel electrophoresis apparatus was obtained from Bio-Rad.

<u>SDS separating gel</u>	<b>7%</b>	<b>10%</b>
40% Acrylamid	0,875 ml	1,5 ml
1,5M Tris pH 8,8	1,25 ml	1,75 ml
A. bidest	2,8 ml	2,15 ml
10% SDS	50 µl	50 µl
10% APS	25 µl	25 µl
TEMED	2,5 µl	2,5µl

<u>SDS collecting Gel</u>		<u>2x Sample buffer</u>	
40% Acrylamid	0,25 ml	SDS	4%
1,5M Tris pH 6,8	0,313 ml	Glycerol	20%
A. bidest	1,9 ml	2-mercaptoethanol	10%
10% SDS	25 µl	Tris/HCl pH 6.8	0,125 M
10% APS	12,5 µl	Bromphenolblue	traces of

<u>Electrophoresis buffer</u>	
Glycin	72g
Tris	15g
SDS	5g
A. bidest	fill up to 500ml

### 3.4.1.5 Western blot

Proteins are blotted on a PVDF membrane (VWR) using a wet-blot system (Bio-Rad).

The blotting sandwich is prepared (avoiding air bubbles) according following order:

1. thick pad
2. 3 filter papers
3. PVDF membrane (activated in methanol)
4. gel
5. 3 filter papers
6. thin pad

The blot is running at 25V over night at 4°C in blotting buffer. The negative charge is on the side of the gel so the negatively loaded proteins can run to the positively charged membrane.

After blotting the membrane is washed in water, dried with methanol and can now be stored at 4°C.

#### 10x Blotting buffer

Glycin        72g

Tris            15g

SDS            1g

A. bidest to 500 ml

#### 1x Blotting buffer

10x blotting buffer    10%

Methanol                20%

A. bidest                 70%

### 3.4.1.6 Ponceau S staining

For visualizing all proteins on the membrane it is incubated in Ponceau S (Sigma) solution for 10min. Ponceau S binds to the positively charged amino groups of the protein and is therefore used to check the transfer quality from the gel to the membrane.

The stained membrane can be photocopied and destained with A. bidest or washing buffer (see 3.4.1.7).

### **3.4.1.7 Immunological detection of protein**

The membrane is incubated over night with the primary antibody solution (antibody diluted in 3% BSA in TBST or 1% non-fat dry milk in PBST) at 4°C. On the next day the membrane is washed 3-5 times during a period of 30min-1h before incubating with the secondary antibody solution (horse radish peroxidase (HRP) conjugated antibody in 3% BSA in TBST or 1% non-fat dry milk in PBST) for 1h at room temperature. After washing 3-5 times for 30min-1h the membrane is covered with detection solution (ECL Plus Western Blotting Detection System, Amersham<sup>TM</sup>, GE Healthcare, UK) and exposed to an x-ray film. Bands are semiquantified by scanning and analyzing using ImageQuant® Version 5.0.

#### Washing buffer (TBST or PBST)

TBS or PBS	1l
Tween	1ml or 0,5ml

## Materials and methods

1 <sup>st</sup> antibody	company	dilution	2 <sup>nd</sup> antibody	dilution	buffer	molecular weight
FGFR4 (H121), #sc-9006, N-terminal	Santa Cruz (Santa Cruz, CA, US)	1:250	rabbit	1:20.000	1% milk in PBS-Tween (0,05%)	95/110kDa
B-actin AC-15, #A5441	Sigma-Aldrich	1:500	mouse	1:2000	1% milk in PBS-Tween (0,05%)	42kDa
MAP Kinase 1/2 (ERK1/2-CT), #06-182	Upstate (Lake Placid, NY, US)	1:5000	rabbit	1:20.000	5% BSA in TBS-Tween (0,05%)	42/44kDa
Phospho-MAP Kinase (pERK1/2) (Thr202/Tyr204), #9101	Cell signaling (Danvers, MA, US)	1:1000	rabbit	1:20.000	3% BSA in TBS-Tween (0,05%)	42/44kDa
S6 Ribosomal Protein (S610), #2217	Cell signaling	1:2000	rabbit	1:20.000	5% BSA in TBS-Tween (0,05%)	32kDa
pS6 Ribosomal Protein (Ser240/244), #2215	Cell signaling	1:2000	rabbit	1:20.000	5% BSA in TBS-Tween (0,05%)	32kDa
FRS (M02), clone 1F7-1D6, #H00010818-M02	Abnova (Taipei City, Taiwan)	1:100	mouse	1:2000	3% BSA in TBS-Tween (0,1%)	57,5kDa
pFRS- $\alpha$ (Tyr196), #3864	Cell signaling	1:1000	rabbit	1:20.000	3% BSA in TBS-Tween (0,1%)	85kDa
GFP, #11814460001	Roche (Mannheim, G)	1:1000	mouse	1:2000	4% milk in PBS-Tween (0,05%)	27kDa
TetR, #631108	Clontech (Mountain View, CA, US)	1:1000	mouse	1:2000	1% milk in PBS-Tween (0,05%)	25kDa
pGSK3 $\beta$ , #9323	Cell signaling	1:1000	rabbit	1:20.000	3% BSA in TBS-Tween (0,05%)	46kDa
GSK3 $\beta$ , #9315	Cell signaling	1:1000	rabbit	1:20.000	3% BSA in TBS-Tween (0,05%)	46kDa
Phospho-PLC $\gamma$ 1(Tyr783), #2821	Cell signaling	1:1000	rabbit	1:20.000	3% BSA in TBS-Tween (0,1%)	155kDa
PLC $\gamma$ 1, #2822	Cell signaling	1:1000	rabbit	1:20.000	3% BSA in TBS-Tween (0,1%)	155kDa
Src (Phospho-Tyr418), #Y011091	Abm (Richmond, BC, CA)	1:1000	rabbit	1:20.000	3% BSA in TBS-Tween (0,1%)	60kDa
Src (Ab-529), #Y21168	Abm	1:1000	rabbit	1:20.000	3% BSA in TBS-Tween (0,1%)	60kDa

**Table 9:** Antibodies used for western blot

### 2<sup>nd</sup> Antibodies

Goat Anti-Mouse HRP-conjugated (#1858413, Pierce, Thermo Scientific, Rockford, IL, US)

Goat Anti-Rabbit IgG-h+I HRP (#A120-201P, Bethyl Laboratories Inc, Montgomery, TX, US)

### **3.5 In vivo experiments**

#### **3.5.1 Tissue specimens**

Tissue specimens of colorectal carcinoma and normal mucosa were obtained from 81 patients undergoing surgery for colorectal cancer. The experiments were examined and approved by the ethics commission of the Vienna municipal hospitals (votum EK 05-004-VK, 24.3.2005) and all patients gave informed consent before tissue collection. Tissue specimens were snap frozen in liquid N<sub>2</sub> after surgery and stored until RNA extraction.

#### **3.5.2 Blood samples**

The study population consists of two cohorts and has already been described, analyzed and published in another context (Feik et al. 2010). Blood samples were taken and analyzed in the lab of Andrea Gsur by Gerhard Führlinger. Statistical analysis was evaluated by Andreas Baierl.

From 2003 to 2006 there has been a province-wide screening project “Burgenland gegen Dickdarmkrebs” initiated by BAKS (Burgenländer Arbeitskreis für Sozial- und Vorsorgemedizin). During this time fecal occult blood tests were taken from 144.588 male and female residents of the Province Burgenland from which 17.028 were found positive. Patients were divided into groups of false positive, low risk adenoma, high risk adenoma and carcinoma. 3.471 blood samples from the study in Burgenland were evaluated in this approach.

Additionally, 14 blood samples of colon carcinoma patients in Vienna which have been collected at the Department of Surgery of the SMZ Süd (by Dr. Stefan Stättner) were integrated. From the same patients also tissue specimens were taken as described above.

The whole study population evaluated in this work can be divided into:

85	carcinoma
278	high risk adenoma
928	low risk adenoma
1.660	control

### 3.5.3 Local tumor growth in SCID mice

$1 \times 10^6$  cells are suspended in 50  $\mu$ l SFM and injected subcutaneously into the right flank of Severe Combined Immunodeficiency (SCID) mice. Tumor size (longitudinal and lateral) is measured periodically using a Vernier caliper. Mice are sacrificed as soon as the tumor reaches a size of 5.000mm<sup>3</sup> or mice showed symptoms of morbidity. Tumor and eventually other organs like lung or liver are harvested, washed with PBS and fixed for 24h in 4% formaldehyde-solution (Histofix). Tumors are washed with PBS and stored in 70% ethanol at 4°C.

Calculation of tumor volume: 
$$\frac{\text{longitudinal} \times \text{lateral}^2}{2}$$

All experiments were carried out according to Austrian regulations and Federation of European Laboratory Animal Science Associations (FELASA) guidelines for animal care and protection.

### 3.5.4 Metastatic in vivo model: tail vein injection

$1 \times 10^6$  cells are obtained in 100  $\mu$ l serum free media and injected into the tail vein of SCID mice. Animals are weighted every 2-3 days to find any alterations. 9 weeks after injection mice are all sacrificed and lungs as well as liver and kidney are removed and fixed as described in chapter 3.5.3.

### 3.5.5 Tissue fixation and paraffinization

Tissue is cut into small pieces and transferred into tissue caps. Final fixation and paraffinization are performed at the Kos Microwave histoSTATION (milestone, Bergamo, I).

## Materials and methods

### Conditions

25min	65°C	ethanol absolute
55min	68°C	isopropanol
1h15min	82°C	melted paraffin

Fixed tissue is finally sealed into paraffin blocks and cut into 4µm slides using a microtome (HM 355 S, Microm, Thermo Fisher Scientific, Waltham, MA, US).

### **3.5.6 Hämatoxylin-Eosin staining**

First tissue is deparaffinized incubating the slides according to the following protocol:

2x	1min	xylol
2x	1min	ethanol 100%
2x	1min	ethanol 70%
2x	1min	water

Nuclei are stained with hämatoxylin (Merck) for 5min. Slides are cleaned with water and incubated shortly (5sec) in Sott's solution (Morphisto, Frankfurt am Main, G). Slides are cleaned for 5min in floating water. Counter staining is done with Eosin (Sigma) for 1min. Slides are washed in water and dried in an ethanol range in ascending order:

1x	dipping 3 times	ethanol 70%
2x	1min	ethanol 96%
2x	1min	ethanol 100%
1x	1min	ethanol:xylol, 1:1
2x	1min	xylol

Slides are mounted with Entellan (Sigma).

### 3.5.7 Immunohistochemical staining

Slides are first incubated for 10min at 65°C and then deparaffinized as described in chapter 3.5.6. To remove peroxidases slides are incubated 10min in 0,3% H<sub>2</sub>O<sub>2</sub> (in PBS) at room temperature. After washing 2x3min in PBS slides are cooked in a steamer in 10mM citrate buffer for 30min and cooled down. Slides are washed 3min in PBS-Tween (0,1%). Tissue on the slide is circuted with a fat marker. For detection the Ultravision LP Large Volume Detection System HRP Polymer (Ready-To-Use) kit (Thermo Scientific, CA, USA) is used. Tissue is first incubated for 5min with ultra V block and then for 30-60min with the first antibody solution: Antibody + goat serum (1:100) in PBS-Tween (0,1%).

Slides are washed 2x3min in PBS-Tween (0,1%) and then incubated for 10min with primary antibody enhancer. Slides are again washed 2x3min in PBS-Tween (0,1%) and incubated for 15min with HRP polymer. After washing 2x3min in PBS-Tween (0,1%) slides are incubated for 2-10 min with DAB substrate (Dako North America, CA, USA) and washed with water. Counter staining is done by very short incubation (2sec) in hämatoxylin (Gill III, Merck). Slides are washed with water and dried in ethanol range (70%, 80%, 96%, 100% and n-butyl-acetate). Slides are mounted with Entellan.

#### Antibodies used for immunohistochemical staining

**Cytokeratin 20** (Ab-5), mouse anti human, (#DLN-14712, Dianova, Asker, N)

**Ki-67**, rabbit anti human, (#A047, Dako)

### 3.6 Statistical evaluation of data

Results obtained from cell culture assays were analyzed by student's t-test or Kruskal-Wallis test depending on the results of normality testing. To evaluate local tumor growth in SCID mice a 2-way ANOVA test was used. For tissue expression a paired sample t-test after obtaining the Gaussian distribution was used. To determine the impact of FGFR4 allelotype on tumor stage, all different stages were compared to stage I using contingency tables and  $\chi^2$  test. Significances are indicated as \*, \*\*, and \*\*\* for significant increase and #, ##, ### for significant decrease at  $p \leq 0,05$ , 0,01, and 0,001 respectively.



## 4 Results

### 4.1 FGFR4 in human colorectal cancer

#### 4.1.1 Genotyping FGFR4 G388R polymorphism in blood samples

To link the FGFR4 G388R polymorphism with the risk of developing CRC, 3471 blood samples of control, low-risk adenoma, high-risk adenoma and carcinoma patients in the course of a prevention study in Burgenland were analyzed in matters of their allelic expression of FGFR4. Table 10 shows the distribution of FGFR4<sup>Arg</sup> homozygous, FGFR4<sup>Gly</sup> homozygous and FGFR4<sup>Arg/Gly</sup> heterozygous genotypes over the four analyzed study-population groups. Evidently, most of the analyzed people have an FGFR4<sup>Gly</sup> homozygous genotype (~50%). Another 41% display a heterozygous genotype whereas only a small portion of ~9% is FGFR4<sup>Arg</sup> homozygous. In the carcinoma group however the percentage of FGFR4<sup>Arg</sup> homozygotes is increased compared to the two adenoma groups or the control group.

	FGFR4 <sup>Arg</sup>	FGFR4 <sup>Gly</sup>	FGFR4 <sup>Arg/Gly</sup>	number
missing	9,9%	51,6%	38,5%	384
control	8,1%	48,4%	43,4%	1.738
low-risk adenoma	8,9%	49,7%	41,4%	970
high-risk adenoma	5,5%	52,7%	41,8%	292
carcinoma	12,6%	48,3%	39,1%	87

**Table 10:** Categories of study population and their genotype in relation to allelic FGFR4 expression

To analyze the involvement of FGFR4 G388R in colorectal tumor development the FGFR4 genotype was correlated with the carcinoma group, the carcinoma group plus the high-risk adenoma group and finally carcinoma plus high-risk plus low-risk adenoma group. Distribution of the FGFR4 genotype over these three groups was compared to the control group. p-values were calculated against the FGFR4<sup>Gly</sup> homozygous group referring this group as the “wildtype”-FGFR4-variant.

## Results

In this study no significant correlation between the presence of FGFR4<sup>Arg</sup> (both heterozygotes and homozygotes) and the risk of getting colorectal carcinoma or diagnosed carcinoma was found. Remarkably, the p-value in the FGFR4<sup>Arg</sup> homozygous group, although not significant, decreases with increasing carcinoma incidence whereas the FGFR4<sup>Arg</sup> heterozygous group behaves conversely.

### Carcinoma

Genotype	Control	Cases	p-value
FGFR4 <sup>Gly</sup>	802	42	0,000
FGFR4 <sup>Gly/Arg</sup>	723	33	0,574
FGFR4 <sup>Arg</sup>	135	10	<b>0,350</b>

### Carcinoma + high-risk adenoma

Genotype	Control	Cases	p-value
FGFR4 <sup>Gly</sup>	802	190	0,000
FGFR4 <sup>Gly/Arg</sup>	723	148	0,210
FGFR4 <sup>Arg</sup>	135	25	<b>0,360</b>

### Carcinoma + high-risk + low-risk adenoma

Genotype	Control	Cases	p-value
FGFR4 <sup>Gly</sup>	802	642	0,000
FGFR4 <sup>Gly/Arg</sup>	723	542	0,267
FGFR4 <sup>Arg</sup>	135	107	<b>0,865</b>

**Table 11:** Genotype of FGFR4 polymorphism and carcinoma incidence  
p-values are calculated against FGFR4<sup>Gly</sup>-homozygous group.

## 4.1.2 FGFR4 expression and G388R polymorphism in human CRC tissue specimen

### 4.1.2.1 FGFR4 expression in human CRC tissue specimen

To assess correlations between the FGFR4 expression and histopathological tumor parameters like size, stage, grade, and in particular invasiveness of the tumor, 81 tissue pairs consisting of a sample from colon carcinoma tissue and normal mucosa tissue of the same patient were analyzed. Additionally, the allelic expression of the tissue pairs

## Results

was assessed and also correlated with histopathological parameter as well as FGFR4 expression.

FGFR4 expression was determined in mucosa and tumor tissue of 81 patients by quantitative real-time PCR using TaqMan assays for FGFR4.  $\Delta$ -ct-values were calculated using GAPDH as control for normalization. X-fold change of FGFR4 expression in tumor tissue was presented as ratio of tumor to normal mucosa (T/N ratio). In 10 cases bad quality of either the tumor or the normal mucosa mRNA revealed no evaluation of the FGFR4 expression.

FGFR4 expression was significantly up-regulated in 48% (34/71) of the tumor tissue compared to normal tissue ( $p=0,0152$ ) with a mean of 2,73 and a standard error of 0,6952. 25% of the tumor specimen displayed even a 2-fold or higher expression of FGFR4 compared to the normal mucosa. The relative expression levels ranged from 0,04 to 33,76.

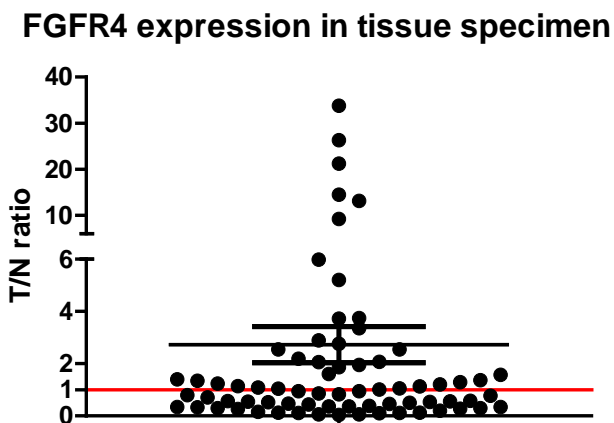


**Figure 48:** FGFR4 expression of 71 colorectal tumor tissues normalized to normal mucosa.

Results are presented as tumor/normal mucosa ratio (T/N). The red line indicates equal expression.

### 4.1.2.2 Correlation of FGFR4 expression and TMN-staging

Depending on the FGFR4 expression ratio tissue pairs were classified into two groups: using 1,5-fold FGFR4 over-expression as a cut-off point tissue pairs were divided into FGFR4 up-regulated tissues ( $T>N$ ) and FGFR4 unchanged or even down-regulated expression ( $T\leq N$ ). 22 tumor tissue pairs had a relative up-regulation of more than 1,5-fold whereas 49 tumor tissue pairs were classified into the  $\leq N$  group. Relating these

## Results

two groups to histopathological parameters like tumor stage, grade, size and lymph node metastasis resulted in no significant correlations indicating that FGFR4 expression had no impact on these parameters in this study.

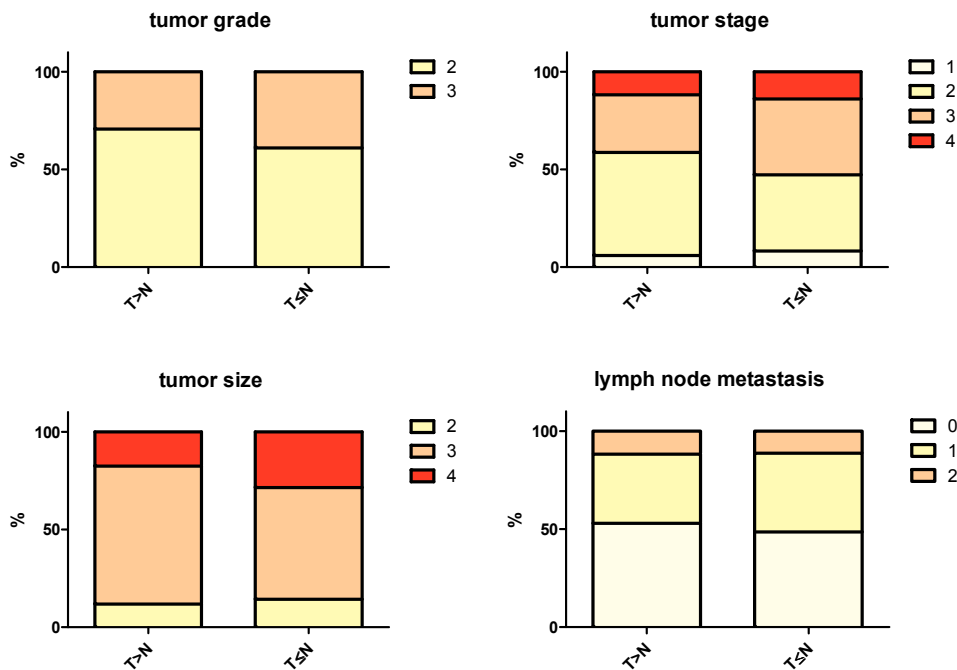


**Figure 49:** Correlation of FGFR4 expression in CRC with histopathological parameters

Tissue pairs were divided into up-regulated FGFR4 expression (T>N) and un- or down-regulated FGFR4 expression (T≤N) groups. Results are presented as percentage of the parameter corresponding classifications.

### 4.1.2.3 Allelic expression of FGFR4 in human CRC tissue specimen

Allelic expression of tissue specimen was assessed by using a TaqMan<sup>®</sup> Genotyping assay. For this purpose at first a calibration experiment was performed by using FGFR4<sup>Arg</sup> and FGFR4<sup>Gly</sup> expression vectors mixed in defined ratios, namely 8:1, 3:1, 2:1, 1:1, 1:2, 1:3, 1:8. Log<sub>2</sub> of the ratios was calculated and plotted against the  $\Delta$ ct-values (FGFR4<sup>Arg</sup>-FGFR4<sup>Gly</sup>). Using the linear equation of the calibration curve (see Figure 50) tissue specimens were related to the mixing ratios by measuring ct-values and calculating  $\Delta$ ct-values.

## Results

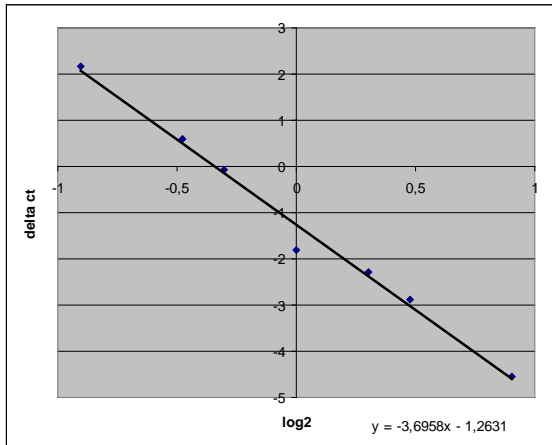


**Figure 50:** Straight calibration line to analyze allelic expression of FGFR4 in tissue specimen

Straight calibration line was calculated by using FGFR4<sup>Arg</sup> and FGFR4<sup>Gly</sup> expression vectors and mixing them in different ratios with each other. Ct-values were measured by real-time PCR and  $\Delta$ ct-values were calculated and plotted against log<sub>2</sub> of the mixing ratios.

Allelic expression was determined from both the tumor tissue and adjacent normal tissue. 45% (35/78) of the analyzed normal mucosa presented a FGFR4<sup>Gly</sup> homozygous expression whereas only 6% (5/78) had the FGFR4<sup>Arg</sup> homozygous expression. In 13% (10/78) of the cases a shift from FGFR4<sup>Gly</sup> to FGFR4<sup>Arg</sup> and in 19% (15/78) a shift from FGFR4<sup>Arg</sup> to FGFR4<sup>Gly</sup> expression could be observed between normal mucosa and the tumor. The remaining 53 tissue pairs showed no shift of allelic FGFR4 expression.

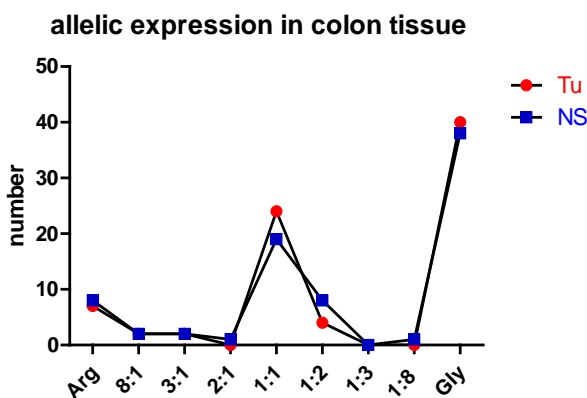


**Figure 51:** Allelic expression of FGFR4 in colon tumor and normal mucosa tissue

Tissues were grouped into nine different categories presenting different mixture ratios of the Arg- and the Gly-allele expression.

#### 4.1.2.4 Correlation of allelic FGFR4 expression and TMN-staging

To correlate FGFR4 expression with histopathological parameters like tumor grade, stage, size or lymph node metastasis tumor tissues were separated into two categories: tumors presenting the Arg-allele (homo- or heterozygote) and tumors with a Gly-homozygous genotype. A comparison between FGFR4 expression and allelic expression in tumor tissue with a mean of 2,853 T/N ratio for Arg and a mean of 2,677 T/N ratio for Gly showed no correlation. The level of FGFR4 expression is therefore independent of the allelic genotype of FGFR4.

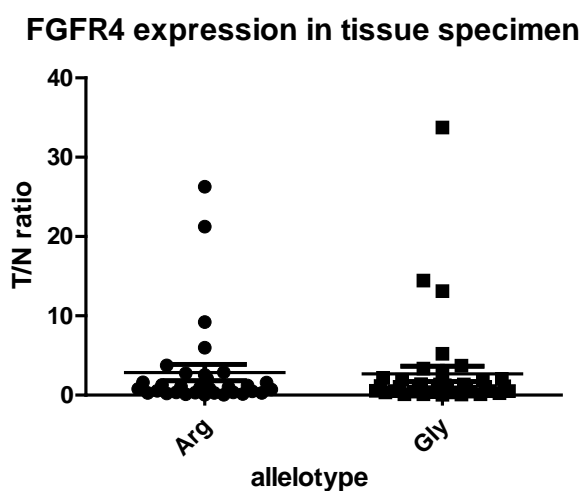


**Figure 52:** FGFR4 expression versus allelotype in human CRC tissue

Tissue specimens are divided into Arg- and Gly-expressing groups. Results are presented as tumor/normal mucosa ratio (T/N ratio)

To correlate the FGFR4 G388R polymorphism with histopathological parameters in human CRC the study population was enlarged by adding 55 carcinoma cases from the Burgenland-study (see chapter 3.5.2) to the 81 tissue specimens. Although in the Burgenland-study results were taken from blood samples and not from tumor tissues histopathological parameters of genotyped Arg-patients, Gly-patients and heterozygous patients were available and were added to the preexisting results of the tumor specimens.

Concerning tumor grade and size no differences between the Arg- and the Gly-group could be found. However, the Arg-group did reach a higher classification concerning lymph node metastasis compared to the Gly-expressing group.

## Results

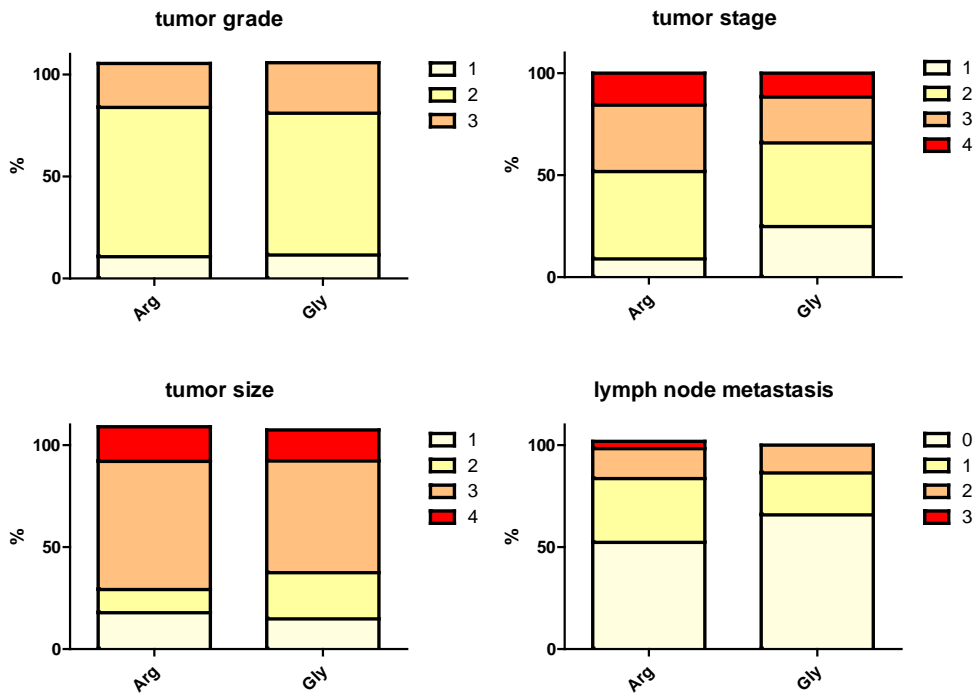


**Figure 53:** Correlation of FGFR4 genotype with tumor histopathological parameters in human CRC

Patients were divided into Arg- and Gly-expressing groups. Results are presented as percentage of the parameter corresponding classifications.

The Arg-allele was more prevalent at higher tumor stages in our study. In stage I the Arg-allele is present in 25% of the cases. This percentage increases with higher stage until 58-59% in stage III and IV. Results of all stages were compared to stage I. For all stages a significant change in the allelic expression was found.

## Results

Stage	FGFR4 <sup>Gly</sup>	FGFR4 <sup>Arg</sup>	Arg (% of total)	different from stage I (p-value)
I	15	5	25	-
II	28	30	52	0,0383
III	16	23	59	0,0134
IV	8	11	58	0,0368

**Table 12:** Correlation of FGFR4 genotype with tumor stage in human CRC

Patients were divided into FGFR4<sup>Arg</sup> homo- or heterozygous and FGFR4<sup>Gly</sup> homozygous groups. The percentage of FGFR4<sup>Arg</sup> positive tumors was calculated for each stage and the different stages were compared to stage I using the  $\chi^2$ -test.



## 4.2 Expression data of CRC cell lines

### 4.2.1 FGFR4 expression in CRC cell lines

One aim of this study was the establishment of a FGFR4 over-expression model for both the FGFR4<sup>Gly</sup> and the FGFR4<sup>Arg</sup> allele as well as the identification of a proper cell model for FGFR4 down-regulation experiments. To find an appropriate cell model all cell lines available in the laboratory were screened concerning their FGFR4 expression by real-time PCR. Results were normalized using GAPDH as a housekeeping gene. SW480 cell line expresses very low levels of FGFR4 and therefore all other data were presented as “fold expression of SW480”.

There is another splice variant of FGFR4 existing. In this variant the transmembrane domain of the receptor is lacking and the receptor may act as a decoy receptor to regulate the cell signaling for the FGFR4 pathway. Therefore, the expression of the soluble FGFR4 was also detected. The results were normalized to GAPDH expression and presented as “fold expression of SW480”.

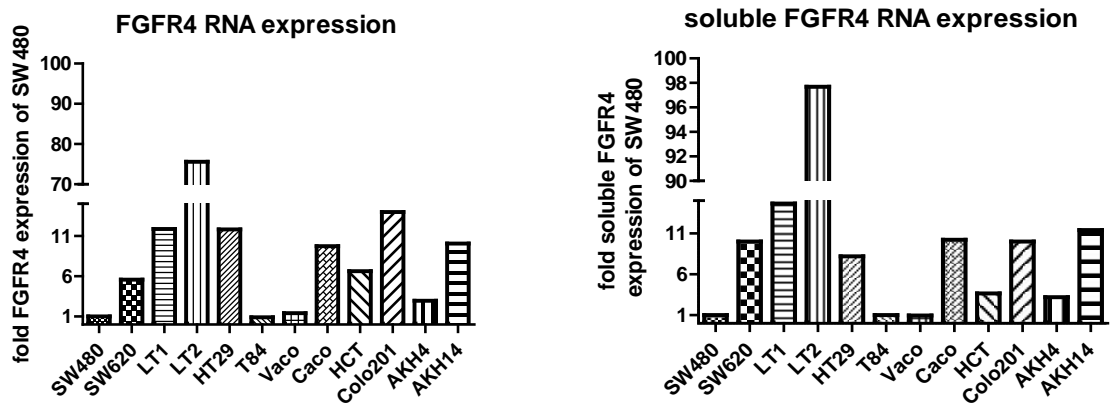


**Figure 54:** FGFR4 expression of CRC cell lines

FGFR4 expression of all available CRC cell lines was assessed by quantitative real-time PCR. On the left panel FGFR4 expression and on the right panel the expression of a soluble FGFR4 splice variant is shown. Results are normalized to GAPDH expression levels and presented as “fold expression of SW480”.

## Results

### 4.2.2 Expression of FGFR4 ligands in CRC cell lines

Apart from the FGFR4 the mRNA expression of diverse FGF's binding to FGFR4 was evaluated. Not for all of them TaqMan probes were available. FGF9, 18, and 19 were evaluated by using real-time PCR whereas for FGF 1, 2, 6, 16, and 17 standard PCR was carried out. For some FGF's only four cell lines with different expression levels of FGFR4 were tested: SW480, SW620 which is a metastasis cell line obtained from the same patient as SW480, the adenoma cell line LT97-2, and Caco-2.

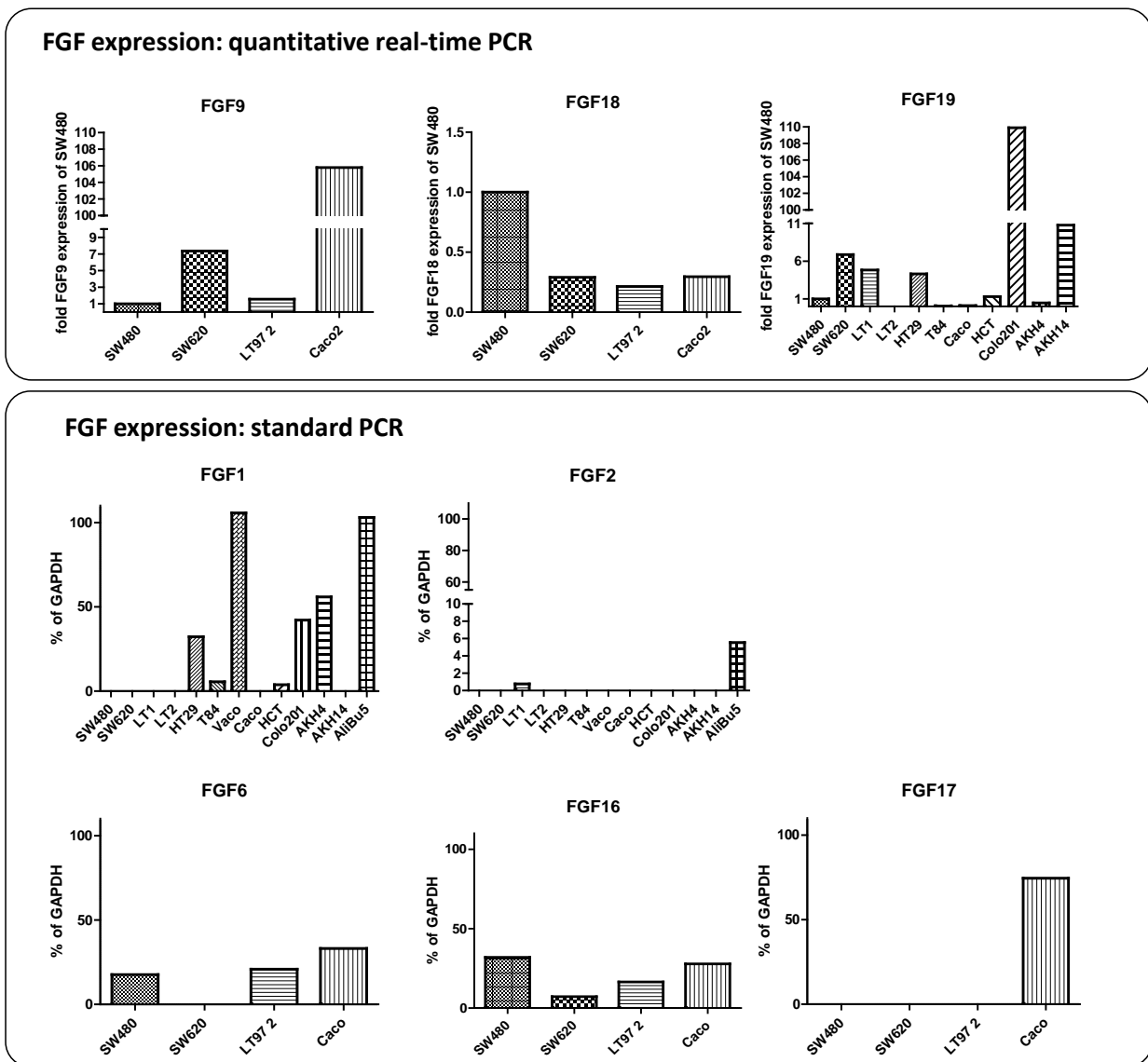


**Figure 55:** Expression of FGFR4-ligands in CRC cell lines

The expression of FGF1, 2, 6, 9, 16, 17, 18, and 19 in CRC cell lines was assessed using quantitative real-time PCR (FGF 9, 18 and 19) or standard PCR (FGF 1, 2, 6, 16 and 17). Results were normalized to the expression of GAPDH and presented as fold expression of SW480 or percentage of GAPDH.

## Results

To assess the allelic expression of CRC cell lines a standard PCR was performed using primer which anneal next to the polymorphism side. Afterwards the PCR product was digested by the endonuclease MspI. The existence of an Arginine at position 388 masks an enzyme cleavage side resulting in a 2-band-pattern for Arg<sup>388</sup> and a 3-band-pattern for Gly<sup>388</sup> (see protocol in chapter 3.2.6).

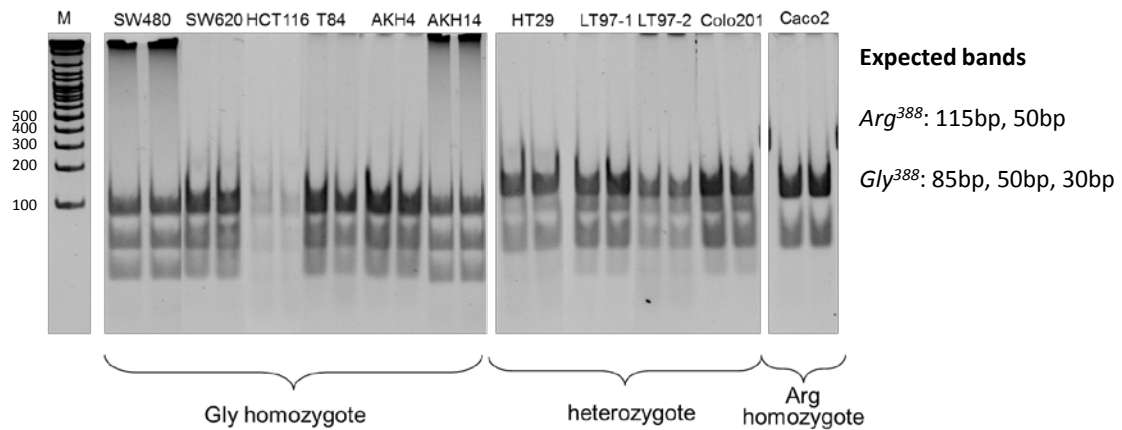





**Figure 56:** G388R polymorphism in CRC cell lines

Restriction fragment length polymorphism of CRC cell lines. Gly<sup>388</sup> homozygotes show three bands at ~30bp, ~50bp and 85bp, Arg<sup>388</sup> homozygotes show two bands at ~50bp and 115bp. Heterozygotes present all bands at ~30bp, ~50 bp, 85bp, and 115bp.

Six of the eleven cell lines tested are Gly<sup>388</sup> homozygous, five cell lines are heterozygous and only one could be identified as Arg<sup>388</sup> homozygous.

Based on the expression results three cell lines were selected for the further experiments: SW480, HCT116 and HT29. SW480 expresses very low amounts of FGFR4 and is Gly<sup>388</sup> homozygous and consequently serves as a good model for investigation on the effects of transfected FGFR4 over-expression in vitro. HCT116 is also homozygous and contrary to SW480 expresses higher amounts of FGFR4 and represents a good model for the effects of FGFR4 down-regulation in vitro. HT29 expresses also high amounts of FGFR4 but unlike SW480 and HCT116 this cell line is heterozygous and expresses predominantly the Arg<sup>388</sup> allele. Furthermore, all three cell lines are easily transfectable in contrast to the only Arg<sup>388</sup> homozygote cell line Caco-2. Caco-2 cells are very difficult to transduce and were therefore not chosen for our experiments.

## Results

Cell line	FGFR4 expression	polymorphism
SW480		Gly <sup>388</sup> homozygote
HCT116		Gly <sup>388</sup> homozygote
HT29		heterozygote

**Table 13:** CRC cell lines chosen for FGFR4 over-expression and down-regulation models

### 4.3 FGFR4 G388R polymorphism in CRC cell lines

#### 4.3.1 Establishment of FGFR4<sup>Gly</sup> and FGFR4<sup>Arg</sup> over-expressing cells

The cell lines chosen for our experiments were transfected each with a control vector (empty pcDNA3 or pcDNA3-GFP), FGFR4<sup>Arg</sup> and FGFR4<sup>Gly</sup> over-expressing vectors by lipofection and electroporation.

All following experiments and results of SW480 have been carried out with three differently transfected batches. To facilitate the presentation of the results all three batches of SW480 transfectants were pooled. For HCT116 and HT29 only one batch of transfectants was used.

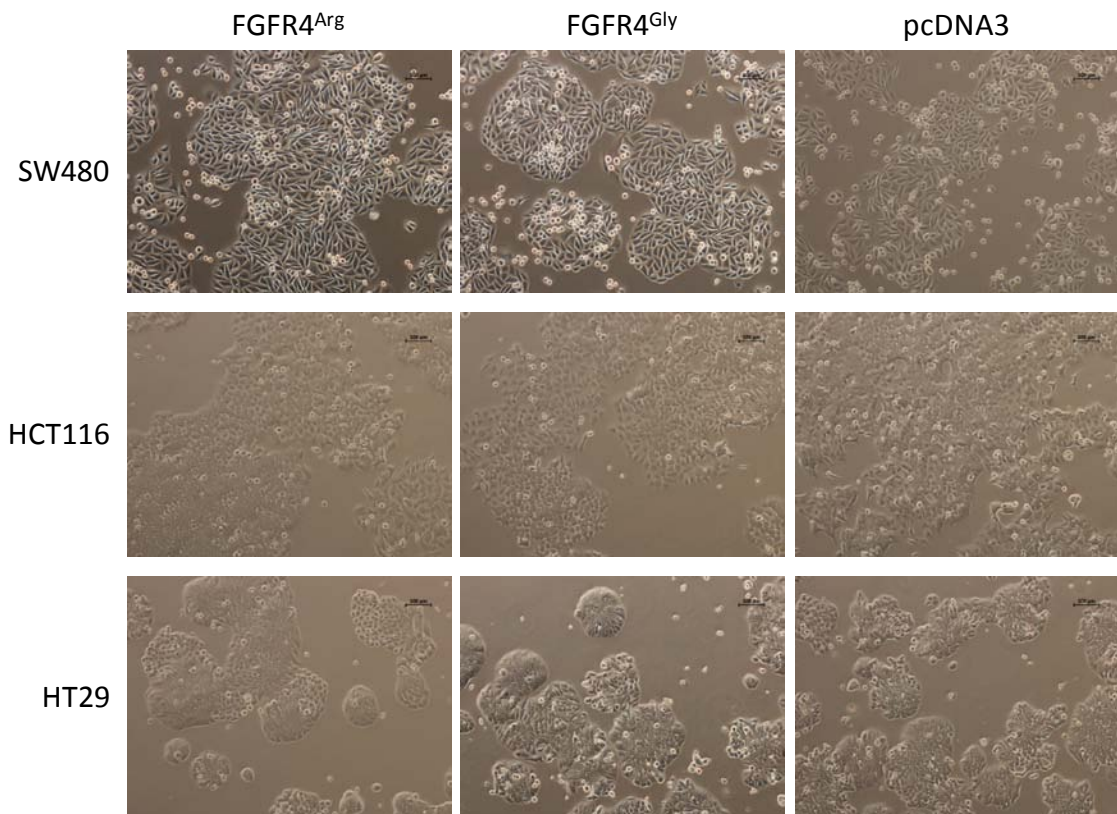


**Figure 57:** Pictures of SW480, HCT116 and HT29 FGFR4 transfectants

Pictures of FGFR4 transfectants and controls were taken from SW480, HCT116 and HT29 at a magnification of 10x.

Cells were transfected by lipofection and selected with G418 for approximately 3-4 weeks. All clones were combined to one clone pool per group. FGFR4 expression was

## Results

assessed both on mRNA- and protein-level. Cells were seeded at densities of 50-70% confluence and RNA- and protein-lysates were harvested 24-48h later, depending on individual growth rate.

FGFR4-mRNA expression was measured by both standard and real-time PCR. At least two results of each batch and group were pooled and are presented in Figure 58. Results are normalized to GAPDH expression and presented as percentage of control.

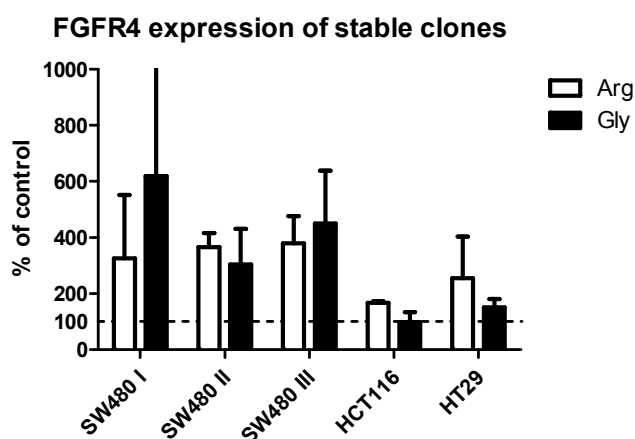


**Figure 58:** FGFR4 RNA expression of transfected SW480, HCT116 and HT29 stable clone pools

FGFR4 expression was measured by both standard and real-time PCR. Results are presented as percentage of control. Arg...FGFR4<sup>Arg</sup>, Gly...FGFR4<sup>Gly</sup>

FGFR4 protein expression was evaluated by western blot for total FGFR4 protein and by FACS-analysis with a PE-labeled FGFR4-specific antibody which determines FGFR4 at the surface. Western blot was performed with two batches of transfected SW480 and  $\beta$ -actin was used as an internal loading control. For both batches total FGFR4 protein was increased for FGFR4<sup>Arg</sup> as well as FGFR4<sup>Gly</sup> transfected cells compared to control.

## Results

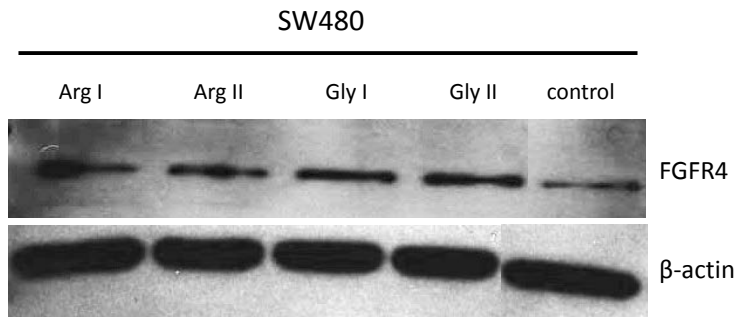


**Figure 59:** Total FGFR4 protein expression of SW480 transfectants

Total FGFR4 protein expression of two batches of transfected SW480 expressing either FGFR4<sup>Arg</sup> or FGFR4<sup>Gly</sup> were analyzed by western blot.  $\beta$ -actin was used as an internal loading control. Arg...FGFR4<sup>Arg</sup>, Gly...FGFR4<sup>Gly</sup>

FACS analysis was carried out at least two times for each cell line. Results were presented as fold-expression of control. In all transfected cell lines the over-expression of the FGFR4<sup>Arg</sup>-protein at the cellular surface was higher than the FGFR4<sup>Gly</sup>-protein. The expression of FGFR4<sup>Arg</sup> ranges from 11-12-fold in SW480 and HT29 to 4-fold in HCT116 compared to control. FGFR4<sup>Gly</sup>-expression was 3-4-fold in SW480 and HT29 and 1,4-fold in HCT116 compared to control.

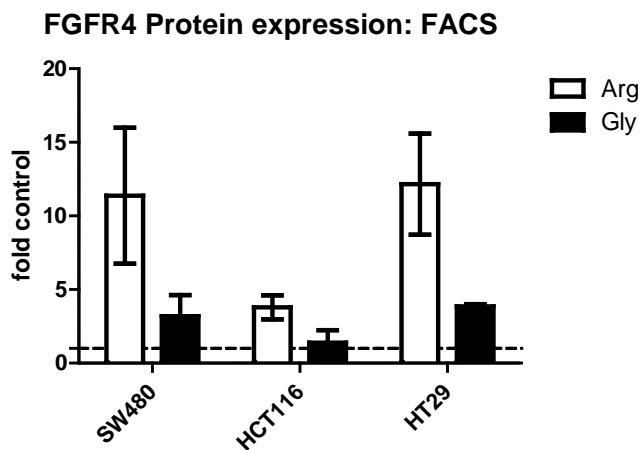


**Figure 60:** Cell surface expression of FGFR4 in SW480, HCT116, and HT29 FGFR4-transfectants

Cell surface expression of FGFR4 was evaluated by FACS analysis. Results are presented as fold control. Arg...FGFR4<sup>Arg</sup>, Gly...FGFR4<sup>Gly</sup>

### 4.3.2 Viability of FGFR4 over-expressing cells

To determine FGFR4 impact on cell growth viability assays were performed for each transfected cell line. Cells were seeded at low densities ( $1 \times 10^4$  cells per well) into 24-well plates and after five days neutral red assays (see chapter 3.1.4.1) were performed.

## Results

For each group six wells were evaluated and the assay was repeated at least three times for each cell line.

Surprisingly, the over-expression of FGFR4 (for both the Arg-variant and the Gly-variant) did not affect cell viability in any cell line. Results are presented in Figure 61 as percentage of control.

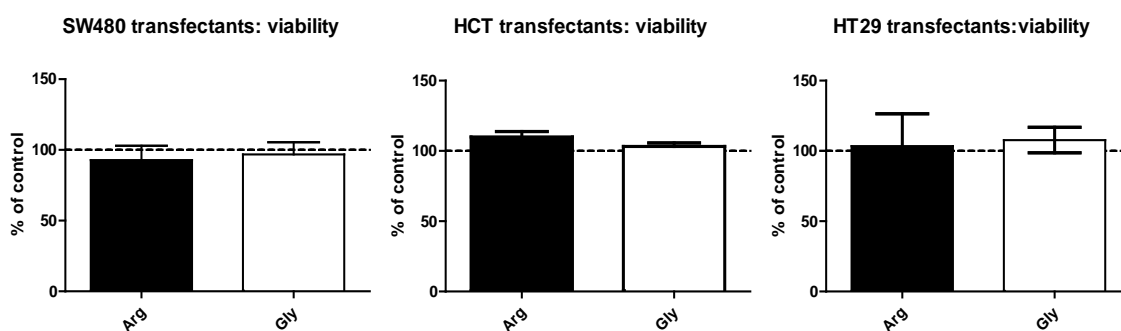


**Figure 61:** Viability of FGFR4<sup>Arg</sup> and FGFR4<sup>Gly</sup> transfectants

Viability was evaluated by performing a neutral red assay. Results are presented as percentage of control and pooled from three different approaches, each six values. Arg...FGFR4<sup>Arg</sup>, Gly...FGFR4<sup>Gly</sup>

### 4.3.3 Proliferation of FGFR4 over-expressing cells

In addition proliferation of FGFR4 transfectants was analyzed using a H<sup>3</sup>-thymidine incorporation assay (according to the protocol described in chapter 3.1.8) three times for each cell line. For each group eight values were measured per approach.

In all cell lines the DNA synthesis of FGFR4 over-expressing cells was higher at lower cell densities compared to the control. At higher densities FGFR4 over-expression did not show any effect concerning cell proliferation in SW480. In HCT116 proliferation was FGFR4-dependently increased in low- and intermediate- density cultures. In HT29 proliferation was significantly increased at all cell densities with FGFR4<sup>Arg</sup> over-expression.



## Results

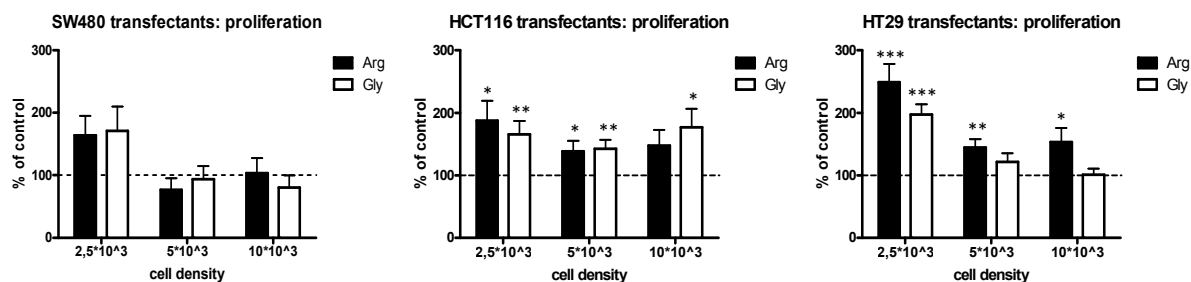


**Figure 62:** Proliferation of FGFR4 over-expressing cells

SW480, HCT116 and HT29 cell lines over-expressing FGFR4<sup>Gly</sup> and FGFR4<sup>Arg</sup> were seeded at three different densities and H<sup>3</sup>-thymidine incorporation assay was performed to assess proliferation. Results are presented as percentage of control and pooled from three different approaches each eight values. \*, \*\*, and \*\*\* = significantly increased as compared to control at  $p \leq 0,05$ , 0,01, and 0,001 respectively; Arg...FGFR4<sup>Arg</sup>, Gly...FGFR4<sup>Gly</sup>

### 4.3.4 Migration of FGFR4 over-expressing cells

To assess the impact of FGFR4 variants on cell migration a filter migration assay was performed according to the protocol described in chapter 3.1.6. For each group triplicates were evaluated and the assay was repeated at least three times for all cell lines.

Migration was stimulated 60- and 30-fold respectively for both FGFR4 over-expressing forms in SW480. Above all FGFR4<sup>Arg</sup> did significantly stimulate migration also when compared to FGFR4<sup>Gly</sup> ( $p=0,0032$ ). Also in HCT116 FGFR4 over-expression increased migration significantly and again the effects were stronger in FGFR4<sup>Arg</sup> expressing cells than in FGFR4<sup>Gly</sup>-expressing cells. In HT29 the case was different: FGFR4<sup>Gly</sup> expressing cells showed a significant ( $p=0,0004$ ) decrease in migration whereas the FGFR4<sup>Arg</sup> transfected cells displayed no difference compared to the control.

## Results

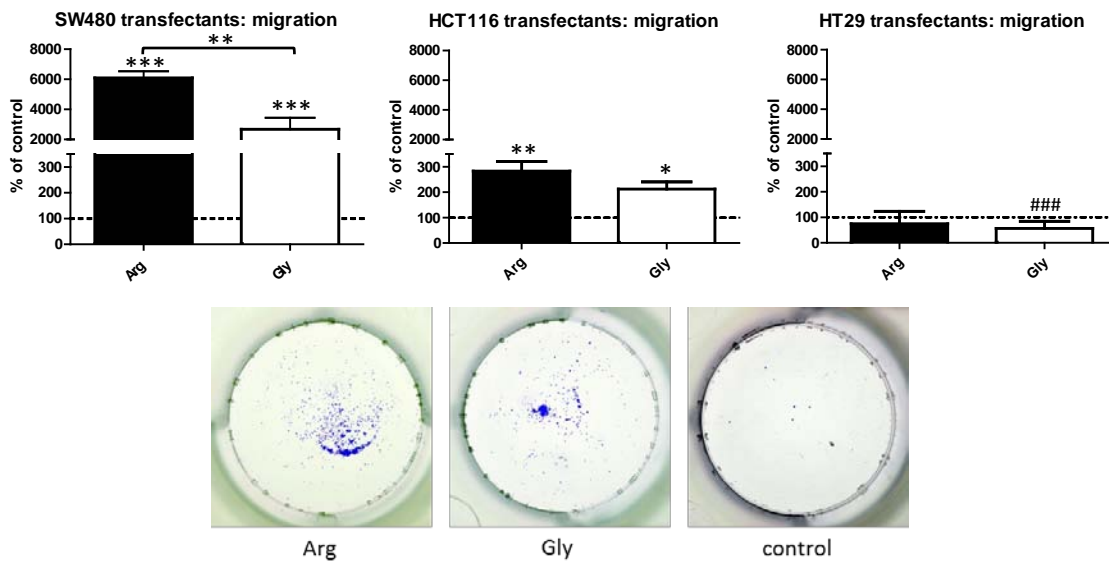


**Figure 63:** Migration of FGFR4 over-expressing cells

Migration of FGFR4 transfectants was assessed by using a transwell-filter-migration assay. In the upper panel results are presented as percentage of control and pooled from three different approaches each three values. In the lower panel pictures of migrated SW480 transfectants are shown. \*, \*\*, and \*\*\* = significantly increased as compared to control at  $p \leq 0,05$ ,  $0,01$ , and  $0,001$  respectively; ### = significantly decreased as compared to control at  $p \leq 0,001$ ; Arg...FGFR4<sup>Arg</sup>, Gly...FGFR4<sup>Gly</sup>

### 4.3.5 Colony formation of FGFR4 over-expressing cells

Colony formation assay was carried out at least three times according to the protocol described in chapter 3.1.5.

In all three cell lines it was observed that FGFR4<sup>Gly</sup> over-expressing cells showed increased colony formation compared to control and to FGFR4<sup>Arg</sup> over-expressing cells which did not differ from the control. (SW480 FGFR4<sup>Gly</sup>:  $p < 0,0001$ ; HCT116 FGFR4<sup>Gly</sup>:  $p < 0,0001$ ; HT29 FGFR4<sup>Gly</sup>:  $p < 0,0001$ )

## Results

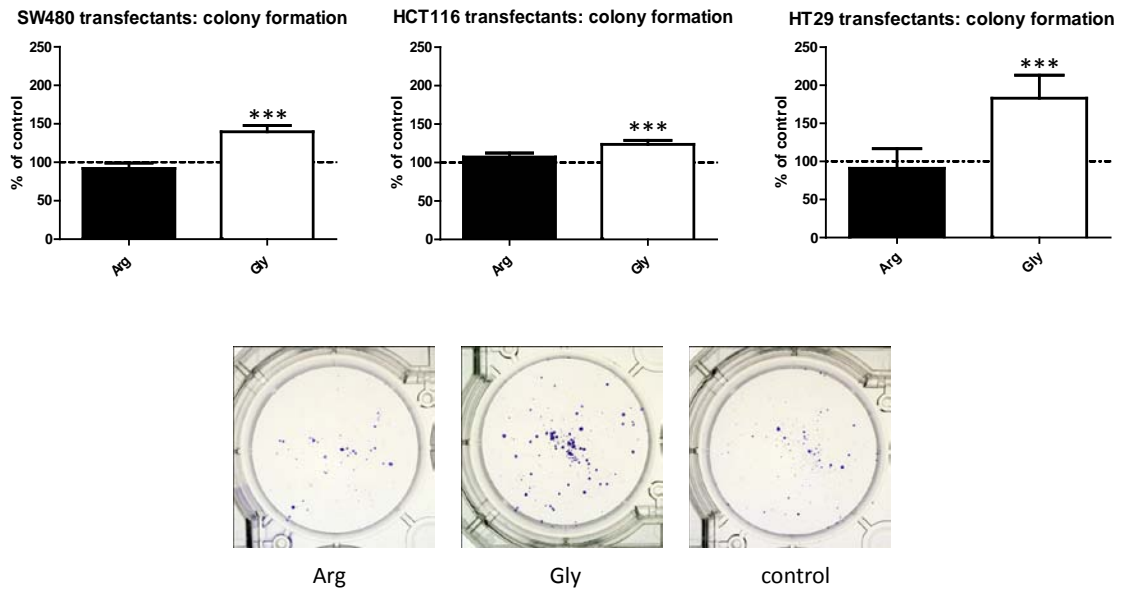


**Figure 64:** Colony formation of FGFR4 over-expressing cells

Formation of single clones of FGFR4<sup>Arg</sup> and FGFR4<sup>Gly</sup> over-expressing cells was assessed by colony formation assay. Results are presented as percentage of control in the upper panel and pooled from three different approaches each six values. In the lower panel pictures of colony formation assays from SW480 transfectants are shown. \*\*\* = significantly increased as compared to control; at p < 0.001; at p Arg...FGFR4<sup>Arg</sup>, Gly...FGFR4<sup>Gly</sup>

### 4.3.6 Anchorage independent growth of FGFR4 over-expressing cells

The outgrowth of colonies in an anchorage independent manner reflects another characteristic of aggressive tumor cells. Cells were embedded into a soft agar matrix according to the protocol described in chapter 3.1.7. After 2-3 weeks colonies were counted microscopically. Soft agar assay was performed three times for each cell line and in triplicates for each group.

SW480, which expresses low levels of endogenous FGFR4, showed a significantly increased ( $p < 0,0001$ ) soft agar growth when FGFR4 was over-expressed. Also in HT29 FGFR4 over-expression significantly stimulated anchorage independent growth independent from allelic expression ( $p < 0,0001$ ). FGFR4 over-expressing HCT116 cells showed a different effect. Whereas with FGFR4<sup>Gly</sup> no increased soft agar growth was observed, FGFR4<sup>Arg</sup> expression decreased growth significantly ( $p < 0,0001$ ).

## Results

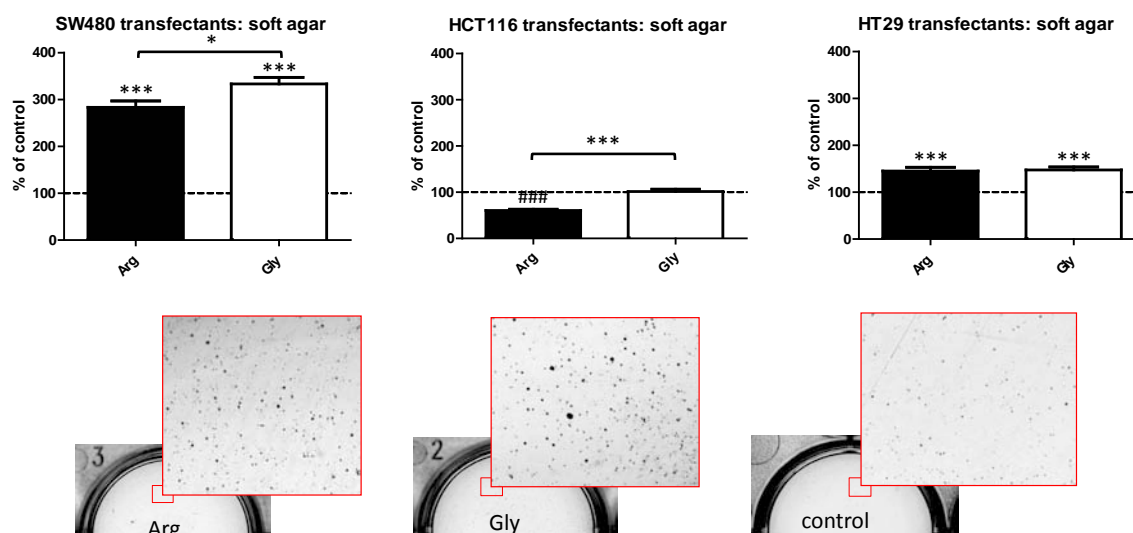


**Figure 65:** Anchorage independent growth of FGFR4 over-expressing cells

The upper panel shows the effect of FGFR4<sup>Arg</sup> and FGFR4<sup>Gly</sup> over-expression on anchorage independent growth in all three transfected cell lines. Results are presented as percentage of control and pooled from three different approaches each three values. In the lower panel pictures of soft agar plates from SW480 transfectants are shown. \*\*\* or ### = significantly increased or decreased as compared to control at  $p < 0,001$ ; Arg...FGFR4<sup>Arg</sup>, Gly...FGFR4<sup>Gly</sup>

### 4.3.7 Signaling of FGFR4 over-expressing cells

Total protein lysates and lysates of membrane proteins from SW480 FGFR4<sup>Arg</sup>, FGFR4<sup>Gly</sup> and control cells were isolated according to the protocol described in chapters 3.4.1.1 and 3.4.1.2. Activation and phosphorylation of direct FGFR signaling targets FRS and PLC $\gamma$  at the cell membrane and also as total protein were analyzed by western blot. Alterations of downstream signaling due to FGFR4 over-expression was described by detection of both the phosphorylated forms and the total protein levels of ERK, S6, GSK3 $\beta$  and Src in total protein lysates.  $\beta$ -actin was used as loading control. For final semi-quantification of signaling proteins ImageQuant® software (Version 5.0) was used.

At the cell membrane FRS phosphorylation was induced by both FGFR4<sup>Arg</sup> and FGFR4<sup>Gly</sup> compared to the control. The presence of the FRS at the cell membrane was decreased in FGFR4<sup>Arg</sup> expressing SW480 compared to FGFR4<sup>Gly</sup> and control. The specific phosphorylation of membrane-localized FRS was increased in both FGFR4<sup>Gly</sup> and FGFR4<sup>Arg</sup> expressing SW480 cells compared to control.

## Results

Total protein of PCL $\gamma$  was up-regulated in the two FGFR4 over-expressing cells. In FGFR4<sup>Gly</sup> expressing SW480 the PCL $\gamma$  was increasingly localized at the cell membrane. However phosphorylation of PCL $\gamma$  at the cell membrane was down-regulated by FGFR4 over-expression compared to control.

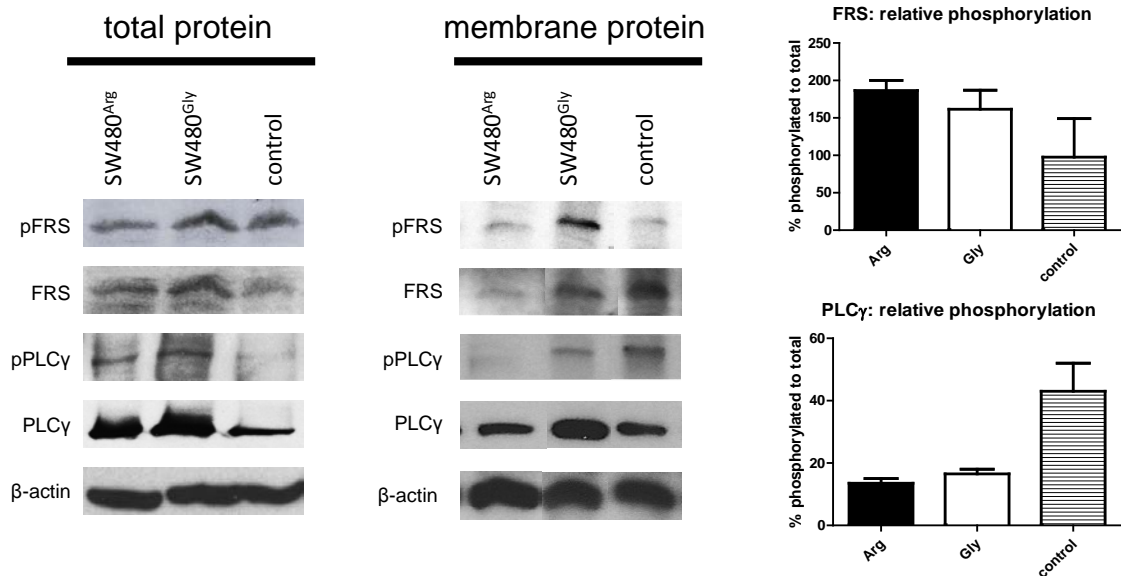


**Figure 66:** Impact of FGFR4 over-expressing SW480 on FRS and PCL $\gamma$

In the left panel western blots of total proteins and in the middle panel of membrane localized proteins are shown. Antibodies detecting phosphorylated FRS (pFRS), FRS, phosphorylated PCL $\gamma$  (pPCL $\gamma$ ), PCL $\gamma$  and  $\beta$ -actin as loading control where used.

In the right panel relative phosphorylation of FRS and PCL $\gamma$  membrane protein is shown. Results are presented as percentage of phosphorylated protein to unphosphorylated protein and analyzed by semi-quantification of membrane protein. Arg...FGFR4<sup>Arg</sup>, Gly...FGFR4<sup>Gly</sup>

Downstream of FRS we found no alterations of ERK in the FGFR4 over-expressing SW480 cells. Phosphorylation of GSK3 $\beta$  was induced by FGFR4 over-expressing SW480 compared to control. Both S6 protein and phosphorylation were up-regulated by FGFR4<sup>Gly</sup> and even more by FGFR4<sup>Arg</sup>.

Src phosphorylation was not up-regulated when normalized to total src-protein in FGFR4 over-expressing cells. Src protein level was increased however in FGFR4<sup>Arg</sup> but not FGFR4<sup>Gly</sup> expressing SW480.

## Results

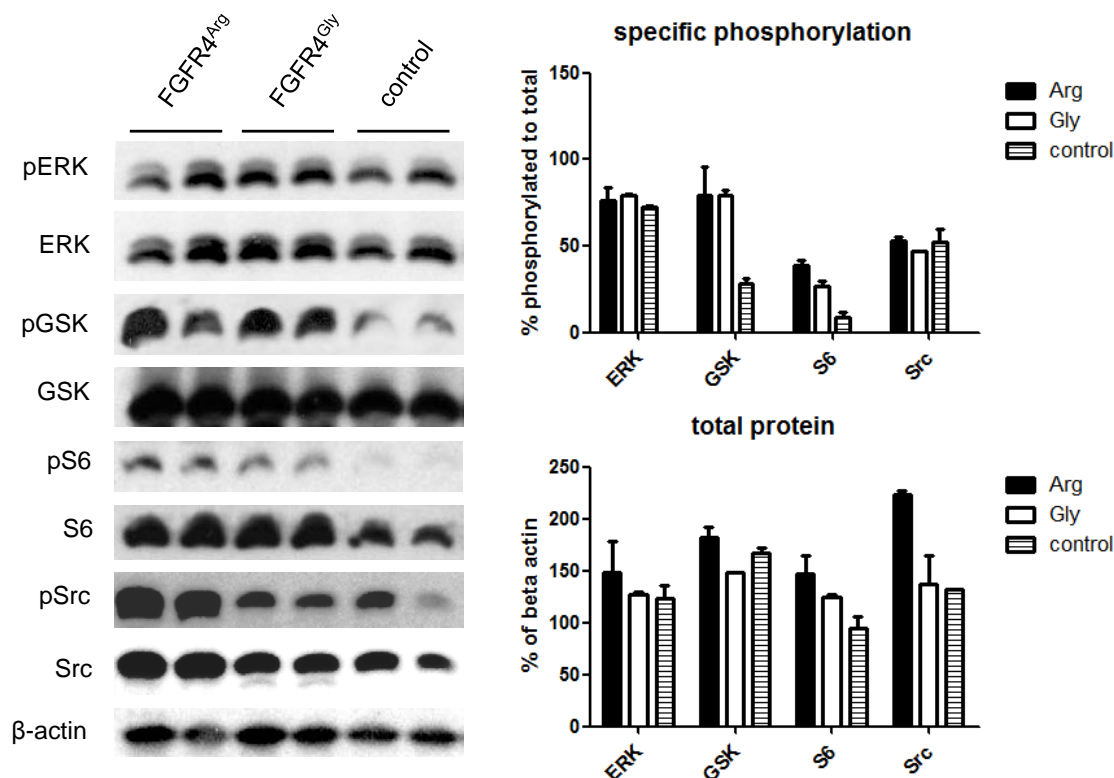


**Figure 67:** Impact of FGFR4 over-expressing SW480 on ERK, S6, GSK and Src

Western blot of down-stream signaling and Src of FGFR4 over-expressing SW480 and control are shown in the left panel. Antibodies detecting phosphorylated ERK (pERK), ERK, phosphorylated S6 (pS6), phosphorylated GSK3 $\beta$  (pGSK), GSK3 $\beta$ , phosphorylated Src (pSrc), Src and  $\beta$ -actin as loading control were used.

On the right side protein semi-quantification is presented. In the upper panel quantified proteins are displayed as percentage of phosphorylated to total protein. In the lower panel total protein is presented normalized to  $\beta$ -actin. Arg...FGFR4<sup>Arg</sup>, Gly...FGFR4<sup>Gly</sup>

### 4.3.8 FGFR4 over-expressing SW480 xenografts in SCID mice

10<sup>6</sup> SW480 cells over-expressing FGFR4<sup>Arg</sup> and FGFR4<sup>Gly</sup> as well as SW480 expressing GFP were injected subcutaneously into SCID mice. For each group four male SCID mice were selected. Tumor volume was measured every 48-72 hours and mice were sacrificed as soon as the tumor volume exceeded a size of 5.000mm<sup>3</sup> or when mice showed symptoms of morbidity. Tumors and organs like lung, kidney and liver were harvested, fixed and embedded in paraffin. Serial sections were obtained and stained as described in chapters 3.5.6 and 3.5.7.

## Results

In the control group one mouse died four weeks after injection without developing a tumor. Consequently, in the group of the control mice only three mice were taken for the experimental analysis.

FGFR4<sup>Gly</sup> xenografts showed more rapid growth of local tumor than FGFR4<sup>Arg</sup> and control xenografts (2-way ANOVA,  $p=0,0002$ ). Mice in the FGFR4<sup>Gly</sup>-group did also develop larger tumors and were sacrificed earlier than mice in the control- or FGFR4<sup>Arg</sup>-group.

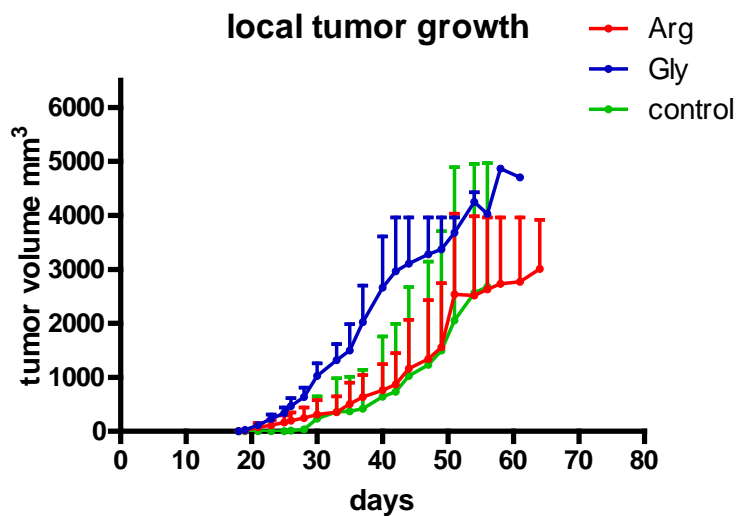


**Figure 68:** Local tumor growth of SW480 FGFR4<sup>Arg</sup>, FGFR4<sup>Gly</sup> and GFP xenografts in SCID mice

SW480 transfectants were subcutaneously injected into male SCID mice and tumor volume was measured every 2-3 days. Arg...FGFR4<sup>Arg</sup>, Gly...FGFR4<sup>Gly</sup>

### 4.3.8.1 Immunohistological evaluation of tumor xenografts

Tumors were stained with hematoxylin & eosin (H&E), cytokeratin 20 and Ki67. Hematoxylin colors the nuclei blue whereas eosin stains eosinophilic structures of the cell and extracellular proteins. Eosinophilic structures are basic like collagen, most part of the cytoplasm and red blood cells which are stained intensely pink. H&E staining was done to compare the morphology of the tumor cells.

Cytokeratins are expressed in a determined pattern in all organs and tissues. Cytokeratin 20 is mainly expressed in the GIT and identifies the cells derived from the injected SW480 transfectants.



## Results

Ki67 is a nuclear protein and associated with cell proliferation. Therefore Ki67 is a proliferation marker because it is present in the nucleus in all active phases of the cell cycle but absent in resting cells.

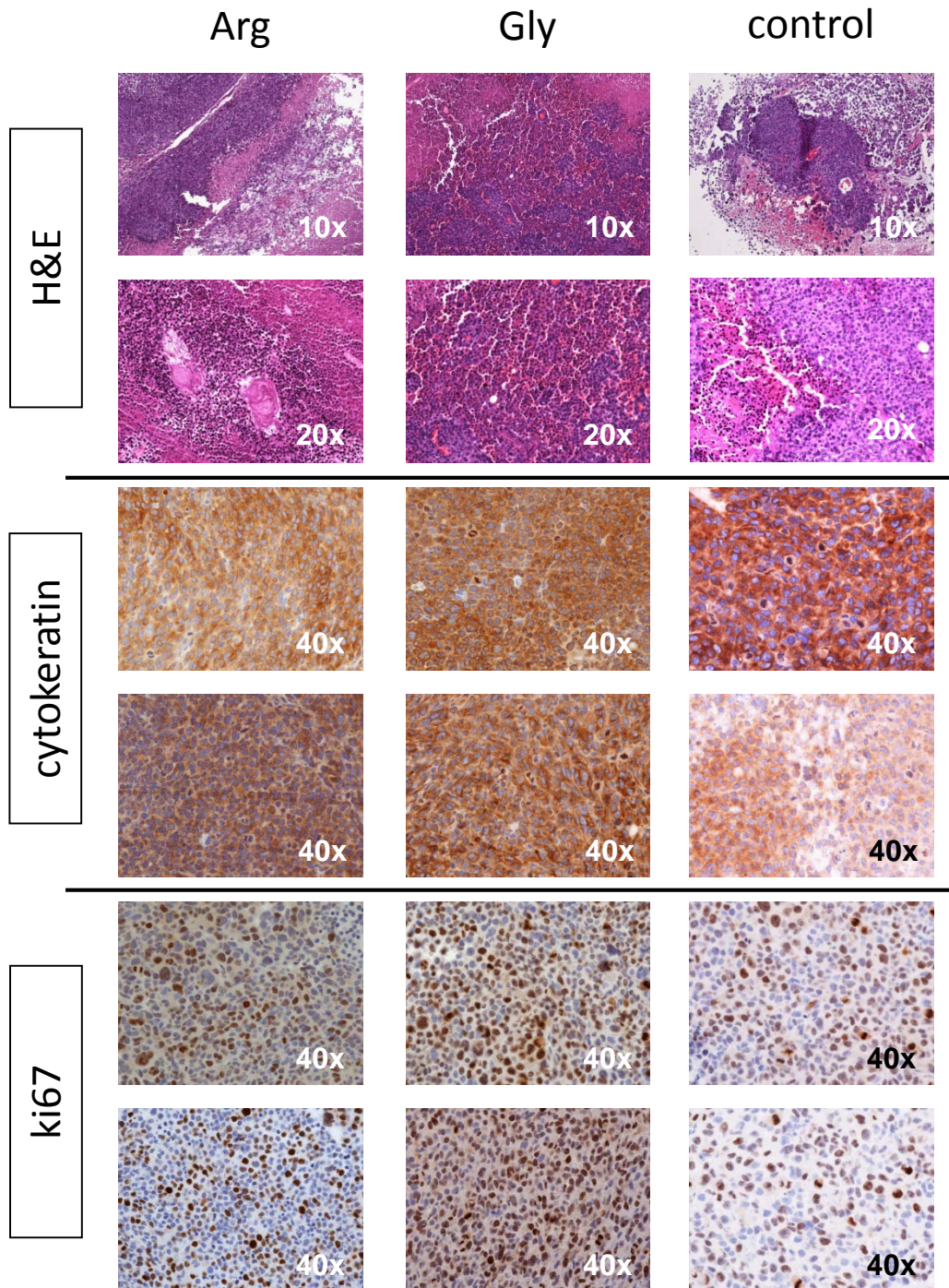


**Figure 69:** Immunohistochemical stainings of FGFR4 over-expressing tumor xenografts

Figure 69 represents for each group two tumor sections stained immunohistochemically by cytokeratine 20 and Ki67 as well as H&E-staining. For cytokeratin 20 and Ki67 a magnification of 40x was used. For H&E staining pictures of different magnifications were taken. Arg...FGFR4<sup>Arg</sup>, Gly...FGFR4<sup>Gly</sup>



## Results

Cytokeratin 20 positive areas were taken to analyze incidence of mitosis and apoptosis in the tumors. Therefore pictures were taken of five different cytoke­ratin 20 positive areas per tumor at a magnification of 40x and mitotic and apoptotic cells were evaluated. Total cell number was determined by counting and the percentage of apoptotic and mitotic cells was calculated. Ki67 positive cells were also counted in five different areas at a magnification of 40x and the percentage of Ki67 positive cells was calculated.

Surprisingly, in the FGFR4<sup>Gly</sup> xenografts significantly more apoptotic nuclei per field in average could be counted than in FGFR4<sup>Arg</sup> and control, whereas mitotic rate was the highest in the control group. Regarding proliferation FGFR4<sup>Gly</sup> had significantly more Ki67 positive nuclei per field than FGFR4<sup>Arg</sup> and control.

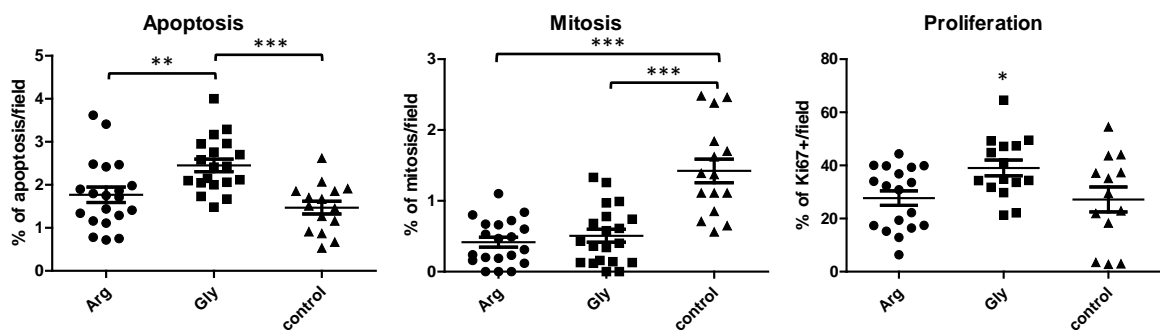


**Figure 70:** Apoptotic-, mitotic-, and proliferation-rate of FGFR4 tumor sections

All cells in five different fields were counted and apoptotic, mitotic and proliferating nuclei were calculated as percentage of total cell number. \*, \*\*, and \*\*\* = significant increase between two comparable groups  $p \leq 0,05$ ,  $0,01$ , and  $0,001$ ; Arg...FGFR4<sup>Arg</sup>, Gly...FGFR4<sup>Gly</sup>

Noticeably the number of cells per field of vision at a magnification of 40x varied significantly between the three groups. In the FGFR4<sup>Arg</sup> group the cell count was highest amounting to about 800 cells, significantly higher than in FGFR4<sup>Gly</sup> tumors with about 600 cells and controls with about 400 cells per field. The difference in cell number per field was highly significant for all three groups.

## Results

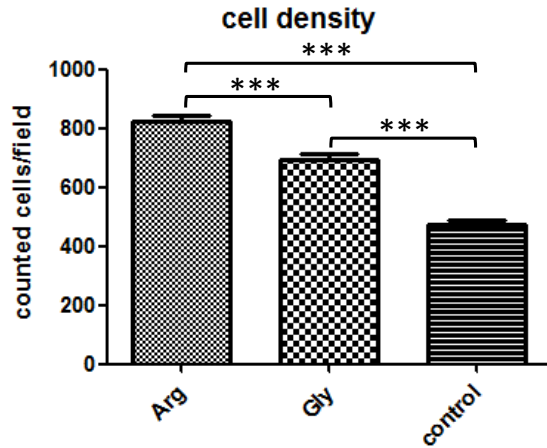


**Figure 71:** Cell density of FGFR4<sup>Arg</sup>, FGFR4<sup>Gly</sup> and control tumor sections

Cell count of five different fields per tumor section was determined. \*\*\* = significant increase between two comparable groups at  $p \leq 0,001$ ; Arg...FGFR4<sup>Arg</sup>, Gly...FGFR4<sup>Gly</sup>

### 4.3.8.2 Immunohistological evaluation of lung sections and metastasis

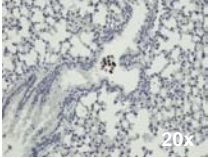
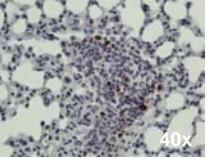
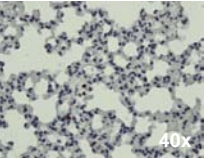
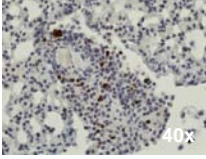
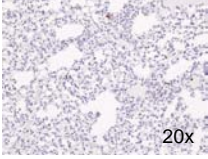
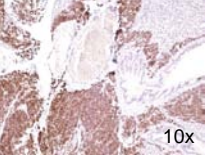
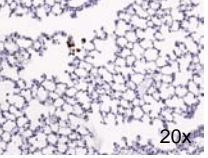
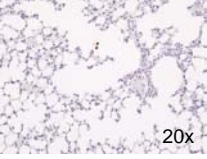
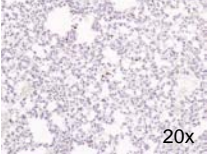
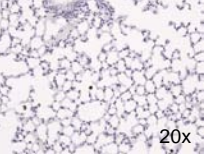
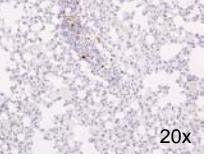
Metastatic tumor cells injected subcutaneously detach from the local tumor and dislocate via the blood stream to the lung where they settle down and grow into metastasis. To detect any metastatic cells lung sections were stained with Ki67 antibody. Lung cells are resting cells and do not proliferate. Consequently, Ki67 positive cells in the lung have to be derived from an actively proliferating origin like a tumor. Lungs were classified into five groups depending on number and position of Ki67 positive cells or areas. For each group scores were given increasing with severity of metastasis (see Table 14)

Score	Description
0	≤ 3 positive nuclei per section
1	4-10 isolated positive nuclei per section
2	more than 10 isolated or/and small aggregations of positive nuclei per section
3	large aggregations and multiple isolated positive nuclei, also close to blood vessels per section
4	extensive areas of positive nuclei per section

**Table 14:** Classification of metastatic score for Ki67 positive stained lungs

## Results

In all of the FGFR4<sup>Arg</sup> xenografted mice micrometastasis could be found. In this group there was no mouse without any Ki67 positive nuclei and two animals reached scores of 3 and 4 whereas in FGFR4<sup>Gly</sup> xenografted mice two mice had no positive staining for Ki67 and the other two reached a score of 2. The control group reached scores of 1 and 2. Consequently, the calculated metastatic score was the highest in the FGFR4<sup>Arg</sup>-group where it was nearly twice as high as in the FGFR4<sup>Gly</sup>-group or in the control-group.

		metastatic score	mouse 1	mouse 2	mouse 3	mouse 4
<b>control</b>	mouse 1	-	data not available			
	mouse 2	1				
	mouse 3	2				
	mouse 4	1				
<b>Arg</b>	mouse 5	3				
	mouse 6	2				
	mouse 7	4				
	mouse 8	1				
<b>Gly</b>	mouse 9	0				
	mouse 10	2				
	mouse 11	0				
	mouse 12	2				

**Figure 72:** Ki67 staining and classification of FGFR4 over-expressing xenograft lungs

Pictures were selected to illustrate metastatic impact. For determination of metastatic score the whole section was evaluated and classified. Mouse 1 died four weeks after tumor injection and was therefore not available for examination. Arg...FGFR4<sup>Arg</sup>, Gly...FGFR4<sup>Gly</sup>

## Results

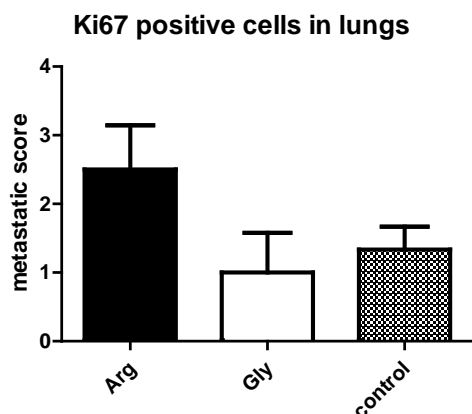


**Figure 73:** Metastatic score of FGFR4 over-expressing xenografts and control

Metastatic score was calculated by evaluating Ki67 positive cells in rodent lungs of four different sections and classification according Table 14. Arg...FGFR4<sup>Arg</sup>, Gly...FGFR4<sup>Gly</sup>

### 4.3.9 In vivo metastasis model of FGFR4 over-expressing SW480 transfectants

To evaluate the metastatic potential of FGFR4 over-expressing transfectants in vivo  $1 \times 10^6$  cells were injected into the tail vein of four male SCID mice per group. Body weight of the mice was observed for a period of 65 days every 2<sup>nd</sup> or 3<sup>rd</sup> day to identify signs of morbidity. Mice were sacrificed at day 65 and lungs were obtained to assess metastatic score.

A rapid loss of body weight could be an indicator for tumor growth. However, body weight of the animals increased steadily throughout the experiment. In the FGFR4<sup>Arg</sup>-group the weight of the mice was slightly higher than in the FGFR4<sup>Gly</sup>- and the control-group.

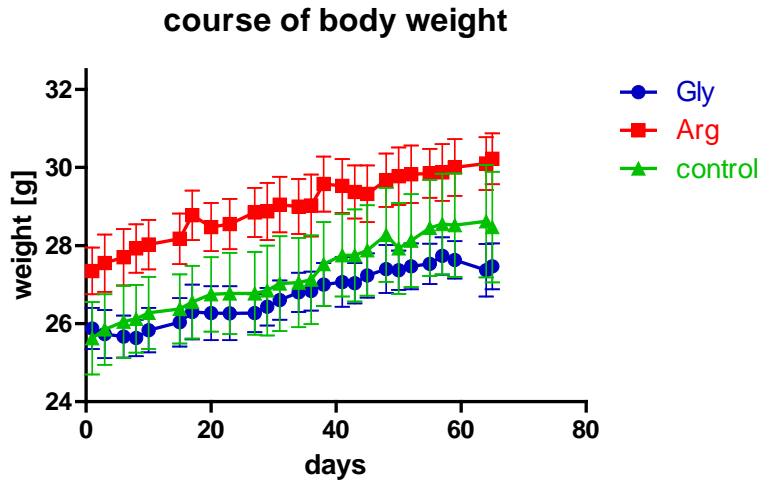


**Figure 74:** Body weight of FGFR4 transfectants in metastasis model in vivo

$1 \times 10^6$  cells of SW480 FGFR4-transfectants and control were injected into the tail vein of SCID mice. Body weight was controlled every 2<sup>nd</sup> or 3<sup>rd</sup> day. Arg...FGFR4<sup>Arg</sup>, Gly...FGFR4<sup>Gly</sup>

From the blood stream cells should preferentially settle in the lung. To find micro-metastasis lungs were again stained with Ki67. All lungs except one lung in the group of FGFR4<sup>Arg</sup> were completely Ki67 negative. The Ki67 positive lung showed small stained nodules and single stained nuclei.

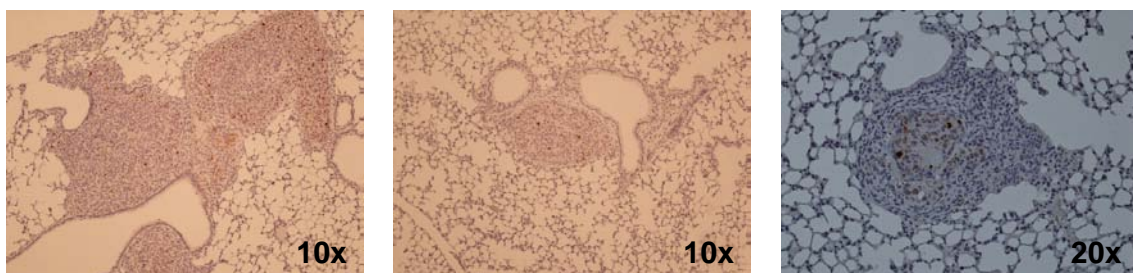


**Figure 75:** Ki67 positive nodules of SW480 FGFR4<sup>Arg</sup> metastasis in rodent lung

Cells were injected in the tail vein and only one mouse (FGFR4<sup>Arg</sup>-group) established metastasis.

#### 4.4 FGFR4 G388R polymorphism and its role in EMT

To find evidence of a connection between the FGFR4 G388R polymorphism and EMT, E-cadherin expression and  $\beta$ -catenin localization were assessed.

##### 4.4.1 E-Cadherin

##### 4.4.1.1 mRNA expression: real-time PCR

mRNA-expression of E-cadherin was measured by quantitative real-time PCR. Cells were seeded and harvested on the next day. RNA was isolated and real-time PCR was performed. This has been carried out 2-3 times. Unfortunately, there were large inter-experimental variations for HCT116 and HT29. For HCT116 values differed from 86%-209% in FGFR4<sup>Arg</sup> and from 120%-275% in FGFR4<sup>Gly</sup> whereas in HT29 values reached from 28%-100% in both groups respectively to control values. E-cadherin mRNA expression of FGFR4 over-expressing HCT116 and HT29 was not significant. SW480 FGFR4 transfectants had a decreased E-cadherin expression compared to control which was statistically significant in FGFR4<sup>Gly</sup> ( $p=0,0067$ ) and failed significance in FGFR4<sup>Arg</sup> ( $p=0,0597$ ).

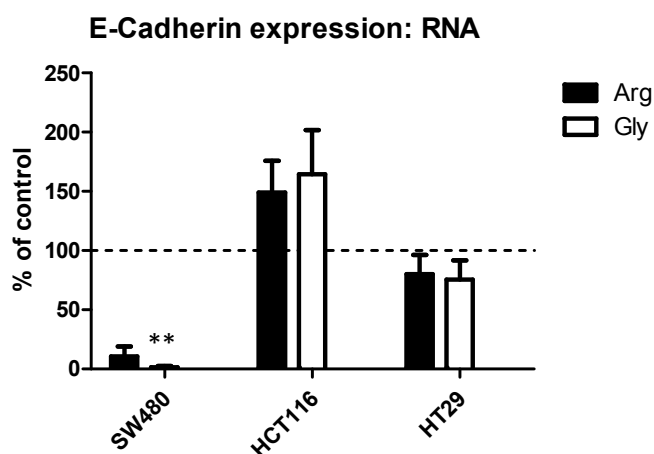


**Figure 76:** E-cadherin mRNA expression of FGFR4 over-expressing cells

E-cadherin expression was determined by quantitative real-time PCR and results are presented as percentage of control. \*\* = significantly increased as compared to control at  $p \leq 0,01$ ; Arg...FGFR4<sup>Arg</sup>, Gly...FGFR4<sup>Gly</sup>

#### 4.4.1.2 Protein expression: FACS

On the protein level expression of E-cadherin was measured by FACS analysis according to the protocol described in chapter 3.1.9.3.

E-cadherin FACS analysis was carried out two times for SW480 and HCT116 cell line and only once for HT29. Although differences between the two measurements concerning E-cadherin expression were remarkably high, the results of FACS analysis reflect results of E-cadherin expression on mRNA level. In SW480 the FGFR4 over-expressing clones showed lower expression of E-cadherin compared to the control. The E-cadherin expression of HCT116 and HT29 FGFR4 over-expressing cells measured by FACS was comparable to the control.

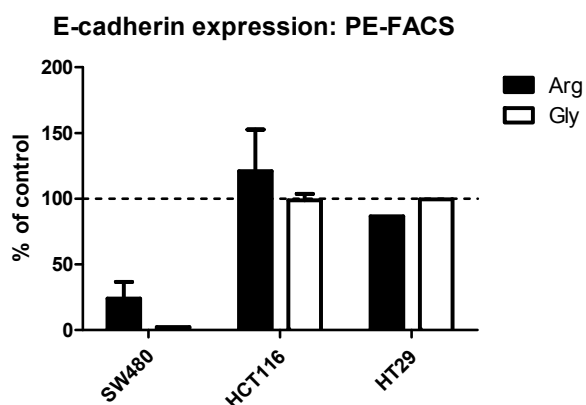


**Figure 77:** FACS analysis of E-cadherin in FGFR4 over-expressing cells

E-cadherin expression was measured by FACS analysis. Results are given as percentage of control and pooled for the SW480 and HCT116 cells from two approaches whereas for HT29 only one value per group was available. Arg...FGFR4<sup>Arg</sup>, Gly...FGFR4<sup>Gly</sup>

#### 4.4.1.3 Protein expression: immunofluorescence staining

To visualize the expression of E-cadherin FGFR4 over-expressing SW480, HCT116 and HT29 were seeded on glass slides, fixed and incubated with an anti-E-cadherin-antibody. The second antibody was coupled to FITC. TO-PRO3-iodide was used as counterstain. Pictures were taken using a confocal microscope at a magnification of 60x.

In SW480 E-cadherin is not highly expressed but in FGFR4 over-expressing cells E-cadherin expression was even further down-regulated compared to the control.

## Results

Concerning HCT116 and HT29 there was no clear difference between FGFR4 over-expressing cells and control visible in the confocal microscope.

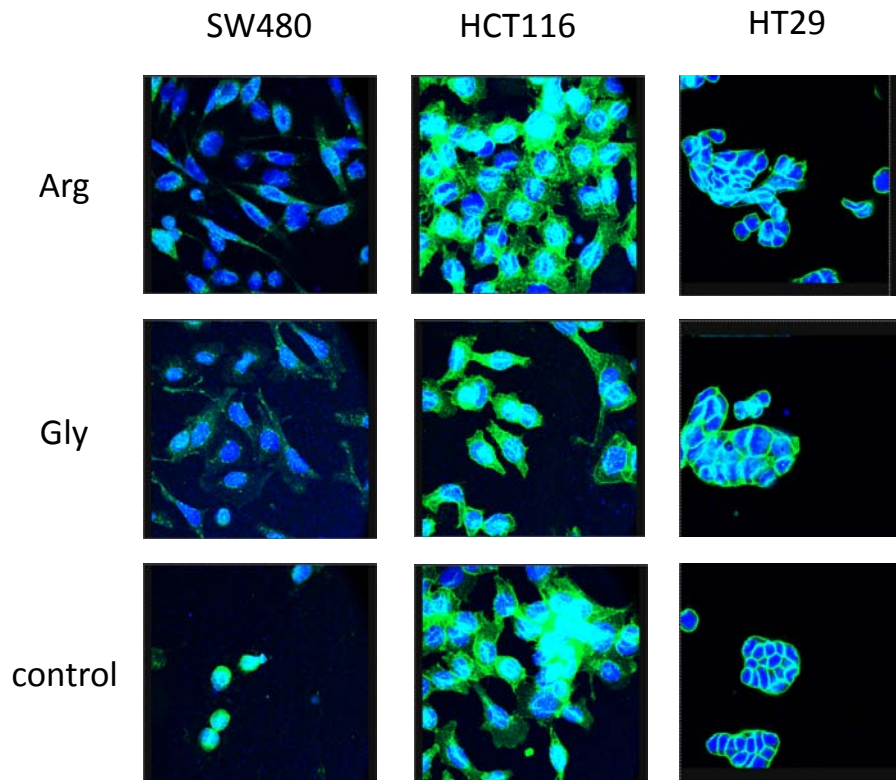


**Figure 78:** Immunofluorescence staining of E-cadherin in FGFR4 over-expressing

Pictures were taken under the confocal microscope at a magnification of 60x. Arg...FGFR4<sup>Arg</sup>, Gly...FGFR4<sup>Gly</sup>

### 4.4.2 $\beta$ -catenin

#### 4.4.2.1 Protein expression: immunofluorescence staining

FGFR4 over-expressing cells were seeded on glass slides, fixed and incubated with an anti- $\beta$ -catenin antibody. Slides were incubated with a FITC-labeled secondary antibody and visualized using a confocal microscope at the magnification of 60x.

Figure 79 shows the local expression of  $\beta$ -catenin in all three cell lines and their transfectants.  $\beta$ -catenin was higher expressed in SW480 than in HCT116 and HT29 where it was predominantly located at the cell periphery. By contrast, the protein was found mostly in the cytoplasm and nucleus in SW480 cells. Differences between FGFR4 over-expressing cells and the control could not be observed.



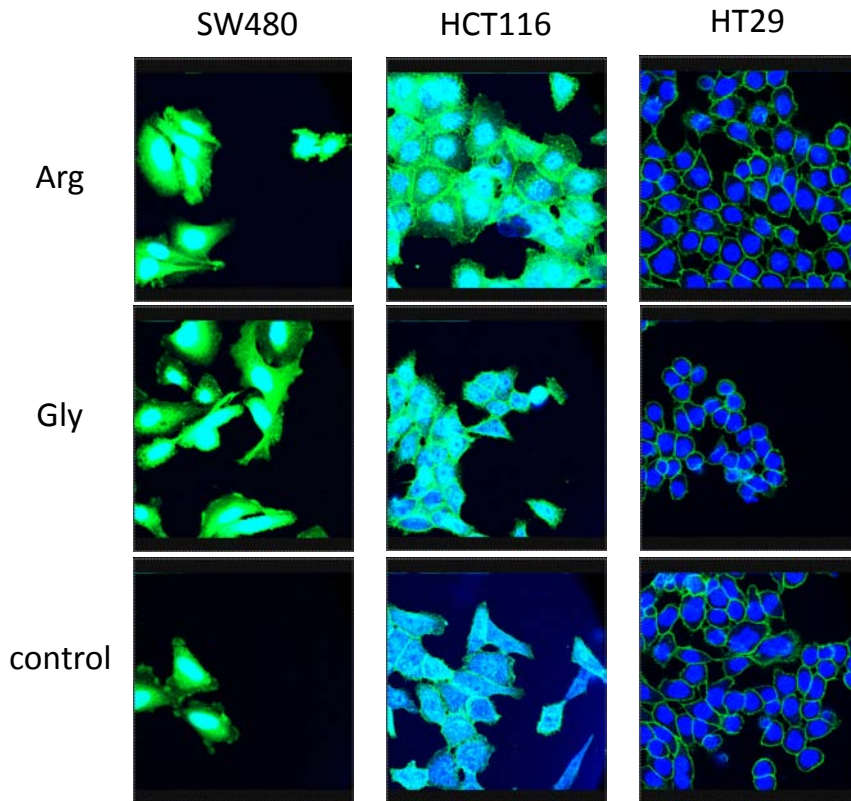


**Figure 79:** Immunofluorescence staining of  $\beta$ -catenin in FGFR4 over-expressing

Pictures were taken under the confocal microscope at a magnification of 60x. Arg...FGFR4<sup>Arg</sup>, Gly...FGFR4<sup>Gly</sup>

#### 4.4.2.2 $\beta$ -catenin localization: luciferase assay

Cells were seeded into 24-well-plate and transfected in triplicates with either a Top vector, where luciferase can only be expressed in the nuclear presence of  $\beta$ -catenin, or a Fop vector, whose binding site for  $\beta$ -catenin is mutated and serves as a negative control. Renilla, a third vector is a positive transfection control and co-transfected with either Top or Fop. 48h later cells were harvested and luciferase activity was measured from the lysates. The assay was carried out two times for all three cell lines.

There was remarkable inter-experimental variation for SW480 cells so that the tendency for higher  $\beta$ -catenin-dependent promoter activity observed in the FGFR4 transfectants (see Figure 80) did not reach significance.

In HCT116 and HT29 cells over-expressing FGFR4  $\beta$ -catenin-dependent reporter activity was down-regulated. FGFR4<sup>Arg</sup> over-expressing HCT116 and HT29 show significantly reduced promoter activity of  $\beta$ -catenin in the nucleus ( $p=0,0130$  and

## Results

p=0,0204). FGFR4<sup>Gly</sup> over-expressing HCT116 had a highly significant reduction of nuclear  $\beta$ -catenin (p<0,0001).

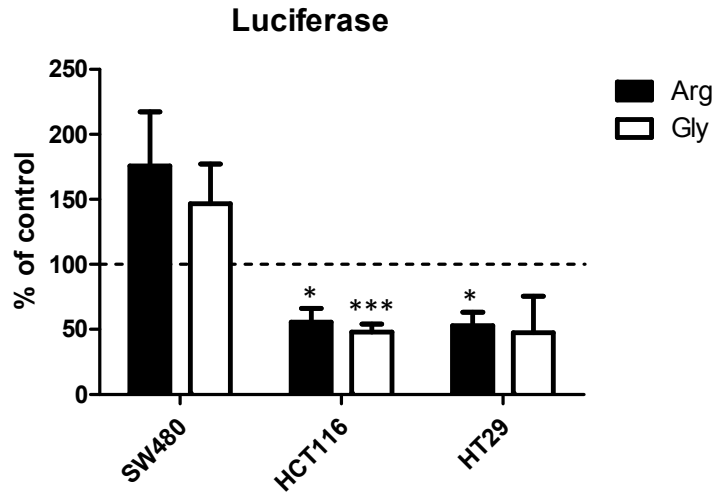


**Figure 80:** FGFR4 over-expression and  $\beta$ -catenin dependent promoter activity

$\beta$ -catenin-dependent luciferase expression of FGFR4 over-expressing SW480, HCT116 and HT29 was detected using the Dual-Luciferase® Reporter Assay System. Results are presented as percentage of control and pooled from two different approaches each three values. \*\*, and \*\*\* = significantly increased as compared to control at  $p \leq 0,01$ , and 0,001 respectively; Arg...FGFR4<sup>Arg</sup>, Gly...FGFR4<sup>Gly</sup>

## 4.5 Down-regulation of FGFR4

Three different approaches were used for inhibiting FGFR4-gene-expression and studying the biological consequences of down-regulation: *siRNA*, *dominant negative adenoviral vector*, and *dominant negative vector under the control of a tetracycline-dependent promoter*. The three CRC cell lines SW480, HCT116 and HT29 used for the FGFR4 over-expression experiments were taken for FGFR4 down-regulating strategies.

### 4.5.1 Down-regulation of FGFR4 via siRNA

Two different siRNAs were obtained and named si1 and si2. First optimization experiments were performed using different siRNA-concentrations, time points and other conditions like change of media after transfection were evaluated. The experiments were done individually for each cell line (SW480, HCT116, and HT29). Transfection was achieved by lipofection using the protocol described in chapter 3.1.15. Based on the outcome of a series of experiments for optimization the following conditions were chosen:

- 10nM siRNA was used
- media replacement after 6h in SW480, after 24h in HCT116 and HT29
- best knock down efficiency after 48h in HCT116 and after 72h in SW480 and HT29

#### 4.5.1.1 Knock down efficiency of FGFR4 on mRNA- and protein-level

Efficiency of knock down was determined from RNA and protein isolated from HCT116 (48h after transfection), SW480 and HT29 cells (72h after transfection).

## Results

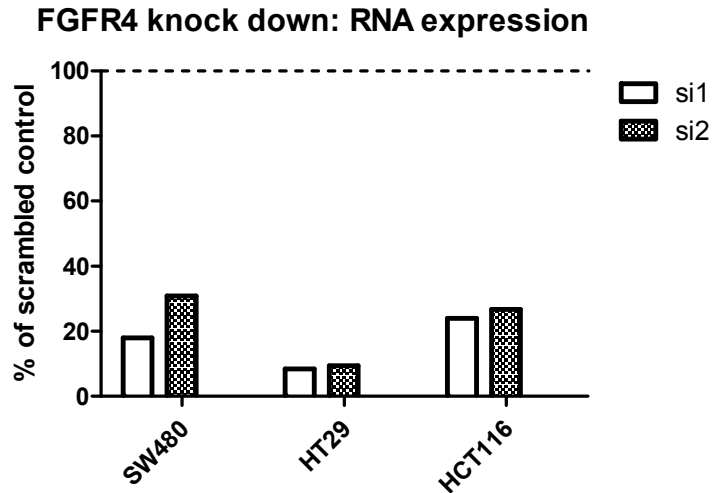


**Figure 81:** mRNA expression of FGFR4 after knock down in CRC cell lines

For each cell line optimized knock down conditions were applied. HCT116 mRNA was harvested 48h after transfection, HT29 and SW480 72h after transfection. FGFR4 expression was determined with TaqMan real-time PCR. Values are presented as percentage of scrambled control. si1/si2 ... siRNA1/siRNA2

In Figure 81 FGFR4 knock down efficiency is shown on mRNA level. For each cell line the optimal conditions for the most effective FGFR4 knock down result were applied. Both siRNAs had similar efficacy and reduced FGFR4 mRNA to 20-30% in SW480 and HCT116 cells and to 10% in HT29. This is also true for Figure 82 which shows FGFR4 knock down efficiency on protein level. Western blot with total protein lysates was performed for SW480 treated with siRNA1 and siRNA2 against FGFR4. A scrambled RNA served as a knock down control.  $\beta$ -actin was used as loading control.

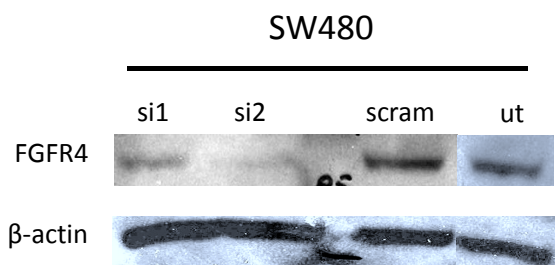


**Figure 82:** FGFR4 protein knock down efficiency of SW480 – western blot

Protein expression of FGFR4 in SW480 72 hours after FGFR4 knock down was detected by western blot. As a loading control  $\beta$ -actin is shown. si1/si2 ... siRNA1/siRNA2; scram ... scrambled control; ut ... untreated cells

## Results

To evaluate the FGFR4 knock down efficiency for HCT116 and HT29, surface expression of FGFR4 was determined by FACS analysis using a directly PE-labeled FGFR4 antibody. Surface FGFR4 expression was decreased by both siRNAs to 20-43% compared to scrambled control.

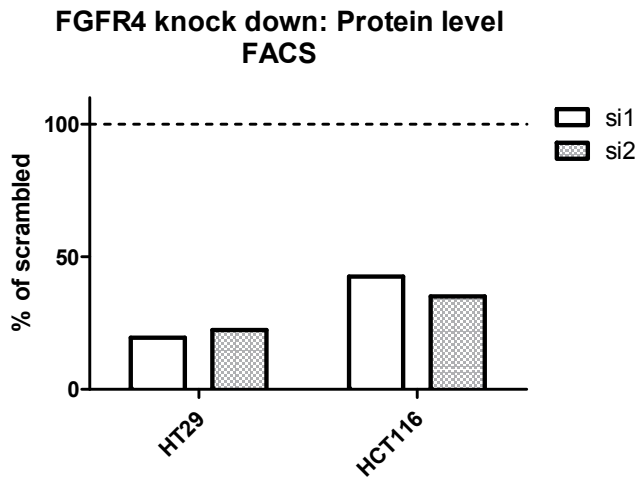


**Figure 83:** FGFR4 protein knock down efficiency of HCT116 and HT29 - FACS

Cell surface FGFR4 was evaluated by FACS analysis using a PE-labeled FGFR4 specific antibody for HT29 and HCT116. Knock down efficiency is presented as percentage of scrambled control. si1/si2 ... siRNA1/siRNA2;

### 4.5.1.2 Viability

Viability was measured using a neutral red assay three days after transfection in three independent experiments for each cell line. Si2 significantly reduced viability in all cell lines with a p-value of 0,0002 for SW480 and in HCT116 and HT29 with  $p < 0,0001$ . With si1 no significant changes in viability of SW480 compared to control were observed, but HT29 showed significantly reduced viability ( $p = < 0,0001$ ). Surprisingly, HCT116 viability was significantly increased after using si1 for FGFR4 ( $p = < 0,0001$ ).

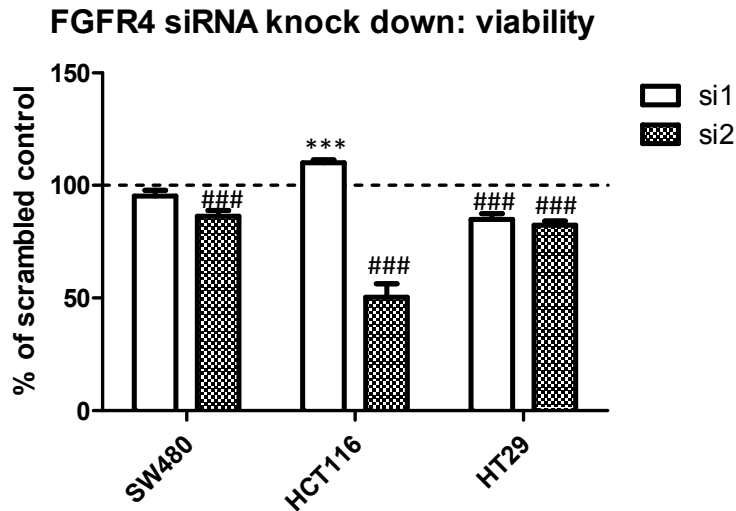


**Figure 84:** Cell viability after FGFR4 knock down in CRC cell lines

Viability was evaluated by neutral red assay. Values are presented as percentage of scrambled control. Results are pooled from three different approaches each at least four values. \*\*\* or ### = significantly increased or decreased as compared to control at  $p \leq 0,001$  respectively; si1/si2 ... siRNA1/siRNA2

#### 4.5.1.3 Proliferation

Cell proliferation was assessed by  $H^3$ -incorporation assay after FGFR4 knock down according to the protocol described in chapter 3.1.8. For each group eight wells were evaluated.  $H^3$ -Thymidine incorporation for FGFR4 knock down was performed three times for all three cell lines.

In SW480 cells FGFR4 knock down at low and intermediate cell densities did not result in differences in proliferation as compared to scrambled control. This changed in high density cultures where both siRNAs significantly reduced proliferation ( $p < 0,0001$  and  $p = 0,0002$ ).

By contrast, in HCT116 no effect of FGFR4 knock down was detected in intermediate and high density cultures but in the low density group FGFR4 knock down reduced proliferation significantly (si1  $p = 0,0126$  and si2  $p = 0,0033$ ).

The strongest effects were measured in HT29 cell lines. Si2 inhibited proliferation significantly at all cell densities as compared to scrambled control ( $p = 0,0071$  for 1.000 cells;  $p = 0,0004$  for 5.000 cells, and  $p = 0,0010$  for 10.000 cells respectively). Si1 was effective in cells with intermediate ( $p = 0,0007$ ) and high density ( $p = 0,0043$ ).

## Results

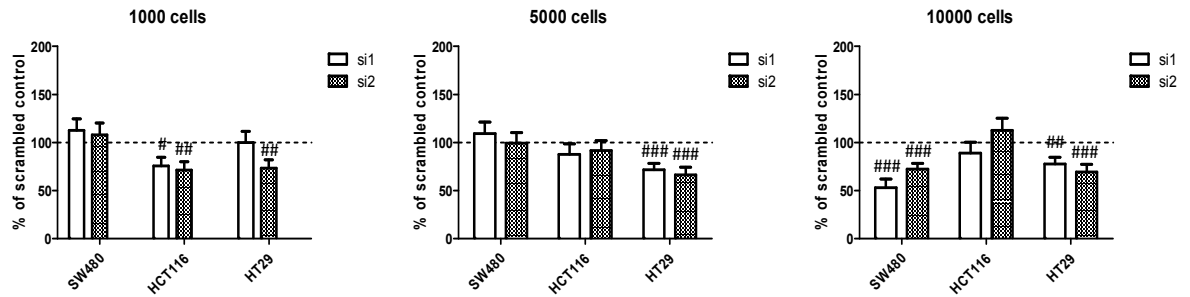


**Figure 85:** Proliferation of FGFR4 knock down in CRC cell lines

Proliferation was assessed by H<sup>3</sup>-incorporation assay. Cells were seeded at the indicated densities and H<sup>3</sup>-thymidine uptake was assayed 24 hours later. Values are presented as percentage of scrambled control and pooled from three approaches each eight values. #, ## and ### = significantly decreased as compared to control at  $p \leq 0,05$ , 0,01 and 0,001 respectively; si1/si2 ... siRNA1/siRNA2

### 4.5.1.4 Colony formation

Clonogenicity was determined using a colony formation assay described in chapter 3.1.5. For each group six wells were used and assay was repeated three times for each cell line.

Colony formation was not reduced by FGFR4 knock down in SW480, it was rather up-regulated significantly with si1 ( $p < 0,0001$ ). In HCT116 only si2 had an impact on colony formation which was significantly reduced ( $p = 0,0163$ ). Colony formation was inhibited considerably in HT29 with a p-value of  $< 0,0001$  for both siRNAs.

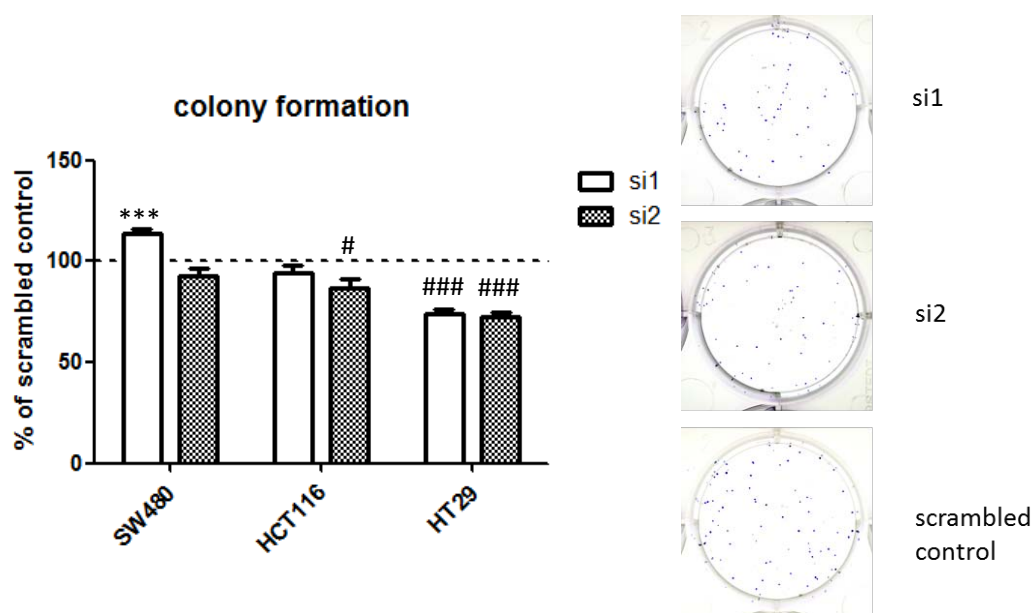


**Figure 86:** Colony formation of FGFR4 knock down in CRC cell lines

Colony counts are presented on the left as percentage of scrambled control pooled from three experiments with six values each. On the right representative photos of colony formation assay from HT29 cell line are shown. #, ## and ### = significantly decreased as compared to control at  $p \leq 0,05$ , 0,01 and 0,001 respectively; \*\*\* = significantly increased as compared to control at  $p \leq 0,001$ ; si1/si2 ... siRNA1/siRNA2

#### 4.5.1.5 Migration

Migration assays were performed following the protocol described in chapter 3.1.6. Assays were carried out in duplicates or triplicates and repeated three times for all three cell lines.

FGFR4 knock down did not inhibit migration in SW480. By contrast, migration in these cells was even stimulated. This was also the case for HCT116 with si1 which stimulated migration significantly ( $p=0,0224$ ), while si2 effectively decreased migration in HCT116 ( $p=0,0375$ ). The strongest inhibitory effect of FGFR4 knock down was observed with HT29: si2 reduced migration in HT29 significantly with a p-value of 0,0003.



## Results

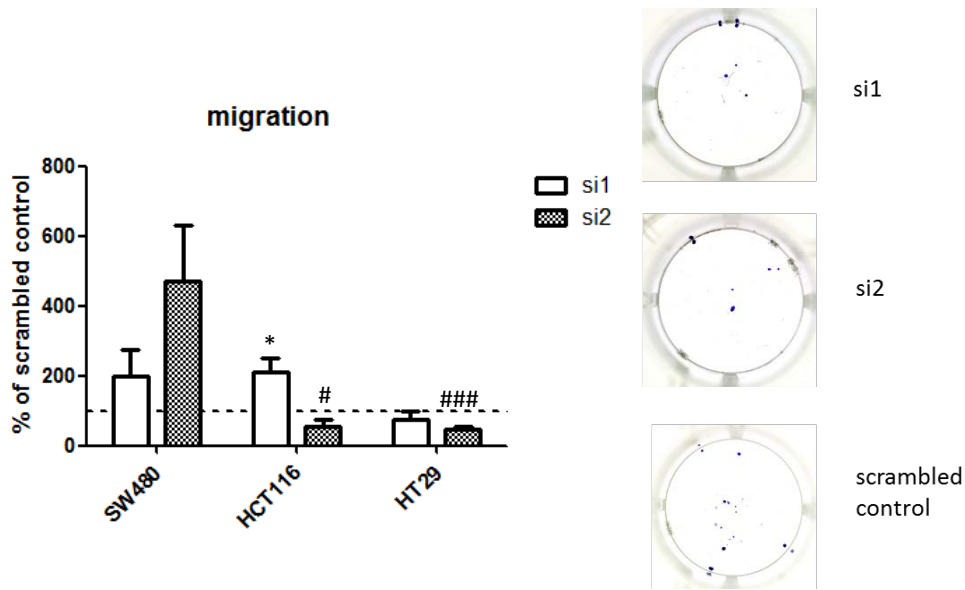


**Figure 87:** Migration of FGFR4 knock down in CRC cell lines

On the left side results from three approaches each three values pooled experiments are presented as percentage of scrambled control. On the right side representative pictures of HT29 migration and FGFR4 knock down with siRNA1 and siRNA2 as well as scrambled control are shown. #, ## and ### = significantly decreased as compared to control at  $p \leq 0,05$ , 0,01 and 0,001 respectively; \* = significantly increased as compared to control at  $p \leq 0,05$ ; si1/si2 ... siRNA1/siRNA2

### 4.5.1.6 Anchorage independent growth

Anchorage independent growth was assessed by soft agar assay performed according to the protocol described in chapter 3.1.7. For each group duplicates were performed and the assay was repeated three times for all three cell lines.

Inhibition of anchorage independent growth was only achieved in SW480 with si2 ( $p < 0,0001$ ). In the other cell lines FGFR4 knock down via siRNA resulted in an increase of growing colonies under anchorage independent conditions which was in some cases significant (HCT116: si1  $p = 0,0052$ , si2  $p = 0,0295$ ).

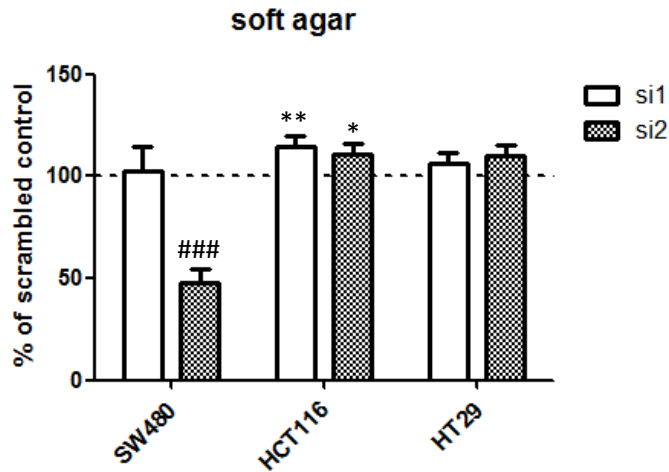


**Figure 88:** Anchorage independent growth of FGFR4 knock down in CRC cell lines

Values are presented as percentage of scrambled control and pooled from three different experiments with ten values each. ### = significantly decreased as compared to control at  $p \leq 0,001$ ; \* and \*\* = significantly increased as compared to control at  $p \leq 0,05$  and  $0,01$ ; si1/si2 ... siRNA1/siRNA2

#### 4.5.1.7 Signaling

The effects of FGFR4 knock down on cell signaling were evaluated from total protein lysates which were obtained according to the protocol described in chapter 3.4.1.1. Phosphoproteins were analyzed by western blot and phosphorylation of ERK and S6 were evaluated.

In HT29 phosphorylation of S6 was stimulated whereas in SW480 it was decreased compared to scrambled controls. Also ERK phosphorylation was stimulated in SW480 compared to scrambled controls.

## Results

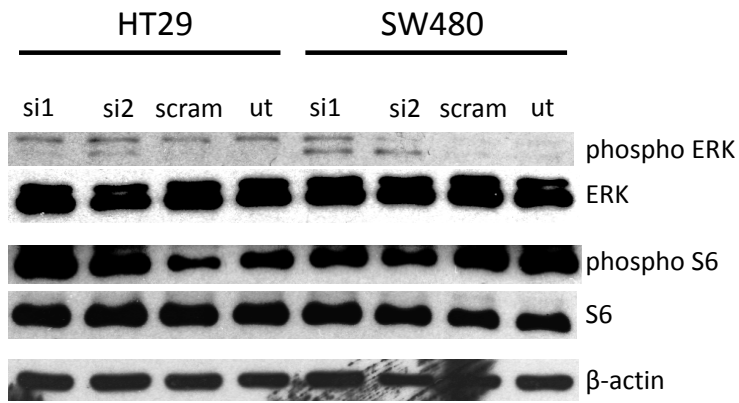


**Figure 89:** Signaling of FGFR4 knock down via siRNA in HT29 and SW480

Phosphorylation of ERK and S6 were evaluated by western blot.  $\beta$ -actin served as a loading control. si1/si2 ... siRNA1/siRNA2; scram ... scrambled control; ut ... untreated cells

### **4.5.2 Down-regulation of FGFR4 via dominant negative adenovirus**

Besides using siRNAs for down-regulating of the FGFR4 an adenoviral approach was implemented. For this purpose a dominant negative construct of the FGFR4 called K5 (see chapter 3.3.1.1) was introduced into an adenovirus. The K5 construct was derived from the FGFR4-sequence by substituting the kinase domain with a cyano-fluorescence protein (CFP). Consequently, the K5 construct is a 78kDa dominant negative FGFR4 protein. GFP expressing virus and an unrelated noncoding virus (Cox as) were used as control. Because of its strong expression GFP virus was used with 1MOI (Multiplicity of Infection) whereas the K5 and Cox as virus were infected with 10MOI.

#### **4.5.2.1 mRNA expression**

Cells were infected with the adenovirus 24h before harvesting the RNA. Expression of the K5 construct was measured by assessing FGFR4 expression using TaqMan quantitative real-time PCR. TaqMan probe binds between exon 8-9 which is next to the transmembrane domain (located at exon 9-10) (Kostrzewa and Muller 1998), and consequently detects also the K5 construct.

FGFR4 expression was up-regulated in all three cell lines which presents a high expression of the K5 construct after 24h in all cell lines. In SW480 the expression of FGFR4 was 3-fold, in HCT116 4-14-fold and in HT29 2-fold higher than in the GFP-control.

## Results

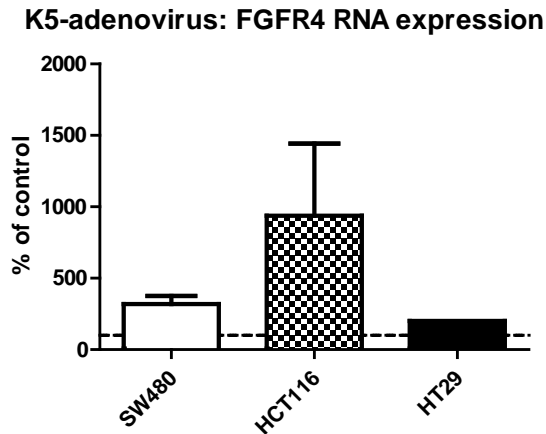


**Figure 90:** K5 mRNA expression of K5-adenovirally infected CRC cell lines: real-time PCR

K5 expression is shown by up-regulated FGFR4 expression detected by using FGFR4 TaqMan kit and quantitative real-time PCR. Results are presented as percentage of control virus and are pooled from two approaches for SW480 and HCT116.

Additionally, standard PCR was performed with GFP-Primers which also detected the CFP in the K5 construct.

In all three cell lines the K5 expression could be detected using a standard GFP-PCR protocol. GAPDH was used as a positive PCR control and loading control. No GFP-band should be present in cells infected by Cox as. The expression of the K5 was even higher than the expression of the GFP infected cells. In the HT29 cells no GFP-band could be detected in cells infected by the GFP virus.

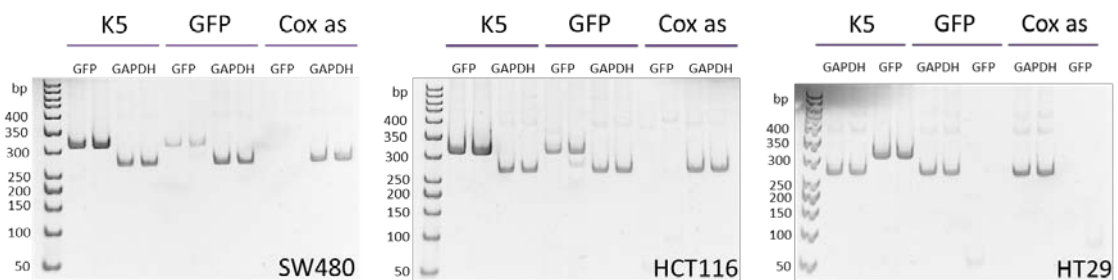


**Figure 91:** K5 mRNA expression of K5-adenovirally infected CRC cell lines: standard PCR

Pictures present gels of PCR-products from all three CRC cell lines infected with K5-, GFP- and the unrelated noncoding virus Cox as. K5 and GFP were detected using GFP-primers which also bind to the CFP domain of the K5-construct. GAPDH was used as a PCR-control.

## Results

### 4.5.2.2 Protein expression

Total protein lysates of SW480, HCT116 and HT29 cells infected with K5, GFP and Cox as virus were harvested after 24h and western blot was performed.

The unmodified FGFR4 protein has a size of 88kDa but phosphorylated and glycosylated the protein reaches a size of ~110kDa. The expression of the K5 construct was evaluated by using a FGFR4-antibody which binds the N-terminal domain of the protein. The K5-band was expected at 80-90kDa because of an original size of 78kDa of the unglycosylated protein. Unfortunately, no signal verifying the K5 expression could be detected for the CRC cell lines when infected with 10MOI.

Figure 92 shows the result of a western blot of HCT116 cells infected with K5 at 1, 10 and 50MOI. Protein lysates were harvested 48h after infection. Only in cells infected with K5 at 50MOI a signal for the K5-protein could be detected. This could not be shown for SW480 or HT29 cells.

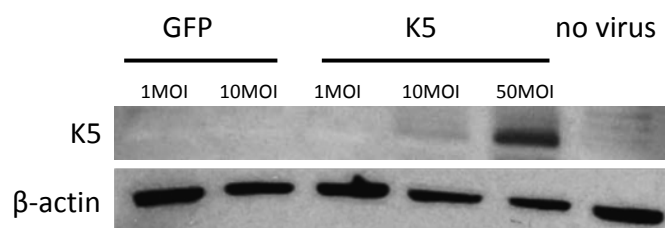


**Figure 92:** Expression of the K5-protein

HCT116 cells were infected with the dominant negative FGFR4 adenovirus K5 and GFP at various MOIs. Protein lysates were harvested after 48h and western blot was performed. The K5-protein was expected to have a molecular weight of 78kDa when unglycosylated, the signal was detected at 90-95kDa with an N-terminal FGFR4 antibody.

### 4.5.2.3 Viability

To evaluate the impact of the dominant negative FGFR4 adenovirus on the viability cells were infected in a plate with K5 and the control virus. 24h later cells were seeded into a 24-well plate. For each group at least 4-6 wells were prepared. Viability was measured after 24h and after five days by using a neutral red assay. Viability was calculated by normalizing on values measured after 24h and the control. The assay was repeated at least three times.

## Results

Viability was significantly decreased in all of the three cell lines when treated with the dominant negative FGFR4 adenovirus (p-values: SW480: 0,034; HCT116: 0,083; HT29: 0,0129) compared to the control.

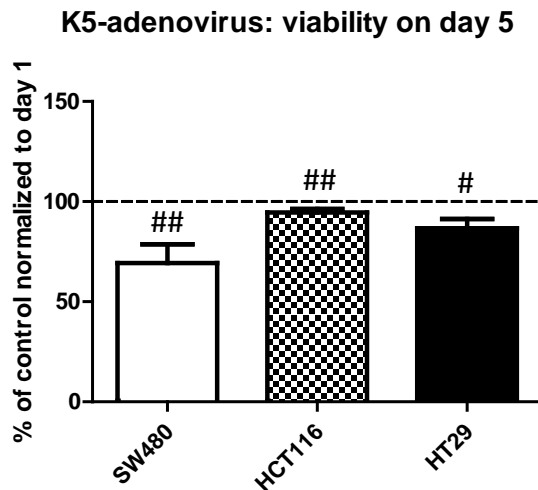


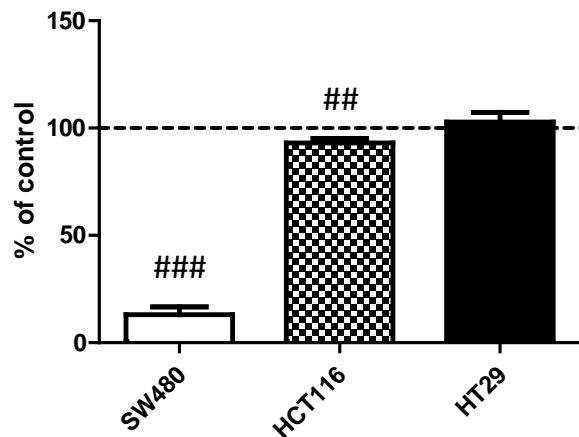
**Figure 93:** Cell viability of CRC cell lines infected with K5 adenovirus

Viability was measured by neutral red assay on day 1 and 5. Results are presented as percentage of control and normalized to day 1. Results are pooled from three different approaches each at least four values. #, ## and ### = significantly decreased as compared to control,  $p < 0,05$ ,  $p < 0,01$  and  $p < 0,001$  respectively.

### 4.5.2.4 Colony Formation

Cells were infected in a plate with the K5 and the control virus. 24h later colony formation assay was performed as described in chapter 3.1.5. For each group six wells were evaluated and the assay was repeated at least three times for each cell line.

Colony formation was down-regulated in cells infected with the K5 adenovirus compared to the control in SW480 and in HCT116 significantly (p-values: SW480:  $<0,0001$ ; HCT116: 0,0063) but not in the HT29 cell line.

**K5-adenovirus: colony formation**

**Figure 94:** Colony formation of CRC cell lines infected with K5 adenovirus

Colony formation of SW480, HCT116 and HT29 infected with K5 adenovirus is presented as percentage of control. Results are pooled from three different approaches each at least six values. #, ## and ### = significantly decreased as compared to control at  $p \leq 0,05$ , 0,01 and 0,001 respectively.

#### 4.5.2.5 Migration

Like for colony formation and viability cells were infected in a plate with the K5 and the control virus 24h before seeding into the transwell filters. Migration was assessed using filter migration assays described in chapter 3.1.6. For each group three wells were evaluated. Experiment was repeated at least three times for each cell line.

Migration was significantly reduced in SW480 cells infected by K5 adenovirus ( $p < 0,0001$ ). In HCT116 cells results differed considerably from experiment to experiment. Also in the HT29 cells the variation of the results was remarkably high. In HT29 cells infected by K5 adenovirus there is a tendency for down-regulated migration when compared to the control.



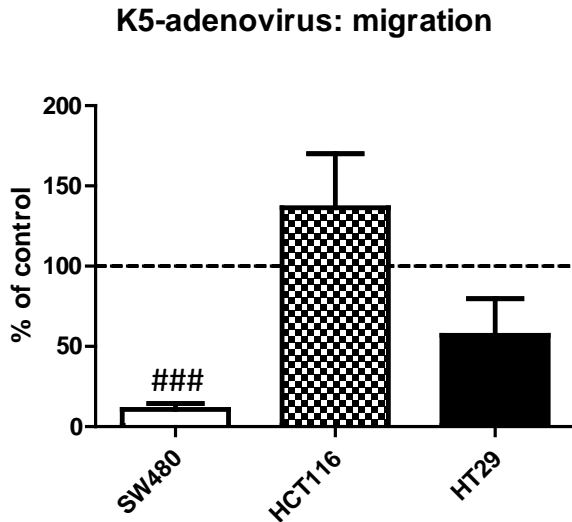


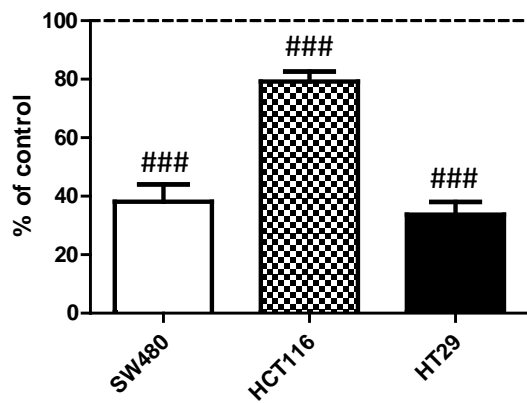
**Figure 95:** Migration of CRC cell lines infected with K5 adenovirus

Cell migration of SW480, HCT116 and HT29 infected with K5 adenovirus was assessed by filter migration assay. Results are presented as percentage of control and pooled from three different approaches each at least three values. #, ## and ### = significantly decreased as compared to control at  $p \leq 0,05$ ,  $0,01$  and  $0,001$  respectively.

#### 4.5.2.6 Anchorage independent growth

To evaluate the influence of the K5 adenovirus on malignant growth, soft agar assay was performed as described in chapter 3.1.7. For this purpose, cells were infected with the K5 and the control virus in a plate 24h prior to seeding them into the soft agar matrix. Colonies were counted after 2-3 weeks. For each group two wells were evaluated.

Infection with the K5 adenovirus significantly reduced malignant growth in all three cell lines ( $p < 0,0001$ ) compared to the control.

**K5-adenovirus: anchorage independent growth**

**Figure 96:** Anchorage independent growth of CRC cell lines infected with K5 adenovirus

Malignant anchorage independent cell growth of SW480, HCT116 and HT29 infected with K5 adenovirus was assessed by soft agar assay. Results are pooled and presented as percentage of control from one approach with ten values for HT29 and at least two approaches (each 10 values) for SW480 and HCT116. #, ## and ### = significantly decreased as compared to control at  $p < 0,05$ ,  $0,01$  and  $0,001$  respectively.

### **4.5.3 Tet-inducible down-regulation of FGFR4**

After using the K5 construct in transient approaches with adenoviral vectors it was our aim to transfect the K5 vector into cell lines and let them stably express the construct. Due to its growth inhibiting effects it was not possible to get stable clones expressing the K5 construct. For this reason it was decided to clone the K5 construct into an inducible tet-off system. Hence, the construct is only expressed when induced in the context of an experiment and it should be easier to obtain stable transfectants because they do not constitutively express the growth inhibiting K5 gene. As for control a GFP construct was also cloned into the tet-off-system.

#### **4.5.3.1 Cloning of a tet-inducible dominant negative FGFR4 construct**

##### *4.5.3.1.1 Excision of K5 and GFP*

First the dominant negative FGFR4 construct K5 and a GFP were excised from their plasmids. To cut out the K5 fragment three endonucleases were used (BcuI, EcoRV and NheI) which results in three pieces. The K5 gene contains 2194bp and the remaining plasmid contains 2284bp which was also cut into two fragments of 1822bp and 462bp size. For GFP excision a restriction digest with BamHI and HpaI was carried out to produce a 856bp GFP gene. Before using a preparative digest of 100µl conditions were tested with a smaller reaction mix (10µl). Samples were loaded on a 1% agarose-gel and quality of the restriction digest was monitored (data not shown). The preparative digest was separated under the same conditions, the correct band was cut out and the DNA was isolated. Amount of DNA was measured.

## Results

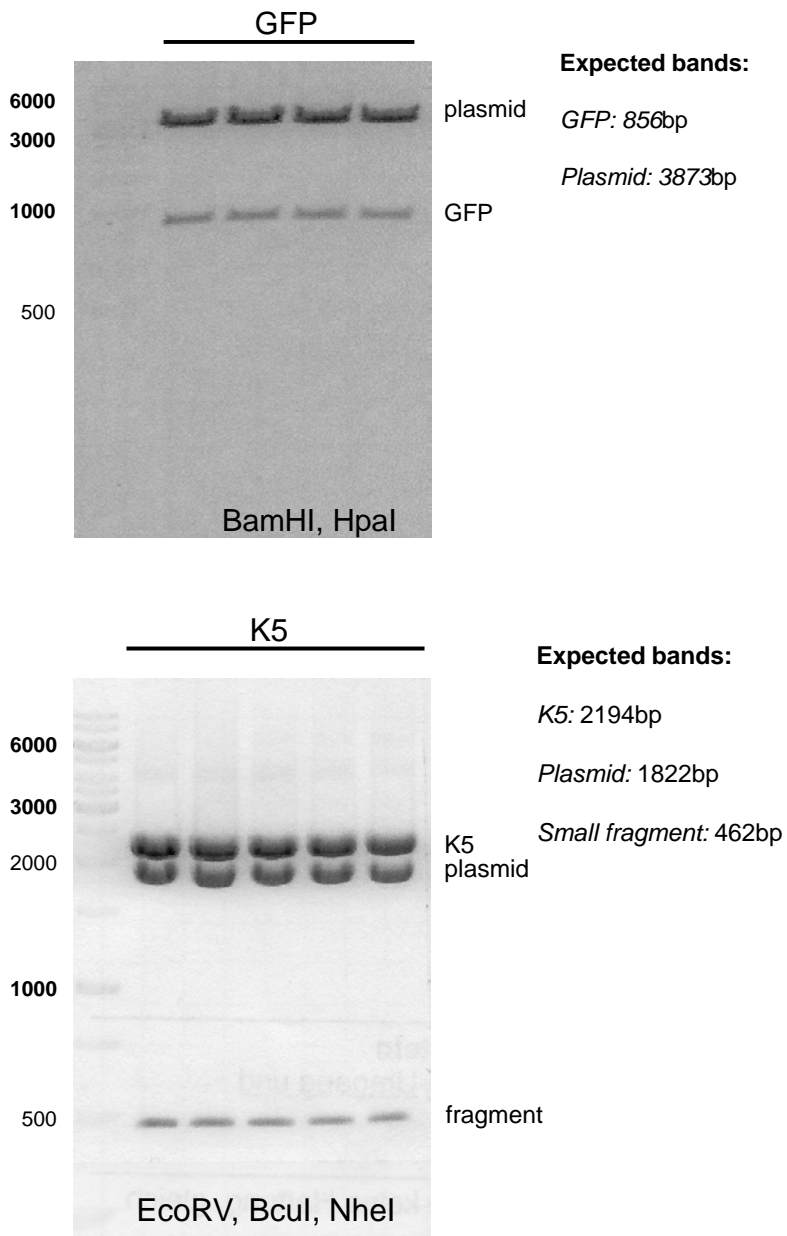


**Figure 97:** Excision of K5 and GFP

The upper panel shows the 856bp GFP-fragment and the 3873bp plasmid-fragment. BamHI and HpaI were used to cut out the GFP fragment.

The lower panel shows the 2194bp K5-fragment cut by NheI, EcoRV and BcuI endonuclease. The remaining plasmid was also cut into two fragments which contained 1822bp and 462bp. Bands are detected on 1% agarose-gel.

## Results

### 4.5.3.1.2 Transformation of *pTet-off* and *pTRE-tight* into *Jm109* bacteria strain

The *pTet-off* vector and the *pTRE-tight* vector were inserted into bacteria (*Jm109* strain) according to the protocol described in chapter 3.3.5. Vector DNA was isolated from a 100ml bacteria culture and verified by a control restriction digest. *pTet-off* was cut with *Bam*H1 and *pTRE-tight* with *Xho*I endonucleases. Fragments were separated on a 1% agarose-gel.

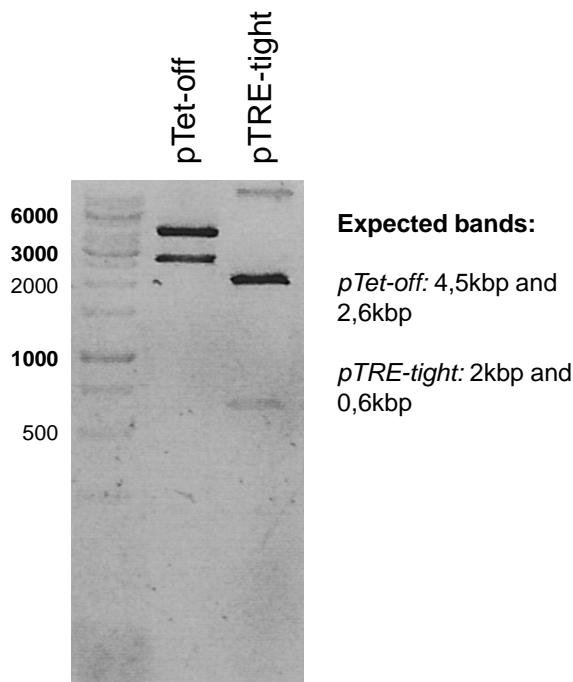


**Figure 98:** Control restriction digest of *pTet-off* and *pTRE-tight*

*pTet-off* was cut with *Bam*H1 and results in two fragments with 4,5kbp and 2,6kbp size whereas *pTRE-tight* was cut with *Xho*I into a 2kbp and a 0,6kbp fragment. Restriction digests were separated on a 1% agarose-gel.

### 4.5.3.1.3 Preparative digest of *pTRE-tight* for cloning

Preparative digest *pTRE-tight* for GFP insert was performed with *Bam*H1 and *Eco*RV. For the K5 insert *Nhe*I and *Eco*RV endonucleases were used. DNA was treated with a calf intestinal alkaline phosphatase (CIAP) to avoid the recircularization and relegation of the plasmid and then separated on a 1% agarose-gel. The correct band was cut out and DNA was isolated.

## Results

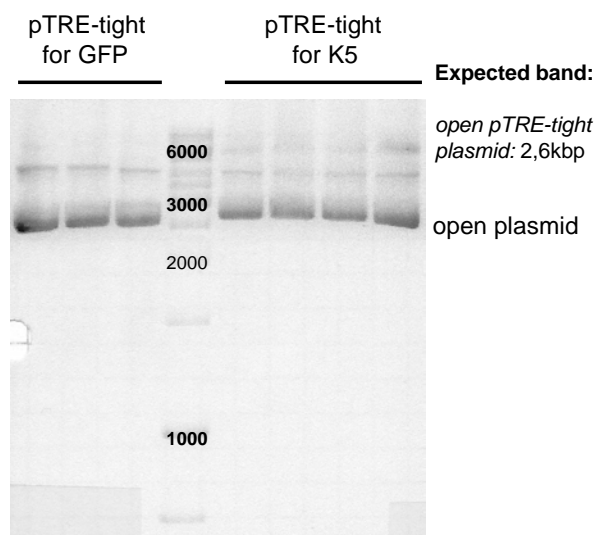


**Figure 99:** Preparative digest of pTRE-tight for cloning

The pTRE-tight vector was cut for the GFP insert with BamHI and EcoRV and for the K5 insert with NheI and EcoRV. The opened plasmid contains a size of ~2,6kbp for both inserts. Bands were separated on a 1% agarose-gel.

### 4.5.3.1.4 Ligation, transformation into XL1Blue bacteria strain and verification

Insert and plasmid were mixed together in defined ratios and incubated with a ligase overnight. A negative control was performed with the vector and insert but no ligase and another with the vector but without the insert. On the next day XL1Blue bacteria were transformed with ligated plasmids and negative controls. Additionally, a positive control (uncut plasmid) was also brought into the bacteria. Bacteria were plated on an ampicillin-containing agar-plate and incubated over night. After 24h five colonies of each plate for the GFP-pTRE-tight and the K5-pTRE-tight constructs were picked and DNA was isolated for control restriction digests with BamHI & HpaI, and DraI. For each group one cloned plasmid was selected after the control restriction digests and larger amounts of DNA were prepared.



## Results

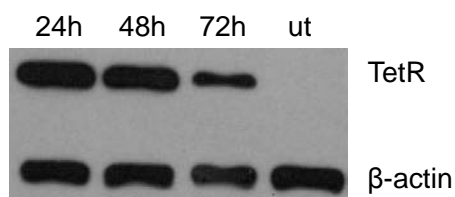


**Figure 101:** Protein expression of TetR in a transient cell model

HCT116 cell line was transfected with pTet-off vector and transient expression of TetR-protein was assessed after 24, 48, and 72hours.  $\beta$ -actin was used as a loading control. ut...untransfected cells

The function of the tet-off system was tested in presence and absence of Doxycycline. Again one million cells were seeded into 6-well-plates per well and transfected with:

- pTet-off and pTRE-tight-GFP (two separate approaches)
- pTRE-tight-GFP: negative control
- pcDNA-GFP: positive control

Doxycycline was added at a concentration of 100ng/ml to one of the pTet-off/pTRE-tight-GFP group. After three days expression of GFP was evaluated by FACS analysis. Each tested group was evaluated as duplicates.

A pcDNA-GFP-vector was used as a positive transfection-control. 60% of the cells transfected with the pcDNA-GFP-vector were found positive with strong expression intensity (mean-value). Only about 19% of the pTet-off/pTRE-tight-GFP transfected cells were positive and the mean of GFP fluorescence-intensity was 2/3 of the positive control. At least 5-10% of the pTRE-tight-GFP transfected cells, which did not receive the pTet-off control element and should not express GFP, were also positive. Their expression-intensity was very low however. The same could be seen with pTet-off/pTRE-tight-GFP expressing cells treated with Doxycycline where 5% of the cells were positive again with very low mean fluorescence intensity.



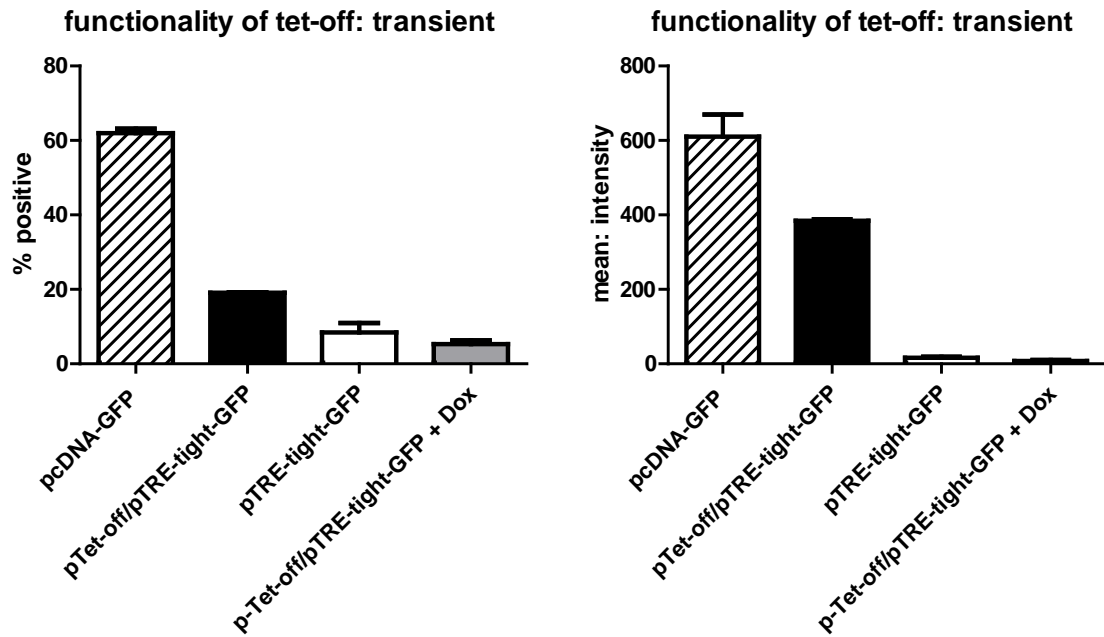


**Figure 102:** Function of tet-off-system in a transient cell model

HCT116 were transfected with pcDNA-GFP (positive control), pTRE-tight-GFP (negative control), and pTet-off and pTRE-tight-GFP +/- Doxycycline-treatment. GFP-expression was evaluated by FACS analysis. On the left panel percentage of GFP-positive cells is presented whereas on the right panel the expression-intensity of GFP was analyzed.

#### 4.5.3.2.2 Establishment of pTet-off expressing stable cells

To establish pTet-off stable cells lipofection of pTet-off-vector and selection was performed according to the protocol described in chapters 3.1.13 and 3.1.14. After 2-3 weeks clones were transiently transfected with the GFP-response plasmid pTRE-tight-GFP and efficiency was evaluated by FACS analysis. 22% of HCT116 stably expressing pTet-off and 8,4% of SW480 stably expressing pTet-off were GFP positive after transient pTRE-tight-GFP transfection.

To increase the number of positive pTet-off-stable cells both stable cell lines were seeded at a density of  $3 \times 10^6$  cells per plate and transiently transfected with the pTRE-tight-GFP-plasmid. 48 hours later GFP-positive cells were sorted out and seeded into a new plate, transfected and sorted for a second time. Sorted cells were split up into two groups: one group permanently treated with Doxycycline and one group without Doxycycline. pTet-off expression of double sorted cells was examined by transient transfection of pTRE-tight-GFP-plasmid and FACS analysis.

## Results

After the second sort nearly 100% of the cells stably expressed the pTet-off vector. Again, SW480 and HCT116 cells transfected only with pTRE-tight-GFP were taken as a negative control to determine the leakiness of the tet-off-system. Although in SW480 48% and in HCT116 30% of the pTRE-tight-GFP transfected cells were positive, the expression intensity was very low. Furthermore, the ability to switch off the signal was determined. pTet-off-stable cells constantly treated with Doxycycline were found to be positive concerning GFP-expression in 28% of SW480 and 40% of HCT116. Nevertheless, the mean-value was again negligibly low. A very low amount (6% in SW480, 1,5% in HCT116) of the double sorted pTet-off stable cells showed positive expression of GFP without transfecting the response plasmid. This is the consequence of the double-sorting-process where each time cells needed to be transfected with the GFP-response plasmid. With passaging most cells lost the transiently transfected pTRE-tight-GFP-vector but a very small proportion still retained it.

## Results

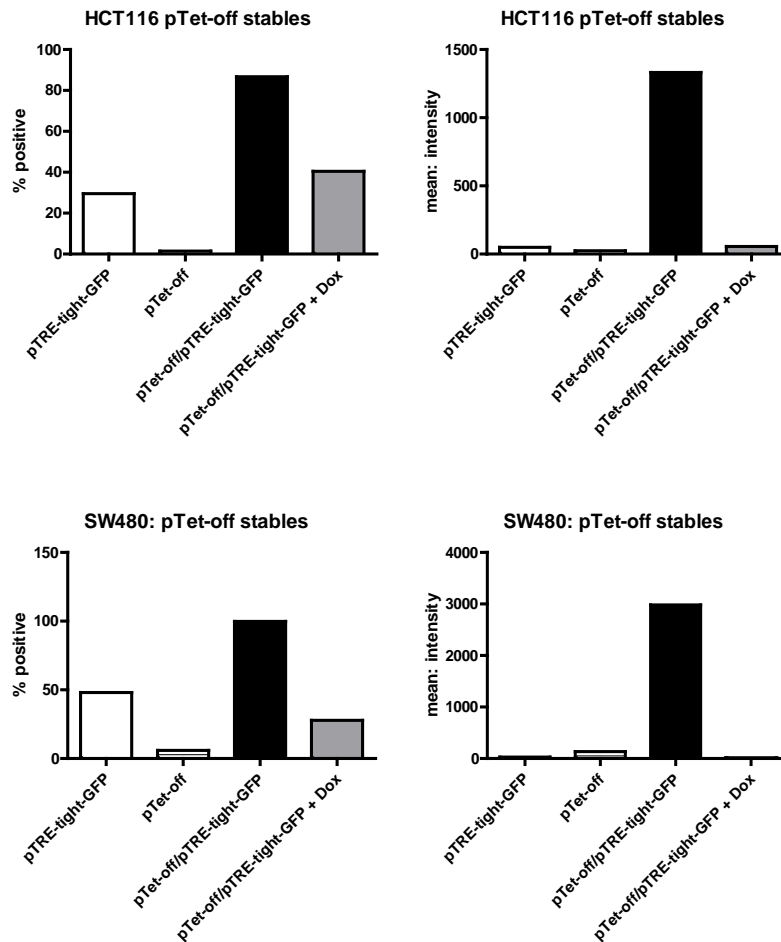


**Figure 103:** Stable expression of pTet-off in SW480 and HCT116

After sorting two times for transient pTet-off/pTRE-tight-GFP positive cells transient transfection with pTRE-tight-GFP was carried out and cells were analyzed by FACS to evaluate the pTet-off expression. Additionally, one group of pTet-off positive cells was treated constantly with Doxycycline to switch off the interaction with pTRE-tight-plasmid. On the left side percentage of positive cells is presented, on the right side the GFP fluorescence intensity represented by the mean value is given. The upper panel shows the results for SW480, the lower for HCT116 cell line.

### 4.5.3.2.3 Establishment of pTet-off/pTRE-tight-K5 and -GFP stable cells

Because the pTRE-tight-plasmid contains no selection marker for eukaryotes a linearized puromycin-resistance-gene was co-transfected. 1/5 of the transfected DNA-amount was presented by the puromycin-resistance-gene.  $4 \cdot 10^5$  pTet-off stable cells constantly treated with Doxycyclin were seeded into 6-well-plates and transfected with pTRE-tight-K5 or pTRE-tight-GFP together with puromycin-resistance-gene by lipofection. After 24h cells were transferred into plates and selection with 0,6 $\mu$ g/ml

## Results

puromycin for SW480 and 0,4µg/ml puromycin for HCT116 was started 24h later. Transfection and selection was performed in the presence of Doxycycline.

Transfection with pTRE-tight-K5 and pTRE-tight-GFP was carried out two times.

Mixed clone pools of SW480 stably expressing pTRE-tight-K5 were established. For HCT116 seven pTRE-tight-K5 stably expressing clones were selected by observation of the CFP fluorescence of the pTRE-tight-K5 under the microscope and isolated.

All pTet-off/pTRE-tight-K5 positive clones (HCT116) and mixed clone pools (SW480) were split into 6-well-plates and incubated with and without Doxycycline. After 72h pTRE-tight-K5 expression was assessed by FACS analysis.

For HCT116 pTet-off/pTRE-tight-K5 the highest expression was 3% positive cells in the absence of Doxycycline and 1,3% under Doxycycline treatment. SW480 pTet-off/pTRE-tight-K5 had an expression of 8,6% and in presence of Doxycycline 0,8%. These two cell populations were used for the following experiments.

For pTet-off/pTRE-tight-GFP positive clones could be picked under the UV-microscope for HCT and SW480 cells. They were also split and raised with and without Doxycycline and GFP expression was analyzed by FACS after a few days.

Based on the on/off ratio of their GFP-expression appropriate pTet-off/pTRE-tight-GFP stable positive clones were chosen. The HCT pTet-off/pTRE-tight-GFP stable clone expresses 76% GFP without Doxycycline and in presence of Doxycycline the signal is down-regulated to 25% expression. For SW480 pTet-off/pTRE-tight-GFP stable clones 72% GFP expression is reached in the absence of Doxycycline and 39% in the presence of Doxycycline.

#### *4.5.3.2.4 Expression of GFP and K5 in pTet-off/pTRE-tight stable cells*

RNA-expression of pTRE-tight-K5 and -GFP was assessed with and without Doxycycline treatment. Cells were seeded at equal densities and RNA was harvested. mRNA expression was measured by quantitative real-time PCR with GFP primer in the presence of SYBR-green.

## Results

Expression of K5 as well as switching off the expression of K5 and GFP by adding Doxycycline could be demonstrated. Results were normalized to GAPDH. Expression of GFP was very high in HCT116 cells whereas K5 expression was quite low. In SW480 the difference between GFP and K5 expression was not as clear compared to HCT116.

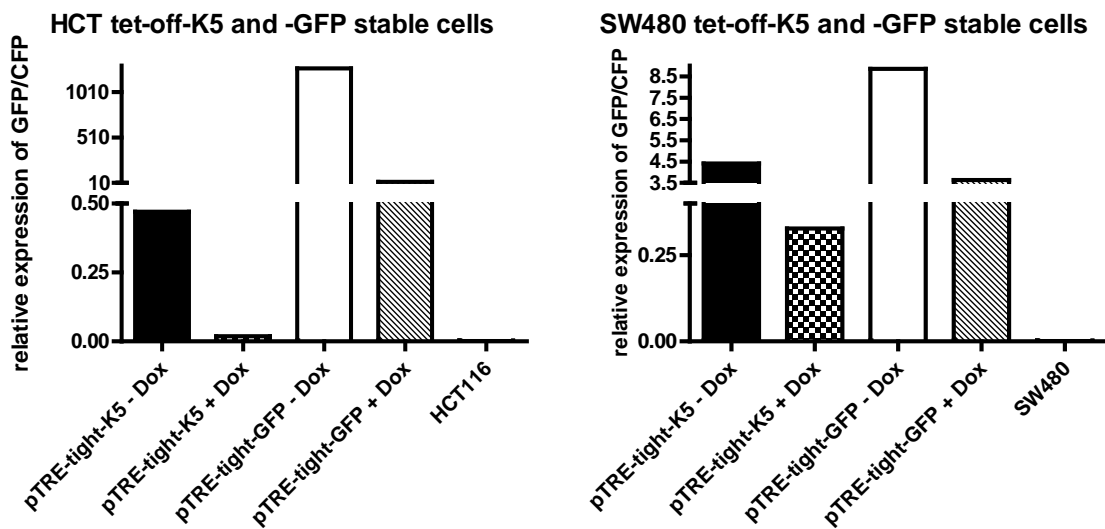


**Figure 104:** mRNA expression of GFP/K5 in pTet-off/pTRE-tight-K5 and -GFP stable cells

mRNA expression of GFP and K5 was assessed by SYBR-Green real-time PCR. Expression was measured in the absence and presence of Doxycycline. Untransfected cell lines were used for negative control. Results are normalized to GAPDH expression.

### 4.5.3.3 Influence of Doxycycline dependent K5 expression on cell biology

#### 4.5.3.3.1 Viability

To analyze the impact of Doxycycline-dependent expression of K5 on cell viability  $1 \times 10^4$  cells per well were seeded into a 24-well plate with and without the presence of Doxycycline. Five days later a neutral red assay was performed. At least four wells per group were evaluated. Assay was repeated three times.

Cells expressing the pTRE-tight-K5 construct showed decreased viability (significant in HCT116:  $p=0,0009$ ). The viability of pTRE-tight-K5 expressing cells was reduced by 26% in HCT116 cells and by only 9% in SW480.

## Results

Comparison of viability of cells with or without Doxycycline showed no differences induced by the antibiotic in any of the groups.

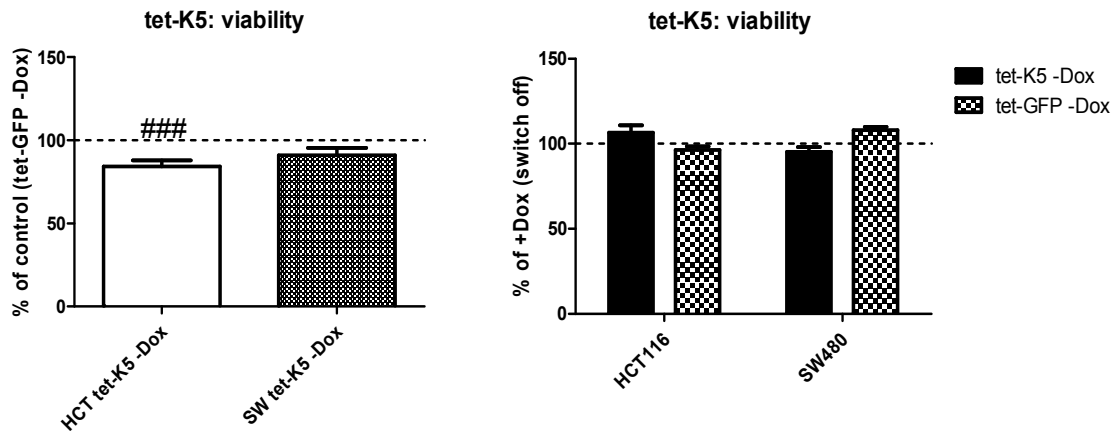


**Figure 105:** Viability of pTRE-tight-K5 and -GFP expressing cells +/- Doxycycline

On the left panel viability of HCT116 and SW480 stably expressing the tet-off-K5 construct without treatment with Doxycycline is presented as percentage of tet-off-GFP expressing control. On the right panel differences in viability concerning presence of Doxycycline in the tet-off-K5 and -GFP expressing cell lines are shown. Results are pooled from three different approaches and presented as percentage of the corresponding cells with treatment of Doxycycline. ### = significantly decreased as compared to control at  $p \leq 0,001$ .

### 4.5.3.3.2 Cell cycle: FACS analysis

Investigating the impact of the K5 construct on cell cycle pTet-off/pTRE-tight-K5 and -GFP stably expressing cells were analyzed by cell cycle FACS with and without Doxycycline.

No Doxycycline-induced differences could be seen.

## Results

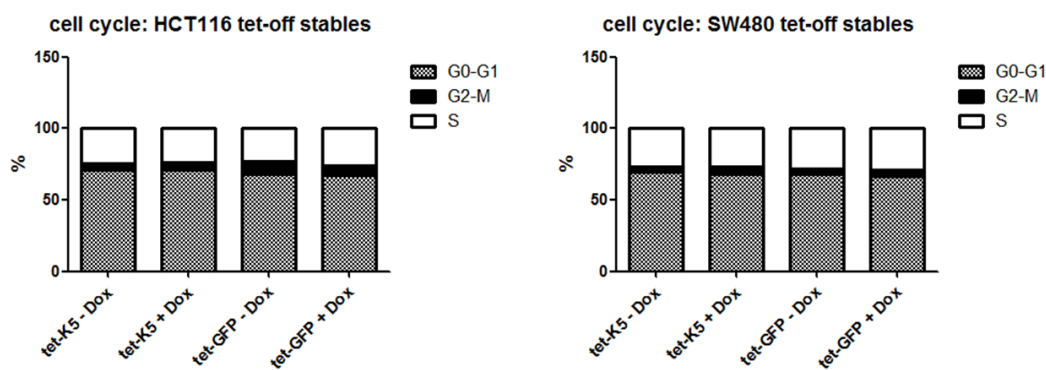


**Figure 106:** Cell cycle of pTRE-tight-K5 and –GFP expressing cells +/- Doxycycline

Cells were treated with and without Doxycycline and after three days cell cycle FACS was performed. On the left panel results are given for HCT116 tet-off stables on the right panel for SW480 tet-off stables.

### 4.5.3.3.3 Apoptosis: JC1-FACS

Our working hypothesis assumed that cells expressing the pTRE-tight-K5 vector had a higher incidence for apoptosis. Consequently apoptotic cells were analyzed by FACS using the mitochondrial tracer JC-1 three days after plating. In SW480 the stable expression of the pTRE-tight-K5 vector in the cells did not cause elevated apoptosis as compared to the controls with Doxycycline. In HCT116 cells expressing the pTRE-tight-K5 apoptosis rate seemed to be even higher when treated with Doxycycline. Surprisingly pTRE-tight-GFP expressing cells without Doxycycline had an elevated apoptosis incidence compared to cells treated with Doxycycline.

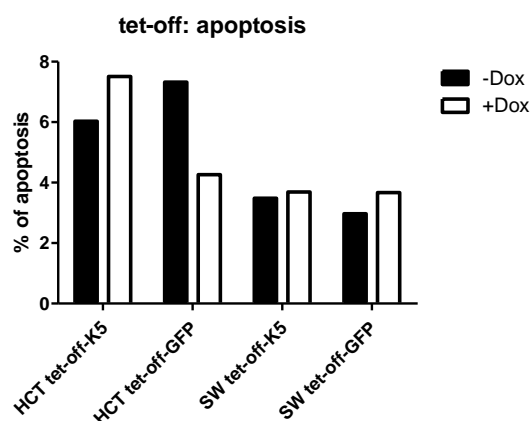


**Figure 107:** Apoptosis of pTRE-tight-K5 and –GFP expressing cells +/- Doxycycline

All groups are presented with and without treatment of Doxycycline. After three days JC-1 FACS was performed. Results are presented as percentage of apoptosis.

## Results

### 4.5.3.3.4 Cell migration

The effects of pTRE-tight-K5 expression on the cells' ability to migrate were assessed by filter migration assay. Cells were treated with and without Doxycycline five days before seeding into the filter-membranes. The assay was carried out two times in triplicates for each group.

Migration seemed to be reduced in the HCT116 pTRE-tight-K5 expressing cells whereas in SW480 cells the K5 expression elevated the ability to migrate.

Regarding the differences in presence or absence of Doxycycline in HCT116 pTet-off/pTRE-tight-K5 stable cells could migrate better in the absence of Doxycycline whereas in the control group pTet-off/pTRE-tight-GFP migration was inhibited by removing Doxycycline. In SW480 cell lines the case was different. pTet-off/pTRE-tight-K5 expressing cells were slightly inhibited in migration by switching on the expression of pTRE-tight-K5 whereas the control group pTet-off/pTRE-tight-GFP migrated better in the absence of Doxycycline.

None of these migration results could be proven as statistically significant.

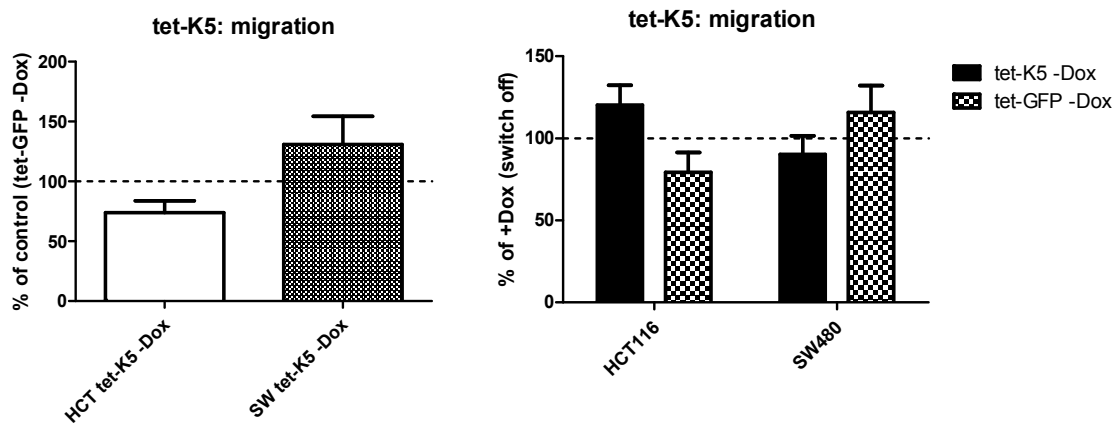


**Figure 108:** Migration of pTRE-tight-K5 and -GFP expressing cells +/- Doxycycline

In the left panel migration of pTRE-tight-K5 expressing stable cells is compared to the control pTRE-tight-GFP. Results are presented as percentage of pTRE-tight-GFP expressing cells. In the right panel migration of pTRE-tight-K5 and -GFP expressing cells is shown in absence of Doxycycline and results are presented as percentage of Doxycycline treated cells. Results were pooled from two different experiments with three values each.



## Results

### 4.5.3.3.5 Colony formation

No significant difference could be found in the pTRE-tight-K5 expressing groups. In HCT116 pTet-off/pTRE-tight-K5 stable cells the ability to build single colonies was slightly reduced whereas in SW480 stable cells it was not altered compared to the control pTRE-tight-GFP.

Switching on the expression of pTRE-tight by removing Doxycycline resulted in slight up-regulation of colony formation in HCT116 cells which failed statistical significance. In SW480 no effect was detected.

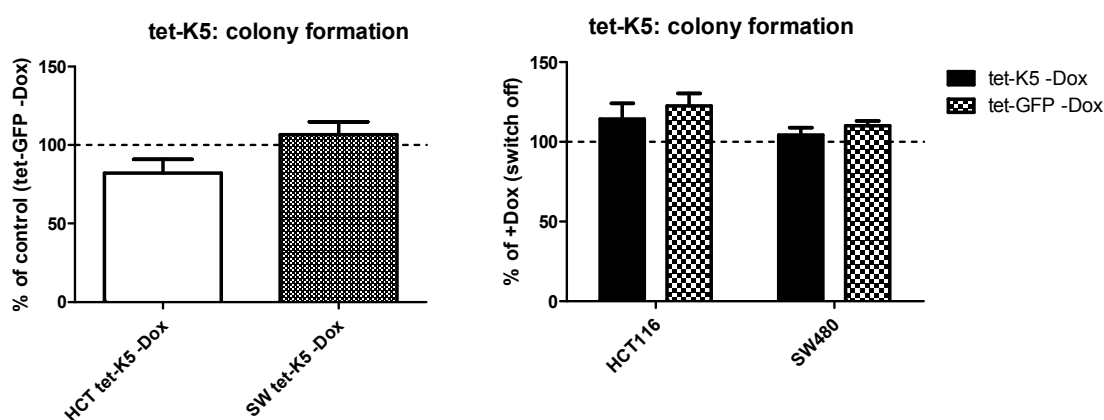


**Figure 109:** Colony formation of pTRE-tight-K5 and -GFP expressing cells +/- Doxycycline

In the left panel colony formation of cells stably expressing the pTet-off and pTRE-tight-K5 constructs is shown as percentage of their corresponding control (pTet-off and pTRE-tight-GFP expressing cells). In the right panel the effect of removing Doxycycline on colony formation is presented for cells stably expressing pTet-off/pTRE-tight-K5 and -GFP. Results are shown as percentage of pTet-off/pTRE-tight-K5 and -GFP stably expressing cells under treatment of Doxycycline. Results were pooled from two different approaches each six values.

### 4.5.3.3.6 Anchorage independent growth

The impact of pTRE-tight-K5 expression on anchorage independent growth was assessed using soft agar assay. Results were evaluated using triplicates and the assay was executed two times.

Surprisingly, anchorage independent growth was significantly up-regulated in cells stably expressing the pTRE-tight-K5 construct (HCT116:  $p < 0,0001$ ; SW480:  $p = 0,0009$ ). No significant changes due to the presence or absence of Doxycycline could

## Results

be reported. HCT116 stably expressing pTet-off/pTRE-tight-K5 showed more colonies when not treated with Doxycycline whereas pTet-off/pTRE-tight-GFP expressing HCT116 had a reduced anchorage independent growth without Doxycycline compared to cells treated with Doxycycline. The same was true for SW480 cells stably expressing pTet-off/pTRE-tight-GFP.

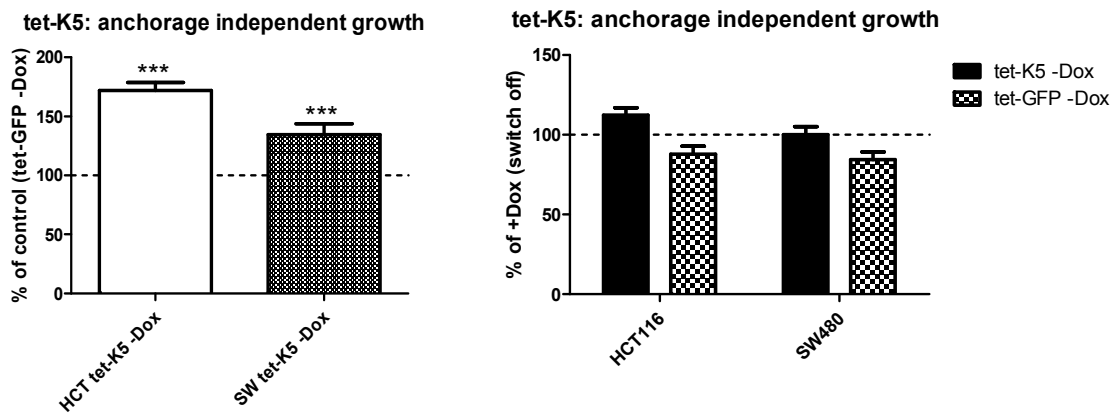


**Figure 110:** Malignant growth of pTRE-tight-K5 and -GFP expressing cells +/- Doxycycline

The left panel shows anchorage independent growth of pTet-off/pTRE-tight-K5 stably expressing cells compared to their control pTet-off/pTRE-tight-GFP expressing cells. In the right panel the effects of Doxycycline on anchorage independent growth for pTet-off/pTRE-tight-K5 and -GFP expressing cells are demonstrated. Results are presented as percentage of pTet-off/pTRE-tight-K5 and -GFP stably expressing cells under treatment of Doxycycline. Results are pooled from two approaches each 10 values. \*\*\* = significantly increased as compared to control at  $p \leq 0,001$ .

## 5 Discussion

As a member of the FGFR family the FGFR4 is involved in the regulation of cell proliferation, differentiation and survival but also in tumor development. Its oncogenic role has so far been described in various cancer types like prostate cancer, breast cancer or rhabdomyosarcoma. In particular the FGFR4 G388R polymorphism was analyzed for different cancers and correlated with increased tumor risk, progression and aggressiveness and decreased survival of the patients. The mechanisms underlying the FGFR4 G388R polymorphism and its effects on cancer patients are not well elucidated so far. One hypothesis is that the polymorphism leads to increased receptor stability and sustained phosphorylation identifying the FGFR4<sup>Arg</sup> as a pro-oncogen (Wang et al. 2008). However, in colorectal cancer the impact of FGFR4 and the G388R polymorphism has only been insufficiently described until now. In this project we analyzed the role of FGFR4 and the G388R polymorphism in the biggest CRC patient cohort so far. In addition we have used three different CRC cell line models to characterize the impact of the polymorphism on cell behavior in terms of growth, migration and adhesion in vitro and in vivo. Furthermore, we tried to discover the influence of the FGFR4<sup>Arg</sup> on cell signaling events. By different approaches for FGFR4 inhibition and down-regulation we aimed to demonstrate the impact of FGFR4 on CRC.

### 5.1 Summary of our results

The results of this project illustrate the importance of FGFR4 and the G388R polymorphism in human CRC. (1) We found a significant up-regulation of the FGFR4 expression in human CRC tissue compared to normal mucosa tissue. 2-fold FGFR4 over-expression or higher compared to normal mucosa was found in 25% of the carcinoma tissue. (2) The presence of the FGFR4<sup>Arg</sup> allele was correlated with higher tumor stage highlighting the impact of the G388R polymorphism on CRC progression. (3) In cell models the FGFR4<sup>Arg</sup> was found associated with cell migration in vitro and with metastasis in vivo. This supports the hypothesis that the allele causes increased tumor aggressiveness. Over-expression of FGFR4<sup>Gly</sup> revealed an increased cell attachment, colony outgrowth and malignant growth. (4) We could also demonstrate reduced cell viability, proliferation, colony formation, migration and anchorage independent growth induced by FGFR4 inhibition or down-regulation in vitro.

(5) With regard to cell signaling both FGFR4 variants stimulated the phosphorylation of GSK and localized FRS to the cell membrane and increased S6 and on protein level whereas a down-regulation of PLC $\gamma$  phosphorylation in FGFR4 over-expressing cells was detected. Localization of the PLC $\gamma$  protein at the cell membrane was elevated in FGFR4<sup>Gly</sup> compared to control and FGFR4<sup>Arg</sup>. In FGFR4<sup>Arg</sup> expressing cells Src protein level was elevated compared to control and FGFR4<sup>Gly</sup>.

## **5.2 Role of the FGFR4 G388R polymorphism in human CRC**

### **5.2.1 Expression of FGFR4 in CRC tissue**

Up-regulation of FGFR4 expression has already been reported in various cancer types like prostate cancer (Sahadevan et al. 2007; Wang et al. 2008), rhabdomyosarcoma (Taylor et al. 2009), breast and gynecological cancers (Jaakkola et al. 1993), head and neck squamous cell carcinoma (Streit et al. 2004) as well as gastric cancer (Ye et al. 2011). FGFR4 over-expression was correlated with higher tumor grade and stage in prostate cancer and rhabdomyosarcoma (Sahadevan et al. 2007; Taylor et al. 2009) but also with higher lymph node involvement in breast and gastric cancer (Jaakkola et al. 1993; Ye et al. 2011) compared to tumors which express low amounts of FGFR4. High expression of FGFR4 was associated with poor clinical outcome and survival (Streit et al. 2004; Taylor et al. 2009; Ye et al. 2011).

In this study 81 tissue pairs consisting of colon carcinoma tissue and a sample of normal mucosa tissue were analyzed. Screening the tissue pairs on mRNA expression of FGFR4 revealed a 2-fold up-regulation of FGFR4 expression in 25% of the tumor specimen. No correlation between FGFR4 expression profile and histopathological parameters were seen.

### **5.2.2 Correlation between FGFR4 allele and expression**

In our study population 45% of the cases were Gly-homozygous and 6% Arg-homozygous which did not differ from the general population. In head and neck squamous cell carcinoma higher FGFR4 expression in Arg-carriers has been reported (Streit et al. 2004). The same was also observed in breast cancer cell lines (Bange et al.

2002). In the lung expression of FGFR4 was not related to the genotype however (Spinola 2005). Similarly, in our study FGFR4 expression level and genotype were not related in human CRC tissue. The association was observed in 11 CRC cell lines however: HT29, Colo201, LT97 and Caco2 that carry FGFR4<sup>Arg</sup> alleles consistently expressed higher levels of FGFR4 than Gly-homozygous cell lines.

### **5.2.3 FGFR4 G388R polymorphism and CRC initiation and development**

To date most of the studies concerning FGFR4 G388R polymorphism and cancer risk could not find any correlation for example in breast cancer (Bange et al. 2002; Naidu et al. 2009; Spinola et al. 2005), prostate cancer (FitzGerald et al. 2009), soft tissue sarcoma (Morimoto et al. 2003) and head and neck squamous cell carcinoma (Streit et al. 2004; Tanuma et al. 2010). However, Ma and colleagues found an increased risk for prostate cancer as well as for benign hyperplasia in Arg/Arg carriers compared to Gly-homozygous people (Ma et al. 2008).

To assess the connection between the FGFR4 G388R polymorphism and the initiation and development of CRC we used the biggest cohort studied so far in this context. 3471 participants in an early detection study in eastern Austria divided into a control group free of tumors in the gut, a low-risk adenoma, a high-risk adenoma and a carcinoma group. In the control group 48,4% had a Gly-homozygous, 43,4% a heterozygous and 8,1% a Arg-homozygous genotype. Regarding the carcinoma patients the percentage of Arg-homozygotes increased to 12,6% whereas the percentage of heterozygotes decreased to 39,1%. Surprisingly in the group of high risk adenoma patients only 5,5% had an Arg-homozygous genotype and the highest percentage of Gly-homozygotes. The low-risk adenoma group had a genotype distribution comparable to the control. This indicates that FGFR4<sup>Arg</sup> conferred a more rapid progression of high-risk adenomas to carcinomas. However, statistical analysis revealed that the difference was not significant ( $p=0,350$ ). For this reason an even larger study population would be necessary.

### **5.2.4 FGFR4 G388R polymorphism and histopathological parameters**

An association between Arg-carriers and lymph node involvement has so far been described for several kinds of cancer. For example Bange et al. showed a positive trend (which failed significance) between Arg-allele and axillary lymph node involvement in breast cancer (Bange et al. 2002). Naidu and colleagues found a significant correlation between Arg-allele and lymph node involvement by analyzing a bigger cohort of breast cancer patients than Bange et al. (Naidu et al. 2009). It has been reported that in lung adenocarcinoma the hazard ratio for being stage II or more was higher for Arg-carriers (Falvella et al. 2009). An earlier study also shows that lung adenocarcinoma patients who carried the Arg-allele were younger at cancer onset. In addition the genotype was associated with an advanced clinical stage as well as nodal status and shorter overall survival. The Arg-allele in this study was significantly more present in higher stages when compared to stage I (Spinola 2005). Additionally, in prostate cancer the presence of the Arg-allele could be related to lymph node metastasis but also to a significant prostate-specific antigen (PSA) recurrence and consequently with occurrence of aggressive disease (Wang et al. 2004).

However, there are also various studies that did not find an association of Arg-allele with nodal status, tumor stage or any other histopathological parameters for instance in breast cancer (Becker et al. 2003; Jezequel et al. 2004; Spinola et al. 2005; Thusbas et al. 2006), lung cancer (Matakidou et al. 2007), soft tissue and osteosarcoma (Morimoto et al. 2003), head and neck squamous cell carcinoma (Streit et al. 2004; Tanuma et al. 2010) and bladder cancer (Yang et al. 2006).

To analyze the importance of FGFR4 G388R polymorphism in human CRC the allelotype was associated with tumor size, stage, grade and lymph node metastasis. For this purpose we analyzed 136 carcinoma patients and divided them into Arg-carriers and Gly-homozygotes. No difference concerning tumor size and tumor grade and allelotype were detected. Although the correlation between lymph node metastasis and allelotype missed statistical significance we can see a trend of Arg-allele associated with lymph node metastasis. Nevertheless, we found a significant correlation between allelotype and tumor staging. The Arg-allele was significantly more present in higher

stages (II, III and IV) compared to stage I. These data totally agrees with the findings from Spinola and colleagues in lung adenocarcinoma. The relevance of Arg-allele and tumor stage becomes even more dramatic when the patients cohort is divided into two groups. 55 of the CRC patients were part of a screening program for early diagnosis of colon carcinoma. In contrast to the other 81 tissue samples which were collected from advanced cases most of the 55 CRC patients were in an early tumor stage and revealed a higher number of stage I and II tumors. Excluding these 55 CRC patients from our analysis resulted in a significant increase ( $p=0,0381$ ) of lymph node metastasis in Arg-carriers compared to Gly-homozygotes. 63% (22/35) of the Arg-carriers suffered from lymph node metastasis whereas in the group of Gly-homozygotes only 38% (12/32) developed metastasis. Furthermore, there was no stage I tissue sample in this subgroup expressing the Arg-allele.

### **5.2.5 FGFR4 G388R polymorphism and survival**

Most of the studies so far found a correlation between the Arg-allele and a short disease-free or overall survival in various cancer types. Poorer survival for Arg-allele carriers above all in node-positive patients has been described for lung adenocarcinoma (Falvella et al. 2009; Sasaki et al. 2008; Spinola 2005), breast cancer (Bange et al. 2002; Thusbas et al. 2006), head and neck squamous cell carcinoma (Dacostaandrade et al. 2007; Streit et al. 2004; Tanuma et al. 2010), prostate cancer (FitzGerald et al. 2009), soft tissue sarcoma (Morimoto et al. 2003), and melanoma (Streit et al. 2006). Additionally, in breast cancer it was also reported that Arg-carriers had less benefit from adjuvant systemic therapy and chemotherapy than Gly-carriers (Thusbas et al. 2006). Only one study associated the Gly-homozygous patients with poor recurrence-free survival (in bladder cancer) so far (Yang et al. 2006).

Data relating the G388R polymorphism in FGFR4 to overall survival and patient recurrence could not be evaluated in this study because of lack of information concerning patient outcome but will be analyzed as soon as data is available.

### **5.3 FGFR4 G388R polymorphism in vivo and in vitro: cell culture model**

To analyze the FGFR4 G388R polymorphism in cell culture three different CRC cell lines (SW480, HCT116 and HT29) with different allelotypes and FGFR4 expression levels were transfected with FGFR4<sup>Arg</sup>, FGFR4<sup>Gly</sup> and a control vector and selected for stable expression. On the mRNA-level a 4-fold over-expression of both FGFR4 allelotypes in SW480 was achieved whereas in HCT116 and HT29 the FGFR4 over-expression was lower and the Arg-variant was better expressed than the Gly-variant. Due to the transfection of the FGFR4<sup>Arg</sup> the Arg/Gly ratio in SW480 shifted from 0:1 to 8:1 and in HCT116 from 0:1 to 1:3. In HT29, which is heterozygote but preferentially expresses the Arg-allele, the Arg/Gly ratio shifted from 1:0 to 1:3 when transfected with the FGFR4<sup>Gly</sup> allele.

More FGFR4<sup>Arg</sup> than FGFR4<sup>Gly</sup> was present on the cell membrane in all three transfected cell lines. This could indicate a higher stability of the FGFR4<sup>Arg</sup> protein which was already reported for prostate cancer. Wang and colleagues described an increased stability and sustained phosphorylation of the FGFR4 due to the G388R polymorphism whereas the Gly-variant needs to be stabilized by a second protein called HIP1 (Wang et al. 2008).

#### **5.3.1 FGFR4 G388R polymorphism and cell growth**

Concerning viability and proliferation no difference was observed in all three cell line models compared to the control. Only in very low density cultures there was a significant increase in proliferation for HT29 and HCT116 but also in SW480 which just missed significance. Viability assays were evaluated five days after seeding so that the cell density might have been too high and no effect of FGFR4 could be observed. Consequently, growth curves of FGFR4 over-expressing cell lines were evaluated in a follow-up study, which showed a significant stimulatory effect of FGFR4 on growth of SW480 cells.

Nevertheless, for anchorage independent growth in soft agar, that permits three dimensional growth, an increase of colony formation in FGFR4 over-expressing cells



was observed for both FGFR4 alleles while FGFR4<sup>Gly</sup> being the stronger inducer. FGFR4<sup>Arg</sup> even decreased growth in soft agar significantly in HCT116.

### 5.3.2 FGFR4 G388R polymorphism and cell migration and cell adhesion

Decreased cell adhesion and consequently increased cell migration are important determinants for metastasis. It has been published that the FGFR4 allelotype clearly affects cell migration. For example in non-tumorigenic prostatic epithelial cell line PNT1A stably expressing FGFR4, migration was stimulated by the Arg-allele (Wang et al. 2004). There are reports about the Gly-variant decreasing cell motility in breast cancer cell lines (Bange et al. 2002; Stadler et al. 2006). In contrast to these reports in our study both FGFR4 alleles significantly increased cell migration in SW480 and HCT116. Both wild type cell lines are Gly-homozygous and in both cell lines the transfected Arg-allele stimulated migration even more than the transfected Gly-variant. However, in a FGFR4<sup>Arg</sup> expression background of HT29 the expression of the Gly-allele decreased migration whereas the transfection of FGFR4<sup>Arg</sup> over-expression vector had no impact on migration compared to control. These findings demonstrate an impact of FGFR4 on migration and a stronger pro-migratory effect induced by the Arg-allele compared to the Gly-allele.

A functional interaction between FGFR and the cell surface protein neural cell adhesion molecules (NCAM) has been described both in the nervous system and in non-neuronal cells. Frequently, FGFR1 and FGFR2 are involved in this association. For example FGFR1 is stabilized and recycled rather than degraded when associated with NCAM (Francavilla et al. 2009). FGFR4 is also reported to associate strongly with NCAM and forming a FGFR4/NCAM/N-cadherin adhesive complex (Ezzat et al. 2004).

Cell attachment and colony outgrowth in all three cell lines were significantly induced by the FGFR4<sup>Gly</sup> over-expressing cells compared to control. The FGFR4<sup>Arg</sup> over-expressing cells did not alter colony formation at all. These findings indicate a correlation between FGFR4<sup>Gly</sup> and cell adhesion. A correlation between FGFR4 G388R polymorphism and NCAM will be analyzed in a continuative project.

### **5.3.3 FGFR4 G388R polymorphism in SCID mouse xenografts**

Consistent with our in vitro findings, SW480-FGFR4<sup>Gly</sup> xenografts in SCID mice formed tumors earlier and grew into bigger tumors than FGFR4<sup>Arg</sup> and control. This was also confirmed by Ki67 staining that was significantly increased in FGFR4<sup>Gly</sup> tumors. Surprisingly, incidence of mitosis was highest in the control group and apoptosis was significantly elevated in both the FGFR4<sup>Arg</sup> and FGFR4<sup>Gly</sup> groups which does not fit the observations described above. This can be explained by the fact that tumors were isolated after reaching maximal size. Consequently, mitosis and apoptosis rate may not be representative for the period of tumor growth.

While FGFR4<sup>Gly</sup> had a greater impact on local tumor growth, FGFR4<sup>Arg</sup> stimulated the formation of micro-metastasis. Tumors growing under the skin metastasize to the lungs where they formed more and larger colonies from FGFR4<sup>Arg</sup>-xenografts than from FGFR4<sup>Gly</sup> or control mice. To confirm these findings a metastasis model in vivo was used by injecting SW480 FGFR4 over-expressing cells and control cells into the tail vein of the mice. Unfortunately, this metastasis model was not quite as successful as expected because only one mouse developed metastasis. We are currently working on another in vivo metastasis model which is more suitable for our FGFR4 cell models.

### **5.3.4 FGFR4 G388R polymorphism and epithelial mesenchymal transition**

FGFR4<sup>Arg</sup> affects tumor cells concerning migration and development of metastasis but also leads to smaller cell morphology. FGFR4<sup>Gly</sup> in contrast increases cell adhesion and local tumor growth. These results led to the hypothesis that FGFR4<sup>Arg</sup> may induce an epithelial mesenchymal transition (EMT). EMT is a process where polarized epithelial cells acquire a mesenchymal migratory morphology. This is of great importance in the embryonic development during gastrulation but is also involved in wound healing, tissue repair and tissue fibrosis. If EMT takes place in carcinoma cells they acquire migratory properties which lead to metastasis and tumor invasion (Thiery 2002). FGF-signaling has already been connected to EMT - for example during embryonic development where FGF-signaling is important for mesoderm induction and gastrulation movements (Hardy et al. 2011). In the context of tumor development the loss of E-cadherin is correlated with the loss of epithelial phenotype and therefore with tumorigenicity. In bladder carcinoma the loss of E-cadherin is associated with a low

expression of FGFR2IIIb. FGFR2IIIb is present in all normal epithelia and important to maintain the epithelial phenotype. Also FGF2 which binds preferentially to the IIIc isoforms and is highly expressed in tumors and wounds is associated with the induction of EMT (Shirakihara et al. 2011). The involvement of FGFR2IIIb/IIIc in EMT has been well investigated. Whether other FGFRs play a role in EMT processes is not clear so far, especially for FGFR4 which lacks the IIIb/IIIc splice variant.

Analyzing the three FGFR4 over-expressing cell models revealed a clear decrease of E-cadherin in the SW480 cells on transcript and on protein level. This did not happen in HCT116 and HT29 transfectants. Additionally, nuclear  $\beta$ -catenin was elevated in the SW480 transfectants whereas in HCT116 and HT29 it was significantly down-regulated. Based on these findings we cannot conclude that FGFR4 expression and allelotype are involved in the induction of EMT. Although in SW480 there might be an impact of FGFR4 leading to a mesenchymal phenotype of the cells it also must be mentioned that SW480 is an undifferentiated cell line and expresses low levels of E-cadherin. This leaves the question open whether the impact of FGFR4 is only seen when E-cadherin is already down-regulated. The influence of FGFR4 on EMT will be the topic of a subsequent project.

### 5.3.5 FGFR4 dependent cell signaling

A point mutation analogous to the G388R polymorphism of FGFR4 has been described in the transmembrane domain of FGFR3 at position 380. Like the G388R polymorphism in FGFR4 a glycine is substituted by an arginine and leads to familial achondroplasia. On the cellular level it results in ligand independent activation of the receptor. In this special case the kinase activation seems to be due to a ligand independent stabilization of the receptor dimers (Webster and Donoghue 1996).

Bange and colleagues report that substituting a hydrophobic amino acid like glycine by a charged amino acid like arginine increases the tyrosine kinase activity. However, they could not find an enhanced tyrosine activity in FGFR4<sup>Arg</sup> transfected breast cancer cell line MDA-MB231 after FGF stimulation. They consequently assume that the activation property of Arg is only subtly changed (Bange et al. 2002). But also in a non-tumorigenic prostate epithelial cell line over-expressing FGFR4<sup>Gly</sup> and FGFR4<sup>Arg</sup> no activation of the tyrosine kinase phosphorylation also in response to FGF2 was found

## Discussion

(Wang et al. 2004). Cell lines obtained from hepatomas and stably over-expressing FGFR4 showed an increased ERK phosphorylation in response to FGF1 and compared to control cells (Huang et al. 2009).

To answer the question whether FGFR4 over-expression activates downstream signaling pathways we used the SW480 transfectants because they mainly express the transfected allele. Analyzing phosphorylation of direct FGFR targets like FRS and PLC $\gamma$  at the cell membrane and also as total protein revealed differences between FGFR4 over-expressing cells and control. FRS expression and activation was not affected in FGFR4 over-expressing cells in the total protein fraction. When localized at the cell membrane phosphorylation was increased by both FGFR4<sup>Gly</sup> and FGFR4<sup>Arg</sup> although FGFR4<sup>Arg</sup> recruited less FRS to the receptor. Downstream of FRS ERK phosphorylation was not affected by FGFR4 over-expression. Nevertheless, GSK3 $\beta$  phosphorylation was increased by FGFR4 over-expressing cells. As described in chapter 1.7.1.6 GSK3 $\beta$  connects FGF-signaling pathway to Wnt-signaling pathway. Phosphorylation of GSK3 $\beta$  results in a down-regulation of its activity which leads to the repression of E-cadherin and translocation of  $\beta$ -catenin into the nucleus (Katoh 2006a). However, in our case increased phosphorylation of GSK3 $\beta$  could be the cause for the down-regulation of E-cadherin and the translocated  $\beta$ -catenin (described above in chapter 5.3.4).

Phosphorylation of S6-kinase is involved in the regulation of cell proliferation and tumor growth, protein translation, cell survival as well as cytoskeletal arrangements (Fenton and Gout 2011). FGFR4 over-expressing SW480 showed an increased S6 protein level as well as increased protein phosphorylation. In our case S6 was analyzed as a pathway indicator. Together with the activation of GSK3 $\beta$  S6 phosphorylation indicates a pathway activation via PI3K leading to activation of cell survival.

PLC $\gamma$  over-expression is correlated with a variety of cancers, colorectal cancer among them, and its signaling is involved in cell growth and survival as well as cell motility (Suh et al. 2008; Tan et al. 2007). PLC $\gamma$  was elevated on total protein level in both FGFR4 over-expressing cell lines. Recruitment to the cell membrane was higher compared to control in FGFR4<sup>Gly</sup> but not in FGFR4<sup>Arg</sup> cells, suggesting a role in the enhanced local tumor growth of SW480<sup>Gly</sup> cells. Phosphorylation of the PLC $\gamma$  localized at the cell membrane was decreased however. Especially FGFR4<sup>Arg</sup> revealed hardly any PLC $\gamma$  phosphorylation at all. As several studies have described a connection of PLC $\gamma$  to

cell adhesion and spreading (Choi et al. 2007; Tvorogov et al. 2005) the decreased phosphorylation may be related to decreased cell attachment and consequently increased cell motility of FGFR4<sup>Arg</sup> over-expressing cells.

In tumor cells PLC $\gamma$  also interacts with Src kinase which could serve as adaptor protein between FGFR and PLC $\gamma$  (Suh et al. 2008; Tvorogov et al. 2005). Src is also recruited by phosphorylated FGFR to FRS and is important for activation and termination of FGFR signaling (Sandilands et al. 2007). Src prevents the association of Cbl to FRS which consequently blocks the ubiquitination of FGFR and its degradation and promotes receptor recycling (Francavilla et al. 2009). Although we found no alterations of Src phosphorylation by FGFR4 over-expression Src protein level was increased in FGFR4<sup>Arg</sup> over-expressing cells. A higher protein level of Src in FGFR4<sup>Arg</sup> expressing CRC cells could contribute to increased receptor stability which has been also described for prostate cancer (Wang et al. 2008). Furthermore, Src plays a crucial role in many cellular processes like invasion, migration, proliferation, angiogenesis and apoptosis. Increased expression of Src is found in 80% of CRC specimens and also associated with increased metastasis and poor clinical prognosis in all stages of colon cancer. Like FGFR4<sup>Arg</sup>, a high expression of Src is also associated with enhanced cell motility (Lieu and Kopetz 2010). Consequently, the more aggressive phenotype of FGFR4<sup>Arg</sup> over-expressing SW480 may be strongly related to an increase in Src protein expression levels.

### **5.4 FGFR4 knock down via siRNA**

In prostate cancer FGFR4 down-regulation by siRNA inhibited proliferation and invasion of prostate cancer regardless of allelotype (Sahadevan et al. 2007). In our study cell viability was significantly reduced in all three cell lines caused by siRNA2. DNA synthesis was significantly inhibited in low density cell cultures by siRNA2 in HCT116 and HT29. In high density cell cultures proliferation of SW480 and HT29 cell lines were significantly diminished by both siRNAs.

Cell migration and colony formation were both inhibited by siRNA2 in HCT116 and HT29 but not in SW480 which expresses very low levels of FGFR4 in SW480 so that a knock down in this cell line does not much impact on protein level.

## Discussion

We could not see any impact of siRNA knock down on anchorage independent growth. This may be due to the quite long incubation period (2-3 weeks): knock down with siRNA is transient and not sustained long enough to prevent growth throughout this period. Surprisingly, in SW480 we saw a clear inhibition of anchorage independent growth when transfected with siRNA2.

In the breast cancer cell line BT-474 which expresses high levels of FGFR4 a siRNA mediated knock down of FGFR4 resulted in an reduction of ERK phosphorylation (Roidl et al. 2009). Investigation of down-stream signaling effects of FGFR4 knock down revealed ambiguous results like up-regulation of pERK in SW480 and HT29 as well as up-regulation of pS6 in HT29 but down-regulation in SW480 compared to a scrambled control. Further analyzes are required to reveal more information on signaling alterations due to FGFR4 knock down.

### **5.5 Tool development for stable and inducible FGFR4 inhibition**

FGFR4 knock down by siRNA resulted in an inhibition of cell viability, cell migration and colony formation. To analyze the impact of FGFR4 inhibition on local tumor growth in vivo siRNA mediated knock down is not an appropriate tool. Due to its transience the siRNA mediated knock down is not stable enough for a period longer than a few days. During tumor growth and cell division the siRNA is diluted out and FGFR4 expression is not altered anymore. For that reason we tried to develop more stable tools for FGFR4 down-regulation.

#### **5.5.1 Introduction of a dominant negative FGFR4 construct**

In the course of former projects dominant negative constructs for FGFR1, FGFR3 and FGFR4 were generated. The dominant negative FGFR4 (K5) construct consists of the extracellular domain and the transmembrane domain of the FGFR4 but its intracellular kinase domain is substituted by a CFP reporter tag. The K5 acts as a decoy receptor and traps FGFR4 ligands but without transmitting a signal. Local tumor growth of SW480 cells transduced with dominant negative FGFR 3 and K5 adenoviral constructs were assessed for a former project on FGFR3IIIc. Whereas local tumor growth was decreased

about 40% (Sonvilla et al. 2010) by the dominant negative FGFR3 construct the K5 construct inhibited the outgrowth of tumors completely (unpublished).

### **5.5.1.1 Influence of dominant negative FGFR4 adenovirus on cell growth, migration and adhesion**

To analyze the mechanisms behind the strong inhibitory effects of the K5 in vitro we used an adenovirus expressing the K5 and transduced the three cell lines SW480, HCT116 and HT29. Although the expression of the K5 construct was detected on the RNA level evaluating the K5 protein was more complicated. High MOIs were necessary for detection of fluorescent cells. Both the CFP tag and the K5 protein could also be verified by western blotting.

Viability and 3-dimensional growth in an agar matrix was significantly down-regulated by the K5 in all three cell lines. These findings are consistent with the in vivo results from our former project. In SW480 also migration and colony formation were significantly reduced whereas in HCT116 only colony formation was significantly inhibited by the K5 construct. HT29 did not show any impact on colony formation when transduced by the K5 and migration was reduced but failed statistical significance.

Although FGFR4 inhibition by siRNA showed only little impact on the low FGFR4 expressing cell line SW480, the effects caused by the K5 adenovirus resulted in a strong inhibition of viability, anchorage independent growth, colony formation, migration and local tumor growth. One explanation could be the ligand spectrum which is affected by a dominant negative decoy FGFR4 receptor. SW480 expresses large amounts of FGF18 which also binds to the FGFR4 and which was found to play a pro-tumorigenic role in colorectal cancer. Decreasing the FGF18 signaling cascade in SW480 results for instance in reduced colony formation (Sonvilla et al. 2008). Trapping ligands like FGF18 affects not only FGFR4 but also other FGFRs – mostly FGFR3-IIIc (Sonvilla et al. 2010). The precise effects of the K5 construct on FGF-signaling need to be explored in a consecutive project.

### **5.5.1.2 Establishment of an inducible tet-off system for dominant negative FGFR4 construct**

In addition to the K5 adenovirus we tried to transfect three CRC cell lines with the K5 plasmid and select stable clones. Probably due to the growth-inhibiting effects of the K5 on the cell lines no stably expressing K5 clones could be selected. Therefore, we decided to use a tet-off system and clone the K5 construct into a Doxycycline inducible vector. A GFP-gene was used as control for in vitro approaches and for testing the function of the inducible gene expression system. Consecutive transfection of pTet-off vector and pTRE-tight-GFP vector resulted in 72-76% GFP positive SW480 and HCT116 cells which under treatment of doxycycline were decreased to 25-39% GFP expressing cells. Presence of Doxycycline not only reduced the percentage but also the intensity of fluorescence of the remaining GFP-positive cells. In addition, transfection of the pTRE-tight-GFP vector without the pTet-off expressing transactivator protein still leads to the expression of the GFP protein in 48% of SW480 and 30% of HCT116.

In summary, the tet-off system worked basically well in our hands but still was too leaky for our purpose. Due to the strong growth-inhibitory effect of the K5 construct we assume that pTRE-tight-K5 expressing cells died right after transfection. Consequently, we could not select cells with an appropriate expression of the K5 construct. Therefore, pTet-off/pTRE-tight-K5 clones, which were selected, showed no impact on cell biological properties like viability, migration, or cell adhesion.

## **5.6 Conclusion**

Based on the results of this study we identified FGFR4 as an oncogene and relevant target for therapy in colorectal cancer. Specifically we could demonstrate oncogenic potential for both polymorphic forms of FGFR4. Concluding from our data FGFR4 G388R is involved in tumor aggressiveness in CRC mediated by changes in cell behavior affecting growth, migration and cell adhesion. Therefore, we suggest the FGFR4 G388R SNP to be regarded as a genetic modifier in colorectal cancer and to play a predictive role in tumor prognosis. The characterization of genetic modifiers as markers predicting increased risk for metastasis development would permit identification of patient groups who will profit from adjuvant treatment. The FGFR4



## Discussion

G388R SNP may be part of a marker set for prognostic testing and classification into “higher” and “lower” risk patients (Drafahl et al. 2010).



## 6 Abstract

The interest in fibroblast growth factors (FGFs) and their receptors (FGFRs) in cancer research constantly increased over the last decade because of the crucial role they play in cell proliferation, differentiation, and migration. During tumorigenesis their expression and activity is frequently deregulated. Especially FGFR4 with its genetic polymorphism affecting the transmembrane domain of the receptor (G388R) is involved in a wide variety of malignancies. The R388 (FGFR4<sup>Arg</sup>) form is associated with increased tumor risk, progression, aggressiveness and decreased survival in various cancer types. In colorectal cancer (CRC) the role of FGFR4 is not well described to date. Therefore, it was the aim of the study to elucidate the impact of FGFR4 and especially the G388R polymorphism on CRC.

Our data show an up-regulation of FGFR4 mRNA expression in 25% of CRC tissue specimen. Moreover, FGFR4<sup>Arg</sup> carriers had an increased risk for higher tumor stage at diagnosis and metastatic lesions than FGFR4-G388 (FGFR4<sup>Gly</sup>) homozygous patients suggesting a role for the FGFR4<sup>Arg</sup> allele in invasion and metastasis. In vitro data, using three different CRC cell lines with differing FGFR4 endogenous expression and genotype, displayed stimulated cell migration but decreased clonogenicity for FGFR4<sup>Arg</sup> whereas over-expression of FGFR4<sup>Gly</sup> had a stimulatory effect on clonogenicity and anchorage independent growth. In vivo FGFR4<sup>Gly</sup> enhanced local tumor growth, while FGFR4<sup>Arg</sup> stimulated metastasis from subcutaneous xenotransplants to the lung. FGFR4 siRNA mediated knock down and a dominant-negative adenoviral construct expressing dominant negative FGFR4 caused down-regulation of cell viability, migration and colony formation CRC cell lines. On the cellular level phosphorylation of FRS2 $\alpha$  was increased by FGFR4 over-expression leading to activation of cell survival pathways independent of the genotype.

Based on the results of this study both allelic forms of FGFR4 have to be regarded as oncogenes and relevant targets for therapy in CRC. While FGFR4<sup>Arg</sup> over-expression was correlated with higher tumor aggressiveness in vivo, mediated by up-regulation of cell migration, over-expression of FGFR4<sup>Gly</sup> stimulated malignant cell growth in vitro and enhanced local tumor growth in vivo.



## 7 Zusammenfassung

In den letzten zehn Jahren haben die Fibroblasten Wachstumsfaktoren (FGF) und deren Rezeptoren (FGFR) in der Krebsforschung immer mehr an Bedeutung gewonnen, nicht zuletzt auf Grund ihrer besonderen Rolle für zelluläres Wachstum, Differenzierung und Migration. Sie sind während der Krebsentstehung häufig von Mutationen betroffen. Vor allem FGFR4, welcher zudem einen Polymorphismus in der transmembranen Domäne des Rezeptors (G388R) aufweist, ist an verschiedensten Krebserkrankungen beteiligt. Die R388 (FGFR4<sup>Arg</sup>) Form wird häufig mit erhöhtem Tumorrisiko, schnellerem Krankheitsverlauf und schlechteren Überlebenschancen in Verbindung gebracht. Da die Rolle des FGFR4 im Dickdarmkrebs bisher nicht ausreichend geklärt war, sollte in dieser Arbeit der Einfluss des FGFR4 und dessen G388R Polymorphismus auf das Kolorektalkarzinom erforscht werden.

Unsere Daten belegen eine erhöhte Expression der FGFR4 mRNA in 25% der untersuchten humanen Dickdarmkarzinomgewebe. Zudem weisen Patienten mit einem oder zwei FGFR4<sup>Arg</sup> Allelen ein höheres Tumor-Staging mit vermehrter Wahrscheinlichkeit zur Metastasierung auf. Folglich wird das FGFR4<sup>Arg</sup> Allel mit erhöhter Tumor Invasion und Metastasierung in Zusammenhang gebracht, was sich in Zellkulturmodellen bestätigte. In drei verschiedenen Kolonkarzinom-Zelllinienmodellen stimulierte FGFR4<sup>Arg</sup> die Migration und hemmte gleichzeitig Zelladhäsion und Koloniebildung. Im Gegensatz dazu stimulierte FGFR4<sup>Gly</sup> sowohl das Wachstum von Kolonien aus dünnen Kulturen als auch das 3-dimensionale, anheftungs-unabhängige Wachstum in einer Agarmatrix. Auch im Tiermodell konnte FGFR4<sup>Gly</sup> mit schnellerem Tumorwachstum assoziiert werden, während FGFR4<sup>Arg</sup> Tumormetastasierung von subkutanen Transplantaten in die Lunge beschleunigte. Hemmung des FGFR4 über siRNA oder ein adenovirales dominant-negatives Konstrukt führten beide zu verminderter Viabilität, Migration und Koloniebildung der Kolonkarzinom-Zelllinien. Unabhängig vom Polymorphismus stimulierte eine erhöhte Expression von FGFR4 Überlebens-Signalwege über die Aktivierung von FRS2 $\alpha$ .

Die Ergebnisse dieser Arbeit identifizieren beide allelische Formen des FGFR4 als Onkogene, welchen in der klinischen Krebstherapie unbedingt Beachtung geschenkt werden sollte. Eine erhöhte Expression von FGFR4<sup>Arg</sup> stimuliert Zellmigration und

## Zusammenfassung

erhöht somit die Tumor-Aggressivität in vivo, während die erhöhte Expression von FGFR4<sup>Gly</sup> malignes Zellwachstum in vitro und in vivo fördert.

## 8 Bibliography

- Abler LL, Mansour SL, and Sun X. 2009. Conditional gene inactivation reveals roles for Fgf10 and Fgfr2 in establishing a normal pattern of epithelial branching in the mouse lung. *Dev Dyn* 238(8):1999-2013.
- Acevedo VD, Ittmann M, and Spencer DM. 2009. Paths of FGFR-driven tumorigenesis. *Cell Cycle* 8(4):580-588.
- AJCC. 26.6.2011. <http://www.cancerstaging.org/staging/posters/colon8.5x11.pdf>.
- Alberts B, Johnson, A., J. Lewis, M. Raff, K. Roberts, P. Walter editor. 2002. *Molecular Biology of The Cell*. 4th Edition ed. New York: Garland Science.
- Allen BL, and Rapraeger AC. 2003. Spatial and temporal expression of heparan sulfate in mouse development regulates FGF and FGF receptor assembly. *J Cell Biol* 163(3):637-648.
- Allerstorfer S, Sonvilla G, Fischer H, Spiegl-Kreinecker S, Gauthofer C, Setinek U, Czech T, Marosi C, Buchroithner J, Pichler J et al. . 2008. FGF5 as an oncogenic factor in human glioblastoma multiforme: autocrine and paracrine activities. *Oncogene* 27(30):4180-4190.
- Ansell A, Farnebo L, Grenman R, Roberg K, and Thunell L. 2009. Polymorphism of FGFR4 in cancer development and sensitivity to cisplatin and radiation in head and neck cancer. *Oral Oncology* 45(1):23-29.
- Armand AS, Laziz I, and Chanoine C. 2006. FGF6 in myogenesis. *Biochim Biophys Acta* 1763(8):773-778.
- Babel I, Barderas R, Diaz-Uriarte R, Martinez-Torrecedrada JL, Sanchez-Carbayo M, and Casal JJ. 2009. Identification of tumor-associated autoantigens for the diagnosis of colorectal cancer in serum using high density protein microarrays. *Mol Cell Proteomics* 8(10):2382-2395.
- Bange J, Prechtel D, Cheburkin Y, Specht K, Harbeck N, Schmitt M, Knyazeva T, Muller S, Gartner S, Sures I et al. . 2002. Cancer progression and tumor cell motility are associated with the FGFR4 Arg(388) allele. *Cancer Res* 62(3):840-847.
- Bartram CR. 2004. Genetische Grundlagen der Kanzerogenese. In: Hiddemann W. HH, Bartram C., editor. *Die Onkologie*. Heidelberg: Springer Verlag.
- Becker N, Nieters A, and Chang-Claude J. 2003. The fibroblast growth factor receptor gene Arg388 allele is not associated with early lymph node metastasis of breast cancer. *Cancer Epidemiol Biomarkers Prev* 12(6):582-583.
- Beenken A, and Mohammadi M. 2009. The FGF family: biology, pathophysiology and therapy. *Nat Rev Drug Discov* 8(3):235-253.
- Behrens J, and Lustig B. 2004. The Wnt connection to tumorigenesis. *Int J Dev Biol* 48(5-6):477-487.
- Berger W, Setinek U, Mohr T, Kindas-Mugge I, Vetterlein M, Dekan G, Eckersberger F, Caldas C, and Micksche M. 1999. Evidence for a role of FGF-2 and FGF receptors in the proliferation of non-small cell lung cancer cells. *Int J Cancer* 83(3):415-423.

## Bibliography

- Berglund ED, Li CY, Bina HA, Lynes SE, Michael MD, Shanafelt AB, Kharitononkov A, and Wasserman DH. 2009. Fibroblast growth factor 21 controls glycemia via regulation of hepatic glucose flux and insulin sensitivity. *Endocrinology* 150(9):4084-4093.
- Berman B, Ostrovsky O, Shlissel M, Lang T, Regan D, Vlodaysky I, Ishai-Michaeli R, and Ron D. 1999. Similarities and differences between the effects of heparin and glypican-1 on the bioactivity of acidic fibroblast growth factor and the keratinocyte growth factor. *J Biol Chem* 274(51):36132-36138.
- Birrer MJ, Johnson ME, Hao K, Wong KK, Park DC, Bell A, Welch WR, Berkowitz RS, and Mok SC. 2007. Whole genome oligonucleotide-based array comparative genomic hybridization analysis identified fibroblast growth factor 1 as a prognostic marker for advanced-stage serous ovarian adenocarcinomas. *J Clin Oncol* 25(16):2281-2287.
- Bosse Y, and Rola-Pleszczynski M. 2008. FGF2 in asthmatic airway-smooth-muscle-cell hyperplasia. *Trends Mol Med* 14(1):3-11.
- Bursch W, Liehr JG, Sirbasku DA, Putz B, Taper H, and Schulte-Hermann R. 1991. Control of cell death (apoptosis) by diethylstilbestrol in an estrogen-dependent kidney tumor. *Carcinogenesis* 12(5):855-860.
- Cabrita MA, and Christofori G. 2008. Sprouty proteins, masterminds of receptor tyrosine kinase signaling. *Angiogenesis* 11(1):53-62.
- Cha JY, Maddileti S, Mitin N, Harden TK, and Der CJ. 2009. Aberrant receptor internalization and enhanced FRS2-dependent signaling contribute to the transforming activity of the fibroblast growth factor receptor 2 IIIb C3 isoform. *J Biol Chem* 284(10):6227-6240.
- Chen H, Ma J, Li W, Eliseenkova AV, Xu C, Neubert TA, Miller WT, and Mohammadi M. 2007. A molecular brake in the kinase hinge region regulates the activity of receptor tyrosine kinases. *Mol Cell* 27(5):717-730.
- Choi JH, Yang YR, Lee SK, Kim IS, Ha SH, Kim EK, Bae YS, Ryu SH, and Suh PG. 2007. Phospholipase C-gamma1 potentiates integrin-dependent cell spreading and migration through Pyk2/paxillin activation. *Cell Signal* 19(8):1784-1796.
- Clevers H. 2006. Wnt/beta-catenin signaling in development and disease. *Cell* 127(3):469-480.
- Colotta F, Allavena P, Sica A, Garlanda C, and Mantovani A. 2009. Cancer-related inflammation, the seventh hallmark of cancer: links to genetic instability. *Carcinogenesis* 30(7):1073-1081.
- Colvin JS, Green RP, Schmahl J, Capel B, and Ornitz DM. 2001a. Male-to-female sex reversal in mice lacking fibroblast growth factor 9. *Cell* 104(6):875-889.
- Colvin JS, White AC, Pratt SJ, and Ornitz DM. 2001b. Lung hypoplasia and neonatal death in Fgf9-null mice identify this gene as an essential regulator of lung mesenchyme. *Development* 128(11):2095-2106.
- Cully M, You H, Levine AJ, and Mak TW. 2006. Beyond PTEN mutations: the PI3K pathway as an integrator of multiple inputs during tumorigenesis. *Nat Rev Cancer* 6(3):184-192.
- Dacostaandrade V, Parisejr O, Hors C, Demelomartins P, Silva A, and Garicochea B. 2007. The fibroblast growth factor receptor 4 (FGFR4) Arg388 allele correlates with survival in head and neck squamous cell carcinoma. *Experimental and Molecular Pathology* 82(1):53-57.
- Dale TC. 1998. Signal transduction by the Wnt family of ligands. *Biochem J* 329 ( Pt 2):209-223.



## Bibliography

- Desnoyers LR, Pai R, Ferrando RE, Hotzel K, Le T, Ross J, Carano R, D'Souza A, Qing J, Mohtashemi I et al. . 2008. Targeting FGF19 inhibits tumor growth in colon cancer xenograft and FGF19 transgenic hepatocellular carcinoma models. *Oncogene* 27(1):85-97.
- Dode C, Levilliers J, Dupont JM, De Paepe A, Le Du N, Soussi-Yanicostas N, Coimbra RS, Delmaghani S, Compain-Nouaille S, Baverel F et al. . 2003. Loss-of-function mutations in FGFR1 cause autosomal dominant Kallmann syndrome. *Nat Genet* 33(4):463-465.
- Drafahl KA, McAndrew CW, Meyer AN, Haas M, and Donoghue DJ. 2010. The receptor tyrosine kinase FGFR4 negatively regulates NF-kappaB signaling. *PLoS One* 5(12):e14412.
- Esteller M, Silva JM, Dominguez G, Bonilla F, Matias-Guiu X, Lerma E, Bussaglia E, Prat J, Harkes IC, Repasky EA et al. . 2000. Promoter hypermethylation and BRCA1 inactivation in sporadic breast and ovarian tumors. *J Natl Cancer Inst* 92(7):564-569.
- Eswarakumar VP, Lax I, and Schlessinger J. 2005. Cellular signaling by fibroblast growth factor receptors. *Cytokine & Growth Factor Reviews* 16(2):139-149.
- Ezzat S, Zheng L, and Asa SL. 2004. Pituitary tumor-derived fibroblast growth factor receptor 4 isoform disrupts neural cell-adhesion molecule/N-cadherin signaling to diminish cell adhesiveness: a mechanism underlying pituitary neoplasia. *Mol Endocrinol* 18(10):2543-2552.
- Falvella FS, Frullanti E, Galvan A, Spinola M, Noci S, De Cecco L, Nosotti M, Santambrogio L, Incarbone M, Alloisio M et al. . 2009. FGFR4 Gly388Arg polymorphism may affect the clinical stage of patients with lung cancer by modulating the transcriptional profile of normal lung. *International Journal of Cancer* 124(12):2880-2885.
- Feik E, Baierl A, Hieger B, Fuhrlinger G, Pentz A, Stattner S, Weiss W, Pulgram T, Leeb G, Mach K et al. . 2010. Association of IGF1 and IGFBP3 polymorphisms with colorectal polyps and colorectal cancer risk. *Cancer Causes Control* 21(1):91-97.
- Feldman B, Poueymirou W, Papaioannou VE, DeChiara TM, and Goldfarb M. 1995. Requirement of FGF-4 for postimplantation mouse development. *Science* 267(5195):246-249.
- Fenton TR, and Gout IT. 2011. Functions and regulation of the 70kDa ribosomal S6 kinases. *Int J Biochem Cell Biol* 43(1):47-59.
- FitzGerald LM, Karlins E, Karyadi DM, Kwon EM, Koopmeiners JS, Stanford JL, and Ostrander EA. 2009. Association of FGFR4 genetic polymorphisms with prostate cancer risk and prognosis. *Prostate Cancer Prostatic Dis* 12(2):192-197.
- Francavilla C, Cattaneo P, Berezin V, Bock E, Ami D, de Marco A, Christofori G, and Cavallaro U. 2009. The binding of NCAM to FGFR1 induces a specific cellular response mediated by receptor trafficking. *J Cell Biol* 187(7):1101-1116.
- Freier K, Schwaenen C, Sticht C, Flechtenmacher C, Muhling J, Hofele C, Radlwimmer B, Lichter P, and Joos S. 2007. Recurrent FGFR1 amplification and high FGFR1 protein expression in oral squamous cell carcinoma (OSCC). *Oral Oncol* 43(1):60-66.
- Frullanti E, Berking C, Harbeck N, Jezequel P, Haugen A, Mawrin C, Parise O, Sasaki H, Tsuchiya N, and Dragani TA. 2011. Meta and pooled analyses of FGFR4 Gly388Arg polymorphism as a cancer prognostic factor. *Eur J Cancer Prev*.

## Bibliography

- Furdui CM, Lew ED, Schlessinger J, and Anderson KS. 2006. Autophosphorylation of FGFR1 kinase is mediated by a sequential and precisely ordered reaction. *Mol Cell* 21(5):711-717.
- Garcia M, Jemal A, Ward EM, Center MM, Hao Y, Siegel RL, and Thun MJ. 2007. *Global Cancer Facts & Figures 2007*. Atlanta, GA: American Cancer Society, 2007.
- Giri D, Ropiquet F, and Ittmann M. 1999. Alterations in expression of basic fibroblast growth factor (FGF) 2 and its receptor FGFR-1 in human prostate cancer. *Clin Cancer Res* 5(5):1063-1071.
- Globoscan I. 11.6.2011. <http://globocan.iarc.fr/>.
- Goldfarb M. 2005. Fibroblast growth factor homologous factors: evolution, structure, and function. *Cytokine Growth Factor Rev* 16(2):215-220.
- Goldfarb M, Schoorlemmer J, Williams A, Diwakar S, Wang Q, Huang X, Giza J, Tchetchik D, Kelley K, Vega A et al. . 2007. Fibroblast growth factor homologous factors control neuronal excitability through modulation of voltage-gated sodium channels. *Neuron* 55(3):449-463.
- Gordon MA, Gil J, Lu B, Zhang W, Yang D, Yun J, Schneider S, Groshen S, Iqbal S, Press OA et al. . 2006. Genomic profiling associated with recurrence in patients with rectal cancer treated with chemoradiation. *Pharmacogenomics* 7(1):67-88.
- Gorringe KL, Jacobs S, Thompson ER, Sridhar A, Qiu W, Choong DY, and Campbell IG. 2007. High-resolution single nucleotide polymorphism array analysis of epithelial ovarian cancer reveals numerous microdeletions and amplifications. *Clin Cancer Res* 13(16):4731-4739.
- Grasl-Kraupp B, Bursch W, Ruttkay-Nedecky B, Wagner A, Lauer B, and Schulte-Hermann R. 1994. Food restriction eliminates preneoplastic cells through apoptosis and antagonizes carcinogenesis in rat liver. *Proc Natl Acad Sci U S A* 91(21):9995-9999.
- Guo L, Degenstein L, and Fuchs E. 1996. Keratinocyte growth factor is required for hair development but not for wound healing. *Genes Dev* 10(2):165-175.
- H. Lodish AB, S. L. Zipursky, P. Matsudaira, D. Baltimore, J. Darnell, editor. 2000. *Molecular Cell Biology*. New York: W. H. Freeman.
- Hacker U, Nybakken K, and Perrimon N. 2005. Heparan sulphate proteoglycans: the sweet side of development. *Nat Rev Mol Cell Biol* 6(7):530-541.
- Hanada K, Perry-Lalley DM, Ohnmacht GA, Bettinotti MP, and Yang JC. 2001. Identification of fibroblast growth factor-5 as an overexpressed antigen in multiple human adenocarcinomas. *Cancer Res* 61(14):5511-5516.
- Hanahan D, and Weinberg RA. 2000. The hallmarks of cancer. *Cell* 100(1):57-70.
- Hardy KM, Yatskievych TA, Konieczka J, Bobbs AS, and Antin PB. 2011. FGF signalling through RAS/MAPK and PI3K pathways regulates cell movement and gene expression in the chicken primitive streak without affecting E-cadherin expression. *BMC Dev Biol* 11:20.
- Harmer NJ. 2006. Insights into the role of heparan sulphate in fibroblast growth factor signalling. *Biochem Soc Trans* 34(Pt 3):442-445.
- Hebert JM, Rosenquist T, Gotz J, and Martin GR. 1994. FGF5 as a regulator of the hair growth cycle: evidence from targeted and spontaneous mutations. *Cell* 78(6):1017-1025.

## Bibliography

- Heinzle C, Sutterluty H, Grusch M, Grasl-Kraupp B, Berger W, and Marian B. 2011. Targeting fibroblast-growth-factor-receptor-dependent signaling for cancer therapy. *Expert Opin Ther Targets* 15(7):829-846.
- Housley DJ, and Venta PJ. 2006. The long and the short of it: evidence that FGF5 is a major determinant of canine 'hair'-itability. *Anim Genet* 37(4):309-315.
- Huang X, Yang C, Jin C, Luo Y, Wang F, and McKeehan WL. 2009. Resident hepatocyte fibroblast growth factor receptor 4 limits hepatocarcinogenesis. *Mol Carcinog* 48(6):553-562.
- Hunter KW, and Crawford NP. 2006. Germ line polymorphism in metastatic progression. *Cancer Res* 66(3):1251-1254.
- Hutley L, Shurety W, Newell F, McGeary R, Pelton N, Grant J, Herington A, Cameron D, Whitehead J, and Prins J. 2004. Fibroblast growth factor 1: a key regulator of human adipogenesis. *Diabetes* 53(12):3097-3106.
- Ichikawa S, Baujat G, Seyahi A, Garoufali AG, Imel EA, Padgett LR, Austin AM, Sorenson AH, Pejtin Z, Topouchian V et al. . 2010. Clinical variability of familial tumoral calcinosis caused by novel GALNT3 mutations. *Am J Med Genet A* 152A(4):896-903.
- Imamura T, Engleka K, Zhan X, Tokita Y, Forough R, Roeder D, Jackson A, Maier JA, Hla T, and Maciag T. 1990. Recovery of mitogenic activity of a growth factor mutant with a nuclear translocation sequence. *Science* 249(4976):1567-1570.
- Inagaki T, Choi M, Moschetta A, Peng L, Cummins CL, McDonald JG, Luo G, Jones SA, Goodwin B, Richardson JA et al. . 2005. Fibroblast growth factor 15 functions as an enterohepatic signal to regulate bile acid homeostasis. *Cell Metab* 2(4):217-225.
- Itoh N. 2010. Hormone-like (endocrine) Fgfs: their evolutionary history and roles in development, metabolism, and disease. *Cell Tissue Res*.
- Itoh N, and Ornitz DM. 2008. Functional evolutionary history of the mouse Fgf gene family. *Dev Dyn* 237(1):18-27.
- Jaakkola S, Salmikangas P, Nylund S, Partanen J, Armstrong E, Pyrhonen S, Lehtovirta P, and Nevanlinna H. 1993. Amplification of fgfr4 gene in human breast and gynecological cancers. *Int J Cancer* 54(3):378-382.
- Jang JH. 2005. Reciprocal relationship in gene expression between FGFR1 and FGFR3: implication for tumorigenesis. *Oncogene* 24(5):945-948.
- Jang JH, Shin KH, Park YJ, Lee RJ, McKeehan WL, and Park JG. 2000. Novel transcripts of fibroblast growth factor receptor 3 reveal aberrant splicing and activation of cryptic splice sequences in colorectal cancer. *Cancer Res* 60(15):4049-4052.
- Jezequel P, Champion L, Joalland MP, Millour M, Dravet F, Classe JM, Delecroix V, Deporte R, Fumoleau P, and Ricolleau G. 2004. G388R mutation of the FGFR4 gene is not relevant to breast cancer prognosis. *Br J Cancer* 90(1):189-193.
- Kan SH, Elanko N, Johnson D, Cornejo-Roldan L, Cook J, Reich EW, Tomkins S, Verloes A, Twigg SR, Rannan-Eliya S et al. . 2002. Genomic screening of fibroblast growth-factor receptor 2 reveals a wide spectrum of mutations in patients with syndromic craniosynostosis. *Am J Hum Genet* 70(2):472-486.
- Kathir KM, Kumar TK, and Yu C. 2006. Understanding the mechanism of the antimitogenic activity of suramin. *Biochemistry* 45(3):899-906.

## Bibliography

- Katoh M. 2006a. Cross-talk of WNT and FGF signaling pathways at GSK3beta to regulate beta-catenin and SNAIL signaling cascades. *Cancer Biol Ther* 5(9):1059-1064.
- Katoh M. 2006b. FGF signaling network in the gastrointestinal tract (review). *Int J Oncol* 29(1):163-168.
- Knights V, and Cook SJ. 2010. De-regulated FGF receptors as therapeutic targets in cancer. *Pharmacol Ther* 125(1):105-117.
- Kohan DE. 2008. Progress in gene targeting: using mutant mice to study renal function and disease. *Kidney Int* 74(4):427-437.
- Kostrzewa M, and Muller U. 1998. Genomic structure and complete sequence of the human FGFR4 gene. *Mamm Genome* 9(2):131-135.
- Kraemer A, Hauser S, Kim Y, Gorschluter M, Muller SC, Brossart P, and Schmidt-Wolf IG. 2009. Phase I trial of metastatic renal cell carcinoma with oral capecitabine and thalidomide. *Ger Med Sci* 7:Doc04.
- Kroemer G, and Pouyssegur J. 2008. Tumor cell metabolism: cancer's Achilles' heel. *Cancer Cell* 13(6):472-482.
- Kunii K, Davis L, Gorenstein J, Hatch H, Yashiro M, Di Bacco A, Elbi C, and Lutterbach B. 2008. FGFR2-amplified gastric cancer cell lines require FGFR2 and Erbb3 signaling for growth and survival. *Cancer Res* 68(7):2340-2348.
- Land H, Parada LF, and Weinberg RA. 1983. Tumorigenic conversion of primary embryo fibroblasts requires at least two cooperating oncogenes. *Nature* 304(5927):596-602.
- Lieu C, and Kopetz S. 2010. The SRC family of protein tyrosine kinases: a new and promising target for colorectal cancer therapy. *Clin Colorectal Cancer* 9(2):89-94.
- Lin PH, Cheng H, Huang WC, and Chuang TY. 2005. Spinal cord implantation with acidic fibroblast growth factor as a treatment for root avulsion in obstetric brachial plexus palsy. *J Chin Med Assoc* 68(8):392-396.
- Liu Z, Xu J, Colvin JS, and Ornitz DM. 2002. Coordination of chondrogenesis and osteogenesis by fibroblast growth factor 18. *Genes Dev* 16(7):859-869.
- Logie A, Dunois-Larde C, Rosty C, Levrel O, Blanche M, Ribeiro A, Gasc JM, Jorcano J, Werner S, Sastre-Garau X et al. . 2005. Activating mutations of the tyrosine kinase receptor FGFR3 are associated with benign skin tumors in mice and humans. *Hum Mol Genet* 14(9):1153-1160.
- Lu SY, Sheikh F, Sheppard PC, Fresnoza A, Duckworth ML, Detillieux KA, and Cattini PA. 2008. FGF-16 is required for embryonic heart development. *Biochemical and Biophysical Research Communications* 373(2):270-274.
- Luo J, Solimini NL, and Elledge SJ. 2009. Principles of cancer therapy: oncogene and non-oncogene addiction. *Cell* 136(5):823-837.
- Ma Z, Tsuchiya N, Yuasa T, Inoue T, Kumazawa T, Narita S, Horikawa Y, Tsuruta H, Obara T, Saito M et al. . 2008. Polymorphisms of fibroblast growth factor receptor 4 have association with the development of prostate cancer and benign prostatic hyperplasia and the progression of prostate cancer in a Japanese population. *International Journal of Cancer* 123(11):2574-2579.

## Bibliography

- Mao L, Lee JS, Kurie JM, Fan YH, Lippman SM, Lee JJ, Ro JY, Broxson A, Yu R, Morice RC et al. . 1997. Clonal genetic alterations in the lungs of current and former smokers. *J Natl Cancer Inst* 89(12):857-862.
- Martinez-Torrecuadrada J, Cifuentes G, Lopez-Serra P, Saenz P, Martinez A, and Casal JJ. 2005. Targeting the extracellular domain of fibroblast growth factor receptor 3 with human single-chain Fv antibodies inhibits bladder carcinoma cell line proliferation. *Clin Cancer Res* 11(17):6280-6290.
- Matakidou A, El Galta R, Rudd MF, Webb EL, Bridle H, Eisen T, and Houlston RS. 2007. Further observations on the relationship between the FGFR4 Gly388Arg polymorphism and lung cancer prognosis. *Br J Cancer* 96(12):1904-1907.
- Matsubara A, Kan M, Feng S, and McKeehan WL. 1998. Inhibition of growth of malignant rat prostate tumor cells by restoration of fibroblast growth factor receptor 2. *Cancer Res* 58(7):1509-1514.
- Metzner T, Bedeir A, Held G, Peter-Vorosmarty B, Ghassemi S, Heinzle C, Spiegl-Kreinecker S, Marian B, Holzmann K, Grasl-Kraupp B et al. . 2011. Fibroblast Growth Factor Receptors as Therapeutic Targets in Human Melanoma: Synergism with BRAF Inhibition. *J Invest Dermatol*.
- Miller DL, Ortega S, Bashayan O, Basch R, and Basilico C. 2000. Compensation by fibroblast growth factor 1 (FGF1) does not account for the mild phenotypic defects observed in FGF2 null mice. *Mol Cell Biol* 20(6):2260-2268.
- Missiaglia E, Selfe J, Hamdi M, Williamson D, Schaaf G, Fang C, Koster J, Summersgill B, Messahel B, Versteeg R et al. . 2009. Genomic imbalances in rhabdomyosarcoma cell lines affect expression of genes frequently altered in primary tumors: an approach to identify candidate genes involved in tumor development. *Genes Chromosomes Cancer* 48(6):455-467.
- Morimoto Y, Ozaki T, Ouchida M, Umehara N, Ohata N, Yoshida A, Shimizu K, and Inoue H. 2003. Single nucleotide polymorphism in fibroblast growth factor receptor 4 at codon 388 is associated with prognosis in high-grade soft tissue sarcoma. *Cancer* 98(10):2245-2250.
- Muenke M, Schell U, Hehr A, Robin NH, Losken HW, Schinzel A, Pulleyn LJ, Rutland P, Reardon W, Malcolm S et al. . 1994. A common mutation in the fibroblast growth factor receptor 1 gene in Pfeiffer syndrome. *Nat Genet* 8(3):269-274.
- Naidu R, Har YC, and Taib NA. 2009. Polymorphism of FGFR4 Gly388Arg does not confer an increased risk to breast cancer development. *Oncol Res* 18(2-3):65-71.
- Narita K, Fujii T, Ishiwata T, Yamamoto T, Kawamoto Y, Kawahara K, Nakazawa N, and Naito Z. 2009. Keratinocyte growth factor induces vascular endothelial growth factor-A expression in colorectal cancer cells. *Int J Oncol* 34(2):355-360.
- NCI. 17.6.2011. <http://www.cancer.gov/cancertopics/cancerlibrary/what-is-cancer>.
- Nicholes K, Guillet S, Tomlinson E, Hillan K, Wright B, Frantz GD, Pham TA, Dillard-Telm L, Tsai SP, Stephan JP et al. . 2002. A mouse model of hepatocellular carcinoma: ectopic expression of fibroblast growth factor 19 in skeletal muscle of transgenic mice. *Am J Pathol* 160(6):2295-2307.
- Nusse R, Brown A, Papkoff J, Scambler P, Shackleford G, McMahon A, Moon R, and Varmus H. 1991. A new nomenclature for int-1 and related genes: the Wnt gene family. *Cell* 64(2):231.

## Bibliography

- Olsen SK, Garbi M, Zampieri N, Eliseenkova AV, Ornitz DM, Goldfarb M, and Mohammadi M. 2003. Fibroblast growth factor (FGF) homologous factors share structural but not functional homology with FGFs. *J Biol Chem* 278(36):34226-34236.
- Olsen SK, Ibrahimi OA, Raucci A, Zhang F, Eliseenkova AV, Yayon A, Basilico C, Linhardt RJ, Schlessinger J, and Mohammadi M. 2004. Insights into the molecular basis for fibroblast growth factor receptor autoinhibition and ligand-binding promiscuity. *Proc Natl Acad Sci U S A* 101(4):935-940.
- Ornitz DM, and Itoh N. 2001. Fibroblast growth factors. *Genome Biol* 2(3):REVIEWS3005.
- Ornitz DM, Xu J, Colvin JS, McEwen DG, MacArthur CA, Coulier F, Gao G, and Goldfarb M. 1996. Receptor specificity of the fibroblast growth factor family. *J Biol Chem* 271(25):15292-15297.
- Ostrovsky O, Berman B, Gallagher J, Mulloy B, Fernig DG, Delehedde M, and Ron D. 2002. Differential effects of heparin saccharides on the formation of specific fibroblast growth factor (FGF) and FGF receptor complexes. *J Biol Chem* 277(4):2444-2453.
- Pai R, Dunlap D, Qing J, Mohtashemi I, Hotzel K, and French DM. 2008. Inhibition of fibroblast growth factor 19 reduces tumor growth by modulating beta-catenin signaling. *Cancer Res* 68(13):5086-5095.
- Plotnikov AN, Hubbard SR, Schlessinger J, and Mohammadi M. 2000. Crystal structures of two FGF-FGFR complexes reveal the determinants of ligand-receptor specificity. *Cell* 101(4):413-424.
- Plotnikov AN, Schlessinger J, Hubbard SR, and Mohammadi M. 1999. Structural basis for FGF receptor dimerization and activation. *Cell* 98(5):641-650.
- Powell SM, Zilz N, Beazer-Barclay Y, Bryan TM, Hamilton SR, Thibodeau SN, Vogelstein B, and Kinzler KW. 1992. APC mutations occur early during colorectal tumorigenesis. *Nature* 359(6392):235-237.
- Powers CJ, McLeskey SW, and Wellstein A. 2000. Fibroblast growth factors, their receptors and signaling. *Endocr Relat Cancer* 7(3):165-197.
- Prie D, and Friedlander G. 2010. Reciprocal control of 1,25-dihydroxyvitamin D and FGF23 formation involving the FGF23/Klotho system. *Clin J Am Soc Nephrol* 5(9):1717-1722.
- Qiao J, Uzzo R, Obara-Ishihara T, Degenstein L, Fuchs E, and Herzlinger D. 1999. FGF-7 modulates ureteric bud growth and nephron number in the developing kidney. *Development* 126(3):547-554.
- Qing J, Du X, Chen Y, Chan P, Li H, Wu P, Marsters S, Stawicki S, Tien J, Totpal K et al. . 2009. Antibody-based targeting of FGFR3 in bladder carcinoma and t(4;14)-positive multiple myeloma in mice. *J Clin Invest* 119(5):1216-1229.
- Rand V, Huang J, Stockwell T, Ferriera S, Buzko O, Levy S, Busam D, Li K, Edwards JB, Eberhart C et al. . 2005. Sequence survey of receptor tyrosine kinases reveals mutations in glioblastomas. *Proc Natl Acad Sci U S A* 102(40):14344-14349.
- Ricol D, Cappellen D, El Marjou A, Gil-Diez-de-Medina S, Girault JM, Yoshida T, Ferry G, Tucker G, Poupon MF, Chopin D et al. . 1999. Tumour suppressive properties of fibroblast growth factor receptor 2-IIIb in human bladder cancer. *Oncogene* 18(51):7234-7243.

## Bibliography

- Roidl A, Berger HJ, Kumar S, Bange J, Knyazev P, and Ullrich A. 2009. Resistance to chemotherapy is associated with fibroblast growth factor receptor 4 up-regulation. *Clin Cancer Res* 15(6):2058-2066.
- Sahadevan K, Darby S, Leung H, Mathers M, Robson C, and Gnanapragasam V. 2007. Selective over-expression of fibroblast growth factor receptors 1 and 4 in clinical prostate cancer. *The Journal of Pathology* 213(1):82-90.
- Sandilands E, Akbarzadeh S, Vecchione A, McEwan DG, Frame MC, and Heath JK. 2007. Src kinase modulates the activation, transport and signalling dynamics of fibroblast growth factor receptors. *EMBO Rep* 8(12):1162-1169.
- Sasaki H, Okuda K, Kawano O, Yukiue H, Yano M, and Fujii Y. 2008. Fibroblast growth factor receptor 4 mutation and polymorphism in Japanese lung cancer. *Oncol Rep* 20(5):1125-1130.
- Sato T, Oshima T, Yoshihara K, Yamamoto N, Yamada R, Nagano Y, Fujii S, Kunisaki C, Shiozawa M, Akaike M et al. . 2009. Overexpression of the fibroblast growth factor receptor-1 gene correlates with liver metastasis in colorectal cancer. *Oncol Rep* 21(1):211-216.
- Schlessinger J, Lax I, and Lemmon M. 1995. Regulation of growth factor activation by proteoglycans: what is the role of the low affinity receptors? *Cell* 83(3):357-360.
- Schlessinger J, Plotnikov AN, Ibrahimi OA, Eliseenkova AV, Yeh BK, Yayon A, Linhardt RJ, and Mohammadi M. 2000. Crystal structure of a ternary FGF-FGFR-heparin complex reveals a dual role for heparin in FGFR binding and dimerization. *Mol Cell* 6(3):743-750.
- Schölmerich J. SW, editor. 2005. Leitfaden kolorektales Karzinom - Prophylaxe, Diagnostik, Therapie. 2. Auflage ed. Bremen: UNI-MED Verlag AG.
- Schulte-Hermann R, Bursch W, Kraupp-Grasl B, Oberhammer F, and Wagner A. 1992. Programmed cell death and its protective role with particular reference to apoptosis. *Toxicol Lett* 64-65 Spec No:569-574.
- Schulte-Hermann R. PW. 2004. Mehrstufenprozess der Kanzerogenese und chemische Kanzerogenese. In: Hiddemann W. HH, Bartram C., editor. *Die Onkologie*. Heidelberg: Springer-Verlag p193-240.
- Sekine K, Ohuchi H, Fujiwara M, Yamasaki M, Yoshizawa T, Sato T, Yagishita N, Matsui D, Koga Y, Itoh N et al. . 1999. Fgf10 is essential for limb and lung formation. *Nat Genet* 21(1):138-141.
- Shankar VN, Ajila V, and Kumar G. 2010. Osteoglyphonic dysplasia: a case report. *J Oral Sci* 52(1):167-171.
- Shaw RJ, and Cantley LC. 2006. Ras, PI(3)K and mTOR signalling controls tumour cell growth. *Nature* 441(7092):424-430.
- Shirakihara T, Horiguchi K, Miyazawa K, Ehata S, Shibata T, Morita I, Miyazono K, and Saitoh M. 2011. TGF-beta regulates isoform switching of FGF receptors and epithelial-mesenchymal transition. *EMBO J* 30(4):783-795.
- Simon R, Richter J, Wagner U, Fijan A, Bruderer J, Schmid U, Ackermann D, Maurer R, Alund G, Knonagel H et al. . 2001. High-throughput tissue microarray analysis of 3p25 (RAF1) and 8p12 (FGFR1) copy number alterations in urinary bladder cancer. *Cancer Res* 61(11):4514-4519.

## Bibliography

- Slamon DJ, Clark GM, Wong SG, Levin WJ, Ullrich A, and McGuire WL. 1987. Human breast cancer: correlation of relapse and survival with amplification of the HER-2/neu oncogene. *Science* 235(4785):177-182.
- Sonvilla G, Allerstorfer S, Heinzle C, Stattner S, Karner J, Klimpfinger M, Wrba F, Fischer H, Gauglhofer C, Spiegl-Kreinecker S et al. . 2010. Fibroblast growth factor receptor 3-IIIc mediates colorectal cancer growth and migration. *Br J Cancer* 102(7):1145-1156.
- Sonvilla G, Allerstorfer S, Stattner S, Karner J, Klimpfinger M, Fischer H, Grasl-Kraupp B, Holzmann K, Berger W, Wrba F et al. . 2008. FGF18 in colorectal tumour cells: autocrine and paracrine effects. *Carcinogenesis* 29(1):15-24.
- Soussi T. 2000. The p53 tumor suppressor gene: from molecular biology to clinical investigation. *Ann N Y Acad Sci* 910:121-137; discussion 137-129.
- Spinola M. 2005. Functional FGFR4 Gly388Arg Polymorphism Predicts Prognosis in Lung Adenocarcinoma Patients. *Journal of Clinical Oncology* 23(29):7307-7311.
- Spinola M, Leoni VP, Tanuma J, Pettinicchio A, Frattini M, Signoroni S, Agresti R, Giovanazzi R, Pilotti S, Bertario L et al. . 2005. FGFR4 Gly388Arg polymorphism and prognosis of breast and colorectal cancer. *Oncol Rep* 14(2):415-419.
- Stadler CR, Knyazev P, Bange J, and Ullrich A. 2006. FGFR4 GLY388 isotype suppresses motility of MDA-MB-231 breast cancer cells by EDG-2 gene repression. *Cell Signal* 18(6):783-794.
- StatistikAustria. 15.6.2011.  
[http://www.statistik.at/web\\_de/statistiken/gesundheit/todesursachen/todesursachen\\_im\\_ueberblick/index.html](http://www.statistik.at/web_de/statistiken/gesundheit/todesursachen/todesursachen_im_ueberblick/index.html).
- Stratton MR, Campbell PJ, and Futreal PA. 2009. The cancer genome. *Nature* 458(7239):719-724.
- Streit S, Bange J, Fichtner A, Ihrler S, Issing W, and Ullrich A. 2004. Involvement of the FGFR4 Arg388 allele in head and neck squamous cell carcinoma. *International Journal of Cancer* 111(2):213-217.
- Streit S, Mestel DS, Schmidt M, Ullrich A, and Berking C. 2006. FGFR4 Arg388 allele correlates with tumour thickness and FGFR4 protein expression with survival of melanoma patients. *Br J Cancer* 94(12):1879-1886.
- Sugi Y, Ito N, Szebenyi G, Myers K, Fallon JF, Mikawa T, and Markwald RR. 2003. Fibroblast growth factor (FGF)-4 can induce proliferation of cardiac cushion mesenchymal cells during early valve leaflet formation. *Dev Biol* 258(2):252-263.
- Sugiyama N, Varjosalo M, Meller P, Lohi J, Chan KM, Zhou Z, Alitalo K, Taipale J, Keski-Oja J, and Lehti K. 2010a. FGF receptor-4 (FGFR4) polymorphism acts as an activity switch of a membrane type 1 matrix metalloproteinase-FGFR4 complex. *Proc Natl Acad Sci U S A* 107(36):15786-15791.
- Sugiyama N, Varjosalo M, Meller P, Lohi J, Hyytiainen M, Kilpinen S, Kallioniemi O, Ingvarsen S, Engelholm LH, Taipale J et al. . 2010b. Fibroblast Growth Factor Receptor 4 Regulates Tumor Invasion by Coupling Fibroblast Growth Factor Signaling to Extracellular Matrix Degradation. *Cancer Res*.
- Suh PG, Park JI, Manzoli L, Cocco L, Peak JC, Katan M, Fukami K, Kataoka T, Yun S, and Ryu SH. 2008. Multiple roles of phosphoinositide-specific phospholipase C isozymes. *BMB Rep* 41(6):415-434.



## Bibliography

- Sun HD, Malabunga M, Tonra JR, DiRenzo R, Carrick FE, Zheng H, Berthoud HR, McGuinness OP, Shen J, Bohlen P et al. . 2007. Monoclonal antibody antagonists of hypothalamic FGFR1 cause potent but reversible hypophagia and weight loss in rodents and monkeys. *Am J Physiol Endocrinol Metab* 292(3):E964-976.
- Sundlisaeter E, Rosland GV, Hertel JK, Sakariassen PO, Almas B, Dicko A, and Sondenaa K. 2009. Increased lymphatic vascular density is seen before colorectal cancers reach stage II and growth factor FGF-2 is downregulated in tumor tissue compared with normal mucosa. *APMIS* 117(3):212-221.
- Takaishi S, Sawada M, Morita Y, Seno H, Fukuzawa H, and Chiba T. 2000. Identification of a novel alternative splicing of human FGF receptor 4: soluble-form splice variant expressed in human gastrointestinal epithelial cells. *Biochem Biophys Res Commun* 267(2):658-662.
- Tan L, Xiao BX, Zeng WS, Lin J, Zou ZP, Xu AM, and Luo SQ. 2007. Antitumour effects on human colorectal carcinomas cells by stable silencing of phospholipase C-gamma 1 with lentivirus-delivered siRNA. *Chin Med J (Engl)* 120(9):749-754.
- Tanuma J, Izumo T, Hirano M, Oyazato Y, Hori F, Umemura E, Shisa H, Hiai H, and Kitano M. 2010. FGFR4 polymorphism, TP53 mutation, and their combinations are prognostic factors for oral squamous cell carcinoma. *Oncol Rep* 23(3):739-744.
- Taylor JGt, Cheuk AT, Tsang PS, Chung JY, Song YK, Desai K, Yu Y, Chen QR, Shah K, Youngblood V et al. . 2009. Identification of FGFR4-activating mutations in human rhabdomyosarcomas that promote metastasis in xenotransplanted models. *J Clin Invest* 119(11):3395-3407.
- Tekin M, Hismi BO, Fitoz S, Ozdag H, Cengiz FB, Sirmaci A, Aslan I, Inceoglu B, Yuksel-Konuk EB, Yilmaz ST et al. . 2007. Homozygous mutations in fibroblast growth factor 3 are associated with a new form of syndromic deafness characterized by inner ear agenesis, microtia, and microdontia. *Am J Hum Genet* 80(2):338-344.
- Thiery JP. 2002. Epithelial-mesenchymal transitions in tumour progression. *Nat Rev Cancer* 2(6):442-454.
- Thussbas C, Nahrig J, Streit S, Bange J, Kriner M, Kates R, Ulm K, Kiechle M, Hoefler H, Ullrich A et al. . 2006. FGFR4 Arg388 allele is associated with resistance to adjuvant therapy in primary breast cancer. *J Clin Oncol* 24(23):3747-3755.
- Trudel S, Stewart AK, Rom E, Wei E, Li ZH, Kotzer S, Chumakov I, Singer Y, Chang H, Liang SB et al. . 2006. The inhibitory anti-FGFR3 antibody, PRO-001, is cytotoxic to t(4;14) multiple myeloma cells. *Blood* 107(10):4039-4046.
- Turner N, and Grose R. 2010. Fibroblast growth factor signalling: from development to cancer. *Nature Reviews Cancer* 10(2):116-129.
- Tvorogov D, Wang XJ, Zent R, and Carpenter G. 2005. Integrin-dependent PLC-gamma1 phosphorylation mediates fibronectin-dependent adhesion. *J Cell Sci* 118(Pt 3):601-610.
- Umemori H, Linhoff MW, Ornitz DM, and Sanes JR. 2004. FGF22 and its close relatives are presynaptic organizing molecules in the mammalian brain. *Cell* 118(2):257-270.
- Urakawa I, Yamazaki Y, Shimada T, Iijima K, Hasegawa H, Okawa K, Fujita T, Fukumoto S, and Yamashita T. 2006. Klotho converts canonical FGF receptor into a specific receptor for FGF23. *Nature* 444(7120):770-774.

## Bibliography

- Uriel S, Brey EM, and Greisler HP. 2006. Sustained low levels of fibroblast growth factor-1 promote persistent microvascular network formation. *Am J Surg* 192(5):604-609.
- van der Walt JM, Nouredine MA, Kittappa R, Hauser MA, Scott WK, McKay R, Zhang F, Stajich JM, Fujiwara K, Scott BL et al. . 2004. Fibroblast growth factor 20 polymorphisms and haplotypes strongly influence risk of Parkinson disease. *Am J Hum Genet* 74(6):1121-1127.
- Vlodavsky I, Miao HQ, Medalion B, Danagher P, and Ron D. 1996. Involvement of heparan sulfate and related molecules in sequestration and growth promoting activity of fibroblast growth factor. *Cancer Metastasis Rev* 15(2):177-186.
- Vogelstein B, Fearon ER, Hamilton SR, Kern SE, Preisinger AC, Leppert M, Nakamura Y, White R, Smits AM, and Bos JL. 1988. Genetic alterations during colorectal-tumor development. *N Engl J Med* 319(9):525-532.
- Vogelzang NJ, Karrison T, Stadler WM, Garcia J, Cohn H, Kugler J, Troeger T, Giannone L, Arrieta R, Ratain MJ et al. . 2004. A Phase II trial of suramin monthly x 3 for hormone-refractory prostate carcinoma. *Cancer* 100(1):65-71.
- Wang J, Stockton DW, and Ittmann M. 2004. The fibroblast growth factor receptor-4 Arg388 allele is associated with prostate cancer initiation and progression. *Clin Cancer Res* 10(18 Pt 1):6169-6178.
- Wang J, Yu W, Cai Y, Ren C, and Ittmann MM. 2008. Altered fibroblast growth factor receptor 4 stability promotes prostate cancer progression. *Neoplasia* 10(8):847-856.
- Wang Q, Bardgett ME, Wong M, Wozniak DF, Lou J, McNeil BD, Chen C, Nardi A, Reid DC, Yamada K et al. . 2002. Ataxia and paroxysmal dyskinesia in mice lacking axonally transported FGF14. *Neuron* 35(1):25-38.
- Wang Y, and Becker D. 1997. Antisense targeting of basic fibroblast growth factor and fibroblast growth factor receptor-1 in human melanomas blocks intratumoral angiogenesis and tumor growth. *Nat Med* 3(8):887-893.
- Warburg O. 1956. On the origin of cancer cells. *Science* 123(3191):309-314.
- Watanabe M, Ishiwata T, Nishigai K, Moriyama Y, and Asano G. 2000. Overexpression of keratinocyte growth factor in cancer cells and enterochromaffin cells in human colorectal cancer. *Pathol Int* 50(5):363-372.
- Webster MK, and Donoghue DJ. 1996. Constitutive activation of fibroblast growth factor receptor 3 by the transmembrane domain point mutation found in achondroplasia. *EMBO J* 15(3):520-527.
- Webster MK, and Donoghue DJ. 1997. FGFR activation in skeletal disorders: too much of a good thing. *Trends Genet* 13(5):178-182.
- Weinberg RA, editor. 2007. *The biology of cancer*. New York: Garland Science.
- Weiss J, Sos ML, Seidel D, Peifer M, Zander T, Heuckmann JM, Ullrich RT, Menon R, Maier S, Soltermann A et al. . 2010. Frequent and focal FGFR1 amplification associates with therapeutically tractable FGFR1 dependency in squamous cell lung cancer. *Sci Transl Med* 2(62):62ra93.
- Weitz J. SA, Kadmon M., Eble M.J., Herfarth C. 2004. Kolon- und Rektumkarzinoma. In: Hiddemann W. HH, Bartram C., editor. *Die Onkologie*. Heidelberg: Springer Verlag.
- WHO. 11.6.2011. <http://www.who.int/mediacentre/factsheets/fs297/en/index.html>.

## Bibliography

- Wiedemann M, and Trueb B. 2000. Characterization of a Novel Protein (FGFRL1) from Human Cartilage Related to FGF Receptors. *Genomics* 69(2):275-279.
- Wiedlocha A, Falnes PO, Madshus IH, Sandvig K, and Olsnes S. 1994. Dual mode of signal transduction by externally added acidic fibroblast growth factor. *Cell* 76(6):1039-1051.
- Xie MH, Holcomb I, Deuel B, Dowd P, Huang A, Vagts A, Foster J, Liang J, Brush J, Gu Q et al. . 1999. FGF-19, a novel fibroblast growth factor with unique specificity for FGFR4. *Cytokine* 11(10):729-735.
- Xu J, Liu Z, and Ornitz DM. 2000. Temporal and spatial gradients of Fgf8 and Fgf17 regulate proliferation and differentiation of midline cerebellar structures. *Development* 127(9):1833-1843.
- Yamaguchi F, Saya H, Bruner JM, and Morrison RS. 1994. Differential expression of two fibroblast growth factor-receptor genes is associated with malignant progression in human astrocytomas. *Proc Natl Acad Sci U S A* 91(2):484-488.
- Yang YC, Lu ML, Rao JY, Wallerand H, Cai L, Cao W, Pantuck A, Dalbagni G, Reuter V, Figlin RA et al. . 2006. Joint association of polymorphism of the FGFR4 gene and mutation TP53 gene with bladder cancer prognosis. *Br J Cancer* 95(11):1455-1458.
- Yayon A, Klagsbrun M, Esko JD, Leder P, and Ornitz DM. 1991. Cell surface, heparin-like molecules are required for binding of basic fibroblast growth factor to its high affinity receptor. *Cell* 64(4):841-848.
- Ye YW, Zhou Y, Yuan L, Wang CM, Du CY, Zhou XY, Zheng BQ, Cao X, Sun MH, Fu H et al. . 2011. Fibroblast growth factor receptor 4 regulates proliferation and antiapoptosis during gastric cancer progression. *Cancer*.
- Yu C, Wang F, Kan M, Jin C, Jones RB, Weinstein M, Deng CX, and McKeehan WL. 2000. Elevated cholesterol metabolism and bile acid synthesis in mice lacking membrane tyrosine kinase receptor FGFR4. *J Biol Chem* 275(20):15482-15489.
- Zhang X, Ibrahimi OA, Olsen SK, Umemori H, Mohammadi M, and Ornitz DM. 2006. Receptor specificity of the fibroblast growth factor family. The complete mammalian FGF family. *J Biol Chem* 281(23):15694-15700.
- Zhang X, Yeung DC, Karpisek M, Stejskal D, Zhou ZG, Liu F, Wong RL, Chow WS, Tso AW, Lam KS et al. . 2008. Serum FGF21 levels are increased in obesity and are independently associated with the metabolic syndrome in humans. *Diabetes* 57(5):1246-1253.
- Zhong W, Wang QT, Sun T, Wang F, Liu J, Leach R, Johnson A, Puscheck EE, and Rappolee DA. 2006. FGF ligand family mRNA expression profile for mouse preimplantation embryos, early gestation human placenta, and mouse trophoblast stem cells. *Mol Reprod Dev* 73(5):540-550.
- Zielonke N. 2010. Krebsinzidenz und Krebsmortalität in Österreich. Statistik Austria.

I have done my best to identify the owners of the copyrights for the images and to get their permission for usage in this thesis. Nevertheless, please contact me in case of any copyright infringements.



## 9 Curriculum vitae

### Personal Data

Name: Christine Filomena Heinzle  
Address: Horneckgasse 12-14, 1170 Wien  
Email: christine.heinzle@meduniwien.ac.at  
Date of birth: 23.07.1981  
Nationality: Austrian

### Education

School:

- 1991-1999 High school, Bundesgymnasium Blumenstraße, Bregenz

Study:

- 1999-2006 University of Vienna, Diploma studies: Nutrition
  - Title of diploma thesis: “Ernährung und Osteoporose”, supervised by Prof. Dr. Elmadfa
- Since 2002: University of Vienna, Diploma studies: Molecular Biology
- 2003: semester abroad at University of Valencia, Spain
- 2008-2011: University of Vienna, Doctoral studies: Molecular Biology
  - Title of doctoral thesis: “The Role of Fibroblast Growth Factor Receptor 4 in Colorectal Cancer”, supervised by A.o.Univ.Prof. Dr. Marian

### Publications

- Kaindl U, Eyberg I, Rohr-Udilova N, Heinzle C, and Marian B. 2008. The dietary antioxidants resveratrol and quercetin protect cells from exogenous pro-oxidative damage. Food Chem Toxicol 46(4):1320-1326.

## Curriculum vitae

- Sonvilla G, Allerstorfer S, Heinzle C, Stättner S, Karner J, Klimpfinger M, Wrba F, Fischer H, Gauglhofer C, Spiegl-Kreinecker S et al. . 2010. Fibroblast growth factor receptor 3-IIIc mediates colorectal cancer growth and migration. *Br J Cancer* 102(7):1145-1156.
- Heinzle C, Sutterluty H, Grusch M, Grasl-Kraupp B, Berger W, and Marian B. 2011. Targeting fibroblast-growth-factor-receptor-dependent signaling for cancer therapy. *Expert Opin Ther Targets* 15(7):829-846.
- Metzner T, Bedeir A, Held G, Peter-Vorosmarty B, Ghassemi S, Heinzle C, Spiegl-Kreinecker S, Marian B, Holzmann K, Grasl-Kraupp B et al. . 2011. Fibroblast Growth Factor Receptors as Therapeutic Targets in Human Melanoma: Synergism with BRAF Inhibition. *J Invest Dermatol*.
- Holzmann K, Grunt T, Heinzle C, Sampl S, Reichmann N, Kleiter M, Hauck M, Marian B. Alternative Splicing of Fibroblast Growth Factor Receptors in Cancer (in press)
- Klampfl T, Bogner E, Bednar W, Mager L, Massoudom D, Kalny I, Heinzle C, Berger W, Stättner S, Karner J, Klimpfinger M, Fürstenberger G, Krieg P, Marian B. Up-regulation of 12(S)-Lipoxygenase Mediates Induction of a Migratory Phenotype in Colorectal Cancer Cells. (manuscript submitted)
- Heinzle C, Gsur A, Hunjadi M, Gauglhofer C, Stättner S, Karner J, Klimpfinger M, Wrba F, Grasl-Kraupp B, Holzmann K, Grusch M, Berger W, Marian B. Differential Effects of the Fibroblast Growth Factor Receptor-4 Polymorphic Alleles (G388R) on Colon Cancer Growth and Metastasis. (manuscript submitted)

## Posters

- PhD Symposium 2010 at the University of Vienna, Vienna, Austria:  
Heinzle C, Hunjadi M, Stättner S, Klimpfinger M, Holzmann K, Grusch M, Berger W, Marian B. *Fibroblast Growth Factor Receptor 4 (FGFR4) G388R Polyphormism in Colorectal Cancer*
- 22<sup>nd</sup> EORTC-NCI-AACR symposium on “Molecular targets and Cancer Therapeutics”, Berlin, Germany:  
Heinzle C, Hunjadi M, Stättner S, Klimpfinger M, Holzmann K, Grusch M, Berger W, Marian B. *Fibroblast Growth Factor Receptor 4 (FGFR4) G388R Polyphormism in Colorectal Cancer*